The Mineralogy And Chemistry Of Micrometeorites

Thesis

THE MINERALOGY AND CHEMISTRY OF MICROMETEORITES

A thesis submitted for the degree of

Doctor of Philosophy

By

Giles Andrew Graham

B.Sc. Hons. (Oxford Brookes University, 1994)

September 1999

Planetary Sciences Research Institute

The Open University

Abstract

Prior to their retrieval from low Earth orbit (LEO), the individual solar cells that make up the '-V2' solar array panel from the Hubble Space Telescope (HST) were prone to hypervelocity (>5 km/s) impact damage from micrometeoroids and space debris. The analysis of such passive collector surfaces allows sampling of micrometeoroids that have not undergone any terrestrial atmospheric alteration and better defines the population of space debris particles below the 1mm size range.

Herein a new approach has been taken to try and identify the nature and origin of impact derived residues generated in the individual solar cells from the HST. A total of 25 solar cells were selected on the basis that they contained impact craters (100-1000μm diameter) rather than larger impact holes (1-3mm diameter), as preliminary studies indicated that they were more likely to retain impact residues. These were subsequently analysed using digitised back-scattered electron imaging, coupled with digitised x-ray elemental mapping and micro-spot analysis to locate, identify and classify the residues.

29 impact craters were located on solar cells. In the analysis of the residues; 3 were identified residues as space debris in origin, 6 unclassified and 20 as micrometeoroid. The space debris derived residues were identified as remnants of a paint fragment, a stainless steel particle and a fragment of a printed circuit board. The micrometeoroid derived residues were sub-classified in terms of mineral chemistry, with apparent mafic- and phyllo- silicates being the dominant components, with minor iron-nickel metal and iron sulfides, suggesting a broadly chondritic origin. Fe-Ni rich residue was also identified that would appear to belong to a group of non-chondritic particles previously unrecognised. Possible refractory or Ca/Al rich inclusions from a primitive micrometeoroid were also

observed as near intact Ca-rich fragments, the textures of the individual grains suggested that they were not merely terrestrial contamination.

Laboratory impact studies, using a light-gas-gun to accelerate small fragments (125-250μm) of known meteorite mineralogies up to 5km/s, and then impact them into solar cells have generated a suite of residues that are analogues of those observed from LEO studies. The silicate minerals generated residues that were intimately associated with the host melt glass. Metallic sulfides and metals generated surface and sub-surface immiscible droplets. Several craters also contained near-intact fragments of minerals.

Overall, despite the small sample set examined, the observed dominance of micrometeoroid to space debris residue chemistry (correlating to particle size range of 8-80 μm) corresponds well to the accepted flux models.

"The world is full of wonders in earth and air and sea,
A man may study all his life and not much wiser be..."

Extracted from the poem "A Wonder" attributed to **James Sowerby** (undated)

Acknowledgements

I would like to thank my supervisors Ian Wright and Monica Grady for instigating this project, and then allowing me to develop the project the way I wanted. Also for covering my papers, abstracts and of course thesis drafts in red pen with constructive criticism that I know have greatly improved the work in this thesis!

I am extremely grateful to Anton Kearsley, of Oxford Brookes University, who has taught me so much about scanning electron microscopy, shown endless enthusiasm for the research and for always using a blue pen instead of a red one! Gerhard Drolshagen, of ESA, is especially thanked for his advice and for supplying numerous samples for this thesis. Tony McDonnell, of the University of Kent, must also be acknowledged for stimulating discussions on space debris, for allowing me to participate in ESA contract 11887/96/NL/JG and for providing funds for several overseas conferences. I am very grateful to Mike Zolensky, of NASA, who helped the selection, and preparation of IDPs used in this thesis and for answering my seemingly endless e-mails. I also thank John Bradley, of MVA and Frans Rietmeijer, of the University of New Mexico, for useful advice, suggestive comments and constructive criticisms of the work. Terry Williams, John Spratt and Chris Jones, Natural History Museum, and Naomi Williams, The Open University are all acknowledged for their time and patience in my initial training in electron microscopy.

Funding for this project was provided by a PPARC /CASE studentship jointly within the 'Earth History, Materials and Processes theme' of the Natural History Museum and the Planetary Sciences Research Institute (PSRI) at the Open University. The PSRI at the Open University, University of Kent, Unispace Kent, PPARC and the Meteoritical Society are all acknowledge for travel funds and inspiration.

Working in the PSRI, has been an interesting experience. There is not enough space on the page to thank everybody, but the following have been particularly good at entertaining me and providing support over the past four years. Claire and Charles are thanked putting up with me as an "office-mate" over the past years. Lee and Ian are thanked for making several overseas conferences extremely entertaining, and Simon for getting a real ball and chain made for my stag weekend! Finally to Dr Bob for advice with the project, getting me into hockey and for being a mate.

Outside of the PSRI, special thanks must go to Mark for being the bestman at my wedding, providing advice on just about everything, getting me extremely drunk on numerous occasions throughout my time at the O.U., for helping me move house on more than one occasion and for "Annie"! Nick is thanked for providing in-depth discussions on how we can "take-over the world" during lunch and again for helping me move house on more than one occasion. Tubbs is acknowledged for many entertaining stories that alas can not be reprinted here. Sarah (aka Pocket rocket) and other members of the O.U hockey club are thanked for allowing me to let off steam by running around like a mad thing. Matt and Meryl made trips to the Natural History Museum enjoyable. Away from the PhD life, Dan, Annette and now little Elise (not that I am implying that it took rather longer than expected to finish this thesis), Simon, Guy and Steph are all thanked for their friendship, support and interest in my work (not that they had much choice!).

Most of all I would like to thank my wife Beth, for her constant encouragement, support and love over the past five years. Without her dedication and patience (with both the thesis and me) this research would not have been completed. *Thank you!*

Table Of Contents

List Of Figures

Chapter 1

Chapter 2

Chapter 3

Chapter 4

Chapter 5

Chapter 6

Chapter 7

List Of Equations

Chapter 2

List Of Tables

Chapter 2

Chapter 5

Chapter 6

Glossary & Acronyms

AMM Antarctic micrometeorite.

AO(S) Aluminium oxide (spherules), debris generated during the burning of solid rocket motor fuel operations.

(D)BEI *(Digitised) Back-scattered electron image.*

CDC Cosmic dust catalogue, since 1981 NASA has used high altitude aircraft to collect IDPs in the stratosphere. The preliminary information (secondary electron image and energy-dispersive spectra) of each particle examined is published by the *NASA Johnson Space Center Office of Curator* in the form of a catalogue. To date there have been 15 volumes of the catalogue published.

CMX The technical name for the borosilicate glass which is the top protective layer of individual HST solar cells.

EDS Energy dispersive spectrometry, the analysis of characteristic X-rays based on their energies.

EMP Electron microprobe, used for the micro-spot elemental analysis both qualitative and quantitative, of a selected area within a sample by the analysis of characteristic X-rays.

ESA European Space Agency.

ETA Back-scattered electron coefficient.

EuReCa European Retrievable Carrier, a reusable unmanned spacecraft that is fitted with technology, science and applications experiments for exposure to space environment. EuReCa was launched in 1992 and after 326 days of LEO exposure was returned to Earth in 1993.

HST Hubble Space Telescope, a co-operative program between NASA and ESA, is a 2.4m reflecting telescope that acts as a space observatory.

HVI Hypervelocity impact.

IDP Interplanetary dust particle, extra-terrestrial material (less than 100μm in diameter) collected in the stratosphere by NASA.

JSC Johnson Space Center, Houston Texas, USA.

LDEF Long Duration Exposure Facility, a large reusable unmanned spacecraft that contains technology, science and applications experiments for long term exposure to space environment. LDEF was exposed LEO for 69 months (5.75 years) from 1984 to 1990.

LEO Low Earth Orbit, orbit with a mean altitude of less than 2000km.

LGG Light-Gas-Gun, a two-stage gun using highly compressed light gas (hydrogen or helium) to accelerate particles to speeds of up to 7 km/s.

MLI Multi-layer insulation blankets used on satellites and other spacecraft.

MM Micrometeorite, extraterrestrial material (less than 1mm in size) collected from *terra firma* locations (e.g. Antarctic and Greenland Ice sheets).

NASA National Aeronautics and Space Administration (USA).

SEM Scanning electron microscope.

SEI Secondary electron image.

Solar Max Solar Maximum, a satellite launched in 1980, designed to assist in the study of solar flares. After technique problems the satellite was serviced in 1984 and as a result exposed spacecraft surfaces and components were returned to Earth for post-flight analysis.

Space Debris Metre to micrometre sized material that is present in LEO that have been generated by the exploration and utilisation of space.

SRM Solid rocket motor fuel.

(D)XREM (Digitised) X-ray elemental mapping.

WDS Wave-dispersive spectrometry, the analysis of characteristic X-rays according to their wavelength.

Chapter 1

Introduction

1.0 Impacts In Space: Extraterrestrial Or Simply Space Junk?

"*It might have been a disused faring, a fragment from an exploded upper stage rocket. It didn't matter. The fragment slammed into the satellite with the force of a large lorry doing 100 miles an hour, destroying the satellite.*" Astronomy Now, (1996).

The popular press (e.g. Astronomy Now, December 1996 and New Scientist, 11th May 1996) frequently writes about catastrophic collisions in low Earth orbit (LEO)[1] that destroy satellites and predictions of the human race imprisoned on Earth by a deadly permanent cloud of debris, a cloud of SPACE DEBRIS. This cloud of debris has been generated since 1957 when humans first started the exploration of space (the launch of Sputnik) and will continue to increase as planetary exploration increases and greater numbers of communications satellites orbit the Earth (e.g. the Iridium communication satellite network, (Scientific American, 1999)). The size of material which makes up space debris is extremely diverse, it can include large metre-sized spent rocket bodies and satellites to millimetre-sized and micron-sized fragments of paints, ablation products from rocket fuels and human waste (National Research Council, 1995). It is debris from the smallest size-range that is of importance to the work presented in this thesis.

However, Earth's orbits have never been void of material, as there has always been constant passage of extra-terrestrial material in various size ranges. In fact over 40,000 tonnes of extraterrestrial material bombards the Earth each year, of which 95% is as

[1] LEO is a orbit with a mean altitude of less than 2000km

"cosmic dust" or micrometeoroids of less than 1mm in size (e.g. Love and Brownlee, 1993). So the question must be raised to whether micrometeoroids pose a threat to space hardware. Beech and Brown, (1993) identified the probability of micrometeoroids impacting satellites during the 1993 Perseid meteoroid as small but non-negligible. A particle impacting onto a satellite can generate a plasma-burst that may be sufficient to disable the electronics. The small but non-negligible probability seemed to become reality when the Olympus communications satellite failed at the height of the Perseid meteor shower in August 1993 (Caswell et al., 1995). As the satellite was never returned to Earth for a detailed post-flight investigation, it is impossible to state unambiguously whether the failure was or was not due to a collision with micrometeoroids. McBride and Taylor (1996) calculated the risk to satellite tethers from micrometeoroids and debris as significant. The investigation of micrometeoroid damage to space hardware surfaces can only be carried out when the surfaces are returned to Earth (e.g. Warren et al., 1989 and Wright et al., 1995a & b).

The timing of this project coincided with the unique opportunity to investigate materials returned from exposure to LEO. The materials made available were individual solar cells from the Hubble Space Telescope (HST) and multi-layered insulation blankets from the European Retrievable Carrier; both these materials contained impact damage ranging from microns to millimetres in diameter. There was therefore the possibility to search for the remnants of micrometeoroids and space debris impactors within hypervelocity impact features preserved on the samples. Such investigations have in the past been problematic (e.g. Carey, 1998), due to limitations in the analytical techniques used to search for impactor remnants. With respect to these problems, scanning electron microscopy has been employed using back-scattered electron imaging and X-ray elemental mapping (Chapter 2) to develop a highly successful protocol for the rapid location and identification of residue material (Chapter 3) in HST solar cells. The generation of laboratory simulated

hypervelocity residues of known mineral projectiles using a light-gas-gun facility (Chapter 4) has assisted in the interpretation of micrometeoroid derived residues. Within Chapter 5 the results of the survey of the HST solar cells are presented and discussed with a view to classification in terms of space debris and micrometeoroid origin. It was hoped that the natural impactors might be sub-classified in terms directly comparable to the many samples obtained from terrestrial collections of cosmic dust (discussed in Chapter 1). Within Chapter 6, the result of the analyses of one particular residue are presented, with the possible consideration that it may represent a class of micrometeoroid which has only been subjected to limited laboratory investigations in the past.

If all the previous objectives can be carried out, then it was postulated that the results would enable the relative assessment of the significance of micrometeoroids and space debris particles (in the 10-100μm diameter size range) within LEO. It will hopefully prove that such investigations can provide substantial information and are a worthy addition to the terrestrial collection of material.

1.1 Origins Of Particles Collected In Space And On Earth

1.1.1 Micrometeoroids

The first identification of dust in the interplanetary medium of the Solar System was by Cassini in the 18th century, with the observation of "zodiacal light" or gengenschein (Sandford, 1987) (the illumination by the sun of dust orbits between it and the Earth). The investigations of microcraters produced in mineral grains in lunar rocks (e.g. Morrison and Zinner, 1976) proved that this was not a passing feature, but has been stable for a considerable period. Particle lifetime in the solar system is essentially short, e.g. 10^4 to 10^5 years (Dohnanyi, 1978; McDonnell, 1988) before effects such as Poynting-Robertson drag,

sublimation, sputtering, collisions and radiation remove particles from the Solar System and they are recycled into the interstellar medium (Dohnanyi, 1978; Brownlee, 1994). Therefore, Solar System sources of this dust material must be from recent past activity and not as long-lived particles dating from the formation of the Solar System. The two widely accepted sources of origin for micrometeoroids are either cometary or asteroidal (e.g Brownlee, 1994). The analysis of the zodiacal cloud by the Infrared Astronomical satellite (IRAS) have identified that cloud is a mixture of cometary (e.g. Liou et al., 1995) and asteroidal (Levasseur-Regourd et al., 1991) dust. Liou et al. (1995), postulated that the contribution of the two was as follows: asteroidal dust contributed approximately 1/4 to 1/3 of the total and cometary dust contributed 3/4 to 2/3 to the total composition. However, the relative proportion of cometary and asteroidal dust accreted by the Earth is a matter of great debate.

Flynn (1990) proposed that the Earth's gravitational focusing favours the collection of particles with low geocentric velocities, therefore as asteroidal particles have lower geocentric velocities than cometary particles they should dominated the collections (section 1.3) of terrestrial dust. Yet, it has been proved that if cometary particles are trapped in a mean-motion resonance with planets, e.g. Jupiter, their eccentricity and inclination can be reduced resulting in encounters with Earth at near asteroidal velocities (Liou and Zook, 1996, 1997). It is also suggested that atmospheric entry (section 1.4.1) can affect the survivability of particles and therefore affect the contribution of material observed in the terrestrial collections of material. It has therefore been postulated that cometary particles are contributing a major element to the dust sample in terrestrial collection (Liou et al., 1996).

It is also possible that minor contributions to the source of material may come from an, as yet, unquantified component from the interstellar medium. Interstellar grains have been

identified entering the Earth's atmosphere by using radar remote sensing techniques (Taylor et al., 1996). Impacts due to interstellar dust were identified by the plasma detectors from the Galileo and Ulysses spacecraft (Grün et al., 1993). As yet the identification of dust particles as interstellar material from the various collections of extraterrestrial material (see section 1.3 for a discussion on the collection techniques) has proved extremely complex. This has been due to several factors, firstly the identification of interstellar material can not simply be based on the physical or chemical properties of suspect particles, but instead must depend upon isotopic investigations (Walker, 1994). As the analysis has to be in-situ, they are normally carried out using an ion-probe (see McKeegan et al., 1985 for a discussion on the technique).

The current limitations in ion-probe techniques requires particle sizes of at least 1μm (Walker 1994). Here-in lies the problem: locating such material in particles where the maximum size of the whole particle maybe only 1-10μm and an interstellar component present on a nanometer scale presents an extremely difficult task. Bradley and Brownlee (1983) located nanometer-sized SiC in dust particles, but concluded that these could have been contaminants and isotopic measurements by ion-probe were not possible. Walker (1995) calculated if 10^3 micrometeorites were analysed using X-ray elemental mapping, the investigation might possibly yield one or two particles suitable for analysis with the ion-probe. Graham et al. (1996a & b) carried out static-line carbon stable isotopic measurements on five specially selected particles, the carbon isotopic measurements of one particle indicated the possible presence of SiC. Detailed electron microscopy and ion-probe measurements of fragments of the same particles did not identify any SiC (Engrand and Maurette, 1997).

Recent attempts at searching for interstellar phases in IDPs have used Fourier Transform Infrared (FTIR) spectrophotometry in laboratory measurements (Bradley et al., 1998) and

infrared spectroscopy from ESA's Infrared Space Observatory (ISO) for space measurements (Bradley et al., 1998), this research is continuing but at present has not identified any SiC. The search for interstellar phases in cosmic dust particles will hopefully be resolved by the development of better analytical instruments such as the Nano-SIMS (Messenger, 1998) that will enable the in-situ mapping for material at a suitable scale within terrestrial collections of IDPs and micrometeorites.

1.1.2 Flux Models: Micrometeoroids

The Earth is constantly being bombard with extra-terrestrial material within the mass range of 10^{-12}g to over 10^{10}g (Yates, 1992). It is possible to calculate the annual amount of material that is accreted by the Earth each year using a number of different methods. Hughes (1978) used radar, visual and satellite techniques to monitor the frequency of meteors. Hörz et al. (1975), determined flux estimates from lunar microcrater counts. In 1985, Grün et al. derived the Grün flux model based on meteoroid flux versus meteoroid mass. The model used data from lunar flux measurements, space craft measurements and radar measurements to calculate the flux and produced an estimate of 30-40x10^6kg per year (Grün et al., 1985). Love and Brownlee (1993) used data obtained from the Long Duration Exposure Facility satellite to obtain a flux estimate of 40±20x10^6kg per year. It is interesting to note that the estimated yield of micrometeoroids is consistent using the different methods (Bland et al., 1996). Olsson-Steele (1988) calculated that 85% of the material accreted annually by Earth is within the size range of micrometeoroids.

1.1.3 Space Debris

The origins of space debris are directly linked to human utilisation of space, as space debris is essentially the pollution of our space endeavour (figure 1.1). Since 1957 when Sputnik was launched, over 4,500 other spacecraft have been launched, of which over

2,200 remain in orbit (National Research Council, 1995). The amount of debris that these launches have put in LEO is significant: for large debris (over 10cm in diameter) it is calculated there are over 10,000 objects in orbit, for medium debris (1mm to 10cm in diameter) possibly over 10 million objects and for small debris (less than 1mm in diameter) the number is predicted to be in the trillons (National Research Council, 1995). For this thesis the size range of debris that is of interest is the small diameter.

This type of debris can be defined as mission-related debris, as they are the result of the deployment, activation and use of space hardware. The more significant mission-related debris is aluminium oxide particles that are formed and released during the burning of rocket fuels during launch and subsequent flight of a rocket. Aluminium oxide particles have been identified in the stratospheric collections of cosmic dust particles (Zolensky and Mackinnon, 1984) (section 1.2.4 and section 1.3.4). Mission-related debris also includes human waste, e.g. a fragment of crystalline urine was collected near-intact by using an aerogel collector fitted to the Mir space station (Hörz et al., 1998). The other source of small-sized debris is defined as fragmentation debris, which is the largest contributor to the total population of catalogued space debris. It is typically made up of fragments and particles generated by the break-up or deterioration of space hardware, e.g. solar cell debris released during an impact event, paint fragments, and thermal blanket debris (National Research Council, 1995). The classification schemes used to identify impact-derived residues have been developed by NASA (Zolensky et al., 1993) and are based on simple elemental signatures which are discussed in-depth in Chapter 3.

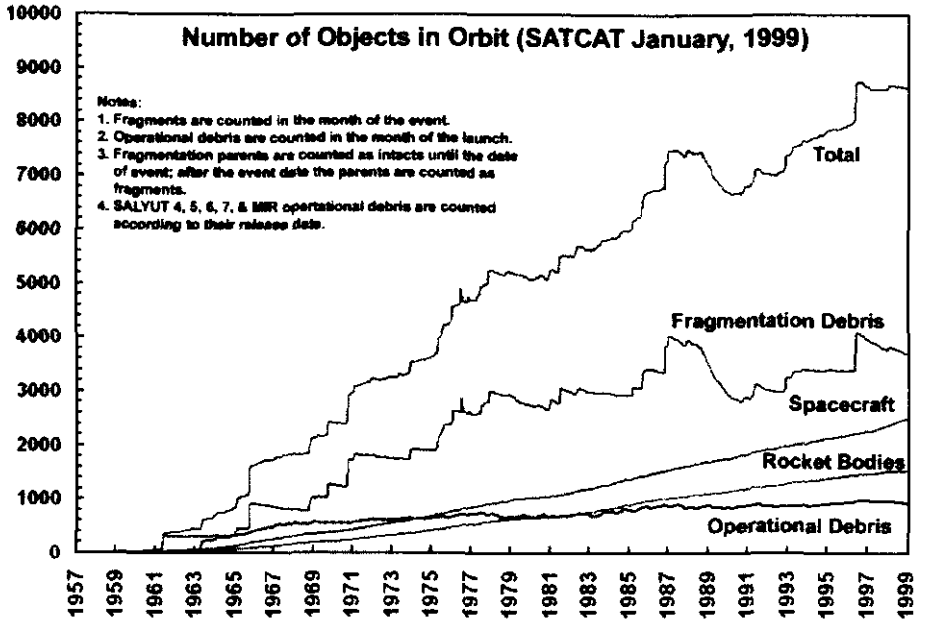

Figure 1.1 shows the increase in catalogued orbital debris from 1960 – 1999. The increase in debris can be compared to the increase in the utilisation of LEO (image courtesy of NASA).

1.1.4 Flux Models: Space Debris

Flux models are required for space debris because they can be used to predict the number of particles that may impact onto a piece of space hardware during its life-time in orbit. The models define the impact flux as a function of particle/debris size and velocity for various space hardware orbital altitudes and inclinations. An example of this is NASA's Engineering Orbital Debris Model (EODM) (Kessler et al., 1991). The model has been updated using data from the Long Duration Exposure Facility (LDEF) (see section 1.3.5 for a description of LDEF) and other sources (Kessler et al., 1996). An in-depth discussion of space debris modelling is given in Orbital Debris – A technical assessment (National Research Council, 1995).

1.2 Compositions Of Cosmic Dust And Space Debris

Cosmic dust material has been extensively investigated (e.g Brownlee et al., 1979; Bradley, 1988 and Maurette et al., 1993), therefore a vast amount of data has been obtained

on its composition in terms of chemistry and mineralogy. Only a general overview of the different types of cosmic dust material are given here, since the work presented in this thesis focuses on identification of micrometeoroid remnants in hypervelocity impact-damaged solar cells that have been highly altered by the impact process (section 1.4.1). Therefore comparisons between the intact chemistries and mineralogies of micrometeorites, interplanetary dust particles and deep sea spherules can only be made at the most simplistic level. The amount of data obtained on space debris within the size of less than 1mm diameter is in complete contrast to that for cosmic dust.

1.2.1 Deep Sea Spherules

The composition of deep-sea spherules can be broadly separated into two groups; i) iron spherules and ii) stony spherules. The iron spherules are composed of either small iron-nickel rich or smaller platinum group element nuggets cores surrounded by iron-oxides (magnetite) (e.g. Brownlee et al., 1984). Unfortunately in most of the iron spherules, the nickel rich core is often weathered away or oxidised therefore leaving particles that are entirely composed of magnetite (e.g. Parkin et al., 1977). The stony spherules are again composed of magnetite but there is an additional olivine component within the spherules and again if not weathered or altered, trace phase of metallic nickel-iron (Heide and Wlotzka 1995). Rare spherules can be composed of the metallic material again surrounded by the magnetite rims, but they can also include small quantities of glass. Unlike the stony spherules, they do not contain crystalline silicate material (e.g. Finkleman, 1972).

1.2.2. Micrometeorites

The size of micrometeorites (MMs) recovered from the Polar Ice Sheets can be from 1μm – 1000μm in diameter. There have been numerous classification schemes (e.g. Taylor and Brownlee, 1991; Kurat et al., 1993; 1994) but this study will adopt that developed by Genge (1996) based on the previous systems. MMs can be broadly separated into two groups; i) coarse grained and ii) fine-grained. The fine-grained material can be sub-classified into; i) melted cosmic spherules and scoriaceous micrometeorites (Kurat et al., 1993); ii) unmelted core micrometeorites, vesicular unmelted micrometeorites and unmelted micrometeorites (Genge, 1996). The cosmic spherules show evidence that they have undergone extreme melting during atmospheric entry, therefore often only relatively refractory relict mineral phases remain e.g. forsteritic (olivine) and or enstatitic (pyroxene) (Klöck and Stadermann, 1994). The scoriaceous MMs differ from cosmic spherules in terms of shape but again the main mineral composition is olivine and pyroxene (Michel-Levy and Bourot-Denise, 1992). Although unmelted micrometeorite particles do show some evidence of melting during atmospheric entry i.e. magnetite rim formation, this rim tends to be discontinuous and the bulk chemistry of the particle would appear to be relatively unaltered.

The mineralogy of these particles consists mainly of hydrous phyllosilicate minerals. These phyllosilicates have normally been thermally metamorphosed and are highly altered during atmospheric encounters. The original chemistry is sometimes preserved and it is therefore possible to identify the pre-entry mineralogy of the particle that is similar to serpentine or smectite in composition (Kurat et al., 1994). The composition of these unmelted MMs can also consist of anhydrous coarse-grained mafic silicates (olivine/pyroxene) (Kurat et al., 1994). The particles may also be a mixture of the two types where the particles consist of

coarse-grained mafic silicates with fine-grained phyllosilicate matrix materials (Klöck and Stadermann, 1994). The unmelted micrometeorites are similar in composition to that of larger carbonaceous chondrite meteorites (Kurat et al., 1994).

So the question must be raised whether these unmelted MMs might contain interstellar material, such as SiC, graphite and diamonds which have been identified in carbonaceous chondrite meteorites (e.g. Murchison) (e.g. Zinner et al., 1989; 1990; Amari et al., 1990 and Russell, 1993). No interstellar material has been identified, although this is partly because the size of such grains would be extremely small (less than 1μm) and the concentration expected to be present within the particles would be very low (Walker, 1994). Therefore they would be difficult to locate in-situ using current iron-probe and SEM X-ray microanalysis techniques (Walker, 1994). The development of new nano-secondary ion mass spectrometry (Stadermann et al., 1999) may resolve this problem if favourable MMs are identified (Messenger, 1998).

1.2.3 Interplanetary Dust Particles (IDPs)

IDPs have been investigated extensively since NASA started collecting them from the stratosphere (see section 1.3.4) in 1981 (e.g. Mackinnon et al., 1982. Bradley, 1988; Schramm et al., 1989). The IDPs can be broadly classified into two groups based on the major mineral components: i) anhydrous mafic silicates and ii) hydrous phyllosilicates (Klöck and Stadermann, 1994). The anhydrous mafic silicates are dominated by either olivines or pyroxenes (Thomas et al., 1993). There is a sub-division of anhydrous IDPs where the particles are dominated by fine-grained microcrystalline aggregates (Klöck and Stadermann, 1994). The aggregates are composed of 5-50nm grains of Mg-Fe silicates, Fe-Ni sulfides and Fe-Ni metal embedded in a fine-grained carbonaceous matrix (Klöck and Stadermann, 1994). The hydrous IDPs are dominated by phyllosilicate mineralogies

(smectites such as saponite and serpentine) although minor anhydrous mineral phases, e.g. Fe-Ni sulfides, Mg-Fe silicates, Mg-Fe carbonates and magnetite may also be identified particularly in smectite IDPs (Klöck and Stadermann, 1994).

Refractory mineral phases, e.g. hibonite, perovskite, spinel and melitite have been identified within matrix material of IDPs (Zolensky, 1987 and McKeegan, 1987). The significance of identifying these refractory phases, it indicates that IDPs may be directly linked to primitive carbonaceous chondrites and their asteroidal origin (Klöck and Stadermann, 1994). Ultra-fine grained chondritic IDPs have been found to consist of smaller sub-grain aggregates (0.05μm-0.5μm) of "glassy" silicate material with embedded Fe-Ni metal and Fe-Ni sulfides (termed as GEMS) (e.g. Bradley, 1988; Bradley, 1994 and Martin, 1995). The implications are that these GEMS particles are relatively unaltered interstellar material, although much further work is required to substantiate such a theory (Martin, 1995).

1.2.4 Space Debris

The composition of space debris particles is directly related to the material that has been placed in space, for example steel alloys, aluminium alloys, solid rocket motor fuel debris and leaked coolant (liquid Na and K) from nuclear reactors powering satellites (e.g. Zolensky et al., 1993). The chemistry of space debris-derived residues as a result of hypervelocity collisions is discussed in-depth in Chapter 5. Apart from LEO collections of material (1.3.5), particles identified as space debris have been identified in the stratospheric collections of IDPs.

The particles are not terrestrial contaminants such as volcanic ash particles which have also been identified in the cosmic dust catalogue (CDC) as they have a distinct elemental

composition of Al_2O_3 - aluminium oxide (termed AO in the CDC). These AO particles have a distinctive spherule shape morphology (therefore termed AOS) and analysis by Zolensky and Mackinnon (1984) revealed that these particles are in fact fragments of orbital or space debris. Significant quantities of aluminium and propellant used in solid rocket motor (SRM) fuel and during the burning of the fuel, ablation products including Al_2O_3, i.e. AOS (Zolensky et al., 1989) are released. The study by Zolensky et al (1989) noted that there was a tenfold increase in the number of AOS identified in the stratospheric collection from 1976-1984 which would indicate the increased problem of space debris .

1.3 Sampling Of Cosmic Dust & Space Debris

1.3.1 Atmospheric Collection

Due to the residence time in the atmosphere of cosmic dust particles (1 to 60 days at altitudes above 20km) (Kasten, 1968), it would seem to provide an excellent environment in which to sample particles. The first attempts at sampling in the atmosphere involved the use of balloons which were fitted with capture cells (Fireman and Kistner, 1961). As the balloons were only able to sample at limited altitudes (up to 37km although usually only few km) the sampling yielded far more terrestrial than extra-terrestrial dust particles. Futher attempts at sampling (ca. 10-20km altitudes) used recoverable sounding rockets (e.g. Hemenway and Soberman, 1962 and Farlow et al., 1970). They were fitted with relatively small collection surfaces and were only sampling at these altitudes for approximately 1 minute. As a result of the small sampling time the yield of extra terrestrial particles was again extremely low. Apart from low collection yields these particles were contaminated by sulfate aerosols (Bigg et al., 1970) The sampling of particles at high altitudes has improved somewhat over the years and present day methods are discussed in section 1.3.4.

1.3.2 Ocean Floors

The first recorded success at the collection of extraterrestrial material from the ocean can be dated back to the voyages of HMS Challenger in the late 1880s. Black magnetic spherules separated from deep ocean sediments during the expeditions were subsequently identified as cosmic dust particles (Murray and Renard, 1884, 1891). Deep-sea spherules were collected in the 1950s by raking the sea-floor (Brunn et al., 1955) and the improvements to analytical technologies (e.g. electron probes) allowed more detailed investigations of individual spherules (e.g. Castaing and Fredriksson, 1958). The studies of the spherules continued in the 1970s (e.g. Finkelman, 1970; 1972) where magnetic raking of the ocean floor was again the method of collection (e..g Brownlee et al., 1979 and Brownlee, 1985).

The origin of these cosmic spherules was subject to much debate, although it was generally assumed that they were simply ablation droplets from meteorites (e.g. Öpik, 1956), extensive work by Parkin et al. (e.g. 1977, 1980 and 1983) postulated a different origin for the particles. They suggested that the particles were debris formed by collisions in the asteroid belt and subsequently spiralled to Earth under Poynting-Robertson drag (Parkin et al., 1980). Blanchard and Davis (1978), to allow a better understanding on the possible alteration effects that occur during the atmospheric transit of extra terrestrial material carried out artificial ablation studies on iron and iron-nickel samples. The studies produced morphological features that were similar to iron meteorite fusion crusts and cosmic spherules extracted from deep-sea sediments. Also Blanchard et al. (1980) analysed spherules which had not been extensively weathered and found that the mineral chemistry was similar to CI chondrites.

Further comparisons between the spherules' mineral chemistry (Mg-rich olivines) and meteorites found a link to C2 chondrites (Steele et al., 1985). The identification of extra

terrestrial platinum-group metals in the spherules by Brownlee et al. (1984) essentially resolved the debate, as these are metallic remnants of the oxidation of the spherules which are ablation products of meteoritic material (McDonnell, 1988). It is widely now accepted that the majority of these spherules are the end result of atmospheric heating processes acting on what were originally small fragments of meteoritic material (Heide and Wlotzka, 1995). Although deep-sea spherules have been well studied, the interpretation of the findings have often been limited by the rather extensive melting the spherules have undergone (e.g. Brownlee, 1985) and terrestial weathering (e.g. Wright et al., 1988). The terrestrial weathering is from the sea-water which etches the spherules, which causes the dissolution of olivine crystals and effects of bulk element chemistry content of the spherules (Brownlee, 1981). Therefore a better collection environment was sought.

1.3.3 Polar Locations

The search for the ideal environment for sampling micrometeorites (MMs) switched from the oceans to Greenland and Antartic Ice Sheets (Maurette et al., 1986). The Ice Sheets are convenient repositories of micrometeorites (MMs) as the ice is clear and clean, and particles can be extracted from it. The ice also preserves the particles as it limits the degree of chemical alteration the MMs suffer from weathering (Maurette et al., 1994).

However, the actual concentration of extra terrestrial material located in the ice is often low, 2-5 micrometeorites in the 100-250μm size range per ton of ice assuming the micrometeorite flux measured at ca. 1 AU in the interplanetary medium (Grün et al., 1985) is the same as that on the Earth's surface and with an accumulation rate approximately 50cm/y. As a result, large quantities of ice/lake basement sediment have to be melted/extracted to recover a sufficient number of MMs.

One of the first ice field locations to be used to recover MMs was lake deposits in the melt zone of Sondre Stromfjord on the Greenland ice sheet (Maurette et al., 1986). The seasonal lakes form during the Artic summers and are fed by the melting ice and it was observed that the basement of these lakes a contained sediment (termed as cryoconite). It was suggested that the cryoconite which is derived from filamentary siderobacteria and mineral sand would also contain a yield of MMs that have accumulated over time (Maurette et al., 1994). The extraction techniques used to remove MMs from cryoconite will not be discussed herein but can be found in Maurette et al., (1994).

The problem of MM recovery from was highlighted during one expedition – only approximately 1000 MMs were found per kg of wet cryoconite (200kg of cryoconite were collected) (Maurette et al., 1994). The MMs recovered were both melted (800 in total) and unmelted (200 in total) in nature and generally greater than 100μm in diameter, although some smaller MMs (50-100μm) were also collected (Maurette et al., 1994). The MMs collected from the cryoconite deposits are generally not used by researchers because they are subjected to chemical attack or alteration from the siderobacteria that effect the origin chemistry (Maurette et al., 1994). However several studies have compared their mineralogy and chemistry with MMs collected from other locations (e.g. Robin et al., 1990 and Beckerling and Bischoff, 1995). Furthermore the chemical techniques, e.g acid dissolution, used for the removal of the cryoconite from the particles may destroy mineral components within the MMs (Yates, 1992).

As well as the particles collected from Greenland, MMs have also been successfully recovered from Antarctic Blue Ice Sheets (e.g. Maurette et al., 1993; 1994). In the 1991 EUROMET expedition, 100 tonnes of ice was melted to recover approximately 20,000 MMs in the 50-400μm size range (e.g. Maurette et al., 1991). Antarctic Micrometeorites have a distinct advantage over the Greenland Ice Sheets, as they are cryoconite-free

(Maurette et al., 1994) which means that the problem of weathering and chemical alteration is reduced (Maurette et al., 1994), but MMs are still affected by atmospheric entry effects (e.g. Flynn, 1989a & b and see section 1.4).

MMs from polar ices have been extensively studied terms of mineral, chemical and isotopic compositions in the 1990s (e.g. Michel-Levy and Bourot-Denise, 1992; Kurat et al., 1993; Wright et al., 1997; Genge et al., 1997 and Engrand and Maurette, 1998). Recently (Taylor et al., 1996) located a new source of MMs from the bottom of the water well at the U.S. South Pole Station.

1.3.4 The Stratosphere

When dust particles enter the Earth's atmosphere they initially encounter at velocities greater than 11km/s. At 80-100km altitude they decelerate slowly and may only be exposed to a maximum temperature of 800°C for a few seconds (Yano et al., 1994). This slow-down in velocity results in a 10^6-fold increase in particles in the stratosphere compared to the flux in near-Earth space (e.g. Rietjmeijer, 1999). The early attempts to collect cosmic dust particles from the stratosphere have already been discussed in section 1.3.1. The first real success at collecting particles in the stratosphere was in 1973 at 35km altitude (Brownlee et al., 1973), where particles of chondritic composition were identified amongst the majority of aluminium oxide particles collected (Brownlee and Hodge, 1973). It is interesting to note that aluminium oxide particles were originally unclassified in terms of origin, as they appeared not extra terrestrial yet they were not of a composition that would have indicated a terrestrial origin. The most probable source of origin was later identified as aerospace materials, i.e. they are space debris particles (Brownlee et al., 1976; Zolensky and Mackinnon, 1984 and Zolensky et al., 1989).

The sampling of cosmic dust particles in the stratosphere in 1970s developed due to better collector cells, the availability of high altitude aircraft and improvements in analytical instrumentation allowing more detailed analysis of the sampled particles (e.g. Brownlee et al., 1977). However researchers who have investigated cosmic dust particles collected from the stratosphere would suggest that much of the development was due to the pioneering research of D.E. Brownlee, to the extent that the particles are often referred to as "Brownlee particles".

Since 1981 NASA has used U-2, ER-2 and WB-57 aircraft to collect interplanetary dust particles (IDPs) (Mackinnon et al., 1982). There are two of sizes of collectors that can be fitted to the aircraft: 1) $30cm^2$ surface area (figure 1.2) and 2) $300cm^2$ surface area. The collectors (composed of "Lexan" a polycarbonate plastic) are coated with silicone oil (dimethyl siloxane) and sealed within airtight containers which are only open to expose the collector surface to the stratosphere or for the collector plate to be removed in the clean-lab at the Johnson Space Centre (NASA).

Stratospheric sampling occurs when the aircraft is at a high altitude (ca. 20km). After the sampling has been carried out the collectors are sealed until the Cosmic Dust Preliminary Examination Team (CDPET) can investigate them at the Johnson Space Centre (NASA) (Zolensky et al., 1994). The information obtained by CDPET is then presented in the Cosmic Dust Catalogues (e.g. CDPET, 1997). IDPs have been subject of numerous studies that have detailed the mineral and chemical composition (e.g. Bradley, 1988 and Schramm et al., 1989), the isotopic composition (e.g. McKeegan, 1986; Carr et al., 1986 and Nier and Schlutter, 1990), the effects of atmospheric entry (e.g. Flynn, 1989a&b; Love and Brownlee, 1991 and Nier and Schlutter, 1993) and the potential origins of the particles (e.g. Bradley and Brownlee, 1991)

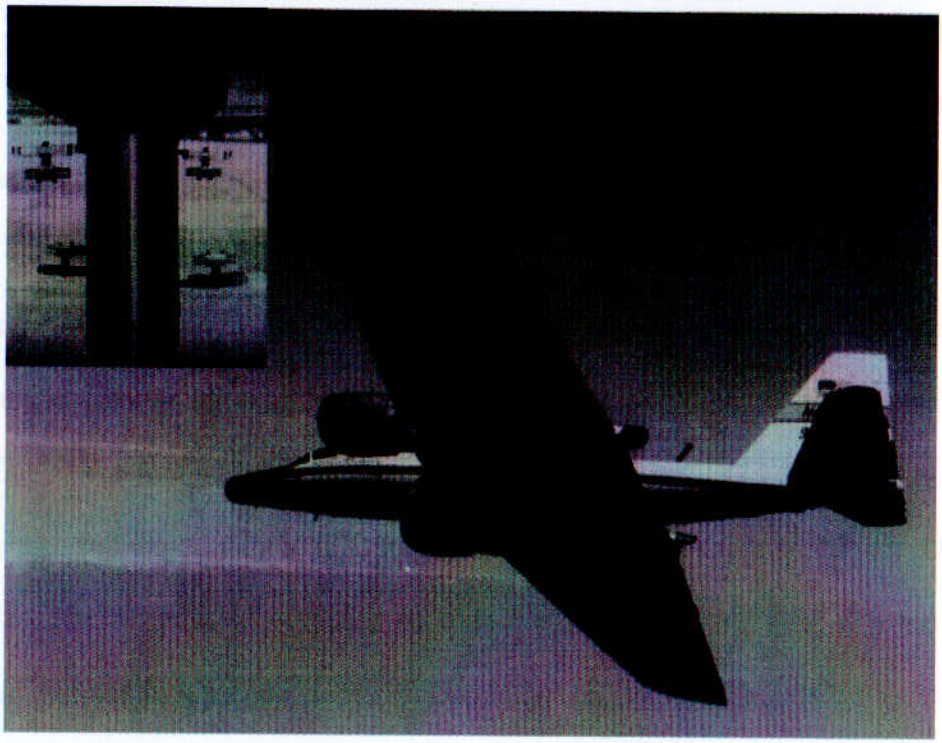

Figure 1.2 NASA's WB-57F stratospheric aircraft (NASA photograph S81-31582), the cosmic dust collectors are fitted on special mounts underneath the wings. The insert (NASA photograph S82-36796) shows four small collector plates (each with approximately 30cm^2 surface area) fitted underneath the wings of the aircraft.

1.3.5 Space

The concept of making direct measurements of cosmic dust in space is not new, spacecraft probes have analysed material using sensitive detectors, e.g. the dust impact detection system on the Giotto Spacecraft which encountered Comet Halley (Zarnecki, 1988). Whilst such probes can yield information on flux and mass distribution of particles, no laboratory investigations can be carried out since the hardware does not return to Earth. The NASA "Stardust" mission (e.g. Brownlee et al., 1997) was launched in February 1999 and will encounter Comet Wild 2 in 2004, where it will capture dust particles coming from the Comet in aerogel collectors. Apart from cometary particles, the craft may also collect possible interstellar material. Once the craft has finished sampling materials, it will retract the collectors and head back to Earth, arriving in 2006 (Scientific American, 1999). Once

returned to Earth, the collected samples will be analysed. Although "Stardust" is part of NASA's discovery class of mission (i.e. "*better, cheaper, faster*"), it is still costing $200 million and is a one-flight mission.

The capture of material in low Earth Orbit (LEO) enables particles to be investigated before they encounter terrestrial atmospheric entry effects, such as heating (see section 1.4.1). One of the first attempts to capture particles intact in LEO was carried out using a microabrasion foil experiment (MFE) which was flown on the space shuttle (McDonnell et al., 1984). The MFE was composed of a double layer foil structure; i) a top layer of aluminium foil and ii) a kapton sheet (McDonnell et al., 1984). The MFE was exposed to the LEO environment for eight days. The foil contained several impact features that had been generated by hypervelocity collision with particles in LEO (McDonnell et al., 1984). The experiment was important as it identified that capture cell technologies worked and were a possible low cost method of particle collection in LEO (McDonnell et al., 1984).

Apart from dedicated experiments such as the MFE, it is also possible to sample the LEO environment using non-dedicated surfaces, e.g. micrometeoroid impact investigation were conducted on Apollo spacecraft surfaces (Cour-Palais, 1974) and surfaces from the Skylab IV mission (Brownlee et al., 1974). Any pieces of space hardware in LEO are prone to hypervelocity collisions with particles present in that environment. These particles can impact at speeds up to 68 km/s (Hörz, 1986), and as a consequence intact fragments of the original impactor are rarely observed on the hard surfaces. Instead, complex and mixed residues of the original impactor and the host substrate (e.g. solar cells) are the common products of the impact, with deformation to the host substrate (e.g. impact craters or holes). Whilst the analysis of such material might seem impossible in terms of yielding any relevant information with regards to the chemistry of the origin impactor, examples where

spacecraft surfaces have been returned to Earth and subjected to post-flight investigations has proved that information about the impactor can be retrieved.

The Solar Maximum satellite was launched in 1980 and after 4.15 years in space was captured by the space shuttle in 1984 so that repair work could be carried out. As apart of the repair mission the thermal blankets and the aluminium thermal control covers were replaced after a total of 1517 days of space-exposure, and returned to Earth (Warren et al., 1989). These two surfaces were investigated in detail as apart of a post-flight investigation which included space debris and micrometeoroid impact studies. Both surfaces contained a number of impact-derived craters and holes with extraneous debris associated with them (Warren et al., 1989).

This debris has been identified as derived from both micrometeoroid and space debris. In terms of micrometeoroid-derived material, iron-nickel sulphides (Schramm et al., 1986), a near intact olivine grain (Rietmeijer and Blandford, 1988) and a hydrate silicate grain (Bradley et al., 1986) were identified. In terms of space debris-derived material, paint fragments were identified on a number of impacts (Bernhard and McKay, 1988). The post-flight analysis of the Solar Max surfaces showed that non-dedicated collectors could yield information on the chemistry of particle populations in LEO. It also indicated that certain spacecraft surfaces can act as very good particle collectors as intact material was retrieved that had not been destroyed by the hypervelocity impact process (Warren et al., 1989).

The Earth often has encounters with meteor streams, e.g. the Perseid Storm (Caswell et al., 1995). Such storms offer the potential to collect cometary material, as the streams are related to comets. In 1985 during Earth's encounter with the Draconid meteor stream (related to comet Giacobini-Zinner), a dedicated collector was placed in LEO (Borg et al., 1993). The experiment was called COMET-1 and comprised high purity metallic

collectors (gold and nickel). The collectors retained not only debris from the stream but also cosmic dust particles from other origins (most likely asteroidal) and space debris. The impactor remnants were identified as residue grains that showed evidence of hypervelocity collision yet it was still possible to carry out detailed elemental analysis of these grains (Borg et al., 1993).

The residue grains which were suspected to be derived from particles in the stream were enriched in carbon and oxygen when compared to other meteoroid derived material and known chemistries from IDPs (Borg et al., 1993). The COMET-1 experiment identified the possibility that impact residues that are micrometeoroid-derived could be classified in terms of origin, i.e. cometary versus asteroidal, from residue chemistry (Borg et al., 1993). It also showed that particles involved in hypervelocity collision can retain volatile elemental chemistries, i.e. carbon and oxygen (see section 1.4.2).

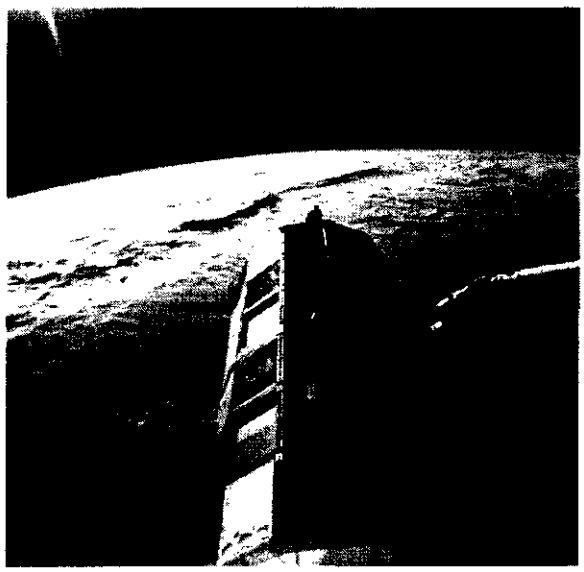

Figure 1.3 NASA's Long Duration Exposure Facility (LDEF) which was exposed to low-Earth orbit for 5.7 years until it was recovered by the space shuttle Columbia in 1990 (NASA photograph S32-8539).

Whilst Solar Max and the COMET-1 experiments provided evidence that extra terrestrial material and space debris could be collected in LEO, perhaps the best known example of LEO collection was NASA's Long Duration Exposure Facility (LDEF) (figure 1.3)

(Zolensky et al., 1994). The MFE, COMET-1 experiments and the surfaces from Solar Max had provided the information to produce collector surfaces that would be able to retain the most information about the original impactor (Zolensky et al., 1994). All of LDEF surfaces were fitted with experiments designed to investigate LEO, including collectors to sample and capture both cosmic dust and space debris (O'Neal and Lightner, 1991).

LDEF was launched in 1984 and was an 11 ton satellite containing 57 experiments to assess the effects of the LEO space environment in terms of ionizing radiation, exposure to atomic oxygen effects on material (those which were and those which might be used on spacecraft) and micrometeoroids and space debris. LDEF and its experiments were exposed to LEO at an average altitude of 458km (Zolensky et al., 1994). LDEF, unlike Solar Max, was gravity gradient stabilised thus its orientation with respect to Earth was fixed (Taylor, 1997). The faces of the LDEF were in the following directions: the east face was the ram direction (leading edge) and therefore a good meteoroid and debris collector (Taylor, 1997). The west face (trailing edge) was in the wake of the ram (Taylor, 1997). The space-facing end was obviously the best natural meteoroid collector surface as there would have been a degree of shielding from space debris, in that it would not be exposed to space debris in circular orbits (Taylor, 1997). It was important to be able to assign likely origins of impactors on the space-facing, leading and trailing edges as it would assist in the identification of residues in terms of micrometeoroid versus space debris.

LDEF was exposed to the LEO environment for 69 months (57 months longer than expected; as retrieval was delayed due to the Challenger shuttle disaster). This gave an opportunity to study the LEO environment for the longest period ever recorded. After the retrieval from LEO, LDEF was party to a very detailed post-flight investigation (e.g. Zolensky et al., 1993; McDonnell et al., 1992 and Yano et al., 1993). The detailed results

from the specific micrometeoroid/space debris analysis (e.g. Bernhard et al., 1993a) will be discussed in Chapter 5 as direct comparisons are made between the residue chemistries observed in LDEF and those observed in solar cells from the Hubble Space Telescope.

In terms of allowing a detailed investigation of LEO, LDEF provided much information but the LEO environment is constantly changing and the increased utilisation means that more space debris is being produced - this is highlighted in (figure 1.1). To truly understand the environment it must be constantly sampled, but missions such as LDEF are not frequently set up, therefore one must rely on other post-flight opportunities that occur.

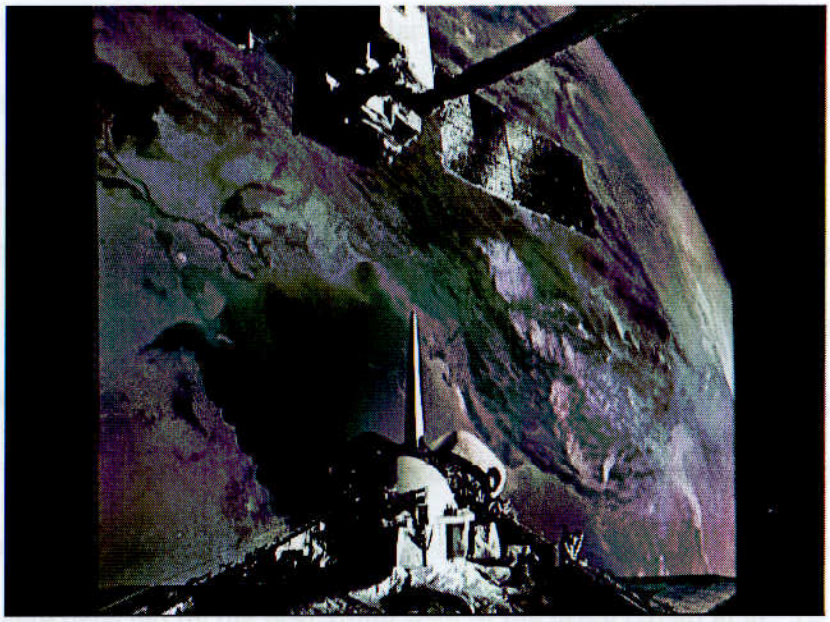

Figure 1.4 ESA's European Retrieval Carrier (EuReCa) which was exposed to low-Earth orbit for 326 days until it was recovered by the space shuttle Endeavour (image courtesy of NASA).

In the early half of the 1990s, two European-based post-flight investigations occurred. The first of these came in the form of ESA's European Retrieval Carrier (EuReCa) (figure 1.4), which was in some respects similar to LDEF as it was a re-useable platform specifically designed to investigate LEO (e.g. Aceti et al., 1994). On the maiden, and so far only flight, the craft contained a dedicated micrometeoroid and debris collector, the Time Band Capture Cell (TICCE) (McDonnell et al., 1995). Yet the main focus of the post-flight

investigation was on the other surface material that cover the spacecraft, such as the Multi-Layer thermal Insulation blankets (MLI) and the individual solar cells from the array panels.

Prior to its return to Earth, EuReCa was in LEO from August 1992 to June 1993 at an altitude of 502-426km (McDonnell et al., 1995). In LEO, EuReCa, unlike LDEF, was in a fixed sun-pointing orientation rather than Earth pointing (Taylor, 1997). This difference in fixed pointing direction implies that it would experience different types of micrometeoroid and debris impact signatures (Aceti et al., 1994). The sun-pointing orientation means that the spacecraft surfaces (particularly the solar arrays) will be exposed to a varying space debris flux and a time-varying Earth shielding (Taylor, 1997). After its retrieval, EuReCa was returned to Earth where it subjected to a detailed post flight investigation (Drolshagen, 1995; McDonnell et al., 1995 and Wright et al., 1995a). As mentioned earlier, apart from the specific micrometeoroid and debris collector (TICCE), detailed impact residue investigations were carried out on the other surfaces from the spacecraft (figure 1.5) (e.g. Wright et al, 1995a). A major focus was placed on the MLI thermal blanket that contained 71 impact features (Aceti et al., 1995) and the solar array panels that contained 851 impacts that were detected by the post-flight scan of the array (Aceti et al., 1995).

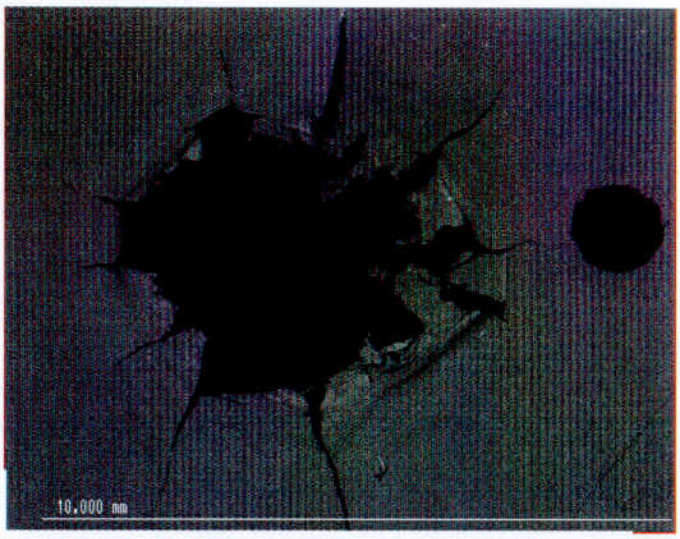

Figure 1.5 Back-scattered electron image of a typical impact feature observed in the layers of the MLI. This particular impact feature is in an aluminium foil layer.

The second opportunity was from the Hubble Space Telescope (HST). The HST (figure 1.6) is a co-operative program between NASA and ESA and is a 2.4m reflecting telescope that acts as a space-based observatory. It was deployed into LEO (614km altitude) on 25th April 1990 by the space shuttle Discovery. The nature of the HST means that it receives routine maintenance in space; as part of the first service mission in December 1993 (Eaton, 1993 and Flam, 1993), the two large arrays of the solar cells that power the telescope were replaced and one was successfully returned to Earth.

Prior to its retrieval the HST array was in a similar sun-pointing orientation and experienced similar time-varying space debris flux and time-varying Earth shielding as LDEF (Taylor, 1997). Exposure to space debris and micrometeoroids was complicated by the fact that the array was shielded from the telescope, but may also have a number of impacts that were generated from secondaries from the main body of the HST (Taylor, 1997). Under the HST post-flight investigation program to study the effects of space exposure, the array was dismantled at ESTEC into individual Solar Cell Samples. In a co-ordinated survey, these were then sent to several European laboratories for characterisation of the impact features and analysis of the micrometeoroid and debris residues (Drolshagen, 1995 and Carey 1998).

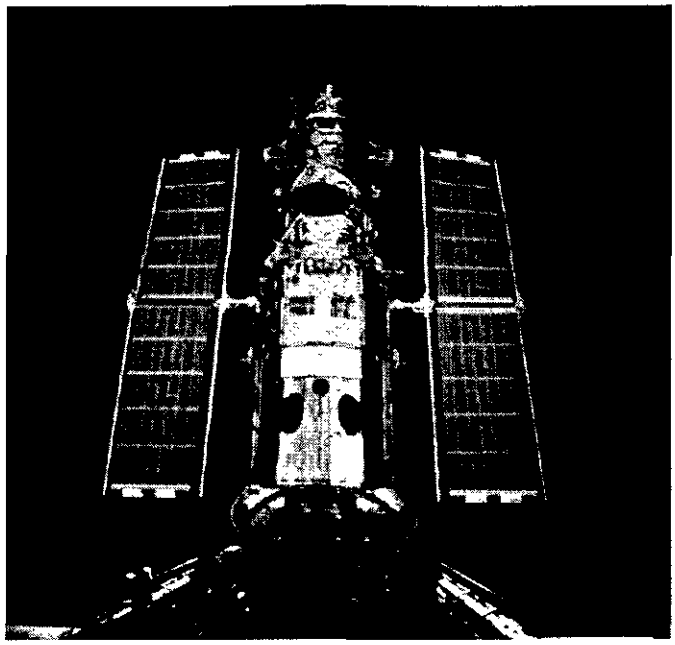

Figure 1.6 The Hubble Space Telescope during the first service mission, the –V2 wing (the array on the right of the image) was returned to Earth after it had been replaced. The –V2 wing has a total area of 28.92m^2 of which 20.73m^2 is covered by solar cells (image courtesy of NASA).

The Open University (U.K.) and the Natural History Museum (U.K.) were part of this survey program and received 26 samples (20 were solar cells and 6 were outer buffer assemblies). The analysis conducted by the Open University and the Natural History Museum were based on optical and scanning electron microscopy. The general findings of this specific study (Wright et al., 1995b) were that 35% of the solar cells (7 out of 20) had been completely penetrated (i.e. a hole had been generated) by the hypervelocity encounter. The study also identified that the HST solar cells were not ideal substrates to search for micrometeoroid residues as they were composed of an extremely complicated multi-element chemistry (the specific composition of solar cells is discussed in depth in Chapter 3).

In contrast the recognition of material that was artificial in origin (i.e. space debris) such as rocket propellant (Al-rich), paint fragments (Ti, C, N, O, Al) etc. was somewhat easier. 65% of the solar cells contained impact features that showed evidence of material

extraneous to the host composition of the solar cells and were deemed to be associated with a space debris origin. Only one impact event was thought to have been created by a natural micrometeoroid, but the findings were not conclusive.

1.4 Atmospheric Entry Versus Hypervelocity Collisions

1.4.1 Atmospheric Entry

All extra terrestrial material, be it meteorites, IDPs or MMs, collected on Earth are subject to mineralogy and chemical alteration during atmospheric transit. In essence particles encounter the Earth at velocities of 11km/s (e.g. Rietmeijer, 1999) and are therefore subject to alteration effects because of the encounter. Essentially when a particle encounters the atmosphere, it undergoes deceleration due to collisions with air molecules (Whipple, 1950, 1951). As a result of these collisions the particles radiate away the energy gained, thus the particle has undergone atmospheric heating (Flynn, 1989a&b). Extensive modelling work has been carried out on both IDPs and MMs to investigate the effect of atmospheric entry, (e.g. Flynn, 1989a; 1989b; Love and Brownlee, 1991 and Genge et al., 1996). It has been suggested that the degree of heating which a given particle undergoes is dependent on its size, density, entry velocity and angle of entry (Flynn, 1989b).

Love and Brownlee (1993) devised a model for IDPs / MMs with a density of $2g/cm^3$, diameters of between 2 – 50μm, entry velocity of 10 – 25km/s and an angle of entry of 45° that would predict the peak entry temperature experienced. For example, a 50μm diameter particle with the specified density and angle of entry and an entry velocity of 12 km/s would have a peak temperature of 1375°C. It was hoped that the modelling would help to distinguish between IDPs of asteroidal or cometary origin. Flynn, (1989b) suggested that 20μm diameter particles with a density of $1g/cm^3$ which were of asteroidal origin would

not be heated above 700°C during entry, whereas particles of cometary origin (perihelia <1.2 AU) would be heated above 800°C during entry.

Nier and Schlutter, 1993, carried out stepped-heating experiments to extract He and Ne on IDPs to attempt a better understanding of thermal history of particles. Unfortunately, the experiments did not unambiguously answer the question. It is an area of IDP research that more work needs to be carried out. The effects of atmospheric heating on both IDPs and MMs apart from obviously melting the particle, may also alter the mineralogical composition of the particle (Flynn, 1989b). A clear example of this process is the production of a magnetite rim around the particle (figure 1.7). The formation of a magnetite rim on IDPs will be discussed further in Chapter 6.

It is also possible that atmospheric heating may result in loss of volatile elements such as He and Ne (e.g. Nier and Schlutter, 1993); S (e.g. Fraundorf et al., 1982), Zn (e.g. Klöck et al., 1992). Complex carbon chemistries within the particles might also be lost. Yet stable carbon isotopic measurements on MMs (e.g. Graham et al 1996a & b), and Wright et al., 1997) have identified carbon-rich phases including amphorous carbon, possible nanodiamonds and silicon carbide which would suggest limited loss. Wright et al. (1997) indicated that the removal of organic C could be due to partial oxidation due to the presence of O in the atmosphere. Electron energy loss (EELS) analysis by Engrand and Maurette (1997) have shown yield carbon contents of MMs up to 7 wt%. Complex polycyclic aromatic hydrocarbons (PAHs) have also been identified in IDPs (e.g. Clemett et al., 1997).

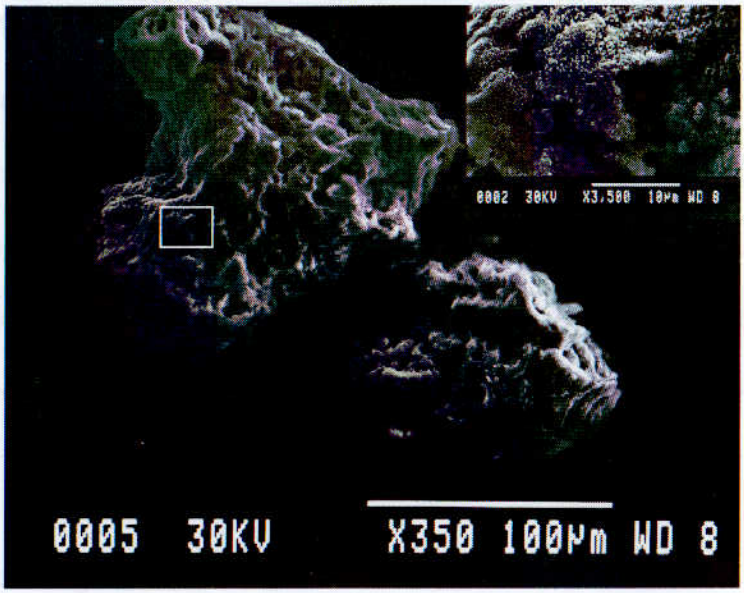

Figure 1.7 Antarctic Micrometeorite with a discontinuous magnetite rim (see insert) covering the particles suggesting that the particles has had limited heating during atmospheric entry to Earth.

It is also possible that IDPs and MMs can become contaminated during atmospheric entry or whilst the particles are dwelling in the atmosphere. After the deceleration of the initial atmospheric entry, it takes between 1 day and 2 months before the particles land on the Earth's surface (Brownlee et al., 1978). The level and type of contamination can be quite varied. For instance IDPs have shown evidence of halogen contamination from Br and Cl which are abundant in the stratosphere (e.g. Arndt et al., 1996). It is also possible that mineralogical contamination can occur, when geological debris in the stratosphere such as volcanic ash particles become associated with the extra terrestrial particle (Reitmeijer, 1988). Apart from the atmospheric environment itself, particles can also become contaminated by the collection method. IDPs are collected using silicone oil collectors and the silicone oil can impregnate the particles; this is particularly a problem with porous particles which despite cleaning, have still been found to contain silicone oil (e.g. Reitmeijer, 1987).

The problem of atmospheric entry on particles is further complicated by the possibility of multiple encounters with the Earth's atmosphere before final entry. Genge et al. (1996)

identified a MM particle which showed evidence (multiple silicate glass rims coating a glassy core) of at least two grazing encounters with the atmosphere. Such an observation would suggest that IDPs and MMs could experience multiple melting, evidence that could strongly alter the chemical and mineralogical composition of a particle. This therefore raises the question whether there is a better environment to capture cosmic dust particles for laboratory investigations other than from terrestrial locations, i.e. space.

1.4.2 Hypervelocity Collisions

The impact damage sustained by returned surfaces from space hardware in LEO would, without question, suggest that the original impactor would have experienced intensive energy transfer when impacting at speeds of ca. 25km/s (e.g. Bernhard et al., 1993b). It is highly likely that such an event would alter the appearance and composition of the remnants retained in the feature. The obvious alteration of the impactor as a result of the impact event is the morphology: rarely in passive collectors surfaces (e.g. HST solar cells and thermal blankets from Solar Max) are intact particles identified (Reitmeijer and Blandford, 1988). Instead, complex residues are observed (e.g. Bernhard et al., 1993a and Brownlee et al., 1993), these are often composed of remnants of the impactor (either micrometeoroid or space debris) and the host substrate.

Numerous attempts have been made to simulating the effect of hypervelocity impact, on the impactor (e.g. Hörz et al., 1983) and on the impacted substrate (e.g. Mandeville, 1972) in terms of morphology (these are discussed in-depth in Chapters 4 and 5). The chemistry of the impactor will also be highly altered; Amari et al. (1991) identified enrichments in refractory elements in Al, Ca and Ti, compared to IDPs collected in the stratosphere, it was suggested that this was as a result of evaporation. Yano et al. (1993) observed that remnants of micrometeoroid impactors identified in LDEF Al-clamps, whilst similar in

composition to chondritic IDPs with regards to Mg, Si, Fe and S elemental signatures, were depleted in Ni and Ca.

Zolensky et al. (1993) observed that individual remnant mineral components identified in impact features from LDEF material showed evidence of intense shock metamorphism, planar deformation to crystal structure and recrystallisation (120° grain intersections on remnant orthopyroxene material). In extreme cases the impactor can be completely vaporised (e.g. Bernhard et al., 1993b). Further discussions on chemical and morphological observations are given in Chapters 4-6). Whilst it is clearly evident that both micrometeoroids and space debris particles are highly altered by hypervelocity impact events, characteristic remnants do remain, for example the chondritic residues identified in an Al-clamp from LDEF (Brownlee et al., 1993). Although the capture of particles in passive collector surfaces in LEO may not preserve material that is better than that sampled from terrestrial collections, it may however sample different material (Yano et al., 1991).

1.5 Overview

The analysis of cosmic dust has been a long-standing concern and fascination to the scientific community. Extensive research has been carried out on the terrestrial collection of IDPs and micrometeorites, with much learnt about mineralogy, chemistry and possible origins. Yet, the fact remains that these collections may have a sample bias and the composition of material may have been altered by atmospheric entry and terrestrial weathering. Therefore, it is important to assess other collections of material when they become available. The timing of this project has coincided with the availability of some scientifically unique material from both the HST and EuReCa. Unlike post-flight investigations, the time-scale and nature of the project allowed development of an analytical methodology that may reveal significant information on the chemistry and

mineralogy of cosmic dust from the zodiacal cloud. It also allowed assessment of the significance of space debris in LEO, in terms of identification of material below the 1mm size range.

Chapter 2

Experimental Methodology

2.1 Introduction

The chemical and mineral analysis of cosmic dust material (both IDPs and micrometeorites) has been carried out using a variety of analytical techniques. These have included scanning and transmission electron microscopes fitted with X-ray elemental analysers (e.g. Bradley et al., 1994), proton-induced X-ray emission (PIXE) (Wallenwein et al., 1987), Synchroton X-ray fluorescence (SXRF) (Flynn and Sutton, 1990), Secondary Ion Mass Spectrometry (SIMS) (application of Time-of-Flight (TOF)-SIMS analysis of IDPS, Stephan et al. (1993)) and high precision, static vacuum carbon stable isotopic mass spectrometry (e.g. Graham et al., 1996a & b and Wright et al., 1997). These techniques are used as they are particularly well designed for small particle analysis (Sutton, 1994) and therefore maybe suited for the analysis of impact residues.

The search for, and particularly the chemical analysis of, impact residues in space hardware is an extremely complex task and sometimes very time consuming. The residues maybe retained in only a limited number of impact features, which can vary dramatically in size from millimetre holes to sub-micron craters. The analytical approach to investigations of impact residues necessarily involves a preliminary rapid survey. Previous investigations that were based on attempts to identify residue chemistry in returned surfaces from low Earth orbit (LEO) (e.g. Warren et al., 1989; Borg et al., 1993) have highlighted the range of analytical techniques that have worked, e.g. scanning electron microscopy (SEM) (e.g. Bernhard et al., 1993a) and those which have not been successful, e.g. secondary ion mass spectrometry (SIMS) (e.g. Borg et al., 1993).

It would be unjust simply to state that SIMS has not proved successful for residue investigation; rather, the use of a highly specialised technique such as SIMS is not appropriate for survey work. SIMS therefore should be used in specific cases to identify much lower concentrations, light elements down to hydrogen and isotopic measurements (Reed, 1996). Isotopic measurements of residues would be particularly useful, as it is this data that would allow unambiguous distinction between space debris and natural micrometeoroid sources of impactor. SIMS was successfully carried out on impact residues identified on the trailing edge capture cell of LDEF (Amari et al., 1993). This would suggest that SIMS is a suitable technique for detailed analysis of impact residue once the residues have been identified by a preliminary survey.

TOF-SIMS was used in the analysis of HST solar cells and the EuReCa foils post-flight surveys (e.g. Stephan et al., 1996). Unfortunately, the construction of the HST solar cells generated analytical problems, including long sample induction time into the sample chamber due to out-gassing. The lack of compositional contrast between the cell layers prevented distinction between host and extraneous material, causing difficulty in locating residues (Stephan et al., 1996). It would appear that for this investigation SIMS is not a suitable technique.

Previous investigations of Solar Max thermal blankets (e.g. Warren et al., 1989), LDEF surfaces (Bernhard et al., 1993a), HST solar cells (e.g. Wright et al., 1995b) have successfully used analytical scanning electron microscopy to search for impact residues. In keeping with these previous investigations, herein scanning electron microscopy has been used extensively in the search for and characterisation of impact residues. The rest of Chapter 2 discusses the experimental details behind the technique and the typical analytical problems, which are involved with the analysis of impact residues.

2.2 Background

Essentially the two most widely used instruments for the analysis of a sample at micron and sub-micron scales are the scanning electron microscope (SEM) and the electron microprobe (EMP). Although they are two different instruments in detail, there are similarities between them, as both are centred on the interactions that occur when a sample is hit by an electron beam (figure 2.1). Therefore, they are relatively similar in design, in that the basic components are a lens system, electron gun, electron collectors and visual/recording cathode ray tubes (CRT) (figure 2.2).

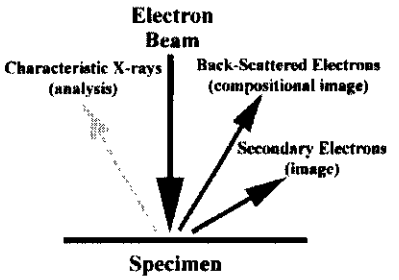

Figure 2.1 A schematic diagram showing the charged particles and electromagnetic radiation that are emitted by a specimen when hit by an electron beam (after Williams and Spratt, 1995).

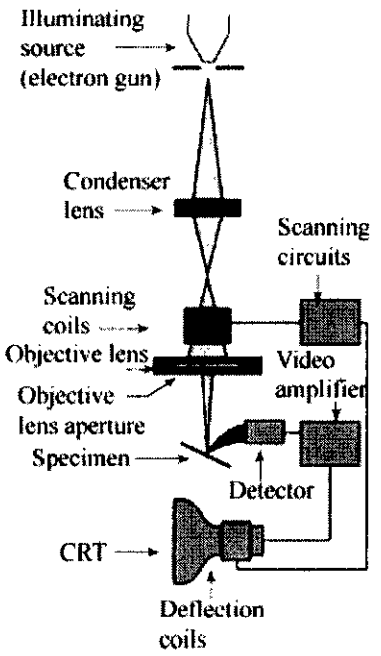

Figure 2.2 A cross-section schematic diagram of a scanning electron microscope. The image is courtesy of Oxford Instruments.

2.2.1 The Scanning Electron Microscope

The traditional use of scanning electron microscopy (SEM) has been as an imaging tool of biological, geological and material samples. It was Zworykin et al. (1942) who first used the SEM to examine the thickness of a sample. Zworykin et al. (1942) postulated and then observed that the secondary electrons (SE) produced by the beam interactions between the sample and the primary electron fired from the electron gun resulted from topographical changes within the sample. The development of detector technologies improved the resolution and amount of topographic information that could be obtained (e.g. Everhart and Thornley 1960).

The back-scattered electrons (BE) also contain imaging information about a sample, although unlike secondary electrons, which are essentially only surface derived interactions, they are produced at a greater depth (1-5μm) and therefore yield compositional and textural information (an in-depth discussion of back scattered electron imaging (BEI) is given in section 2.4). The addition of an X-ray spectrometer to an SEM facility enables the ability to carry out both quantitative and qualitative elemental measurements (section 2.3 discusses the X-ray spectrometry).

2.2.2 The Electron Microprobe

The electron microprobe (EMP), unlike the traditional use of the SEM, is used for micro-spot elemental analysis, both qualitative and quantitative, of a selected area within a sample by the analysis of characteristic X-rays. For example analysis of individual silicates grains within the matrix material of a micrometeorite (Genge et al., 1997).

The discovery that a sample emitted X-rays when excited by electrons (Moseley, 1913) led to the development of X-ray spectrochemical analysis, because the X-rays produced were

characteristic of the elements within the sample (e.g. Goldstein, 1981). This is essentially the fundamental origin of microanalysis by the EMP, although it was not until the late 1950s that the first commercial EMP was produced by CAMECA (Williams and Spratt, 1995).

The development and improvements of the X-ray spectrometers used to analyse the X-rays (see further discussion of X-ray spectrometry in section 2.3) and increased beam stability has increased the use of EMP in all aspects of geological, biological and material sciences. A more detailed description of the electron probe is given in Reed (1995).

2.2.3 Summary Of SEM & EMP Basic Principles

The uses of the SEM and EMP would appear to be fundamentally different. The SEM has traditionally been used for imaging analysis whilst the EMP for chemical analysis. Yet, the development of X-ray detectors for the EMP has also been employed upon for the SEM. The addition of an X-ray spectrometer to a SEM can enable both qualitative and quantitative elemental measurements to be obtained (Reed, 1995).

So, the discussion of which system is most suited to analysis work proposed for this project is based on the different X-ray and imaging detectors available.

2.3 X-ray Spectrometry: WDS Versus EDS

2.3.1 Background

There are two main types of X-ray detection employed with an EMP or SEM: wavelength dispersive spectrometry (WDS) and energy-dispersive spectrometry (EDS). In order to appreciate the difference between the techniques it is necessary to consider briefly the

nuclear interactions that produce the X-rays from the sample under investigation. The classic representation of the atom according to the Rutherford-Bohr model is that of negative electrons in orbit around the positively charged nucleus. The number of electrons orbiting around the nucleus is equal to the atomic number (**z**), which in the neutral state is the same as the number of protons. As the atomic number increases so does the number of orbits available for electrons.

The energy of an electron does not vary continuously but is quantized, i.e. restricted to discrete or individual energy values (quantum numbers) and as stated by the Pauli exclusion principle, no two electrons may have the same spin number (Holtzclaw et al., 1991). The electron orbital is characterised by the principal quantum number (**n**); as the quantum number increases the distance from the nucleus increases (Holtzclaw et al., 1991). The inner orbitals form closed shells assigned K(n=1), L(n=2) M(n=3) etc. (figure 2.3a). All the orbitals of a specified **n** therefore belong to the same shell and have the same energy (Atkins, 1990).

The characteristic X-rays that are used for quantitative and qualitative elemental measurements are produced by the electron transitions between energy levels in the inner shells for samples that are of a solid state (figure 2.3). Apart from elements with low atomic numbers, these shells are normally full (Reed, 1996), and so allow the removal of an inner electron, certain conditions must be attained. If the electron beam is sufficiently energetic, it may eject an inner shell electron **K**, **L** or **M** leaving the atom in an ionised state. Subsequently the atom reverts to its original state, and it is during this that the transition of electrons from one shell to another occurs. It is possible during the transition that the excess energy (which ionised the atom) can be released as photon of electromagnetic radiation. The photon energy corresponds to emission within the X-ray

band of the electromagnetic spectrum and such a quantized photon is referred to as a characteristic X-ray (Goldstein, 1981).

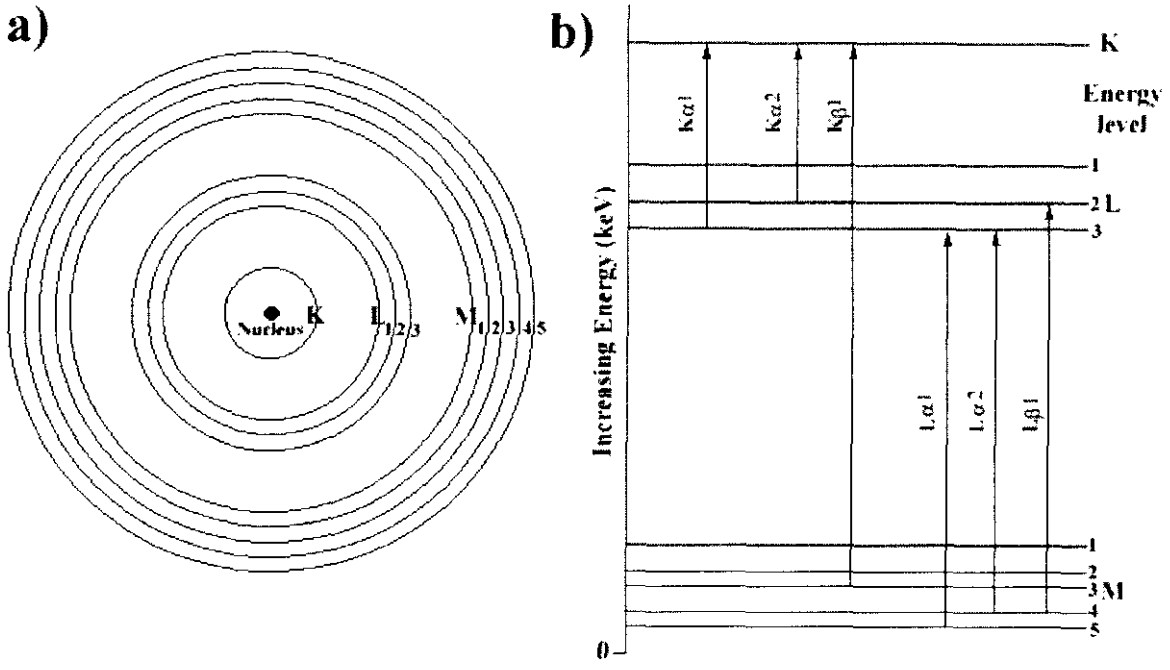

Figure 2.3 a) Schematic representation of the inner electron shells surrounding the nucleus of an atom; b) energy level diagram showing the transitions between the electron shells shown in (a). It is these transitions which produce the characteristic X-rays that can be used for elemental analysis under the SEM or EMP.

Apart from the characteristic X-rays that are produced by excitation of elements in the specimen, a second broad-band emission of X-rays will be sampled by the detector. The deceleration of the electrons from the beam in the coulombic field of the atom core causes the electrons to experience a quantum jump to a lower energy state, with the emission of a photon (Goldstein, 1981; Reed, 1996) leading to the formation of a continuous spectrum of X-ray energies, often referred to as bremsstrahlung radiation. This bremsstrahlung spectrum can limit the detectability of characteristic X-rays when they are low in intensity (Reed, 1996).

For detailed elemental chemical analysis in both analytical scanning electron microscopy and electron microprobe analysis the X-rays, particularly the characteristic ones must be

detected and measured. There are essentially two basic ways in which these X-rays may be measured; one is based on the energies of the X-rays (energy dispersive spectrometry EDS) and the other is based on the wave lengths of the X-rays (wavelength-dispersive spectrometry WDS) (Williams and Spratt 1995).

2.3.2 Wavelength-Dispersive Spectrometry Versus Energy-Dispersive Spectrometry

Wavelength-dispersive spectrometry (WDS) obtains both quantitative and qualitative chemical analysis by measuring the characteristic X-rays according to their wavelength (Reed, 1996). The characteristic X-rays which are emitted when a sample is bombarded by electrons are dispersed in a WDS initially by a crystal of known structure (typical crystals used are Lithium Fluoride (LiF), Pentaerythritol (PET) and Thallium Acid Phthalate (TAP)). This acts to separate segments of the wavelength spectrum that can be made individually to strike upon an X-ray detector.

Analysing Crystal	Element Range
PET	K-alpha lines: Si to Cr L-alpha lines: Rb to Eu M-alpha lines: Lu to Bi and Th to U
TAP	K-alpha lines: F to Si L-alpha lines: Cr to Zr M-alpha lines: La to Pt
LiF	K-alpha lines: Ca to Rb L-alpha lines: Sb to U

Table 2.1 showing the typical analysing crystals used in a WDS and the elemental range each crystal is capable of analysing (source data http://www.gps.caltech.edu/facilities/analytical/probe.html).

The characteristic X-rays are deflected according to Bragg's law (figure 2.4 and equation 2.1). The line intensity produced by this deflection is then measured by an X-ray detector (Williams and Spratt, 1995). As the angle at which the X-rays hit the crystal is changed, a different part of the spectrum of X-rays is diffracted to the detector which may correspond to a different characteristic emission from another chemical element (more detailed

descriptions of WDS can be found in Goldstein et al, 1981 and Reed, 1996, amongst others). Whilst the spectrometer can detect a varying range of θ values, a number of crystals are required to analyse the range of elements from Be to U. Therefore, a typical WD system will have spacing for four or five interchangeable crystals within the detector.

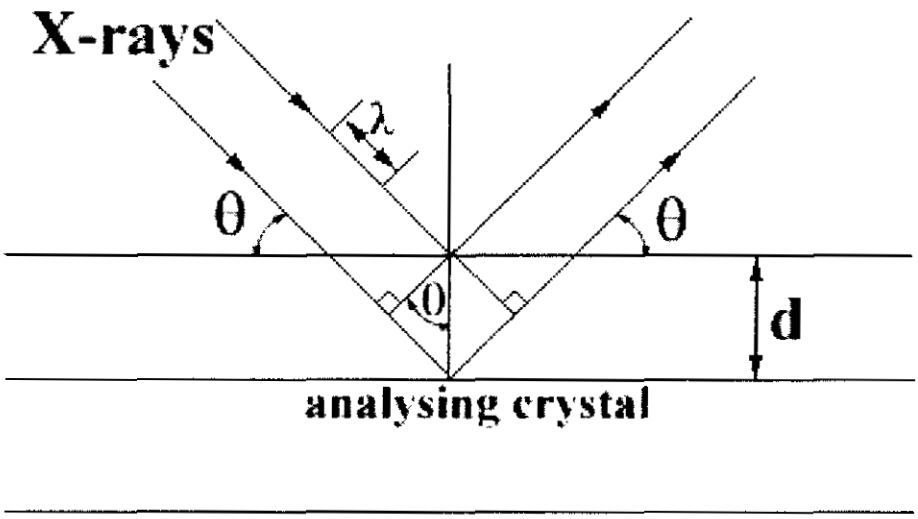

Figure 2.4 Shows a diagram representing Bragg reflection for X-rays of wavelength λ hitting an analysing crystal with interplanar spacing ***d***. The relationship of the variables in this diagram are resolved by Bragg's Law (equation 2.1).

$$n\lambda = 2d\sin\theta$$

Equation 2.1 Bragg's Law: where: **n** is the order of reflection; λ is the wavelength; ***d*** is the interplanar spacing of analysing crystals and θ is the incident angle within the crystal (after Goldstein et al., 1981).

The WD detector can therefore only analyse elements sequentially as it requires movement of crystal and detector from the peak position for one characteristic emission to another. (table 2.1 shows the elemental ranges for the different crystals used in the detector). Therefore when carrying out multi-element mapping (which is desirable for the work described herein), the analysing crystal and the detector must be moved. This can result in substantial analytical time required to investigate a sample.

The benefit of using the WD system is that a greater spectral resolution can be obtained, which resolves the contribution of even closely spaced wavelengths and therefore reduces the peak overlap problems that can occur with spectra obtained using an ED detector.

The major disadvantage for using a WD system for the study of impact residues in space hardware is that a WD system requires a higher specimen beam current, e.g. 50nA compared to typical 2nA required by an ED system. This high specimen beam current is concentrated into a submicrometre beam irradiating the sample for perhaps minutes.

It is known that a higher beam current can cause effect or damage to samples (e.g. Williams and Spratt, 1995). The top protective surface of the solar cells (Berthoud, 1995) are coated with sub-micrometre thin film composed of elements including Mg+F (not stoichemetric MgF_2), Na and K. It is possible, although this would be only a minor contribution, that the influence of the electrostatic field produced by a high electron beam current would cause ionisation of the elements (Mg^{2+}, Na^{+} and K^{+}). The evidence of this ionization, would be a subsequent move or migration of these elements (Reed, 1996) (figure 2.5).

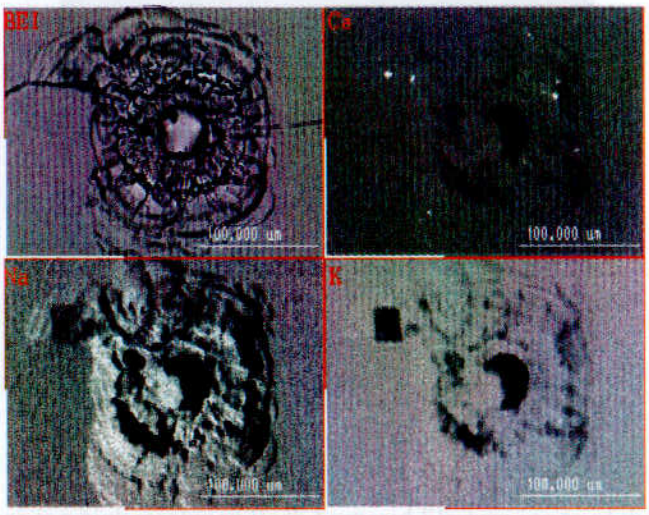

Figure 2.5 Back-scattered electron image and digitised X-ray elemental maps for Ca, Na and K. From the Na and K maps it is clearly possible to see the migration which has occurred from the previous investigation of the cell under a CAMECA SX100 electron probe (the dark rectangular boxes within the maps).

A demonstration of the thermal heat damage caused by an increased beam current is shown in (figure 2.6). Here a calcite fragment has been analysed using a WDS after the particle was initially imaged using a field-emission scanning electron microscope. The X-ray map for Na and K in (figure 2.5) has identified the area where the WDS analysis had been carried out. The first image in (figure 2.6a) shows a high resolution BE image the of the calcite particle: here there is no evidence of thermal damage. In the second image (figure 2.6b) obtained using a conventional SEM after the particles had been analysed using the WDS, the particle shows out-gassing as a small dark halo (in BE image) that has appeared around the particle edges. This was not observed when imaged or analysed using the EDS.

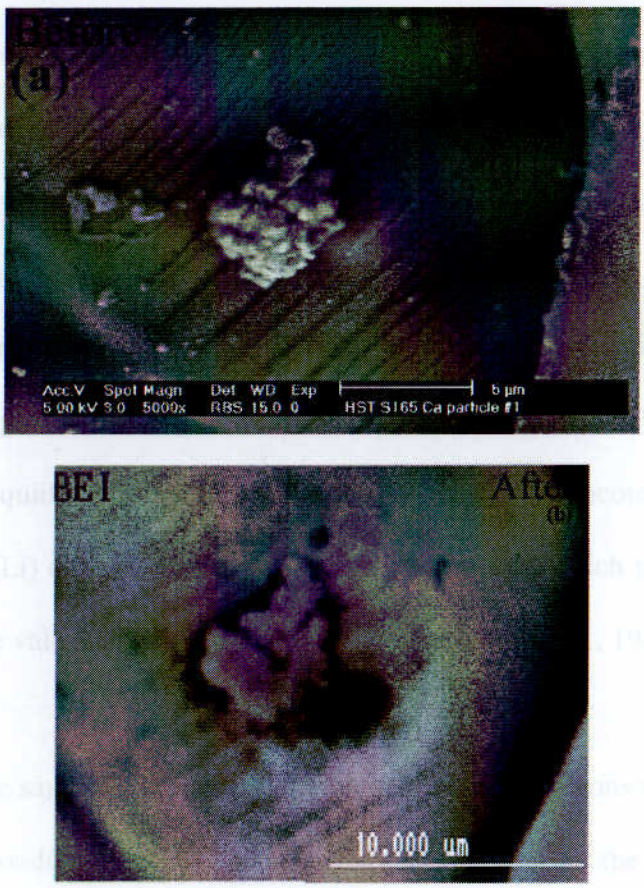

Figure 2.6 The first image is a high resolution Back-Scattered Electron image of the individual calcite grain before elemental analysis using a WDS fitted to a CAMECA SX100 electron probe. The second image is a BE image of the same grain after it has been examined under the electron probe, the dark halo around the grain edges is evidence of out-gassing generated by "cooking" the grain under the electron probe.

The WDS can not be used to map large impact features as the X-ray elemental maps produced would become defocused at magnifications below x2000 (Williams and Spratt, 1995). As the impact features selected for this thesis are between 100-1000μm in diameter it likely that the initial X-ray maps will be carried out at low magnification, typically x250.

WDS mapping would only be applicable on the detailed investigations of residues after they have been located. Due to the analytical disadvantages outlined above, it was decided that it would not be suitable to investigate the samples in this thesis with either an EMP or SEM fitted with WDS.

The energy dispersive X-ray spectrometer (EDS) creates a characteristic spectrum of X-rays based on their energies. All the emitted energies are detected simultaneously rather than sequentially as with WDS (Williams and Spratt, 1995). A typical ED system consists of a solid-state detector, in which lithium atoms are implanted (drifted) into a silicon wafer (this type of detector is termed a Si (Li) ED detector). The emitted X-ray signal from the sample passes through a thin Beryllium (Be) window into the Si (Li) detector which has been cooled using liquid nitrogen (Goldstein et al., 1981). The incoming X-ray photon is absorbed by the Si (Li) crystal, which has a band structure in which the conduction states are empty, whilst the valence band states are filled (Goldstein et al., 1981).

The absorption of the sample's emitted X-ray photon causes electrons to be promoted from the valence to the conduction band and thus leaving a "hole" in the valence band. The movement of electrons and "holes" in opposite directions generates a short pulse of current under applied bias voltage (Goldstein et al., 1981 and Reed, 1996). The produced current pulses are proportional to the energy of the X-rays emitted. Hence the pulses are sorted according to size, to produce an X-ray energy spectrum in which individual characteristic

peaks can be identified (figure 2.7). It is these individual peaks that relate to the different elements and it is from there which elemental concentrations can be calculated (Williams and Spratt, 1995).

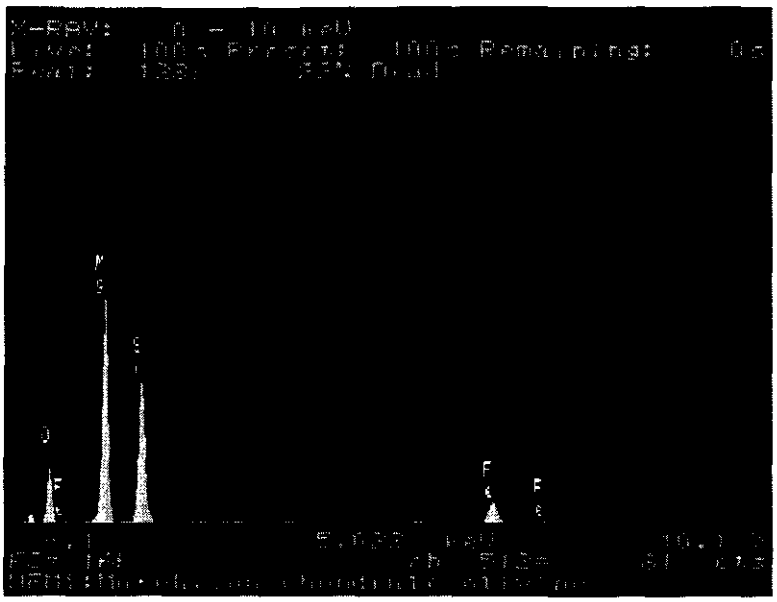

Figure 2.7 An energy dispersive spectrum obtained from a qualitative micro-spot analysis of a sample. The characteristic peaks identified correspond to the elements O, Mg, Si, and Fe. This particular spectrum was obtained from an olivine chondrule from the Murchison meteorite.

Because the Si (Li) detector has to be constantly cooled using liquid nitrogen (to prevent Li migration in the detector), there is a danger that this will act to condense water vapour; clearly a build-up of an ice film on the detector surface would reduce the efficiency of the detector (Bishop et al., 1992). For this reason, a thin metallic window is employed between the detector and the vacuum of the main SEM/EMP system. The Be window described above is commonly used, but in this configuration the detector only allows the analysis of elements with atomic numbers greater than Na. To allow detection of the "light elements", (i.e. those lighter than Na), the EDS has to be fitted with an "ultra-thin" window which is composed of a thin foil (approximately 1.5μm) of an organic film (e.g. Mylar) coated with aluminium. When it is fitted in place of the Be window it allows the detection of elements down to B, including C, N and O.

The major benefits of using an EDS instead of a WDS is that rapid multi-element analysis can be carried out due to the simultaneous detection method used. The EDS also uses a low beam current thus specimen damage is reduced (and in particular the migration of alkali elements). The disadvantages compared to a WDS include poorer peak resolution thus there is the possibility of important peak overlaps and the detection limits are poorer (0.2-0.5 minimum wt % for EDS compared to 0.02-0.05 wt % for WDS) (Williams and Spratt, 1995).

2.3.3 Digitised X-ray Elemental Mapping

X-ray micro-analyses of a sample can be carried out in a number of different ways. Apart from qualitative EDS (e.g. section 2.3.2), it is also possible to acquire chemical elemental information from a sample using X-ray mapping. The distribution of an element can be demonstrated by measuring the intensity of the characteristic X-ray line of the element whilst the beam is rastering across the sample - this produces an elemental map.

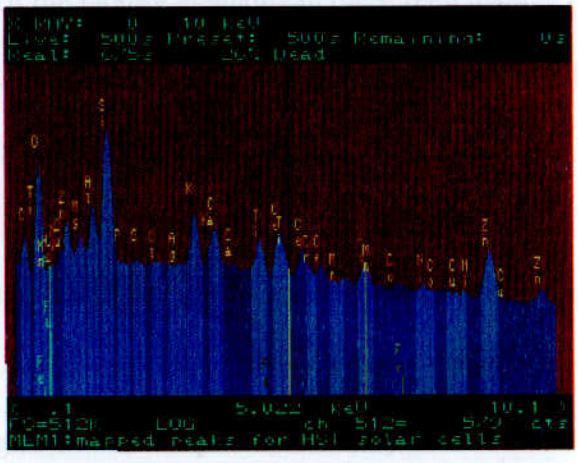

Figure 2.8 The ED spectrum shows the range of total energy range identified using an ED detector within this range different elements have characteristic energy signals. When carrying out X-ray elemental mapping it is possible to map for one individual element or a number of elements. In the ED spectrum the light blue light identify the energy bands which have been selected for mapping. the energy band which are used from the elemental mapping from HST solar cells.

X-ray elemental maps can produce detailed information which has not been revealed from the BE or SE images of a sample, such as subtle chemical zoning of composition (Williams and Spratt, 1995). The method of X-ray mapping used herein is based on EDS rather than a WDS. As has been described in section 2.3.2, the EDS detector collects the whole X-ray spectrum at once, which means that elemental maps can be acquired from a number of energy-bands or "windows" within the entire range of the spectrum (figure 2.8) whilst the beam is in one location. The computer rastering of the beam position allows the EDS system at Oxford Brookes University to collect the maps digitally, although this is now the standard method of collection older software may not allow this type of collection.

The benefits of acquiring the maps by this method are that the image processing and analysis techniques can be applied to the finished map (Reed, 1996). In digitised X-ray elemental mapping (DXREM) the number of X-ray photons for each window recorded at each sample point are stored in the computer system. The resulting X-ray map is constructed by converting the number of photons for each energy band (i.e. element) into brightness modulation of the picture elements in the screen display (Reed, 1996). The final DXREM image consists of an array of pixels (picture elements) (with y coordinates at 0-78 of x coordinates spacing aspect ratio).

The Oxford Instruments eXL at Oxford Brookes University can acquire maps at 128x128, 256x256 and 512x512 pixel resolutions (Reed, 1996). These pixel arrays are essentially point samples within grid boxes at specific x and y directions, the beam resides at the geometric centre of the box for a defined "dwell time" (e.g. 40ms) during which X-rays are counted. Using this method of acquisition, a total number of 16384 individual micro-spot analyses are carried for a 128x128 map of one frame (figure 2.9). This process is then

repeated for a defined number of frames, with the addition of new frames to give the map greater data depth (i.e. dynamic range) thereby smoothing back-ground noise.

The number of frames and the pixel resolution at which a map is carried out both affects the total acquisition time, for example a single frame 128x128 map (with a dwell time of 40ms) takes approximately 15 minutes to complete, where as a single 256x256 map (again with the same dwell time) takes approximately one hour.

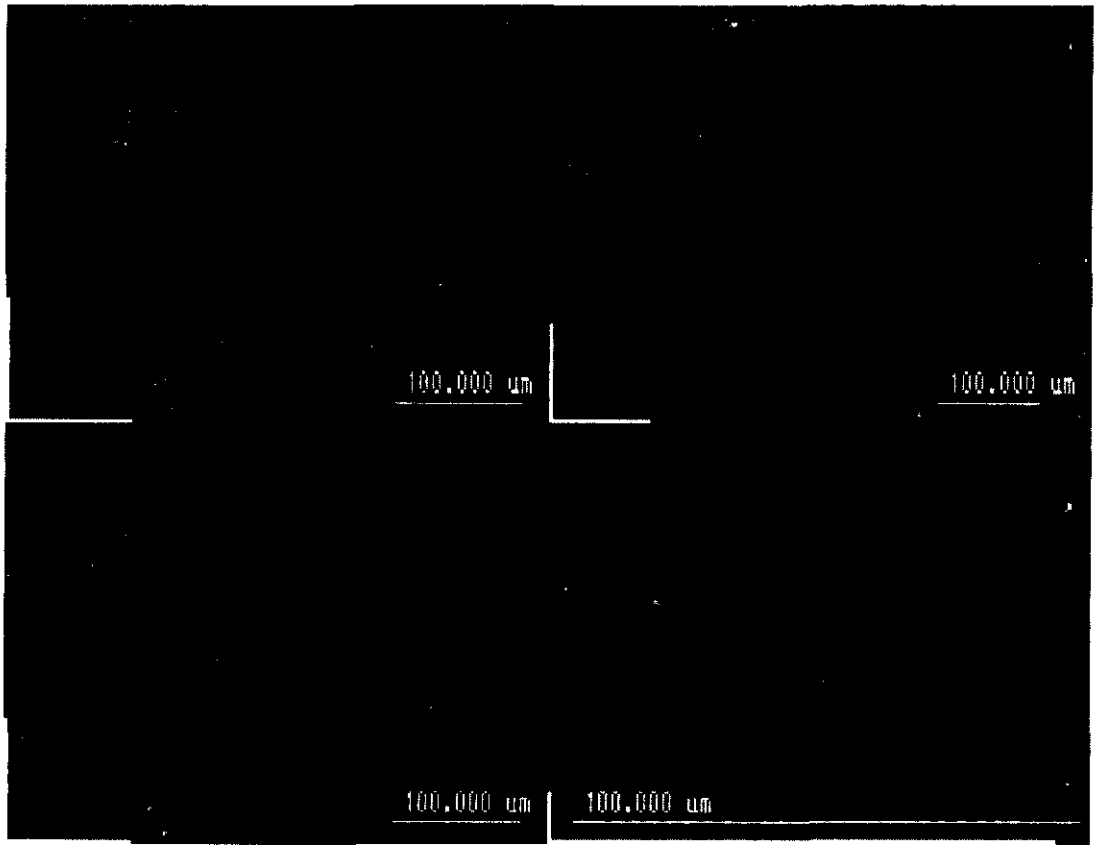

Figure 2.9 The top left-hand BE image is of an area with a sample which will be mapped at a pixel resolution of 128x128. The bottom left-hand image is a BE image of the same area after it has been mapped, the darkness in colour is due to beam damage. The top right-hand BE image shows the 128x128 pixel array, each black square within the array represents a point of analysis (in total 16384 individual points of analysis have been carried out). The bottom right-hand BE image shows a zoomed-in section of the grid (image courtesy of A.T. Kearsley).

Ideally, DXREM should be carried out at the highest pixel resolution using the largest number of frames. However, this inevitably leads to a total acquisition time that is impracticably long. Thus there must be a trade-off between total acquisition time, image resolution and data depth. For the ED system at Oxford Brookes University, the DXREM often carried out at 128x128 pixel resolution but for 60 frames and hence the image has good data depth and takes approximately 12-15 hours to complete. It can also be carried out at 256x256 pixel resolution for 12-15 frames - here the image resolution is enhanced but the data depth is slightly lower. This set up has an acquisition time of between 10-15 hours. The analytical difficulties involved with DXREM are discussed in section 2.5.

2.4 Back-scattered Electron Imaging

2.4.1 Principles Of Back-scattered Electron Imaging

As has already been highlighted, (section 2.2) when an electron beam is incident upon a sample, the electrons undergo a number of elastic and inelastic collisions with the atomic nuclei of the surface of the sample (Bishop et al., 1992) (see Goldstein et al. (1981) for an in-depth discussion). These collisions generate a number of charged particles (figure 2.1) including back-scattered electrons. Back-scattered electrons are primary beam electrons that are scattered out of the surface of the sample; the fraction of these electrons re-emitted with respect to the primary beam is defined as the back-scattered coefficient (ETA) (Bishop et al., 1992). Thus unlike secondary electrons, back-scattered electrons (BE) can be used to identify different elemental compositions (Bishop et al., 1992).

Now, although stated in section 2.2 that the intensity of BE was due to the atomic number of the target nuclei, in detail the ETA of a sample is not directly linked to the mean atomic number of the compound. Rather, the ETA of a sample is related to the weight fractions for each element present multiplied by individual ETAs (equation 2.2) (Bishop et al.,

1992). Therefore the contrast produced in the BE image is a complex function of the different elemental compositions present within the sample (Bishop et al., 1992).

$$\eta Compound = \Sigma(\eta_x * \text{wt fraction}_x) + (\eta_y * \text{wt fraction}_y) + (\eta_z * \text{wt fraction}_z)$$

Equation 2.2 Back-scattered coefficient for a compound XYZ. Where η is the back-scattered coefficient and ***wt fraction*** *is the weight fraction of the element in the compound* (After Bishop et al., 1992).

2.4.2 BE Detectors

There are two different types of detector which are commonly used to detect these back-scattered electrons: the scintillator and solid-state (Figures 2.10 a and b respectively).

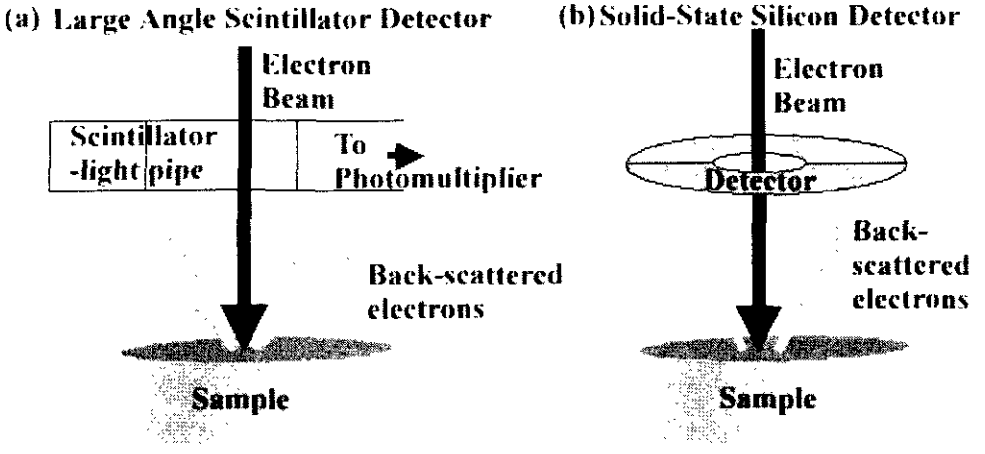

Figure 2.10 Schematic drawings of the two types of electron detector: (a) scintillator detector (b) solid-state detector (based on diagrams from Goldstein, 1981 and Reed, 1996).

It was recognised from the outset that the choice of detector was extremely important because the compositional contrast between the anticipated residues and their host was

considered likely to be very subtle. Back-scattered electrons (BE) unlike secondary electrons, travel in essentially straight line due to their relatively high energy (Reed, 1996).

The result of this means that the detector has to be within close proximity to and preferably above the sample to enable the collection of sufficient BE from an image. Both the solid-state and specialised scintillator detectors (shown in figure 2.10 a and b) do this.

A second important factor regarding the performance of BE detectors is the linearity (i.e. proportionality) of the signal output with regard to the back-scattered electron energy. Essentially as the energy of electrons increases, the contrast or brightness of an area within the image increase, for example a carbon rich area will appear much darker than a chromium rich area (Kearsley, 1989).

A solid-state detector produces a near linear response to the increase in the energy of electrons (figure 2.11a), which means that under favourable conditions the back-scattered electron image can be used as method of identifying different chemical components within a sample (Kearsley, 1989). A scintillator detector unfortunately produces a non-linear response (figure 2.11b) at the higher energy of electrons, and therefore may produces more ambiguous results.

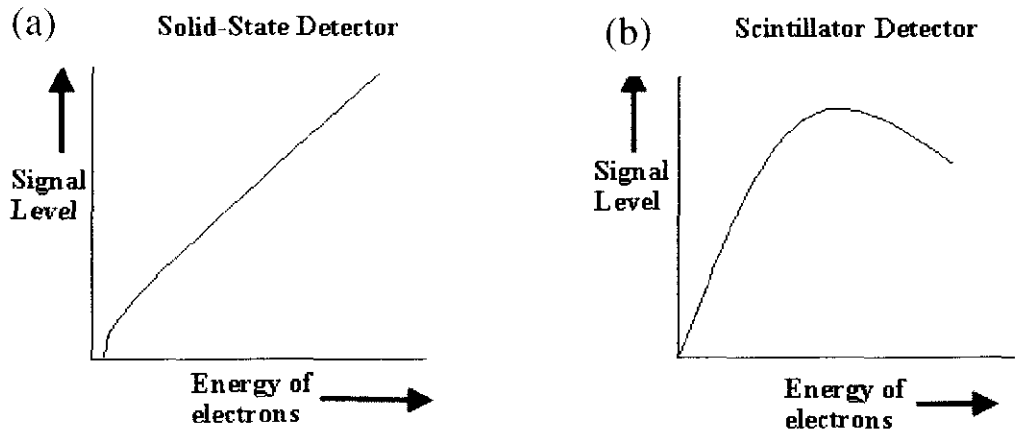

Figure 2.11 Shows the respond of signal levels (i.e. image contrast brightness) to an increase in energy of electrons for (a) the solid-state detector and (b) the scintillator detector (based on diagrams from Goldstein, 1981).

The BE detector at Oxford Brookes University is a Jeol dipole solid-state detector. As with the X-ray elemental mapping, the BE images are collected digitally and are enhanced by repeated Kalman frame averaging software (a technique whereby each frame is added to the next and the average at each pixel is calculated). This means that the usual random fluctuation (noise) in brightness from pixel to pixel that occurs in scanning images is reduced and thus generates a clearer BE image.

2.5 Analytical Problems

Under normal conditions, micro-analysis and imaging work is carried out on a specimen which has been specially prepared. For the study of geological specimens, this essentially means that a polished thin section is produced from the sample. For the sample studied herein such a procedure would require modification. In the case of a cosmic dust particle of some description, it would be possible to conceive a technique whereby a thin slice would be produced from the sample using a cutting medium. One of the sides of the cut slice would be lapped (polished) using an aluminium oxide or silicon carbide abrasive. The slice would then attached to a standard glass preparation slide and is again lapped using an Al source. The surface is then polished using extremely fine aluminium oxide leaving a flat sample of approximately 30μm thickness (Reed, 1996).

However for the study of space hardware, (e.g. HST solar cells, the EuReCa MLI blankets) it is not possible to prepare polished sections. Instead the samples, with their impact features, were examined under the SEM as a complete specimen (figure 2.12). Inevitably this caused a number of classical electron microscopy problems.

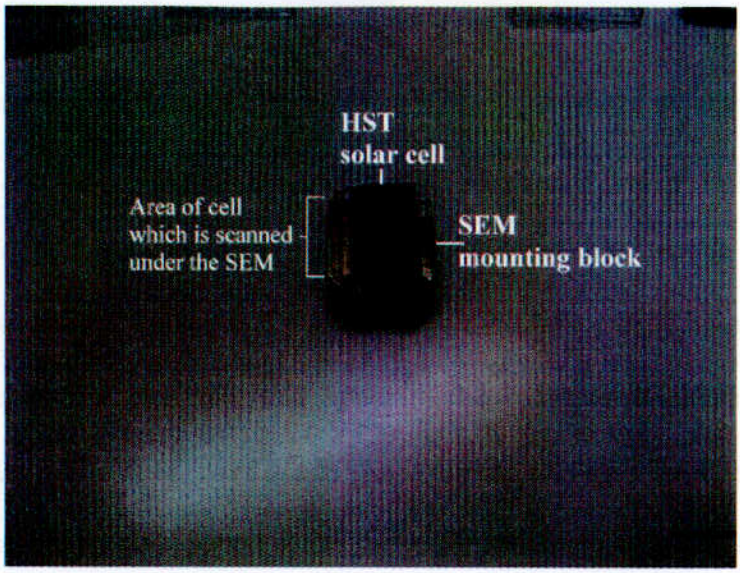

Figure 2.12 HST solar cell on a Oxford Brookes sample mount prior to being admitted into the SEM. The black line at the bottom right-hand corner of the image represents a scale bar (2.1cm).

2.5.1 Coating

The HST solar cells, as typical of most specimen surfaces examined under the SEM, are non-conductors of electricity and therefore a path for the current in the electron beam must be provided by coating the solar cell with a conductive layer. The standard method for coating a sample is to use carbon (C), aluminium (Al) or gold (Au). As X-ray micro-analysis was to be carried out, an Au coating is not used because of the X-ray lines that it produces: the M-lines for Au are at 2.1 – 2.1 kV which overlaps the K-lines for P and S (Reed, 1996). Therefore the HST solar cells were carbon-coated (approximately 30nm thickness), description on the methodology of sample coating are given in Reed (1996).

As the impact features (particularly the craters generated in the HST solar cells) have a complex relief, there is a possibility that sample coating will not be of even thickness over the entire specimen. Upon subsequent analysis, this will result in charging (i.e. electric charge build up where the non-conductive areas in the sample are scanned), resulting in bright patches within the SE image where no information can be seen (figure 2.13.).

If this charging is severe, then the sample may experience thermal and radiation damage and if the charging is sufficiently high, the primary electron beam may even be decelerated (Goldstein et al., 1981). Although the problem of charging is clearly visible in HST solar cells, in SE mode (figure 2.13) it can be reduced by imaging the crater in BE mode. Back-scattered electrons are not substantially affected by the surface deflection that occurs with lower energy secondary electrons that generate the charging (Goldstein et al., 1981), although on certain substrates even this is not adequate to stop charging occurring. One impact feature examined was located in the supporting stiffener substrate for the solar cells (section 3.7.5). The composition of this stiffener is extremely complex, made up of silicone resin layers and individual glass-fibre cross weaved together (see Chapter 3 figure 3.8 for a cross-section view of this substrate). As the impact had penetrated into the glass-fibre layers, it was not possible to apply an even carbon coat to every individual glass-fibre, and so when examined under the SEM, charging rapidly occurred. To counter this effect, the analysis of this impact feature was carried out at a lower accelerating voltage (10-15kV instead of 20kV) and beam current. The reduction of the accelerating voltage is one of the classical ways in which to deal with such a problem (Goldstein et al., 1981).

Figure 2.13 SE image of a HST solar cell containing an impact crater. The application of an uneven coating has resulted in a charging effect to occur, the bright areas within the image identify this.

In addition to the problem of uneven or uncoated areas of the sample, it is possible to generate coating artefacts that can also cause surface contamination and the possible miss-identification of possible residue material. The technique used to coat the samples is a standard thermal evaporation method, and therefore it is possible that fragments of carbon (1μm in diameter) may be deposited on the sample and thus cause surface contamination. Such contamination is a by-product of the technique, so it is impossible to reduce the problem. Caution must therefore be used when dealing with extraneous surface material which is composed of carbon.

2.5.2 ED Detector Geometry – Shadowing Effect

The standard position of the ED-detector fitted to the Joel SEM at Oxford Brookes University has a mounting and aperture design that is set up to the optimum for quantitative analysis of polished surfaces at a 40° take-off angle. This inclined position of the detector means that when analysing craters, that are uneven and have depth, it is possible to create a partial topographic shadow-effect. This shadow-effect means that little or no useful X-ray information is returned to the detector, subsequently an area of darkness appears in the image (figure 2.14). As a consequence of this effect it is necessary to constantly rotate the sample in order to cover an entire area within a crater. It would also be possible to reduce the effect of the shadowing by changing the take-off angle of the ED-detector from 40° to 70°. Such an increase in take-off angle would place the detector within the line-of-sight of the primary electron beam and would have to be purpose-built.

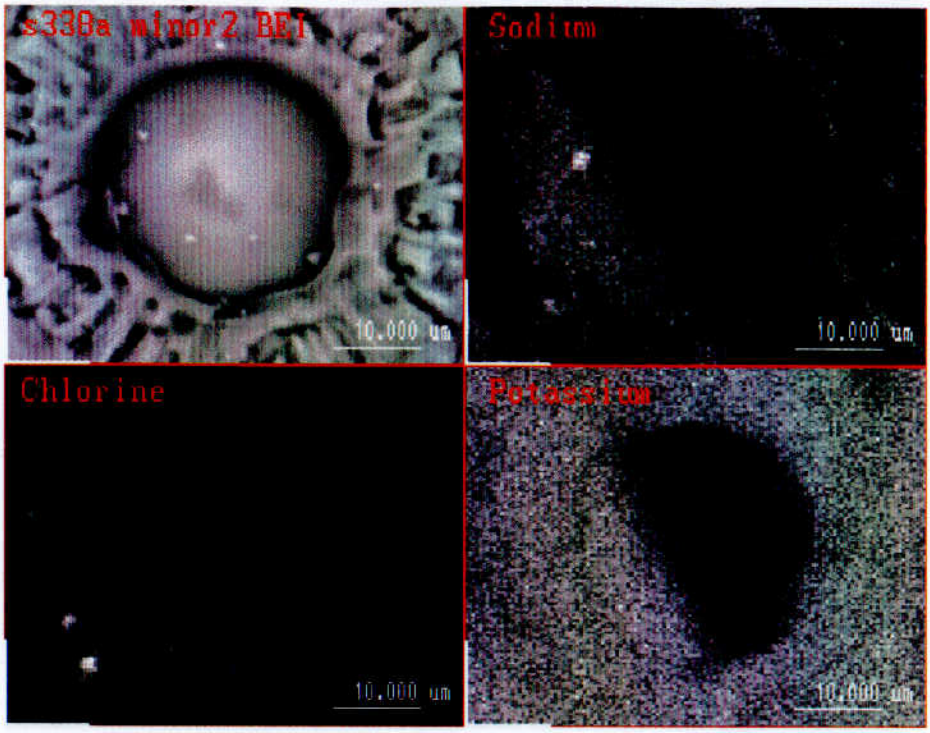

Figure 2.14 Shows a BE image of a melt pit, the three X-ray elemental maps shows the analytical problem that is encountered when dealing with an uneven surface. The morphology of the crater pit means that the line of sight of the ED detector is obscured resulting in a shadowing effect (clearly identified in the potassium and sodium maps).

2.5.3 Edge & Topographic Effects

The major problem associated with the investigation of uneven surfaces under the SEM is the complexity and range of electron interactions. This is particularly a problem when obtaining a secondary electron image at the rim or 'edge' of the crater. At this rim or 'edge', the interaction and sampling volumes are small because of the beam penetration effects (Goldstein et al., 1981). The increased surface/volume ratio can enable more secondary electrons to be collected due to more interactions close to the surface (Goldstein et al., 1981). The creation of more electrons means that the signal detected can be enhanced, and as a result, the rim of the crater can appear brighter than expected in the SE images. This is referred to as an edge effect.

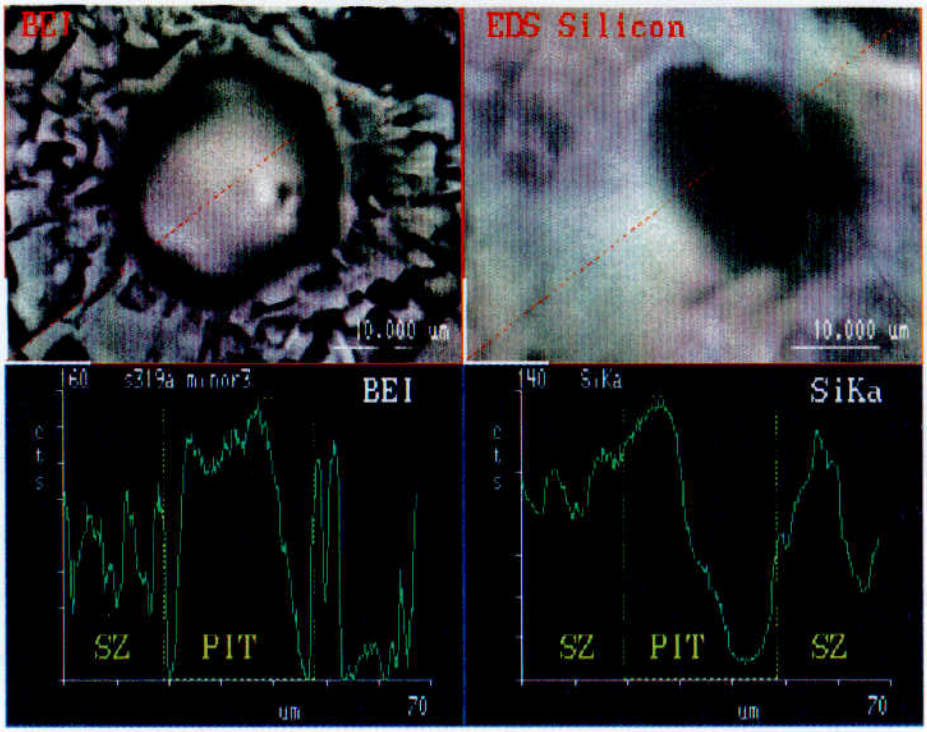

Figure 2.15 BE image of a crater (the red dotted line represents the linescan transverse taken across the crater). The line scan profile beneath the image identifies the topographic effect within the crater edges the count rate of detectable back-scattered electrons drops dramatically, whereas in the crater pit the count rate increases equally dramatically. The X-ray elemental map for Si identifies the shadowing effect. As with the topographic effect in the BE image, the line scan profile for Si shows the variation in the number of counts detected (image courtesy of A.T.Kearsley).

Topographic effects can also be observed in BE images (figure 2.15), although here it is due to a different interaction. The number of BE detected is dependent on the angle between the electron beam and the surface of the sample. Therefore, when BE-images are obtained for a crater, there is a possibility that the morphology of the crater may affect the image.

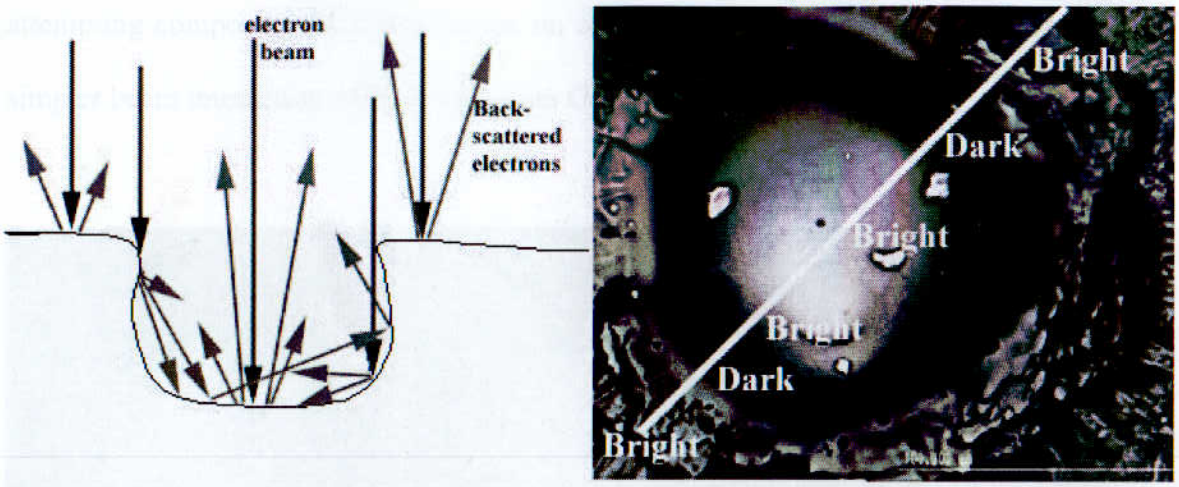

Figure 2.16 Shows a schematic diagram of the profile of the crater in the BE image. The diagram shows the trajectories of the back-scattered electrons (the grey arrows) as the electron beam moves across the crater profile. The white line in the BE image represents the transverse across the crater profile.

The topographic effect can be observed by examining a crater profile (figure 2.15 and figure 2.16). In figure 2.16, the flat surface of the sample prior to the descent into the crater allows the "normal" scattering of back-scattered electrons (see figure 2.17 at 0^{o} tilt) therefore a bright zone is observed in the BE image because a high proportion of the back-scattered electrons are being detected. Then, the descent down the crater wall identifies that the back-scattered electrons now show forward scattering (see figure 2.17 at 20^{o} and 45^{o} tilt). The result of which is that the number of back-scattered electrons detected at that point is considerably dramatically reduced (i.e. almost zero), resulting in a darker zone being observed in the BEI. The crater pit is essentially flat, so the number of back-scattered electrons detected increases at this point reflected in a brighter zone in the BEI. As the profile moves back up the crater wall, the BEI again contains a darker zone.

Finally as the profile moves away from the crater the BEI contains a brighter zone as the forward scattering has been reduced. The forward scattering of back-scattered electrons is affected by an increase in tilt angle. This is demonstrated by computer generated Monte Carlo electron trajectory simulations (figure 2.17). The effects highlight the difficulty of

attempting compositional interpretation on an uneven surface. A detailed description of simpler beam interaction effects is given in Goldstein et al. (1981).

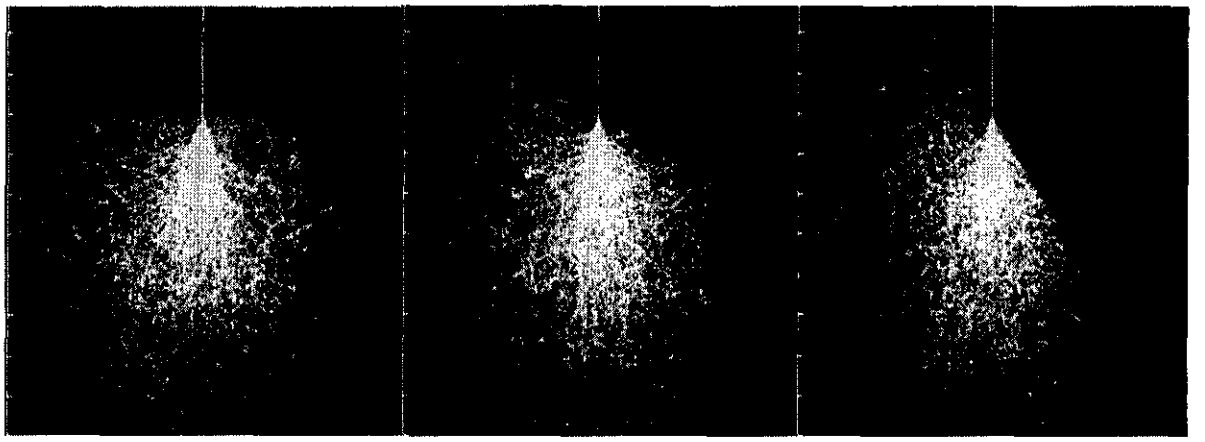

Figure 2.17 *Monte Carlo electron trajectory simulations for a silicon target at 20 kV and at increasing angles* of tilt at 0°, 20° and 45° respectively. Back-scattered electrons tend to travel in straight lines therefore as the angle of tilt increases the level of forward scattering increases. The image is courtesy of Oxford Instruments.

2.5.4. Absorption & Fluorescence

It has previously been shown that the uneven topographic surface of the craters can generate image artefacts. The uneven surface, however, can also generate data-interpretation problems in the X-ray micro-analysis. The main problems are absorption, fluorescence and geometry, which are typically considered as separate problems (e.g. Reed, 1996); herein they always occur together and are considered as a single problem.

The ideal analysis of samples would involve a flat surface in a position where the angle to the electron beam and the detector are known. Under these conditions, the measured X-ray intensities from the sample would only differ from those of a suitable standard because of composition (Goldstein et al., 1981). When characteristic X-rays are escaping to the detector, they will travel a certain distance within the sample and are therefore susceptible to absorption. This will result in the interaction with the atoms of the various elements in the sample, and so the intensity of X-rays measured by the detector will be reduced

(Goldstein et al., 1981). The morphology of the specimen can have a strong effect on the escaping intensity of the X-rays.

This essentially means that the location of the electron beam impact point on the sample in relation to the position of detector is an important factor. If a beam is focused on to an area of the sample that is facing the detector, then the absorption path is low and so a relatively unaltered spectrum can be collected (figure 2.18). However, if the beam is focused on an area facing away from the detector, then the absorption path is increased. The effect of this on the collected spectrum is that the low energy X-rays are not sampled efficiently, and the spectrum exhibits a "roll-off" effect (figure 2.18).

In Chapter 6, *microanalysis* was carried out on IDP particles. The effect of absorption again poses a problem, as the analysis is not carried out on a flat surface. As with the rough surface of the craters, the effect of absorption will be reduced or intensified relative to the positions of the electron beam and the detector.

As well as absorption, the characteristic X-rays of a specific element may be excited by other X-rays from other elements, if the energy of the latter exceeds that of the critical excitation energy of the former, i.e. fluorescence (Reed, 1996). This fluorescence effect always occurs due to the part of the bremsstrahlung line with energy above the critical excitation of the element of interest, yet this bremsstrahlung fluorescence is not as problematic as that generated by other elements (in HST solar cells, the characteristic elemental fluorescence is often generated by a Si peak).

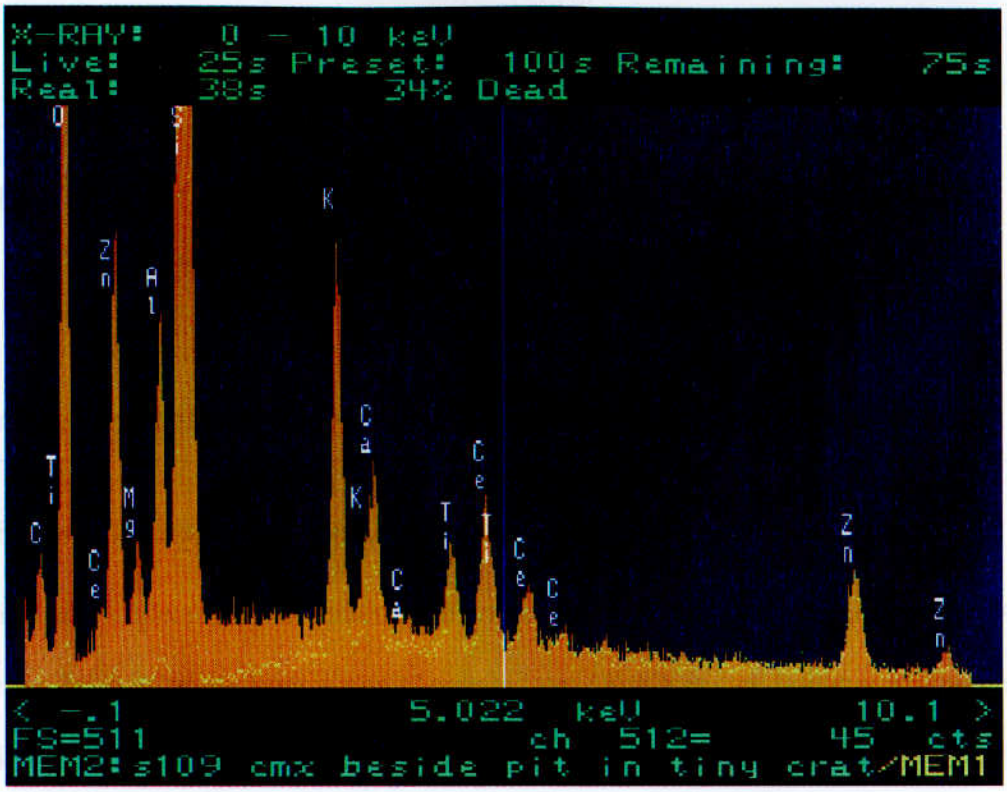

Figure 2.18 ED spectrum obtained for both a flat (the solid spectrum) and in the shadow zone of the melt pit on a solar cell (yellow dotted line). The yellow dotted line represents the spectrum obtained from the analysis of a point within a crater. The absorption effect is identified by the characteristic "roll-off" effect that the spectrum exhibits at the low kV.

2.5.5. Summary

The analysis of an uneven surface is does not provide ideal analytical conditions, and as has been highlighted here, can generate a number of artefacts. Whilst these artefacts can cause errors of data interpretation, an appreciation of all the potential problems means that their effects can be effectively accounted for. Problems of this nature have been taken into consideration in the rest of this project and no specific reference is drawn to individual cases where artefacts were encountered.

Chapter 3

The Development of Analytical Techniques for the Analysis of Impact Residues

3.1 Sample Selection, Post-Flight Survey & Early Analysis Attempts

3.1.1 Sample Selection: HST Solar Cells Versus EURECA Thermal Blankets

Previous dust collectors, i.e. dedicated micrometeoroid and space debris collectors, have been composed of single high purity elements, e.g. aluminium and gold, with the intention of making extraneous residues easier to identify. Clearly, the rationalisation behind using a single element collector was that any impact feature containing a complex elemental chemistry would be easily distinguished from the host itself. However, the LDEF investigations of the aluminium and gold collectors proved that this was not the case as it was difficult to locate residues (e.g. Bernhard et al., 1993(a) and Brownlee et al., 1993). The LDEF studies also highlighted a further complication in using aluminium collectors, since one of the main sources of space debris is from solid rocket motor (SRM) ablation products, which are identified by the presence of Al-oxides. Analytical equipment, for example an SEM, would not be able to identify the difference between Al-metal and Al-oxides unless fitted with a light element detector (Bernhard et al., 1993b).

Herein, various pieces of space hardware returned to Earth have been analysed to assess impact damage and the nature of hypervelocity dust in Low Earth Orbit. In each case, the hardware was designed and constructed for purposes other than micrometeoroid capture. Following on from the work of Wright et al. (1995a; 1995b) it seemed possible that such non-dedicated collectors were fortuitously quite promising. The goal herein was to push the analytical techniques to the limit and learn what could be achieved. Clearly if

successful, this would demonstrate the wide applicability of such studies, especially since various bits of space hardware are returned to Earth at regular intervals.

The timing of this project offered a unique opportunity to study two different sources of space hardware with impact damage from prolonged exposure to LEO. The two sources of hardware are individual solar cells from the -V2 wing of the Hubble Space Telescope (HST), which was successfully returned to Earth after it was replaced during the first service mission (Eaton, 1993; Flam, 1993), and the multi-layer insulation (MLI) blankets from the returned European Retrievable Carrier (EuReCa) spacecraft (Drolshagen, 1995). Both of these materials show evidence of extensive hypervelocity impact damage and thus both are suitable for detailed investigation for potential evidence of impactor origin and thoroughly assess the relative importance of micrometeoroids and space debris.

The two types of space hardware are very different in composition. The solar cells are a brittle composite consisting of a borosilicate glass (technically known as CMX glass) which is a protective top layer for the underlying silicon solar cells supported by an adhesive substrate containing a fibre-glass backing tape (figure 3.1). The elemental chemistries of the individual components within the solar cells can be summarised as follows (Berthoud, 1995): B,Si,O (CMX); Si (solar cell); Si, Ca, Al and Mg (adhesive substrates).

There are essentially two types of EuReCa thermal blankets (Aeritalia Space Systems group, 1989). Type 6 MLI (figure 3.2) which was the main type used to cover the exposed surfaces of EuReCa consists of (1) an upper layer of woven teflon-coated fibre-glass known as β-cloth; (2) a layer of kapton-coated with aluminium with a top coat of acrylic on the inner surface; (3) 19 alternating layers of kapton coated on both sides with aluminium and acrylic and 20 layers of Dacron net; (4) is a thick kapton layer coated on

the inner surface with aluminium and acrylic. The elemental chemistries of the individual components within the thermal blankets can be summarised as follows from Berthoud (1995): F, Si, Ca, O, C (β-cloth); Si, Al, Ca, Mg, O (fibre-glass layer in β-cloth); C, O, (75 μm single aluminised kapton); C, O, Al (7.5 μm double aluminised kapton); C, O (Dacron net – each strand approximately 15μm in diameter) and Si, Zn, O (paint PSG-120-FD).

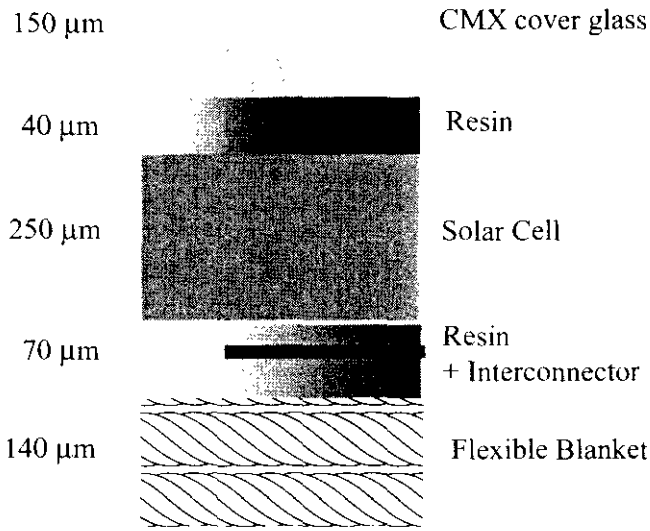

Figure 3.1. A cross-section drawing of a solar cell based on the ESA schematic (Berthoud and Paul, 1995).

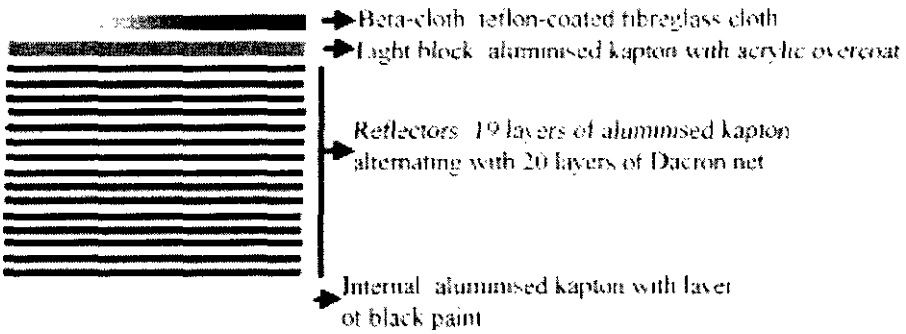

Figure 3.2 A diagram of a Type 6 multi-layer insulation (MLI) blanket from EuReCa based on the ESA schematic (Carey, 1998).

Neither the HST solar cells nor the EuReCa MLI blankets would appear to be ideal substrates upon which to search for remnants or residues of micrometeoroids as both contain key elements (Si, Ca, Al, Mg) which have previously been used as indicators for

particles of natural origin (Zolensky et al., 1993). Since both substrates pose analytical problems the choice of hardware for study was based on other factors; the most significant factor was to assess which of the two substrates was most likely to yield information on the origin of any impact particle, i.e. which would be most likely retain enough quantities of residue that could be analysed under the analytical SEM. Information on the nature of an impactor is clearly only possible if original material is retained in the impact feature.

The brittle nature of the cells offers the potential, if the impact feature generates a crater rather than a hole (figure 3.3) then it is possible that material might be retained and in quantities that may be analysed. The nature of the MLI blankets means that impactors penetrate through a variable number of layers of the blanket, depositing material on all of the layers it traverses. Secondly, although the aluminised kapton layers are flexible, the β-cloth of the MLI blankets is not and like any brittle substrate, shatter when involved in a hypervelocity impact event. This shattering means that fragments of β-cloth are deposited on the subsequent aluminised kapton layers generating secondary debris which has a similar chemistry to micrometeoroid debris. It would be almost impossible to distinguish unambiguously the elemental difference between a Mg-Fe residue (i.e. the remnant of an olivine-rich micrometeoroid impactor) and Mg-Fe debris from β-cloth.

It is likely that the hypervelocity impact event would have altered both to such a significant degree that textural morphological differences would be ambiguous as well. Thus, the search for impactor debris would be extremely time-consuming, as every layer impacted would have to be analysed. Wright et al. (1995a) have concluded that only 8% of all impact features were caused by natural samples. Since one of the aims of this thesis was to investigate the mineral chemistry of micrometeoroids, and as MLI blankets would appear not to yield the highest potential to retain or harbour such material, the blankets were not studied.

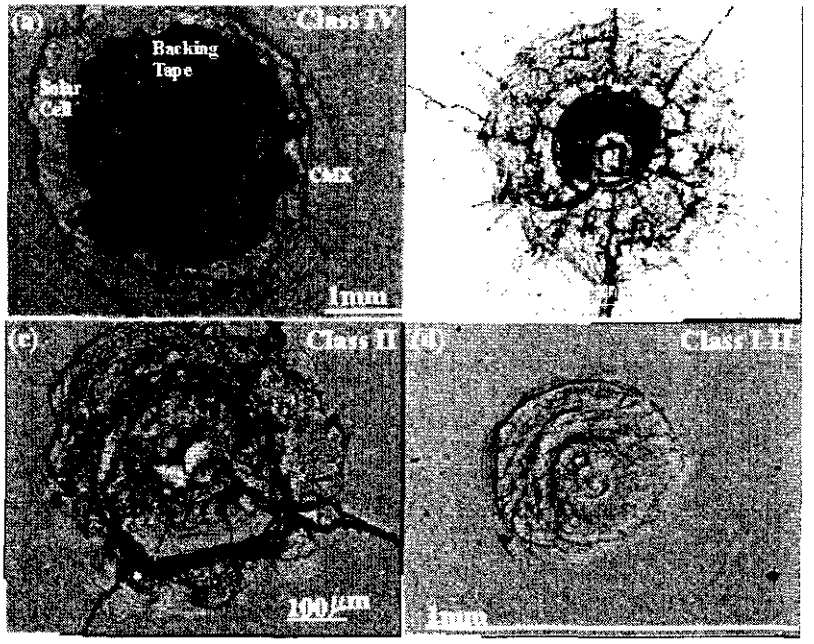

Figure 3.3 Back-scattered electron images of the various types of impact features identified in the HST solar cells. The craters are classified by morphology based on the criteria used by Herbert and McDonnell (1997).

3.1.2 Previous Attempts To Identify Impact Residues In HST Solar Cells

As outlined above, solar cells are composite structures that contain elemental constituents (e.g. Mg, Si and Ca) which, in previous studies (e.g. Bernhard et al., 1993b), have been used as indicators of impact residues. Because of the brittle nature of solar cells, the majority of the projectile residue (if not lost due to later spallation) is found located in the central melt pit. This is in distinct contrast to the typical impact features generated in the Al and Au substrates from the various LDEF experiments (Bernhard et al., 1993b) where the impact events generated craters of simple ductile morphologies (Hörz et al., 1983 and Melosh, 1996) and often residues were located within the cavity of the entire crater bowl.

For brittle substrates such as the solar cells the typical impact features (figure 3.3,) consist of complex radial and conchoidal fractures with extensive spallation zones. Therefore in the solar cells, the melt pit (if one is retained instead of detachment to create a hole) is often the result of mixing of both the cell and the impactor material. As such, impact residues are often complex consisting of up to five major components: (1) impactor

fragments; (2) impactor melt; (3) mixed impactor and cell melt (this can be composed of several different cell substrates depending on crater depth and damage); (4) cell fragments and (5) cell melt.

Thus, for impacts in solar cells, the identification and subsequent classification of any extraneous material is complicated and in some residues may prove to be ambiguous. This ambiguity was clearly identified in the original post-flight survey for residue chemistries were the number of solar cells which were classified as unknown was as high as 62% of the total number investigated (Carey, 1998).

3.1.3 Preliminary Survey Of HST Solar Cells

To assess whether HST solar cells would be suitable substrates to document the nature of particles in LEO a preliminary electron microscopy survey was carried out using a Jeol JSM 820 SEM fitted with an integrated Kevex DELTA energy dispersive X-ray analyser (EDX) for qualitative analysis and a Hitachi S2500 SEM fitted with a LINK Analytical system AN10000 ED X-ray analyser. The typical operating conditions for either SEM were an accelerating voltage of 15kV, a beam currently of 1nA and a working distance of 39mm. The samples were all carbon-coated to reduce the effects of electrical charging during analysis (see Chapter 2.5.1).

The samples were initially investigated using secondary electron imaging, which enabled the individual impact to be classified in terms of morphology (using the classification scheme in figure 3.3): (1) complete hole (generally 1mm diameter or greater) where all the layers of the solar cell had been penetrated (**CLASS IV**); (2) impact crater (200μm-1000μm diameter) which had penetrated varying layers of the cell but not completely penterating the entire structure (**CLASS III**); (3) impact crater (<200μm), which only

penetrated the very top layers of the cell structure, i.e. the protective top CMX glass and the silicon cell layer beneath (**CLASS I-II**). The maximum depth of this type of crater is approximately 220μm.

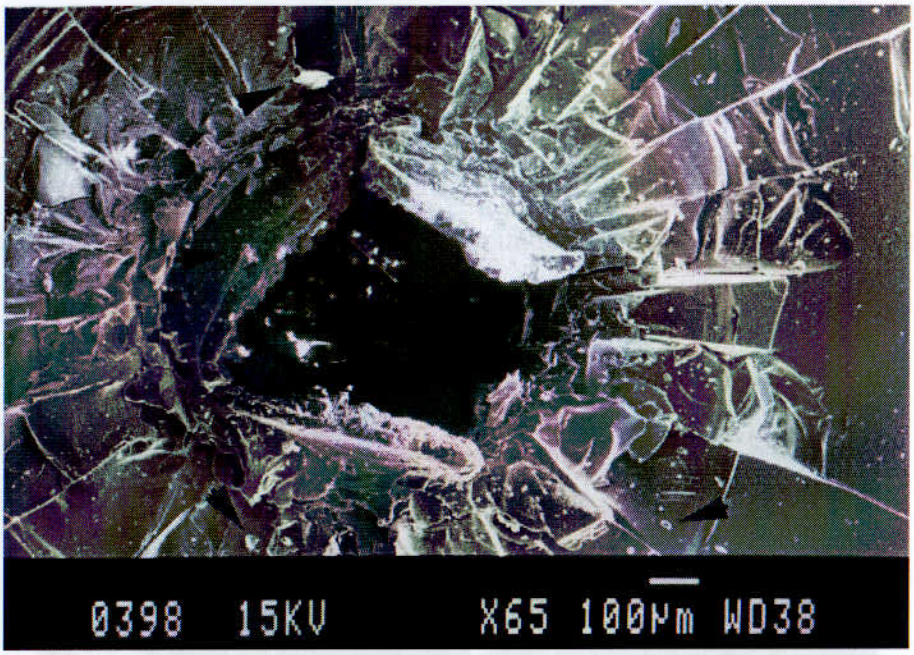

Figure 3.4 A secondary electron image of a large impact hole (CLASS IV, as described in text) investigated in the preliminary survey. From the image, it is possible to see the extensive shattering that occurs to the CMX glass during an impact event. The black arrows identify fragments of debris material which have been generated by the impact event but their origin is from the solar cell itself rather than the impactor.

For the preliminary EDS investigation one of each of the three types of impact feature (above) were examined. It was extremely difficult to locate any extraneous material in the sample containing the impact hole (CLASS IV) which was a 1mm diameter feature with extensive damage to the cell. However, micron-sized debris fragments could be located in the secondary electron image (SEI) (figure 3.4). The debris comprised fragments of the upper layers of the cell (most likely fragments of the borosilicate CMX cover-glass) which had been shattered and re-deposited during the impact event. As before, whilst there appeared to be abundant, micron-sized debris fragments in the craters, EDS spot analysis revealed that the fragments were mainly small pieces of re-deposited solar cell.

Two solar cells containing impact craters which had penetrated just the upper layers of the cells (type CLASS III) were also found to contain abundant, micron-sized fragments when examined in SE imaging but as with the previously examined samples these were identified as host debris. Solar cells with top surface impacts (CLASS I-II) proved difficult to analyse for residual impact material because the extensive shattering which accompanied those shallow impacts meant that it was impossible to give the sample an even carbon coat (and, as such, sample charging under the SEM was a major problem).

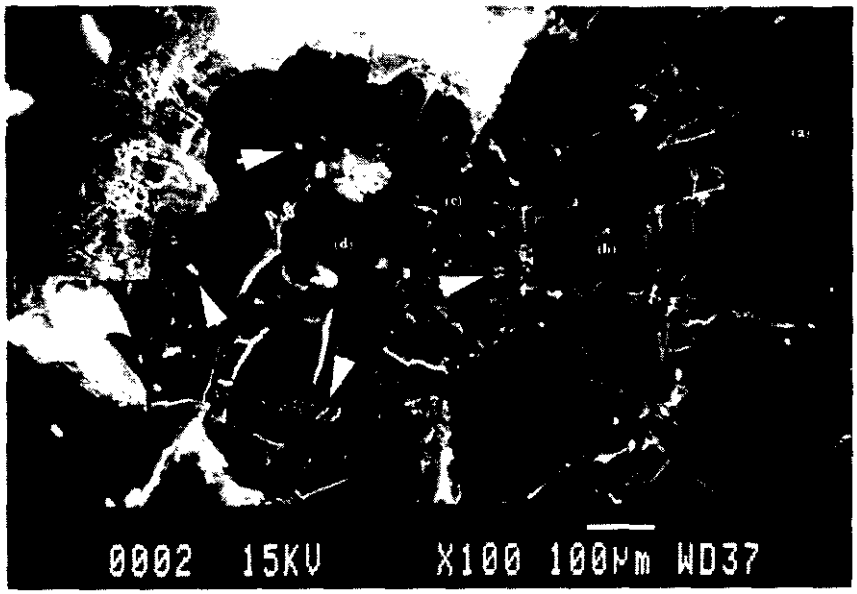

Figure 3.5 A secondary electron image of an impact crater (CLASS III) showing a stepping morphology (a) is the top borosilicate CMX layer of the solar cell showing fracture damage; (b) extensively shattered CMX layer, note that area where the crater has formed there has been complete detachment of CMX; (c) the top of the silicon layer, the white arrows identify debris fragments, these are unlikely to be extraneous debris, but rather fragments from the shattered CMX glass layer; d) the inner crater within the silicon layer.

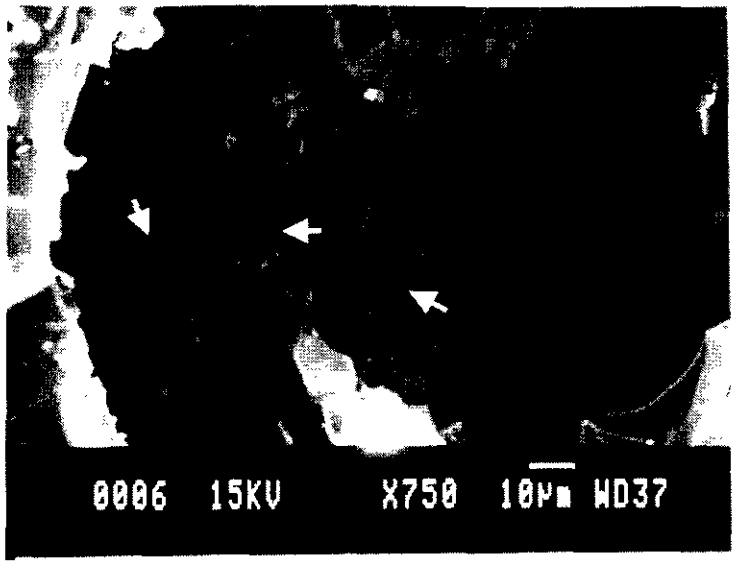

Figure 3.6 A secondary electron image of the inner crater identified in figure 3.5. The white arrows point to the debris material that appears to have a melt texture and is therefore possible impactor remnants.

The preliminary examination of the four impact features suggested that single EDS spot analyses of individual debris fragments associated with a crater was both time-consuming and rarely a profitable method of searching for impactor remnants. It should be stated here that this was the approach used by Wright et al. (1995b) which must have suffered in the same way. In an effort to overcome these problems, the final sample in this preliminary investigation was treated to a somewhat to a different analytical approach. The impact crater that was studied (figure 3.5) was a large conchoidal fracture (1mm diameter), which comprised a stepped morphology, a crater platform (350µm diameter) and a crater pit (100µm diameter).

As with the previous samples there was abundant debris located on the crater platform, but this appeared to be particulate and unmelted in texture, and was considered likely to be debris from those layers that were removed by the impact. Instead of single spot analyses the entire crater was subjected to X-ray elemental mapping (whilst the Kevex EDX software did not allow digitised acquisition, the basic principles of X-ray elemental mapping are the same, see section 2.3.3 for a discussion). Therefore, at a pixel resolution

of 256 x 256 and for 1 frame, the inner crater (figure 3.6) was mapped for the following elemental distributions: Si, Ti, Al, Ca, Mg, Ce and Na. This combination of elements was used as they the most likely elemental combinations for remnant micrometeoroid or space debris material (Zolensky et al., 1993).

Detailed study of the X-ray maps identified a residue that was enriched in Mg and Fe compared to the host (due the dated nature of the output device of the Kevex EDX software it was not possible to include the elemental result sheet of the mapping in this chapter as it did not reproduce well). It was apparent that X-ray mapping had identified material extraneous to the solar cell. Indeed enrichments of key elements such as Mg and Fe strongly suggested an impact by a natural micrometeoroid. Following on from mapping the residue and the surrounding area were subject to detailed ED spot analysis. It very quickly became obvious which areas contained the Mg/Fe signal (impact melt) and which did not (underlying solar cell, or melt cell material). The presence of elemental chemistry from the solar cell composition in the residue suggested that an extremely complex melt process must have occurred during the impact event.

For this particular crater it was not possible to classify the residue in mineralogical terms (e.g. olivine or pyroxene), but using the LDEF criteria (Zolensky et al., 1993) the residue would have been assessed as natural. It was concluded that the impactor was a probable Mg-Fe silicate dominated micrometeoroid.

3.1.4 Conclusions From The Post-Flight Investigation & The Preliminary Survey.

A discussion of attempts by other scientists to identify impact residues in the HST solar cells was given in Chapter 1.5 and section 3.1.2 of this chapter. The conclusions for these investigations (e.g. Wright et al., 1995b) and possible improvements in the efficiency of

analytical surveys were stated in work package 4 of the "Micrometeoroid & Debris Flux and Ejecta Models" contract (ESA contract no. 11887/96/NL/JG) (Carey, 1998). The initial investigation by the author (section 3.1.3) was presented at the 31st COSPAR meeting, in a session on space debris and resulted in the Graham et al. (1997a) publication (see appendix 5). The requirements for the improvements in analytical methodology and chemical classification of residues in solar cells can be summarised as follows:

Since there are a large number of individual solar cells with varying degrees of impact damage (from shallow oblique craters < 10μm in diameter, to large holes of mm dimensions), to optimise the chances of detecting a remnant of the impactor, samples must be selected accordingly. The best hope of accomplishing this is to use a class III impact, e.g. the residue identified in Graham et al. (1997a) was in a 500μm diameter crater.

Once appropriate impact features have been identified, analytical protocols must allow rapid screening for potential impact residues. Techniques such as TOF-SIMS (Chapter 2.1) require typically 12 – 20 hours for the sample to be evacuated prior to analysis (Stephan et al., 1995). Such a long wait is due to the composition of the solar cell (e.g. outgassing of the silicon adhesive) (Stephan et al., 1995). Therefore, it is not viable in terms of analytical time to use such a technique as a search tool, but rather to further characterise the residues once found. Scanning electron microscopy would seem an appropriate method, yet the micrometeoroid residue described in section 3.1.3 (Graham et al. (1997a)) took approximately 30 hours of analytical time to locate, so improvements are required.

The composition of the solar cell is extremely complex, as it contains elemental signatures which in previous studies (e.g. Zolensky et al., 1993) have been used to identify micrometeoroid residues (e.g. Mg and Ca). It is important to obtain qualitative ED spectra of the cell components that have not been altered by an impact event. This will allow

comparisons to be made between altered and unaltered cell material and therefore identify any possible enhancements in the essential elements (e.g. Mg and Ca), i.e. an ED spectra is obtained on the surface away from the impact feature.

To date, the investigations on space hardware, apart from specific physical collector experiments (e.g. Bernhard et al., 1993a) have generally concentrated on flux modelling for micrometeoroids (e.g. Grün et al., 1985) and space debris (Kessler et al., 1989). For flux modelling (i.e. calculating the mean annual value of a defined particle population impacting on to a defined surface) it is only necessary to provide a simple distinction between artificial (space debris) and natural (micrometeoroid). In the absence of an effective distinction, some assumptions may be made here. For instance, large holes may be ascribed to natural (fast moving) samples, whilst small craters may be considered to be relatively low velocity space debris – clearly it is necessary to search for absolute ways of distinction.

Furthermore LEO collections are also scientifically interesting in their own right and allow an examination of natural particles which have not experienced any of the selection effects that occur when materials enter the terrestrial environment (Zolensky et al., 1994). Thus, it is important not merely to distinguish natural samples but to extract the maximum yield of information regarding their nature. Ultimately it would be hoped that the LEO particles could be sub-classified in terms of mineralogy (mafic- or layer- silicates) and groupings (hydrous or anhydrous) thereby providing information that is comparable with both IDPs and micrometeorites, e.g. as summarised by Klöck and Stadermann, (1994).

The work described in the rest of this chapter is an account of the development of survey techniques which allowed the rapid and reliable identification of impact residues in

hypervelocity impact (HVI) produced craters and meet the kind of challenges expounded by Carey (1998).

3.2 Evolution Of Protocols Associated With Sample Selection

An original set of HST solar cells analysed by Wright et al. (1995b) comprised large impact features, with crater diameters up to 2mm. Of the 26 samples that were analysed in that study, 35% were full-thickness penetration holes (CLASS IV) rather than craters (Figure 3.7). Whilst these were easy to locate, being readily visible to the naked eye, they offered little opportunity for retention of impactor material (section 3.1.3). In the present study, impact holes of CLASS IV were avoided in preference to craters of CLASS II-III.

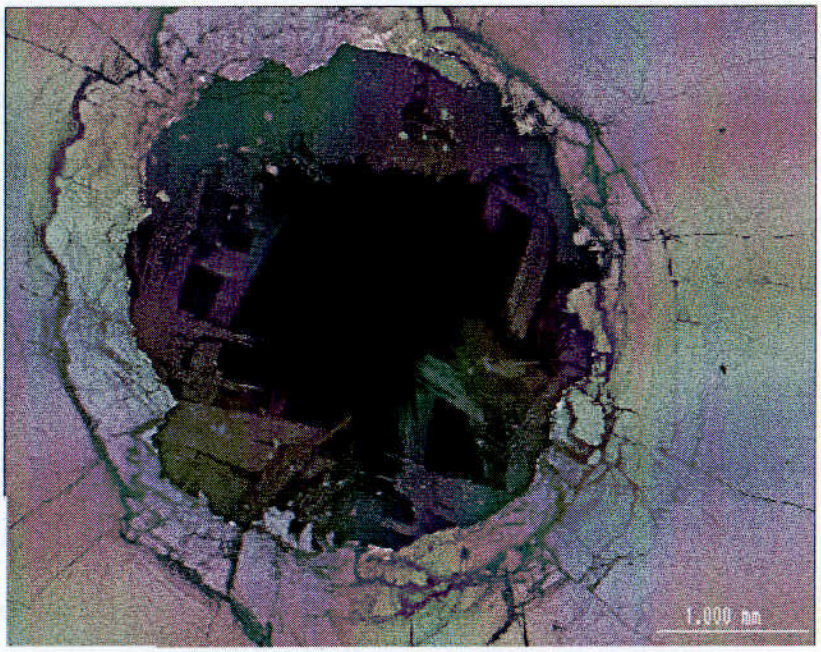

Figure 3.7 A back-scattered electron image of a typical impact hole (CLASS IV) investigated by Wright et al. (1995). The impact has generated extensive damage to the cell and there is little trace of residual material (the broken criss-crossed material evident in the lowest layer is where the impactor has ripped through the backing tape of the solar cell).

The micrometeoroid residue identified in Graham et al. (1997a) was in a smaller class III crater, suggesting that if small features were studied (i.e. classes I-III) there might be a better chance of preservation of impactor material. From this observation a further 25

individual solar cells (appendix 1 contains optical images of these samples) were requested from ESA/ESTEC for residue analysis; all of these samples contained the smaller impact features.

3.3 Detailed Analysis Of An Individual Solar Cell

Since the HST solar cells were not designed as collectors for LEO particles, their constitution had not been optimised for this purpose. Indeed they had been constructed specifically to provide a degree of durability in LEO and thus resistant to possible impact damage from micro-particles. As such some of the compositional details remain proprietary information to the manufacturing companies of the solar cells (e.g. Pilkingtons, U.K. and Matra Marconi Space, U.K.). However, it was clearly going to be impossible to search for impact residues without understanding in detail the composition of the host. Thus it was necessary firstly to undertake a complete analytical examination of the component parts of the cell.

When the HST solar cell studies of Wright et al. (1995b) were carried out, all that was available at the time was a schematic diagram of the cell, and brief manufacturers details of the composition (figure 3.1). It is clear that for the kind of detailed work that was hoped to be pursued herein, the previous level of understanding of cell composition was nowhere near adequate. To redress this situation a non-impacted solar cell was mounted in epoxy resin and cut to produce a transverse polished section. The section was then examined under the SEM using back-scattered imaging (figure 3.8) and elemental X-ray mapping to constrain the composition (appendix 2 shows the detailed maps) in great detail.

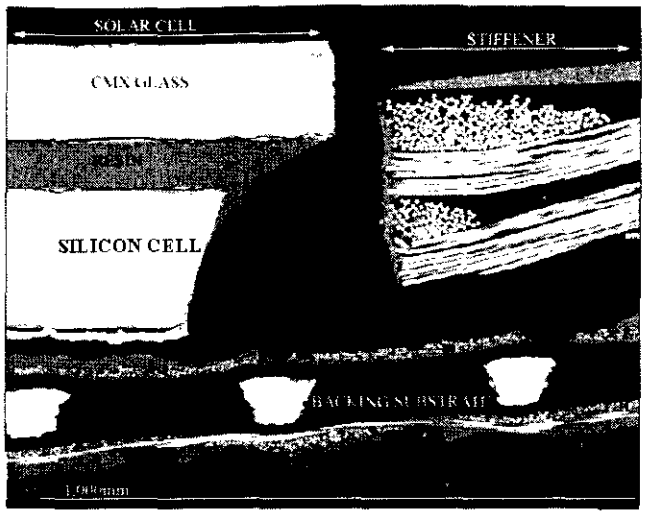

Figure 3.8 A back-scattered electron image of a cross-section made through an individual solar cell and the supporting resin stiffener.

In brief, the cells are made of a top, protective borosilicate CMX cover glass (150μm thick) which has an upper, ultra-thin Mg and F coat on the surface (which acts as an anti-reflective layer). The cover glass is bonded by a 40μm thick layer of *silicone resin* (DC 93500) to the underlying silicon solar cell (250μm thick), below which is a 0.9μm layer containing Al and Ti (figure 3.9) supporting a silver connector strip which runs through the cell (and through which the electrical power is transmitted).

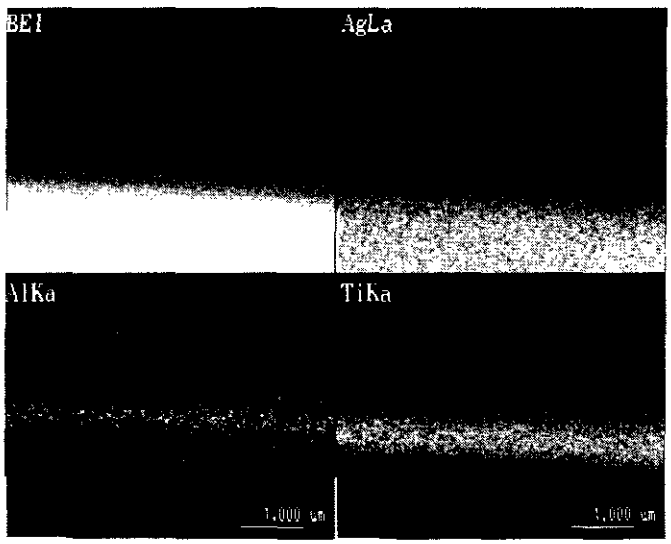

Figure 3.9 Shows the presence of the Ti and Al layer within the Ag connector (all images are to the same scale).

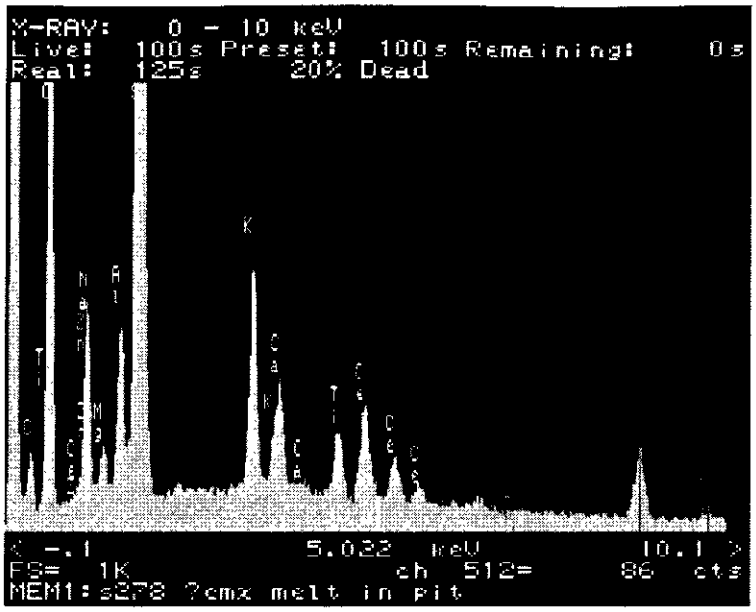

Figure 3.10 An Energy-Dispersive spectrum identifying the elemental composition of the CMX glass.

Under the connector there is a second layer of silicone resin (RTV S691) (70-80μm) which is bonded to a fibre-glass backing tape (100μm thick). The main elemental components of the cell can be summarised as the following: CMX glass (figure 3.10) - Si, Ce, K, Zn, Ti, Mg and F; upper silicone Resin - Si; Solar cell - Si, lower silicone Resin (containing silver connector) - Si, Ag, Ti/Al; Backing tape - Si, Ca, Al, Mg.

3.4 Classification Of Impact Residues

In previous studies, the classification of impact-derived residues in space hardware as either micrometeoroids or space debris, is based on that used during the post-flight analyses of hardware returned from LDEF (e.g. Zolensky et al., 1993). Unfortunately the chemistry of the HST solar cells complicates the identification of extraneous melt residues, because elemental "fingerprints" used previously as indicators of micrometeoroid origin (e.g. Si, Mg and Ca), are fundamental constituents of the cells themselves. Identification of extraneous material is further complicated by the fine-scale mixing that occurs between melted host and impactor.

However, the detailed characterisation of the host solar cell composition carried out in section 3.3 enables such effects to be observed and, in consequence, it has been possible to propose a classification scheme which allows distinction between micrometeoroids, space debris and contamination.

3.4.1 Space Debris

ED spectrum and X-ray elemental maps that contain the following are used as indicators of impactors of artificial origin (i.e. space debris):

- Mainly Ti + possible minor C,N,O (paint fragment)
- Mainly Fe + variable Cr, Mn + possible trace Ni (specialised steels)
- Mainly Al + minor Cl, O, Cr (rocket propellant)
- Mainly Sn + Cu (computer or electronic components)
- Enrichments in Mg, Si, Ce, Ca, K, Al, Zn (glass impactor, possibly from other solar cells)

The presence of the Ti/Al layer within the solar cell (section 3.3) complicates the identification of artificial impacts since Ti has been traditionally used as an indicator of paint fragments. In the HST survey of Wright et al. (1995b), solar cells containing Ti, Al, Ag were ascribed to artificial debris particles, such as paint fragments; on the basis of the work herein it is clear that Ti/Al elemental compositions could be due to host chemistry and have no bearing on impactor origin. Thus, whilst Ti on its own is probably a good indicator of paint fragments, when observed along with Al and Ag, it is more likely to represent a melt from the host solar cell.

3.4.2 Micrometeoroids

HVI events may well modify the original chemical composition of an impactor, fractionating volatile from refractory elements. Thus micrometeoroid residues may not

retain the stoichiometric chemical signature of their parent mineral; in which case analytical results may not easily be compared to those of mineral standards. Notwithstanding such difficulties, ED spectra and X-ray elemental maps of residues that contain the following are used as indicators of a micrometeoroid origin:

- Mg + Si enrichments above the expected concentration of the cell + Fe (mafic silicates, e.g. olivine or pyroxene)
- Fe + S (Fe-sulfides)
- Fe + Ni minor or trace + S (Fe-Ni sulfides)
- Fe + Ni concentration at meteoritic levels (metal)

In reality because of the complexity of any original micrometeoroid (being a poly-mineralic composite) it is entirely possible that a single impactor could produce any number of the above.

3.5 Contamination

Apart from the classification criteria given for residual material of either micrometeoroid or space debris origin, there is a strong possibility that the solar cells may also be subject to contamination. There are several different possible sources of contamination, arising from laboratory handling, to ground exposure, to LEO itself whereby contaminants are effectively imparted at low velocity and are thus only loosely bound. The possible sources of contaminants are given below.

3.5.1 Salt Crystals

The origin of alkali-halide crystals (KCl/NaCl) as both surface particles and impact residues is open to a certain degree of speculation. The HST solar array was retrieved from LEO by the Space Shuttle, which was itself launched from the Kennedy Space Centre (KSC) at Cape Canaveral (Florida, U.S.A.). As the KSC is located near to the coast, the

localised atmosphere unquestionably contains oceanic sea-spray, and thus there is the possibility of contamination from this source during launch or subsequent recovery. This source of contamination was documented in the case of LDEF studies (e.g. Crutcher et al., 1991 and Zolensky et al., 1993).

Further to this, ESTEC (in the Netherlands), where the solar array was taken after retrieval, is also located near to the coast and even though the array was stored in clean-room facility there is still a possibility of contamination with maritime air. A second source of salt crystals is from human waste products (urine) in LEO (Wright et al., 1995 and Hörz et al., 1998). Although in any particular instance either sea-spray or human waste, are the most plausible sources of salt crystals, there is also the possibility that if located in a crater and as a result of HVI, the origin of the crystals could be extra-terrestrial. On LDEF surfaces, NaCl and KCl particles were identified yet the origin remained undefined (Crutcher et al., 1991).

The recent discovery of halite (NaCl) and sylvite (KCl) in the Monahans H5 ordinary chondrite meteorite (e.g. Gibson et al., 1998), along with known salts from carbonaceous chondrites (e.g. Barber, 1981) and martian meteorites (e.g. Wenthworth and Gooding, 1988 and Bridges and Grady, 1999) have shown that salt crystals can be contained within a surprising range of meteorites. Therefore, it is impossible that during collisions between small bodies, individual salt crystals could be released. Unfortunately, it would be almost impossible to prove the extraterrestrial origin of such particles simply from the mineralogy or chemical compositions.

3.5.2 LEO Contamination

During the 1320 days that the HST was in orbit, a Russian 'RORSAT' nuclear-powered satellite in a higher orbit was reported to have had a leakage in the coolant system. These systems are known to be cooled by liquid Na and K, which when exposed to space would form globules. These would pose a threat to satellites such as the HST in LEO as they spiralled down towards Earth by gravitational attraction. Enrichments of Na and K were identified in several impacts in HST solar cells (Heiss and Stadermann, 1995), but since these were associated with Mg and Ca, it seems more likely that these resulted from the CMX host melt rather than an exotic origin. It is entirely likely that globules of Na could produce impact damage on space hardware and not necessarily leave a remnant of itself. This could go some way to explaining craters with no detectable residues.

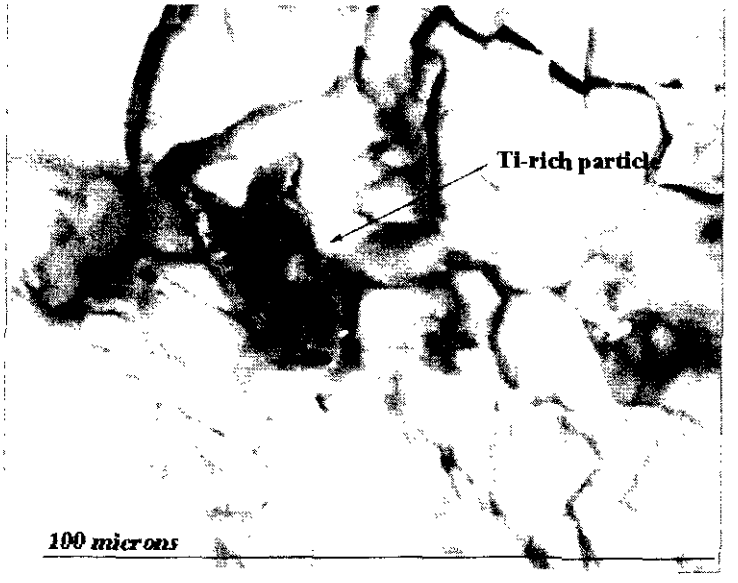

Figure 3.11 A back-scattered electron image of a Ti-rich particle that was found associated with a micrometeoroid-produced impact crater. The particle is fused to the spall zone of the crater. Although the particle is extraneous to the cell composition, it was not responsible for the impact damage.

One of the solar cells examined in the present study (Chapter 5.1) contained an impact crater that was clearly generated by a natural micrometeoroid yet it also contained a Ti-rich particle in a matrix rich in C, N and O, suggestive of a paint fragment and associated

bonding polymer. This fragment was fused to the rim of the crater (figure 3.11) but no melt zone was observed. This implies that it is possible for cells, or indeed any space hardware, to collect low velocity particles that may or may not be the cause of impact damage. This finding shows a complication to post-flight investigations, since it is clearly possible to misidentify the cause of damage.

3.5.3 Terrestrial Artificial Contamination (TAC)

Although once returned to *terra firma*, the HST solar array was stored in a clean-room facility at ESTEC, there are still a number of possible artificial sources of contamination that could have been imparted on the ground. The cutting of the array into individual solar cells could produce fragments of the cell itself, or particles from the stainless steel cutting tool (Drolshagen, personnel communication). Furthermore, if the cells are not handled with clean gloves they may be susceptible to contamination from skin particles, fingerprints etc. Also there may be contamination from the clean-room clothing, as identified in LDEF studies (Crutcher et al., 1991). Furthermore since a number of mechanical devices (e.g. hoists) were used to suspend the array within the clean room it is possible that small drops of lubricants or abraided metal fragments may have contaminated the cells. A common feature of all forms of TAC is that they are represented by loosely attached particles on the cell surface and are not necessarily associated with an impact feature. Such particles are generally not a problem when using the SEM as they are removed either during pumping or subsequent charging when hit by the electron beam.

3.5.4 Laboratory Contamination

Whilst all the samples, once they had arrived in our laboratory, were handled with extreme care, it is possible that prior to introduction into the SEM, they may have become contaminated during preparation. For instance, to prevent charging during analysis (see

Chapter 2.5) the samples are coated with a layer of carbon. Since carbon is one of the target elements of interest this might be considered unwise. However, in practice it is almost always possible to distinguish between the carbon from coating and any particulate carbon from an extraneous source. The carbon in the coating gives very little X-ray absorption or X-ray signal.

To ensure the electrical conductivity of a carbon-coated sample surface, a small amount of silver paint is used to connect the coat to the sample holder. Although caution is taken not to contaminate an obvious impact crater with the paint, it is clear that in the process a minor impact feature may become compromised. However, silver paint has a very distinctive and easily identified ED spectrum; furthermore the unmelted texture of the dried paint is different from that of impact residues.

3.6 New Analytical Protocol For Searching For Impact residues

For the 25 HST solar cells samples specially requested from ESTEC for this study, a preliminary survey was carried out using a Zeiss-Axioplan universal optical microscope (at the Open University) at x10, x20, x40 magnifications, to locate impact features. These were subsequently examined using a Leitz Wild M8 optical microscope fitted with a Sony DKC5000 digital camera (at the Natural History Museum).

The detailed examination was carried out using a Jeol JSM 840 scanning electron microscope (SEM) fitted with an Oxford Instruments e-XL X-ray energy dispersive spectrometer (EDS) (at Oxford Brookes University). The samples were carbon-coated to reduce the effects of electrical charging during SEM investigation. The analytical work was carried out at an accelerating voltage of 20kV with a beam current of 2nA and working distance of 32mm. In a few cases high-resolution imaging in secondary and back-

scatter modes were carried out on a Philips XL FEG SEM (at the Natural History Museum); for this the analytical conditions were an accelerating voltage of 5 kV and a working distance of 15mm.

The SEM investigations initially used digitised back-scattered imaging (BEI) of the impact crater at a low magnification (<x250), but at a high pixel resolution (512 x 512 point matrix with repeated Kalman frame averaging to increase signal-to-noise ratio in the final image). The impact pit was then examined at higher magnification (>x250) to identify any areas of melt that contained residual material from the impactor. Areas of interest were then mapped for 22 characteristic X-ray intervals at low resolution (each frame of 128 x 128 pixel resolution took approximately 15 minutes to complete). Higher resolution and magnification maps (e.g. 256 x 256 pixel map) with repeated frame averaging (e.g. 12 frames) to yield high contrast were then carried out if required (these took typically up to 12 hours to complete).

For the purpose of identification between artificial and natural residues, low-resolution maps were adequate in most cases. However higher resolution map, were essential for more detailed research especially where potentially interesting residues of micrometeoroid were encountered. Following the identification of an interesting residue by X-ray mapping a more detailed classification was obtained from EDS spot analysis (1μm spot diameter). These semi-quantitative analyses (100 seconds was the usual analysis time) produced ED spectra that could be compared to schemes outlined in section 3.4. To reduce the possibility that an individual residue was only a melt from the cell itself, additional ED spectra were collected from any local host melt. The ED spectra of unmelted CMX glass would always be collected away from the impact site to provide a "clean" spectrum thereby acting as a calibration check on the instrument. The data handling software of the SEM allowed the ability to overlay different spectra, which meant that it was possible to

identify any minor chemical variations that were apparent from cell to cell. The same software was used to detect any enrichments in elements that could be diagnostic of an impactor (e.g. Mg) and to compare any particle residue spectra with those obtained from known meteorite mineralogies (the latter provided by A.T. Kearsley at Oxford Brookes University).

3.7 Experimental Methodology

3.7.1 Optical Survey

In previous investigations (e.g. Mandeville et al., 1995) optical microscopy has played an important role in the description of crater morphology. However, morphological information alone does not constrain the origin of individual impactors. Herein a preliminary optical survey was conducted to select impact features that were considered most likely to contain residue material (i.e. crater classes I, II and III). Normal scanning magnification for investigating solar cells is at x5 or x10 using a binocular microscope. Using a petrographical microscope at higher magnification (>x20) it was possible to assess whether or not debris or melt material was present within the crater pit (which in turn suggested whether a sample was worthy of further detailed investigation). Residual materials located by optical microscopy often appeared as black, metallic, fibrous particles above the underlying substrate of the solar cell (figure 3.12).

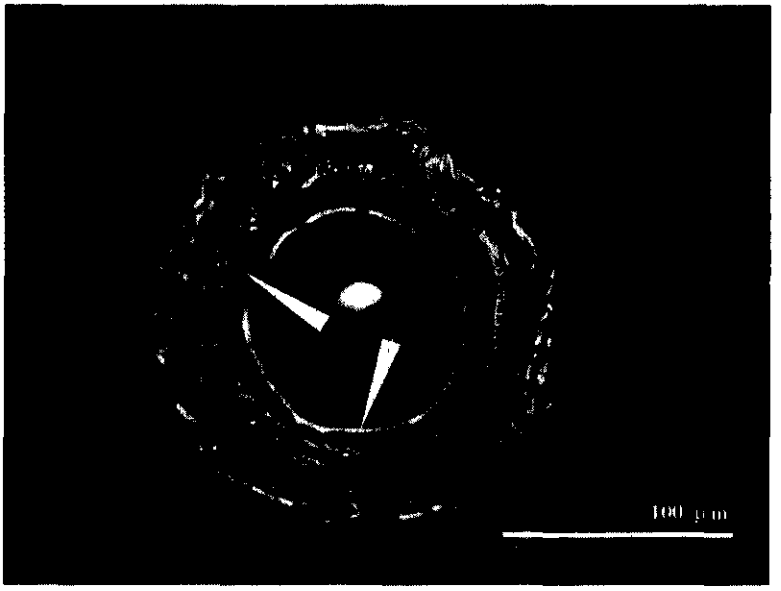

Figure 3.12 An optical image of an impact crater (x40 magnification), the white arrows identify dark particulate material within the crater that may be fragments or residue from the impactor.

3.7.2 Digitised Back-scattered Electron Imaging

Once potentially interesting residues were identified by optical methods, they were analysed on the SEM and digital images were collected using the frame averaging software as before (see Chapter 2.4). BSE images collected in this way show information not only of topography but also, more importantly, of compositional contrast between individual pixels (see Chapter 2.4). In this way it was possible to distinguish the elemental chemical changes within the different layers of the cells and also where extraneous matter had been added (figure 3.13).

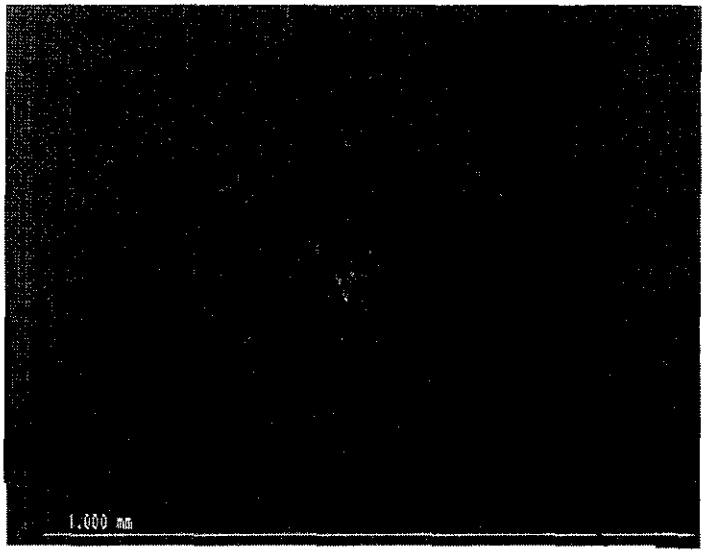

Figure 3.13 A BEI of an impact crater. The bright and dark areas in the crater pit are residue components and the dark area around the crater lip is melted resin from the cell.

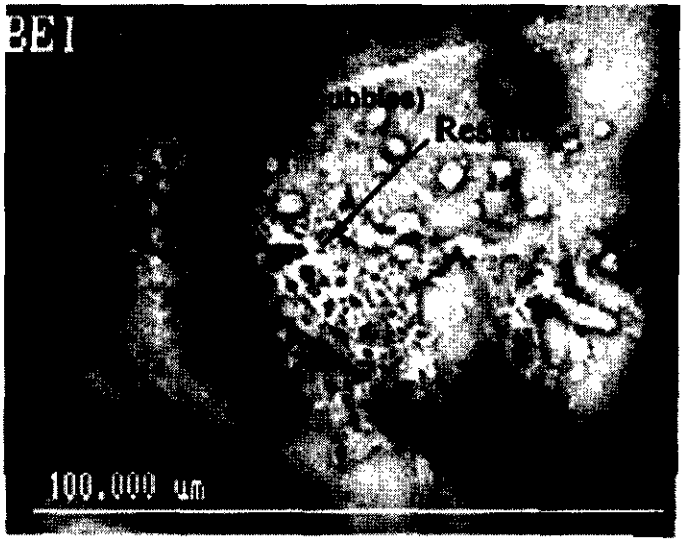

Figure 3.14 The BEI of a impact residue which has a distinctive vesicular texture within the melt. The dark areas within the residue could indicate volatile retention during rapid quenching.

Most impact residues under BEI were found to have distinctive, textural appearances (discussed in more detail in Chapters 4 and 5) when compared to the surrounding host (figure 3.14).

In a number of cases it was observed that the impactor and the cell were fused together, resulting in a complex melt with the possibility that the residue of the impactor was

embedded within the layers of the cell, leaving little or no trace at the surface. A major benefit of BEI was that it was possible to locate compositional differences to a depth of about 1μm below the surface of the crater pit (Figure 3.15) thereby allowing detection of embedded impactor melt.

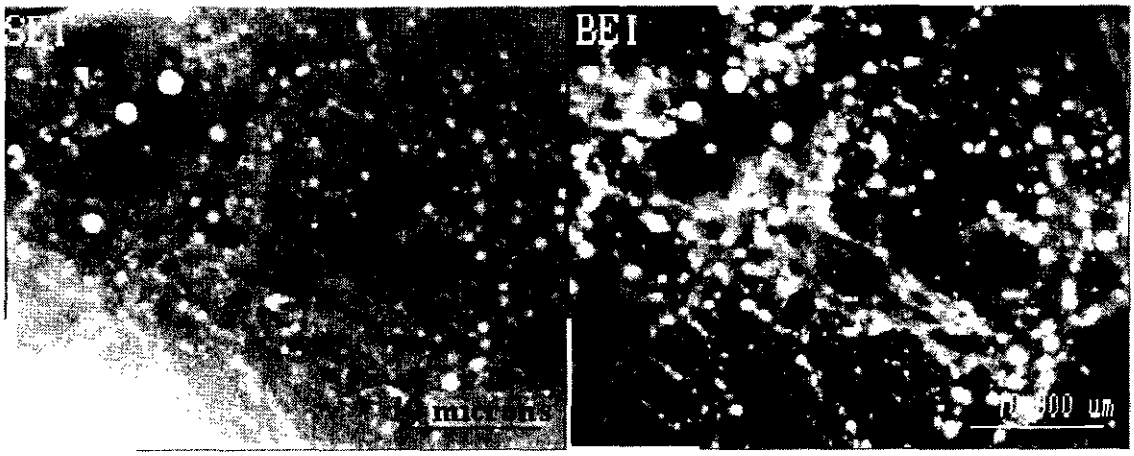

Figure 3.15 Two views of the same area of sample: (a) is a secondary electron image (SEI) and (b) a BEI. Impactor melt is clearly visible in (a) where it is manifest as globules of μm dimensions. Note, these features are present on the surface of the crater pit. (b) shows the tremendous advantage of using BEI where melt globules can be seen extending down into the surface layers of the cell.

3.7.3 Digitised X-ray Elemental Mapping (DXREM)

In previous investigation of HST solar cells by Wright et al. (1995b) individual micro-spot analyses (similar to those described in section 3.6) were used to try and identify possible impactor materials. Herein DXREM was employed to map the entire area under investigation (see Chapter 2.3) and is a far more sophisticated approach than micro-spot analysis.

Once an area containing possible residue had been identified using BEI, the same feature was then subjected to analysis by DXREM. During initial work, only a limited number of elements were selected - Mg, Fe, S, and Ni - these being chosen to reflect the chemistry of

the expected impactors. Unfortunately, this approach was not particularly successful, as the concentration of some of these particular elements was below the detection limits of ED at individual analysis points. Consequently the number of elements mapped was increased to include those used to identify both artificial and natural residues (sections 3.4.1 and 3.4.2) and those that compose the composition of the cell (figure 3.16). The complete list of the 22 elements that were analysed by DXREM in the majority of this work is as follows: C, N, O, F, Na, Mg, Al, Si, S, P, Cl, K, Ca, Ba, Ti, Ce, Cr, Mn, Fe, Ni, Cu and Zn.

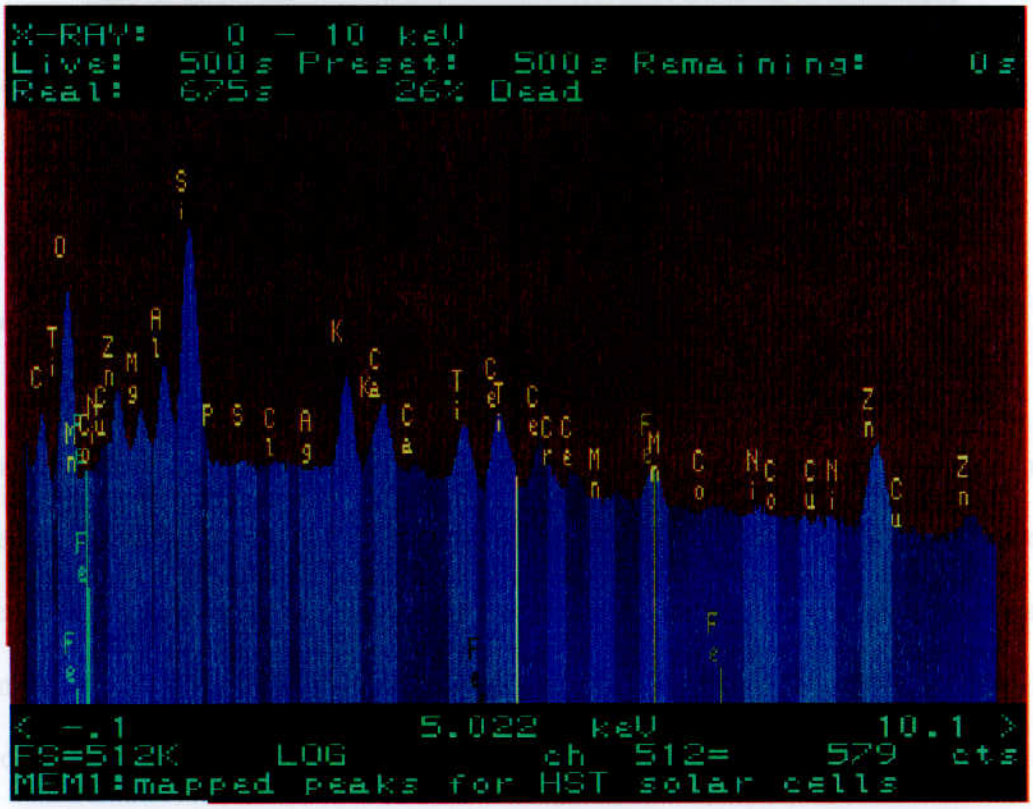

Figure 3.16 A ED spectrum showing some of the 22 characteristic energy bands (the pale blue bands on the spectrum) that are used for mapping.

By analysing for these 22 characteristic elements it was possible not only to identify extraneous elements, but also to detect elemental enrichments or depletions compared to the cell composition. From the ensuing elemental maps, it was then possible to infer the components of an impactor (e.g. figure 3.17). Note that X-ray maps show elemental

variations at depths far greater than those that are apparent during BEI. Indeed during DXREM, elemental variations are detected at up to 5 μm beneath a sample surface.

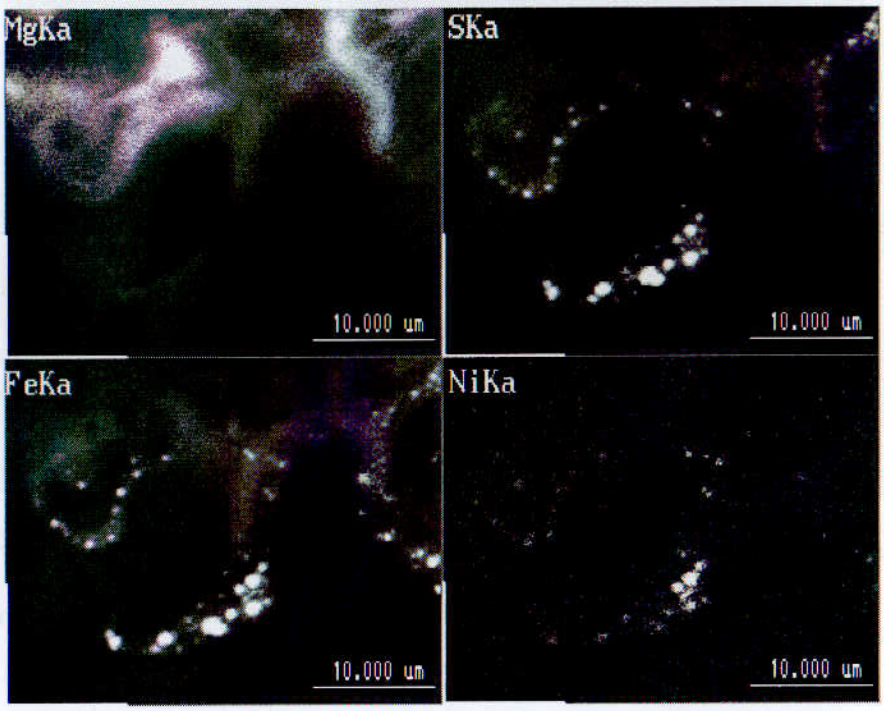

Figure 3.17 DXREM identifying different elemental components within a residue.

Appraisal of data from low magnification (<x50) X-ray maps was used to identify minor elemental variations across the surface of the solar cell substrate. This rapid process (1 frame 128x128 elemental map takes approximately 15 minutes to complete) was used to determine the number of impact craters present on a sample. Since the solar cells are coated with an ultra-thin Mg and F layer (section 3.3), it is apparent that because of an impact event this layer is often removed. Therefore it is possible to locate impact features rapidly on a sample by mapping for these two elements and where they are depleted it is likely that an impact feature will be observed (figure 3.18). In addition, the Mg and F maps clearly define the parameters of the impact features, this is particularly important when carrying measurements to assess crater damage.

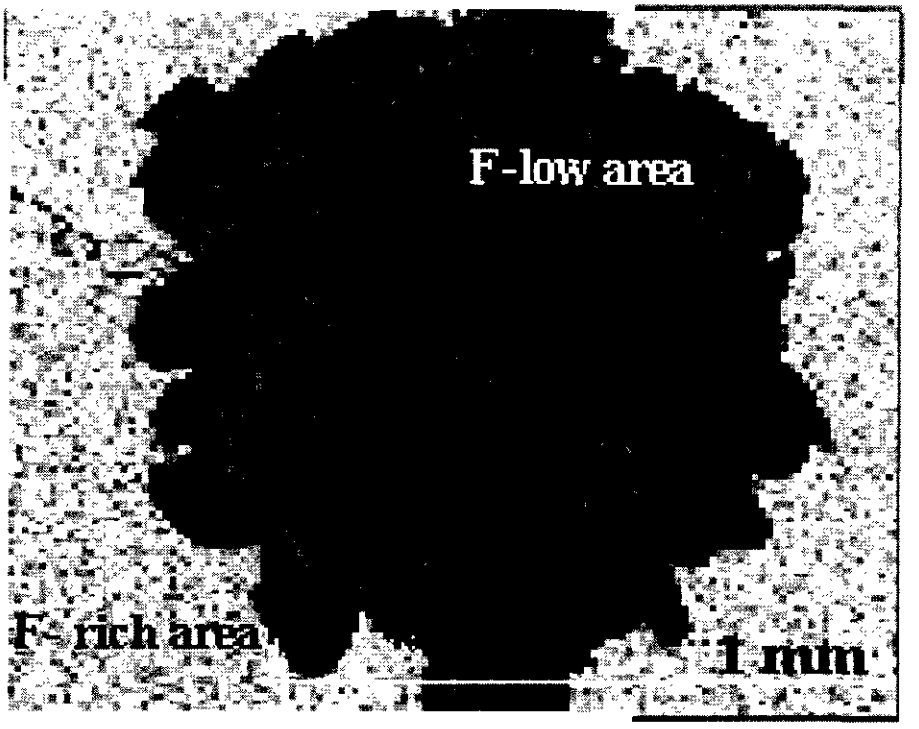

Figure 3.18 The DXREM for the F, highlighting the use of the mapping to locate impact features and to define the maximum extent of damage generated by an individual impact event.

3.7.4 Qualitative Micro-spot Analyses

Measurements of the precise elemental composition of most impact residues was not possible due to the small size of the areas under investigation (maximum size of an individual residue component is 10μm diameter), the complexity of the melt and the fact that residues were often located deep within a crater (quantitative measurements ideally require flat surfaces). All of these problems prevent full analytical correction using ZAF routines[2](see Reed, 199); thus the chemical composition of residues can only be considered qualitative.

The X-ray maps of an impact feature (section 3.7.3) help in the location of dry melt residues, but this does not necessarily allow detailed assessment of the mineral form of the impactor and by extension the likely parent material. One way to improve the chances of delivering the nature of the impactor is by micro-spot analysis using the ED detector in

ultra-thin-widow (UTW) mode. In this way ED spectra are collected not only from the residue, but also the surrounding cell melt and the CMX glass at a point away from the impact site (which acts as a standard). It is then possible to identify minor variations in the composition of elements that appear in both the cell and in the impactor (e.g. Si and Mg is the case of a natural micrometeoroid). Also, the ED spectra will yield elemental concentrations that the X-ray maps do not identify clearly (e.g. Ni in a Fe-S rich residue). Furthermore, the light elements C, N, O and F, are determined as well.

To assist the classification of possible mineralogical origins for the natural residues, work by A.T. Kearsley (Oxford Brookes University) on meteorites had included a digitised catalogue of a number of ED spectrum of known meteorite mineralogies (e.g. figure 3.19). By using the spectrum overlap software it was possible to compare (where possible) clean residue spectra with a known mineral spectrum to give a more detailed identification of the residue.

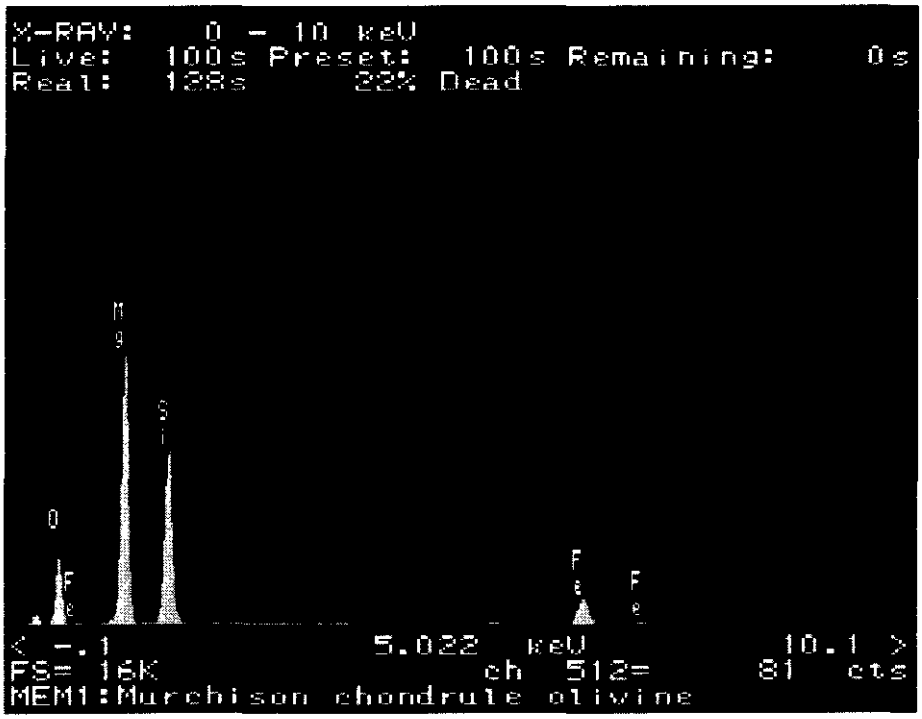

Figure 3.19 A typical ED spectra obtained from meteorite. in this example it is from a olivine chondrule in the Murchison Meteorite.

[2] ZAF: Z stands for atomic number, A stands for absorption and F stands for fluorescence

3.7.5 An Example Of The Application Of BEI & DXREM

It was found that the combination of BEI and DXREM proved highly successful in the location and identification of residues within the solar cells studied (the results will be given in Chapters 4 and 5). To assess whether the techniques could be used on other types of impact features, a sample which had been completely penetrated by an HVI was also studied. The class IV impact hole chosen was probably one of the most difficult to study because it was in one of the stiffener bars of the solar array rather than a cell (figure 3.20a). However, it was deemed important to investigate materials such as the stiffener because they may have proved a better passive collector of debris. The stiffener itself was known to be composed of several layers of silicone and sulphone resins interwoven with glass fibres. The glass fibres complicate imaging of the crater because they do not provide a smooth surface onto which a continuous conductive carbon coat can be applied. Thus, when the sample was placed under the SEM, charging effects were observed which precluded SEI of the crater. In contrast digitised BEI allowed the effect of the charging to be reduced and a high-resolution image was produced (Figure 3.20b).

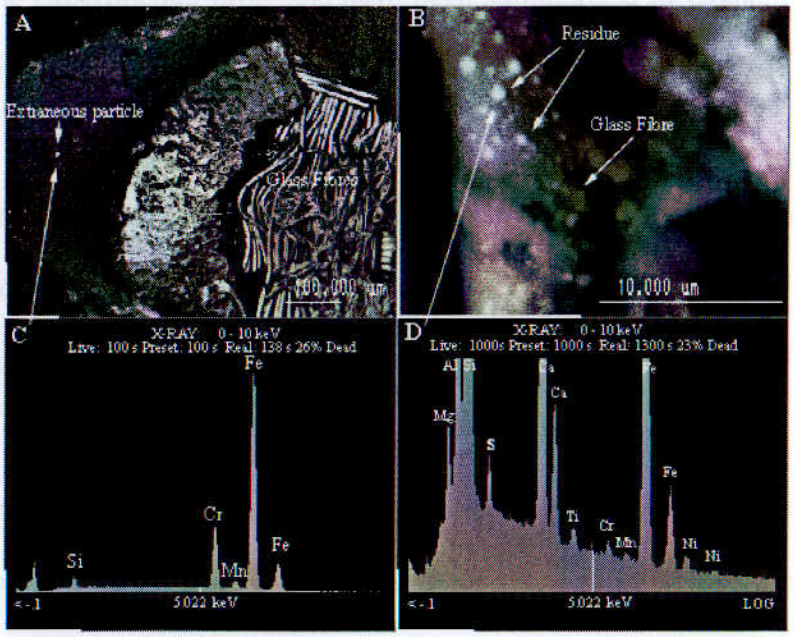

Figure 3.20 (a) The BEI of the impact into the stiffener material, (b) High resolution BEI of an individual fibre, (c) ED spectrum obtained from the bright particle on the lip of the crater (d) ED spectrum obtained from the fibre in (b).

The BE image (figure 3.20a) showed bright particles on both the crater lip and on the glass fibres within the crater. A higher magnification image of individual fibres indicated that residue had been fused onto them (figure 3.20b). X-ray maps of the crater and the individual fibres within, showed not only the different compositions of the stiffener layers but also discrete areas slightly enriched in Fe, Ni and Cr (figure 3.20c & 3.20d). The elemental composition (especially the high Cr) would suggest an impactor of artificial origin, i.e. a metal alloy such as stainless steel. The location and subsequent identification of a residue in such a complex substrate proved that the techniques employed in this study can be used on various types of substrate from the 'simple composition' of the solar cells to a composite glass-fibre stiffener.

3.8 Summary

The purpose of this chapter has been to demonstrate how a combination of analytical techniques was able to assist the identification and classification of impact residues in HST solar cells. The experimental protocols have been summarised in Graham et al. (1997b). The main findings of the developments are as follows:

The complex chemistry of the impact damaged hardware (solar cells in this case) must be fully understood to enable an effective distinction between melted host materials and impactor residues.

To assist in the classification of impact residues into broad categories such as space debris and micrometeoroids, all possible sources of contamination must be identified.

The use of both digitised BEI and XREM enables the rapid identification and classification of impact-derived materials.

Further classification of impacts containing residue material suspected to be natural in origin (i.e. mafic residues) can be enhanced by comparing the ED spectrum obtained from melt residues with known ED spectra from meteorite specimens.

The investigations for micrometeoroid residues should focus on the classes I-III impact craters (Herbert and McDonnell, 1997) as these are most likely to retain residues (Carey, 1998), a suggestion previously made by Graham et al. (1997a).

Chapter Four

Simulated Projectile Shots into Solar Cell Substrates Using A Light-Gas-Gun

4.1 Introduction

The fundamental purpose of a chemical analysis of an impact residue is to assign an origin for the impactor. Yet in practice this has proved extremely complicated, as the composition of the residue is not simply a melt product of the impactor; it is instead a complex mix of the host substrate and the impactor. The analysis is further complicated by the presence of two populations of material: micrometeoroid and space debris. As a result, much of the laboratory-based investigation inevitably concentrate on distinguishing residues of micrometeoroids from those of space debris (e.g. Zolensky et al., 1993 and Bernhard et al., 1993a & b) utilising elemental chemical analysis (Zolensky et al., 1993).

Sometimes this is fairly straight forward; e.g. the presence of Ti, C, N, O is unambiguously the signature of a paint fragment. When it comes to natural samples, however, identification of the residues as 'Mg- or Fe-rich" does not define the mineralogical origin which could of course be a mafic silicate (e.g. olivine or pyroxene) or phyllosilicate (e.g. saponite). It is unlikely that a residue will retain any diagnostic crystallographic information on a sufficiently coarse scale to allow rapid detailed determination of origin. It would therefore seem necessary to use other characteristic features of the residue in conjunction with the elemental analysis to enable a qualitative mineralogical classification rather then simply distinguishing a residue from space debris.

The ability to identify other characteristic features is complicated by the fact that many of the residues identified in the HST solar cells would appear to be polymineralic in origin and therefore it is not possible to assign specific features unambiguously. Coupled with this there are possible interactions with the host chemistry as well, which may affect the overall appearance and chemical composition of the residue, or the individual components within. However, the detailed analysis of specific micrometeoroid residues from LDEF by Brownlee et al. (1993), identified a number of textural features in residues that, in part, seemed dependent on specific mineral compositions and structure. Thus, it would seem that textural morphology might be a suitable feature, to help identify mineralogy.

In order to study this idea, a number of projectile types were accelerated to hypervelocity using the Light Gas Gun (LGG) facility at the University of Kent (e.g. Mackay, 1994), and subsequently impacted into HST solar cells. The need for laboratory generated impact residues was partly due to the success of the rapid identification technique summarised in Graham et al. (1997b). Previous chemical analyses of residue material in HST solar cells by various European laboratories had identified a high percentage of impactors of unknown origin (42-62%), (Carey, 1988).

Yet analysis of the HST solar cells using the combination of digitised back-scattered electron imaging and X-ray elemental mapping (Chapter 3) seemed to reduce the percentage of unknowns to 21%, enabling a more confident classification in terms of micrometeoroid or space debris origin. The ramifications of this new work and the conclusions of Graham et al. (1997b) were clearly significant. As such there became a moral imperative to validate the new results. This chapter discusses the initial validation shots and the development of the program to include a well-defined suite of mineral projectiles that should enable better classification of micrometeoroid residues.

4.2 Initial Validation

(This program was part of ESA contract 11887/96/NL/JG - Micrometeoroid & Debris Flux & Ejecta Models" (MADFEM) – The findings of this program were reported in the executive summary of Graham et al. (1998) and as part of work package 8 covered in the final report by Unispace Kent et al. (1998)).

Following on from the development of the analytical technique described in Chapter 3, it was considered necessary to validate the methodology for MADFEM, so as to provide a comparison with other techniques (Carey, 1998). In order to fulfil this requirement, three simulated impacts were carried out using the light gas gun (LGG) facility at the University of Kent (shots carried out by M.K.Herbert as part of his M.Phil studies at the University of Kent). So that the validity would be considered rigorous a blind test was carried out. This involved receipt of solar cells with impact damage, but with the nature of the impactors being withheld. The object was to see if the technique of Graham et al. (1997b) could successfully identify the impactors.

4.2.1 The Light Gas Gun

The LGG facility at The University of Kent uses a two-stage gun (figure 4.1). The basic working principles of the LGG are given in Taylor, (1997) and can be summarised as follows. First of all the projectile is loaded into a sabot (figure 4.1) which is then put into the LGG and evacuated. A shotgun cartridge filled with gunpowder is ignited when the firing pin hits the cartridge primer. A solid nylon (other materials cannot be used as they would reduce the velocities which could be produced) piston is accelerated by the detonation of the gunpowder in the cartridge and travels down the pump tube (Taylor, 1997). The piston compresses a light gas (hydrogen or helium can be used), which is at an initial pressure of 40-45 atmospheres. The resulting pressure peak ruptures a bursting disk

(it is this disk which separates the launch tube and experimental chambers from the pump chamber). Behind the burst disk is the sabot which holds the projectiles; the rupture of the burst disk allows the sabot to be accelerated by the gas pressure down the launch tube, which causes the sabot to separate. The separate sabot fragments and the remnants of the burst disk are intercepted by the stop plate, and the projectiles are then blasted into the experimental chamber (Taylor, 1997). The firing of multiple projectiles is known as the buckshot technique and is used for all the simulated shots in Chapter 4.

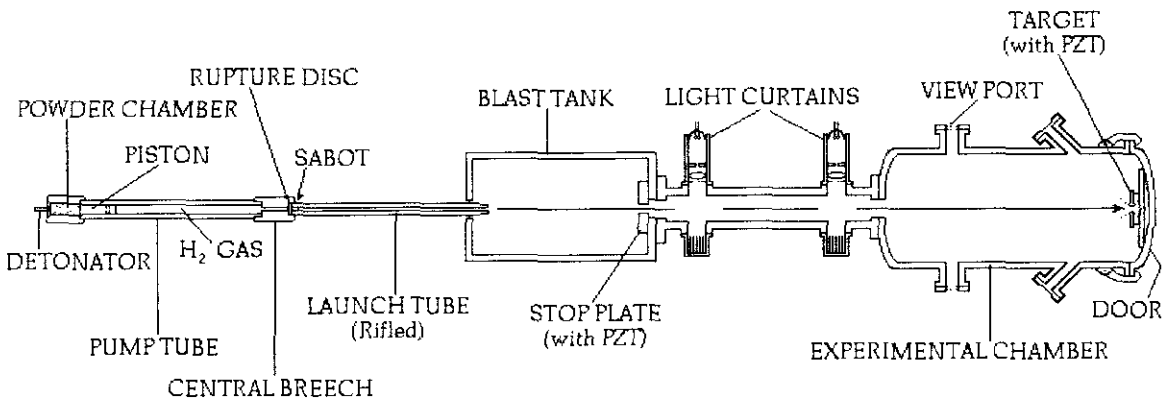

Figure 4.1 A schematic diagram of the Light Gas Gun at the University of Kent (Image courtesy of The Unit for Space Sciences & Astrophysics, The University of Kent).

The simulated impacts were carried out using the following analytical protocol; projectiles (up to 400μm in size) were accelerated into the solar cell target at velocities up to 5 km/s (velocities were calibrated from time-flight measurements using piezo-electric transducers, obtained as the particles traversed the 2 light curtains, figure 4.1) at zero angle of incidence (i.e. perpendicular to target plane). The residues from these experiments, (the samples were labelled A or B) were then analysed under the SEM at Oxford Brookes University using the analytical protocol described in Chapter 3.

4.2.2 Analysis Of Unknown Samples A & B

The samples sent to Oxford Brookes University, were part of a larger program being carried out at the University of Kent, therefore the shot numbers (21-23) relate to that program. The following is a summary of the findings for the analysis of shots 21-23:

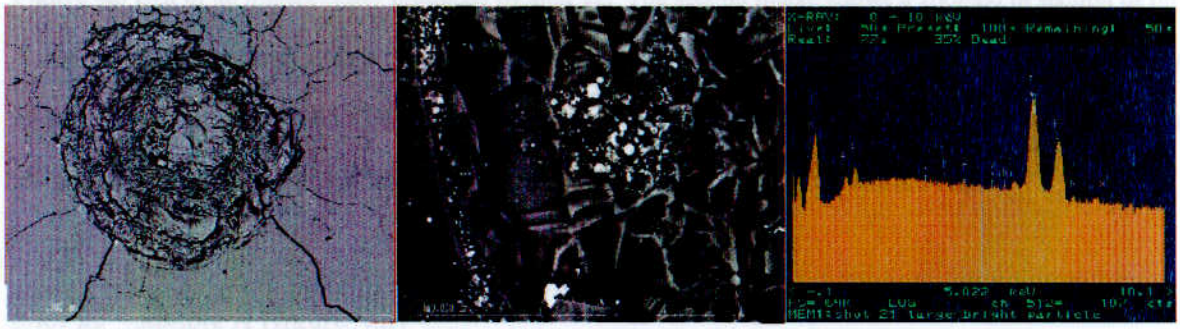

Figure 4.2 BEI of an impact crater. The second image shows a zoomed in section of the crater seen in the first image. It is clearly possible to see bright globules located on the melt surface most likely produced by shot 21. The ED spectrum obtained for the residue identified enrichments in Fe, Mn and Ni, Cr and would therefore be suggestive of a metallic origin.

Shot 21 - sample B (figure 4.2)

All of the craters examined under the SEM contained both residues and debris material. From ED spectra and X-ray elemental maps, the extraneous elemental signatures were identified as Fe, Pb, Al associated with Cu and minor Ti. It was therefore concluded that the impactor was steel of some description. In fact it transpired that the projectiles were martensitic stainless steel AISI 420 ball-bearings (elemental composition Fe, Cr, C, Si, P, S, Mn). The identification of Cu+Al, Pb and minor Ti as contaminants are discussed in section 4.2.3.

Figure 4.3 BEI of an impact crater produced by shot 22. The second image shows a zoomed in section of the crater seen in the first image. It is clearly possible to see a vesicular residue located on the melt surface most likely produced by shot 22. The ED spectrum obtained for the residue identified enrichments in Na, Mg, Ca and Si (highlighted by the dotted lines) and would therefore be suggestive of a silicate origin.

Shot 22 - sample A (figure 4.3)

Whilst there were three large impact craters (200 - 500μm in diameter) generated by shot 22, unfortunately these all contained spalled melt zones and conchoidal fracture surfaces which meant that subsequently no residue chemistry could be identified. Thus it was necessary to study the smaller craters (<100μm in diameter), which did not contain spalled melt zones and which contained residues enriched in Ca, Si, Mg and Na above the expected levels of the cell composition. Faced with such an analysis from a space-exposed cell we would have concluded that the impactor was natural in origin. In fact the projectiles were soda-lime glass, and were meant to simulate natural (chondritic) material). Shot 23 was fired using sample 'A' again and therefore will not be discussed again as it is a repeat of shot 22.

4.2.3 Contamination Problems

The detailed analysis of the simulated impacts has highlighted a contamination problem with the LGG facility as certain elemental signals (Cu associated with Al, Pb and minor Ti) identified were extraneous to the original impactor chemistries. To limit the possible sources of contamination, various working parts of the gun were analysed under the SEM,

including the burst disk and sabot. The analysis (figure.4.4) of the burst disk (mainly Al in composition) identified Cu and tiny Fe-bearing particles on the surface. The identification of the Cu identifies one of the contaminants; furthermore the Fe identified in the impact craters from shot 21, could be contamination products as well as impactor material. It is suggested that if such experiments were carried out again that the current burst disks be replaced with high purity materials. As yet it has not been possible to identify the source of the Pb or Ti signals, but it is suggested that these may arise from previous shots (using other types of projectiles), as the LGG by its nature cannot be an "ultra clean" facility.

The analyses also revealed a distinct problem in the composition of the martensitic stainless steel AISI 420 ball-bearings, which appears not to be homogeneous between samples. This is particularly a problem with the Cr content of the ball-bearings which is variable (figure. 4.5). Through calibration of the X-ray signals it is possible to state that Cr varies from 0-15wt%. Whilst this is not a problem for studying the simulated crater morphology, it is for elemental analysis. Thus, it is suggested that pre-screening of artificial impactors is carried out under the SEM if the experiments are aimed at defining residue chemistry.

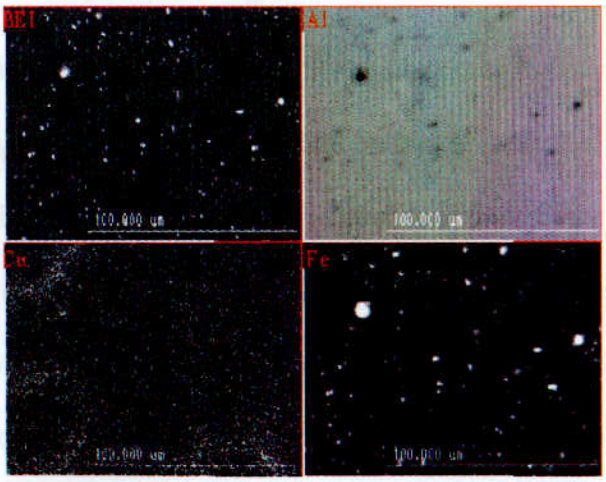

Figure 4.4 shows the X-ray elemental maps obtained from the analysis of a burst disk. The BE image clearly identifies a number of bright particles on the surface of the disk and from the X-ray elemental map for Al, they are not composed of the host material. The bright particles would appear to be Fe-rich whilst there is a uniform background concentration of Cu across the entire disk surface.

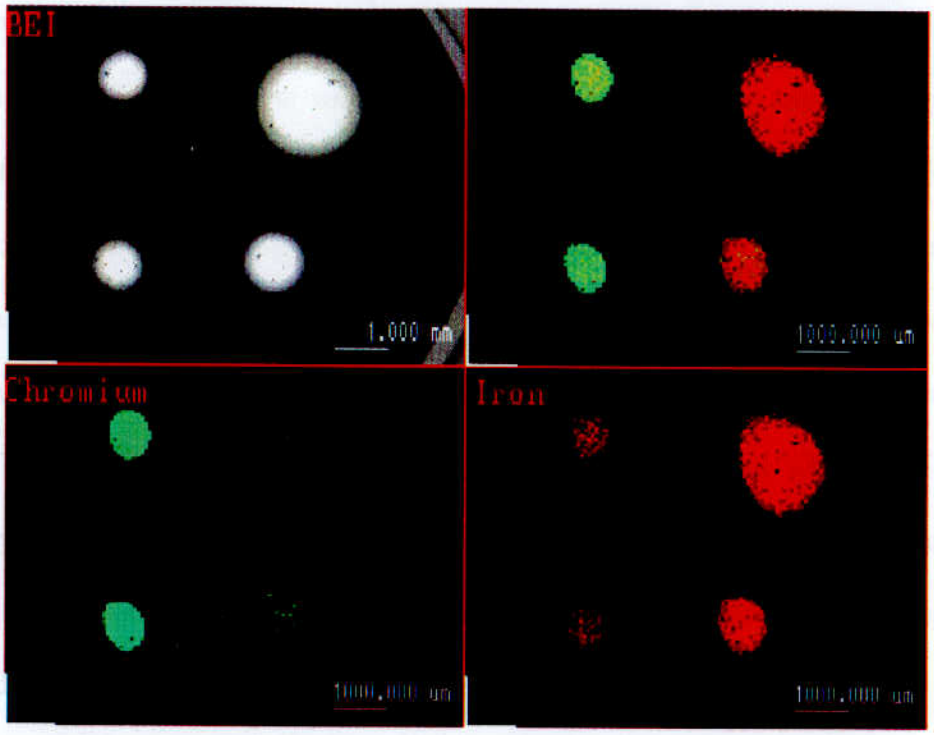

Figure 4.5 The BE image shows that the ball-bearings are different sizes. The X-ray elemental map for the chromium composition (coloured green) show that the four balls all contain varying levels. The X-ray elemental map for the iron composition (coloured orange) show that the four balls all contain varying levels. The final map (top right-hand corner) shows the overlap map for the chromium and iron maps clearly show that the balls are not of a standard composition.

4.2.4 Summary Of The Validation Program

The main aim of the analysis of the three unknown shots was to prove that the combination of digitised BE imagery and X-ray elemental mapping and the protocol described in Chapter 3 were useful in the identification of impact residues. Since correct assignment of the residue remnants of the three unknown shots was obtained, it can be assumed that the methodology of analysis was validated. Apart from the validation of the analysis protocol, the simulated shot program also highlighted the possibility that impact residues may have very distinctive morphologies which are related to the chemical composition of the original intact projectile/particle.

For example, the metallic projectiles produced residue remnants which were immiscible droplets (figure 4.2) compared to the soda-lime glass projectiles (essentially silicate in composition) which produced vesicular morphologies (figure 4.3). This therefore raised the important possibility that residues could be classified not only using the remnant elemental chemistry but the textural morphology as a characteristic feature to support the elemental data obtained. This would resolve the problem of distinguishing between the possible origins of the suspected natural micrometeoroid residues where the elemental chemistry simply identified Mg and Fe enrichments but the original intact particle could be a variety of different silicate materials. The development of the simulated shot program is discussed in section 4.3 of this chapter.

The initial shot program also identified that there was a potential contamination issue with the LGG in terms of additional projectiles from the various internal working components of the gun also impacting onto the target material. This generated misleading impact features or deposited material in impact features causing the mis-identification of the residue material.

Whilst this is a noteworthy problem the detailed analysis of various gun components supplied by the University of Kent (figure 4.4) has identified the sources of the contamination and these can be readily located and classified in the target material when present and therefore distinguished from the projectile remnant chemistry.

4.3 The Mineral Shot Program

4.3.1 Introduction

The investigations of materials derived from hypervelocity collisions in LEO are complex mixed residues of the remnants of the original impactor and the host substrate. It is rarely

based on intact fragments. This complex mixture is particularly difficult to decipher when the suspected impactor is of natural origin. The initial simulated shot program used only simple basic analogues to represent potential space debris and micrometeoroid impactors.

The shot program was then developed to test whether residue texture as well as composition would prove a diagnostic feature for different mineral compositions. This would prove particularly useful when sub-classifying residues which originated from the various silicate minerals. It would also allow the assessment of the survivability of certain minerals and lastly the possibility of investigating the effect of hypervelocity impact events on the composition of an impactor in terms of volatile loss.

The concept of generating laboratory impacts to simulate the suspected effects of hypervelocity collision is not new. Much of the previous work was based on assessing the degree to which the chemical composition of an impact melt reflects the chemistry of the original impactor (e.g. Hörz et al., 1983). Experiments by Hörz et al. (1983) involved impacting synthetic silicate projectiles into Au and Cu targets using a LGG. The targets in these experiments were both ductile substrates, and thus the interaction between the impactor and the host was substantially different to those observed in the brittle glass, resin and silicon laminate of the HST solar cells.

In the Hörz et al. (1983) experiments, the impact craters were simple bowl shaped features with copious amounts of projectile material preserved as thin glass liners covering the walls and the base of the craters. The textures observed for the synthetic silicates were similar to those observed in the initial shot program (section 4.2.2), i.e. vesicular in nature. Unfortunately the Hörz et al. (1983) experiments were derived to assess the impact effects for large planetary surfaces rather than for micro-scale impacts in spacecraft surface. Therefore in terms of assessing the differing nature of residue morphologies associated

with differing chemical composition, the work falls short and is similar in nature to the initial shot program discussed in section 4.2.

So this section reports on the observations made on residues generated by the University of Kent's LGG using known mineralogy projectiles. The use of well-characterised samples is an essential first step to enable positive identification of impactor mineralogy, and thus enhance the interpretation of the complex, natural polymineralic residues observed in the HST solar cell impact craters. The use of both hydrous and anhydrous mineralogies would allow an important sub-classification of residues, which are currently simply identified as probable silicates. This could be a significant move forward in the identification of micrometeoroid material particularly in terms of assessing the potential origins of the material.

4.3.2 Methodology

Prior to firing the projectiles in the LGG, the important task was to select mineralogies which were simple yet realistic analogues of the individual components known to be present within extra-terrestrial materials. The representative selection was as follows: olivine; enstatite; diopside; serpentine; pyrrhotite; kamacite; anorthite; albite; nepheline; sodalite; spinel; alumina and calcite. This selection was based on the review of literature on the topic of meteorite mineralogy, for example Heide and Wlotzka, (1994).

The selected mineral samples were obtained from the Mineralogy Department of The Natural History Museum and from the Geology Department, Oxford Brookes University. For the selected minerals, simple polished sections were produced. This allowed pre-screening of the samples prior to being fired using the LGG and therefore checked to verify that the samples were homogenous in composition. It is important that the samples

are homogenous, as the main aim of the program was to observe whether certain mineral compositions would produce diagnostic residue textures.

The pre-screening examination involved both BEI and X-ray elemental mapping of the samples under the SEM, if a sample was found to be inhomogenous then it was removed from the shot program and a suitable replacement found. Once the samples had passed the pre-screening process they were crushed by hand using a pestle and mortar and sieved to yield individual grains with sizes between 125 and 250μm in diameter. As well as the individual mineral grains, a polymineralic powder was also prepared using crushed matrix from the Orgueil CI carbonaceous chondrite. This was used to represent a possible analogue for a hydrous micrometeoroid impactor. The powders were then sent to the University of Kent where they were individually mounted into the LGG as described previously in this chapter and accelerated into HST solar targets at impact velocities not exceeding 5km/s.

The impacted substrates were returned and examined initially under an optical microscope, revealing abundant craters, ranging from μm to mm scale. A detailed examination was then carried out using the combination of BE imaging and X-ray elemental mapping under the SEM using the protocol discussed in-depth in Chapter 3.6.

4.3.3 Results

Interpretations of the most significant results from the simulated shots are discussed in Chapter 5.3 and therefore only a general summary of the findings is given here. The textural morphologies of the residues were highly variable but would seem comparable with those observed and discussed in Chapter 5 and in previous LDEF investigations (e.g. Brownlee et al., 1993).

The residues can be broadly classified as having the followi ɔgical types (figure 4.6): i) vesicular melt, in residue from Orgueil matrix. The vesicular nature may be due to release of vapour from hydrous mineral phases (e.g. phyllosilicates); ii) concentrated, embedded melt within the host melt, seen in residues of olivine and pyroxene; iii) Surface globules that appear to be quenched immiscible-liquid droplets, possibly condensates from a gaseous state. These retain volatiles such as sulfur in FeS residues and iv) Near-intact particles. Appendix 3 contains the BE images and the X-ray elemental maps for the selected mineral shots.

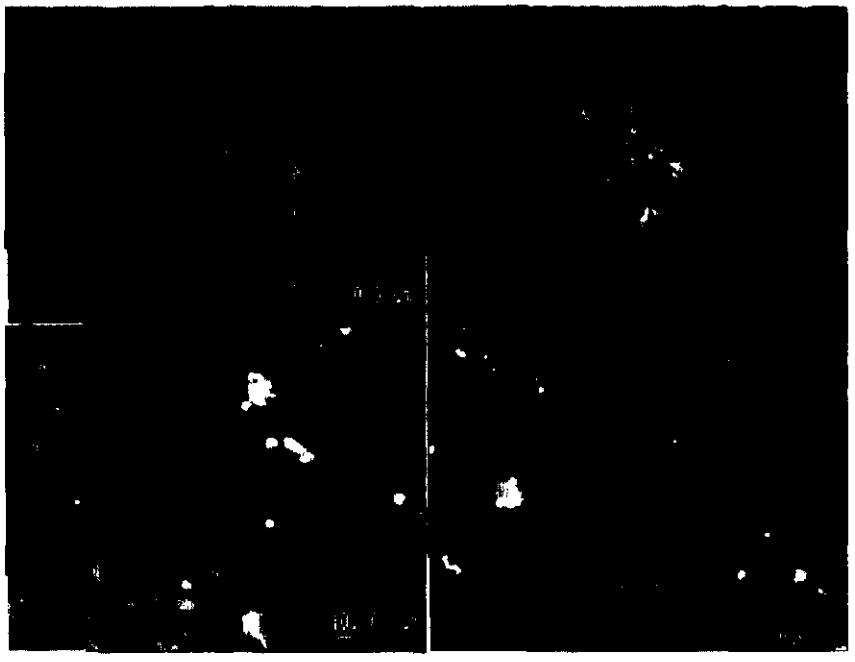

Figure 4.6 BE images of the typical textural morphologies preserved in the impact craters generated by the mineral shots: (i) embedded; (ii) surface droplets (the scale bar represent 100μm); (iii) vesicular and (iv) particulate (the scale bar represents 10μm) (the black arrows identify the residue textures).

4.3.4 Discussion

The effect of hypervelocity impact processes on the chemistry of the residual material remaining is variable. In some cases the residue fragments give a near stoichiometric ED spectrum (figure 4.7), whilst in others it is clearly possible to note the lost volatiles. This

area of research still requires much work to be carried out, but the initial results suggest that further study would be profitable.

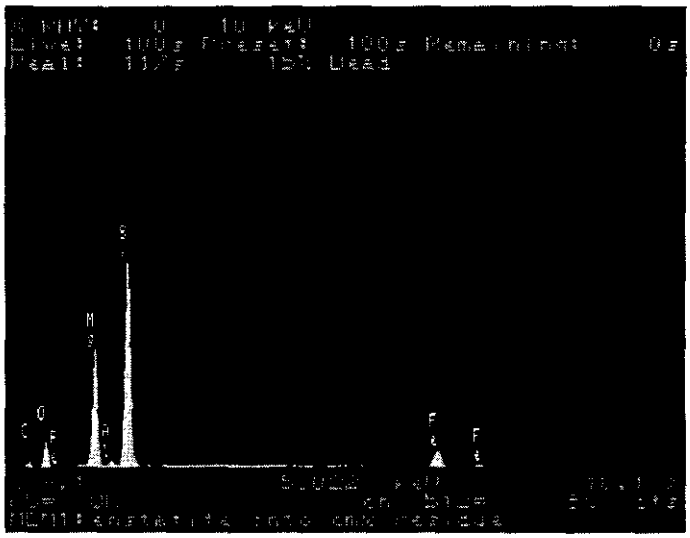

Figure 4.7 The ED spectrum obtained for the enstatite residue. It would appear that there has been little or no change to elemental abundance from the original projectile chemistry prior to firing in the LGG.

For the following projectiles, near intact particulate residues were observed: calcite, spinel, alumina, albite and olivine shots. The surface textures of these residues indicate that melting had occurred and they were not simply contamination products from LGG. It is not possible from the BEI or SEI to assess whether any crystallographic information was retained in these particles.

Such observations will only be possible if residue material can be extracted and made into sections that can be investigated under a TEM. Initially it was considered that calcite fragments from one of the simulated shots could be used in this way. However, this was not pursued because of fears that the calcite shot fragmented within the LGG before impact on the target material. It is possible that this problem can be overcome by mixing the calcite fragments with another mineral powder (for instance diopsite).

A vesicular melt residue was observed in the Orgueil matrix shot which at first glance was thought to be from the release of vapour from hydrous mineral phases (e.g. phyllosilicates). It should be noted that this texture could also arise from the devolatilisation of calcium carbonate, sulfates, organics, etc. However neither saponite and serpentine were found to generate any craters with residues that could be analysed, (all that was present were contaminants or melt pits produced by spallation). It would seem likely that the projectiles disintegrated prior to impacting the target (an observation which may ultimately have the capacity to constrain the formation of hydrous IDP residues). If the mineral shot program is continued it is strongly advised that saponite and serpentine shots are repeated (possibly using different mineral grains since one of the goals is to distinguish between anhydrous and hydrous mineralogies).

Caution has to be taken when a vesicular melt is observed in an impact feature that has penetrated the silicone layer of the cell (class III impact), as this may not be representative of hydrous mineral phases. It was found that the enstatite projectile generated a deep impact crater; the back-scattered electron imaging identified vesicular melt feature within the pit (figure 4.8). Since enstatite is an anhydrous mineral it is unlikely that the texture is related to the impactor. Rather it is considered that since the impact feature was class III (i.e. penetrated the silicone layer, see Chapter 3.1.1) the vesiculation was due to chemical interaction (e.g. dehydration and or decarboxylation) within the silicone layer of the cell immediately beneath hot silicate melt generated by the impact process.

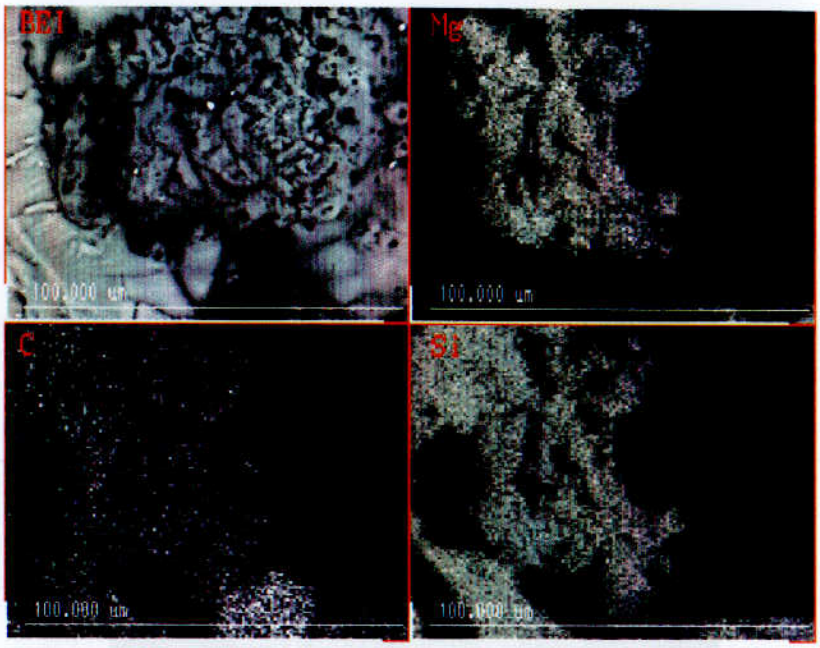

Figure 4.8 The BEI image identifies a vesicular melt material which is in stark contrast to the CMX melt which can be observed at the left-hand end of the image. The X-ray maps of this area identify the vesicular melt to be enriched in Mg. This is from the impactor. The maps also identify that the vesicular melt is associated with an area of Si and C that are from the silicone host melt.

For the pyrrhotite experiment a large number of impact craters were produced (as a natural consequence of the buck-shot technique). Approximately 200 of these had diameters (The diameter measurement for a crater is quoted as D_{CO} (Conchoidal spallation), see section 5.2.1) comparable to those common in HVI from LEO (D_{CO} 100-2000 μm). The large number of craters, and the appropriate variation in crater diameter, offered the opportunity to quantify the retention of residue with respect to crater size. To this end, 116 craters (D_{CO} 100-1700μm) were examined for residue. 111 (96%) of these contained FeS residue, 3 were unclassifiable (spalled melt) and 2 were contamination from the LGG.

In other words, 111 out of 114 craters (i.e. 97%) contained evidence of FeS melt. It is clear from this that an FeS-bearing meteoroid would leave diagnostic evidence in an impact residue. This supports the observation that in the HST solar cells examined in this thesis with HVIs identified as natural, 13 out of the 20 (65%) retained metal sulfide

residues. Clearly one would like to extend this work to residue material from all of the other types of mineral shots employed herein. Furthermore to allow direct comparison with the retention of debris in LDEF craters (e.g. Bernhard et al., 1993a) laboratory HVI must use similar ductile targets (e.g. Al-blocks). Such experiments would form a logical extension of the present study, to be followed by a similar SEM survey of the craters.

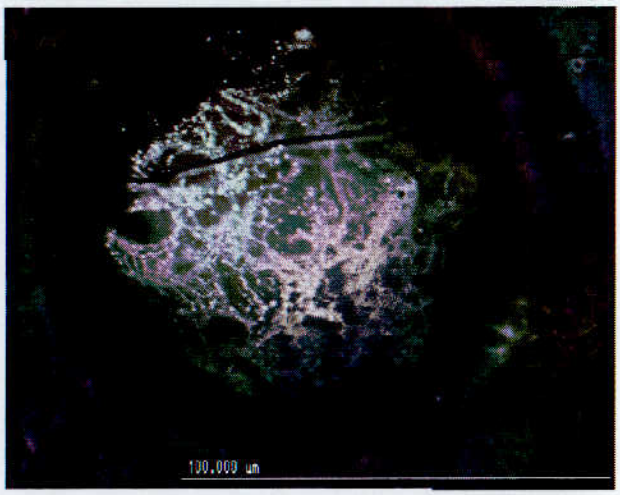

Figure 4.9 BE image of a typical impact crater observed in LEO derived impact crater. This crater was generated by the impact of a Fe-Ni rich micrometeoroid. The concave surface of the melt pit is enriched with residue (the bright globules).

The shot program was essentially designed to allow investigation of residue textures of projectiles with known chemical and mineralogical compositions. Due to the low velocity impact (ca. 5km/s) it has been possible to observe feature which normally do not survive in LEO impact events, where the impact velocity can be much greater (ca. 20km/s).

The typical impact structure observed in HST solar cells is shown in (figure 4.9). This crater shows complex radial and conchoidal fractures with a broad spallation zone. The majority of the projectile residue (if not lost due to spallation) is located in the central melt pit. Understanding mechanisms of melt formation is extremely important, as it gives an insight into the likelihood of residue recognition. It appears that the melt zone is a thin layer of mixed host and projectile material which is inflated by gas, and uplifted into a melt

bubble (Figure 4.10). This usually bursts and collapses to form a concave pit lining (figure 4.9). Further work is required to understand fully the formation of these craters and their residues.

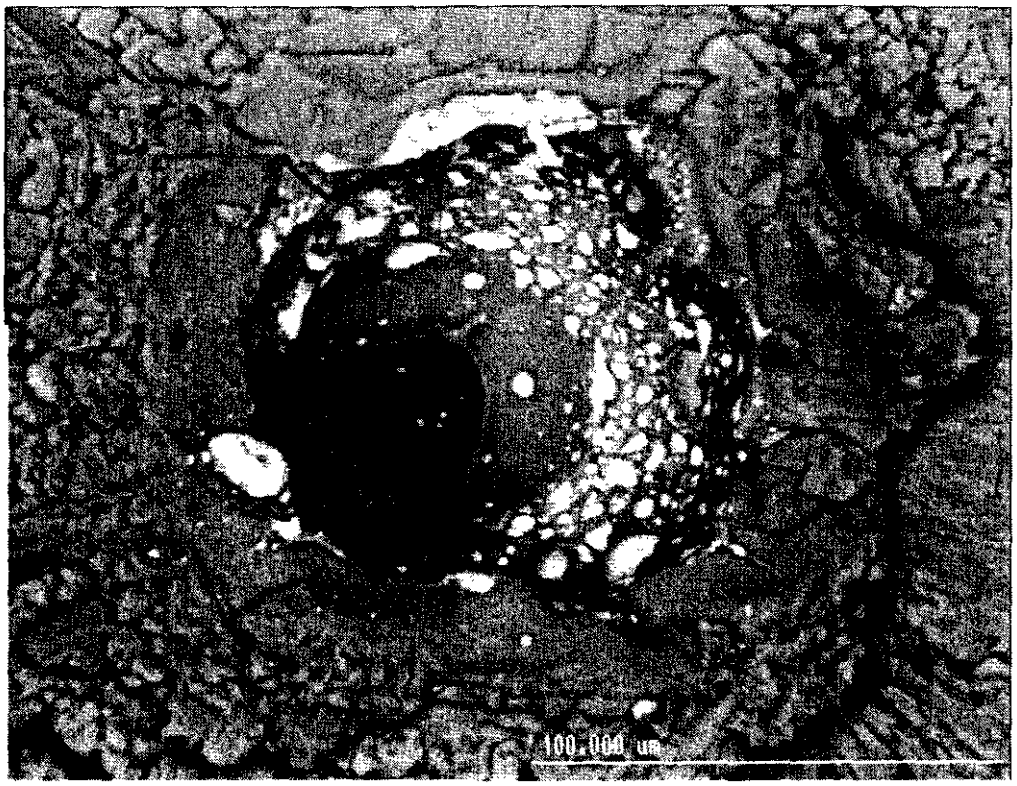

Figure 4.10 BE image of the melt bubble, frozen before collapse. The crater was generated by the pyrrhotite shot and the residue material clearly seen deposited on the surface of the thin bubble layer.

The rigorous interpretation of HVI-derived residues in space hardware is a complex task. Crater size and accompanying degree of damage to the host can vary to a great extent (e.g. for the HST sample, crater diameters range from approximately 50 to 3000μm D_{CO}), with penetration through just the cover glass surface to the entire cell and stiffener thickness (e.g. Herbert and McDonnell, 1997).

To date an insufficient number of larger craters on solar cells have been investigated to be able to assess whether residue can be routinely found in craters greater than 1500 μm in diameter. In this study a further limitation lies in the relatively small number of individual samples yet examined, and it is therefore very important to establish an efficient sampling

method for a larger survey. To yield the maximum information on the LEO environment, it is essential to understand the likelihood of debris retention within a given crater size.

4.3.4 Summary

The mineral shot program was designed to enable a better understanding of residue textures observed in LEO derived impact craters. The simulated shots have produced different residue textures which have been readily observed in the LEO derived craters. Some of which would appear to be very characteristic of composition, e.g. metallic sulfides and metals producing immisicible-liquid droplet condensates. The intention of the shot program was to produce a series of diagnostic residues that could be used in comparative studies with those observed in LEO-derived craters. This has only been a partial success as it has not been possible to resolve whether the vesicular residue textures are characteristic of remnant hydrous minerals.

As the same textures can be generated by the melting of the silicone layer of the cell if the impact penetrates beyond the top CMX glass layer. It was also not possible to substantiate if hydrous minerals would produce vesicular residues as the two hydrous minerals (saponite and serpentine) failed to generate any craters and it is suspected that the projectiles completely desintegrate within the LGG. It is hoped that further shots using these minerals could be carried out as the distinction between possible hydrous and anhydrous residue is very important in terms of deriving the parental origin of the impactor. In terms of residue chemistry and texture the shot program has generated more questions than answers, yet it has also given an important insight into the possible mechanism for the deposition of residue material within the melt pit of the craters although substantial further work is required.

Chapter 5

Chemical Analysis of Impact Residues Generated in LEO by Hypervelocity Collision of Micrometeoroids & Space Debris into Solar Cells from the HST

5.1 Introduction

This chapter describes the results of an investigation into the nature of impact residues recorded in solar cells returned to Earth from the HST. During the period of this thesis work, many of the results and observations described in the previous chapter were presented at international conferences e.g. The 31st and 32nd Scientific Assembly of the Committee On Space Research (COSPAR). As a consequence of this the data have been incorporated into three scientific papers which have been published in the following internationally renowned journals: Advances Space Research and the International Journal of Impact Engineering. The papers concerned are Graham et al. (1999a, b and 2000), all three were peer-reviewed. Rather than include the papers as written, Chapter 5 instead consists of extracts from the submitted three papers.

To conform to the requirements of the examination board of the Open University the following changes have been made: page numbers are consistent with the rest of the thesis. The introductions and experimental sections of each paper have not been included to avoid repetition with what has already been discussed at greater length in Chapters 1, 2 and 3 respectively. A few minor stylistic changes have been made to enable the extracts to fit together logically.

The subsection headings used in each paper are reproduced herein, but with a numbering system that is consistent with the present chapter. Section 5.2 discusses the general results of the project in terms of which is the dominant impactor in the 100-1000μm size range craters. Sections 5.3 and 5.4 will discuss the specific chemical and textural observations of the impact residues.

The investigation of the HST solar cells involved examination of 25 of them under the SEM. The 25 solar cells contained 29 impact craters. All these papers refer to the results of the investigation; therefore a tabulated form of these will only be reproduced once here in the introduction. Table 5.1 contains information on the sample identification number (this is the allocation number used by ESA rather than a position number within the entire array), the crater diameter, elemental information if obtained and the classification in terms of morphology and chemistry.

HST Sample I.D	Morphology	Diameter (Dco)	Elemental Data	Classification
S160	Circular	1364	Sn, Cu	Debris
S161	Circular	457	Fe, Ni, S	Meteoroid
S161	Circular	423	Mg,Fe, Si	Meteoroid
S165	Oblique	447	Mg, Fe, Ni, S, Si	Meteoroid
S165	Circular	176	Ca, Na, Cl, Al, C & O	Meteoroid
S166	Circular	638	No Analysis	Spalled Melt
S167	Circular	1028	Mg, Fe, Si & Fe, Ni, S	Meteoroid
S176	Circular	1037	No Analysis	Spalled Melt
S178	Circular	527	Mg, Fe, Si	Meteoroid
S179	Oblique	605	No Analysis	Spalled Melt
S180	Circular	501	Fe, Ni	Meteoroid
S180	Circular	99	Fe, Ni & S	Meteoroid
S181	Circular	596	Mg, minor Fe, Si	Meteoroid
S182	Oblique	538	Mg, Fe, Ca, Al, C, O, Si	Meteoroid
S183	Circular	1246	No Analysis	No residue
S204	Circular	416	Fe, S, minor Ni	Meteoroid
S278	Circular	434	Mg, Fe, Ni, S	Meteoroid
S278a	Circular	91	Fe, trace Ni, S	Meteoroid
S162	Circular	950	Mg, S, Fe, Ca, K	Meteoroid
S163	Oblique	650	No data	Unclassified
S164	Oblique	830	Mg, S, Fe, Ni	Meteoroid
S164	Circular	385	Mg	Meteoroid
S169	Circular	1010	No data	Unclassified
S170	Circular	515	Fe, S, Ni	Meteoroid
S170 (not SA)	Circular	1030	Fe, Cr, Ni, Ti	Debris
S175	Circular	250	Mg, Fe, Ni, S	Meteoroid
S177	Circular	530	Fe, Ni	Meteoroid
S275	Circular	153	Ti, C, N, O	Debris
S276	Circular	500	Fe, S	Meteoroid

Table 5.1 Shows the results for the 29 investigated impact craters for this project.

5.2 Hypervelocity Impacts In Low Earth Orbit: Cosmic Dust Versus Space Debris (Extract from Graham et al. (1999a))

5.2.1 Results

The surfaces returned from the solar array, unlike many of the previous studies already mentioned, are brittle in nature. Thus, instead of simple crater morphologies, they produce complex radial and conchoidal fractures with extensive spallation zones during the crater forming process (Rival et al., 1998). Therefore it is necessary to define the terminology used to describe the crater morphology (figure 5.1).

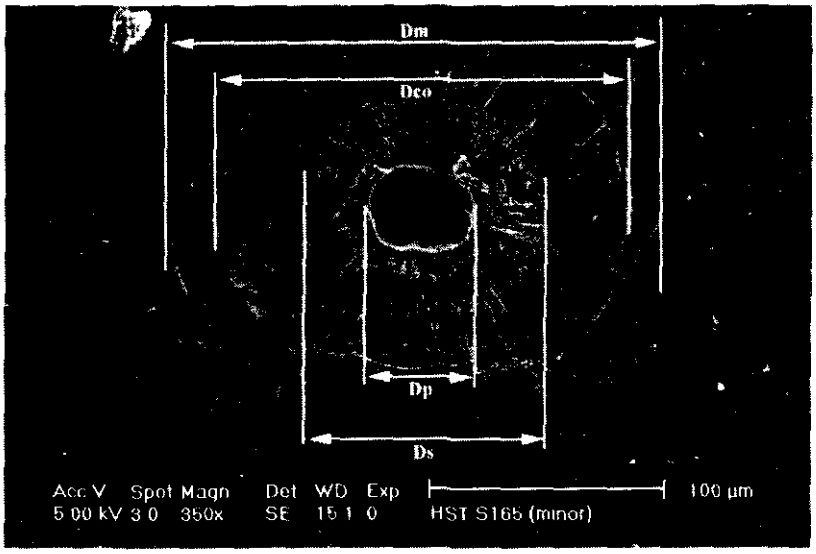

Figure 5.1 A SEI image of a typical impact crater. The impact terminology can be defined as the following: D_P = central pit (melt pit); D_S =shatter zone, this area is highly fragmented; D_{CO} = Conchoidal spallation; D_M =Maximum damage detected at an impact site.

Residues of micrometeoroid origin were identified as Mg-silicates (possibly olivine or pyroxene), Mg-Fe silicates (possibly phyllosilicates); Fe-sulfides; Fe-Ni-sulfides; Fe-Ni metal and calcite fragments associated with Mg-Fe non-silicates (possibly Mg-Fe carbonates). These components were identified as either single or multi- component

residues, their detailed chemistry is discussed in Graham *et al.* (1999b). The space debris residues were identified as derived from paint (EDS spectra with Ti, C, N and O); metallic fragments (EDS spectra with Fe, Cr, Mn and trace Ni in sensible ratios for stainless steel) and printed circuit board (PCB) components, (figure 5.2).

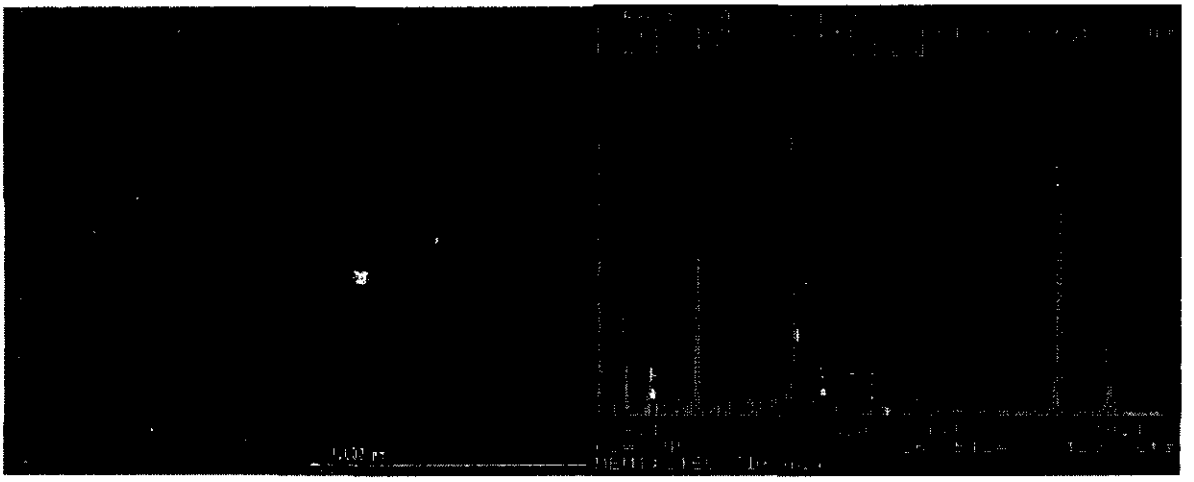

Figure 5.2 BEI image of an impact crater with bright particles in the crater pit. EDS spectrum containing Sn and Cu suggesting an artificial origin (possibly PCB fragments).

5.2.2 Crater Analysis

When discussing the chemistry of the impactor it is important to be able to determine the approximate size of the original impactor. This is significant because it will determine which of the terrestrial collections of dust the residues are compared with, i.e. stratospheric collected IDPs range between 1-100μm in diameter whereas micrometeorites range between 50-200μm. The estimation of original particle size is calculated from the D_{CO} measurement from the crater, the methodology of the estimation is discussed in depth in the report from Unispace Kent 1998. The 29 craters investigated are Class I – II impacts, with D_{CO} = 100 – 1000 μm (figure 5.3). Calibration of the D_{CO} measurements indicates that the impacting particle size range was 8-80μm diameter.

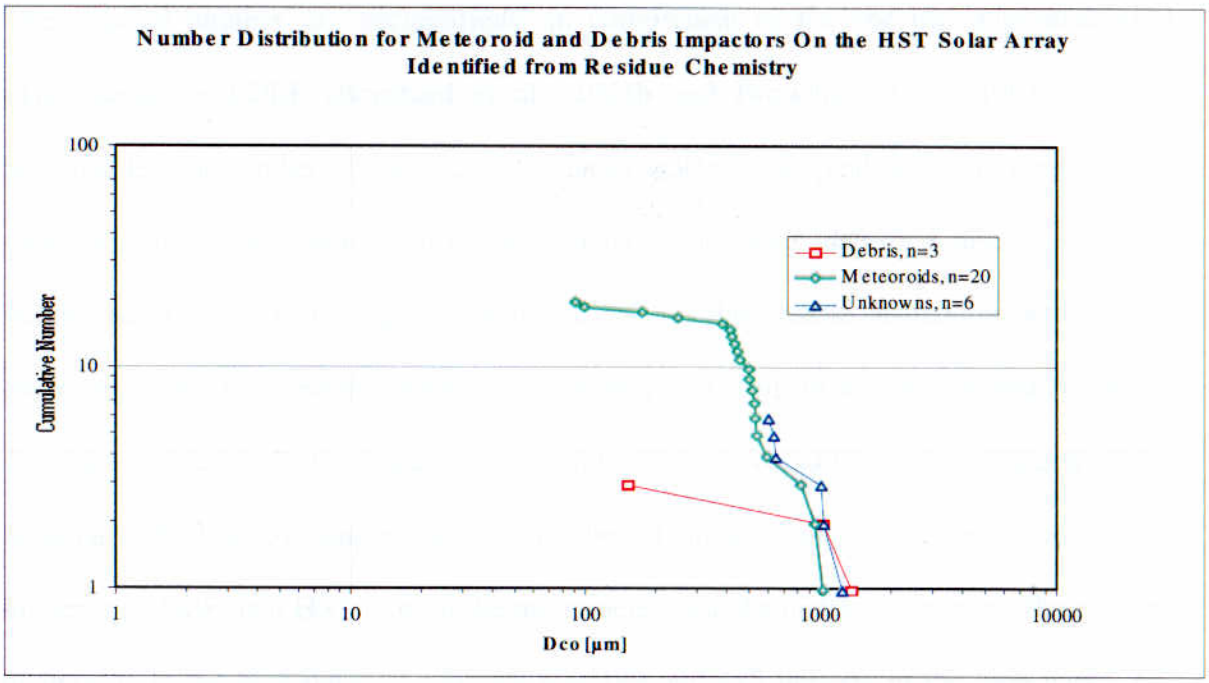

Figure 5.3 Number Distribution for Micrometeoroid and Debris Impactors Vs Conchoidal Diameter (This plot was produced by A.D.Griffiths at University of Kent using the data supplied in table 5.1).

5.2.3 Discussion

The proportion of identified residue is in marked contrast to previous studies of LDEF and HST solar cells, in which up to 75% of the impact craters were 'unclassified'. This increase in identified residues may be due to a number of factors apart from use of digitised BEI and X-ray mapping. The earlier investigations (Wright et al., 1995b) used larger Class III-IV impact craters (as defined by Herbert and McDonnell, 1997), with D_{CO} up to 2mm. Such craters show substantial impact damage to the cell, and there is no trapping mechanism for residue material comparable to that seen in the smaller Class I-II craters of this investigation. Earlier studies (e.g. Rival et al., 1997) also found that the complex cell composition made interpretation of residues extremely difficult, particularly for micrometeoroid residues. The problems of complex cell chemistry have been overcome by detailed analyses of cell cross-sections, enabling recognition of minor variations in the chemistry of the melt, and thus distinction between host and extraneous material.

The reduced number of 'unclassifieds' in comparison to the specific micrometeoroid experiments on LDEF (Bernhard et al., 1993b and Brownlee et al., 1993) may be attributable to a number of factors: 1) the analytical methods and detectors employed in these original studies were insufficiently sensitive to have identified discrete residues within the craters (i.e. the light elements (C, N, O) that enable distinction between the chemistry of the host and the impactor - for example Al-foils of a collector, and Al-oxides from space debris); 2) the impact process into Al and Au surfaces caused much of the material to be lost; 3) sample bias: the number of impact craters investigated was much higher for LDEF than HST (e.g. in the micrometeoroid chemistry experiment, the number of impacts in the high-purity Au-targets was 199 and 415 impacts in the high-purity Al-targets, Bernhard et al., 1993a). This is substantially more than the 29 impacts observed herein which were specifically selected on the basis that they were of a size which was known to commonly contain residue; 4) the impact features identified in craters on LDEF cannot be applied as "absolute" average conditions for any set of impacts feature identified on any space hardware (Bernhard et al., 1993a).

Our data suggest that the Class I-II impact craters on HST are dominated by micrometeoroid-derived residues (69%), possibly from relatively low, oblique impact velocities. Previous studies (Flynn, 1990 and Brownlee et al., 1993) suggest that particles of asteroidal origin might have orbital parameters of this nature. The dominance of natural residues raises the possibility that LEO may harbour a previously under-estimated population of micrometeoroids, although the nature of the HST orbit (all of the array surfaces were exposed to earth- and sun- facing environments) means that it is not possible to confirm this hypothesis. However, re-examination of known orbital-orientation surfaces of LDEF using our techniques might well resolve whether such findings are significant in number on earth-facing surfaces.

5.3 The Collection Of Micrometeoroid Remnants From Low Earth Orbit (Extracted from Graham et al. (2000))

5.3.1 Results & Discussion

The residues were identified as: 3 of artificial origin, 20 of natural origin and 6 were unclassified (spalled melts, where it is assumed the residue was lost during the impact process). The residue material identified was present in varying degrees of abundance and textural appearances within the central melt pit, the spall zone and the fracture cracks of the impact craters. The craters are essentially located in the top layers of the solar cell composite, which means that the host composition in the melt mixture containing the residue is that of the borosilicate glass. Thus the residue textures appear as: vesicular glasses, embedded concentrate glasses, thin 'wispy, glasses, surface immiscible globules and near-intact particles, (these are discussed further in section 5.4). Due to the limited number (29) of samples analysed and the possible bias present in the selection of a specific size range of craters, it is not possible to compare the significance of the results obtained here and those from LDEF experiments (Bernhard et al., 1993a) where over 600 impact features were observed. However although quantitative comparisons are not possible, it is possible to compare the HST and LDEF results qualitatively, in terms of the impact chemistry.

Both IDPs and Antarctic micrometeorites (AMMs) are identified in terms of the major mineralogical components (e.g. Klöck and Stadermann, 1994), thus the natural impact residues must be sub-divided and classified in these terms so that direct comparison with IDPs and AMMs chemistry can be made. Thus to be able to make such comparisons, the residues must be classified in terms of mafic silicates (olivine and pyroxene) and layered silicates with phylliosilicates (e.g. saponite).

5.3.2. Mafic Origin Of Residues

Elemental signatures of Mg, Si and Fe within a residue are an indication of possible mafic origin, although previous studies have highlighted that such an elemental combination without minor S or Ni, is not an unambiguous signal for meteoritic olivine and could be solid rocket motor ablation debris (Laurance and Brownlee, 1986). The Mg-Fe residues identified in the solar cells are components within a polycomposite residue, where the Mg-Fe component is the dominant chemistry, with minor associated Fe-Ni metal and Fe-Ni sulfides (figure 5.4). This combination of elemental components is strongly suggestive of a mafic origin and similar residues were identified in the high purity Al/Au micrometeoroid collectors from LDEF (Brownlee et al., 1993). The residue chemistries, if assumed to be mineralogical remnants, are typical of those of intact IDPs or AMMs (Genge et al., 1997). The mafic residues identified are observed as embedded and vesicular melt glass within the host melt (Graham et al., 1998), therefore it is generally difficult to obtain a diagnostic signal that would enable the sub-classification of whether the residue is olivine- or pyroxene-dominated. However, one of the embedded glass residues contained (Mg+Fe) / Si ratios directly comparable with forsterite olivine (a specific mafic silicate identified in meteorites) (figure 5.5). It is not possible to conclude that this is the original composition of the olivine or whether it had undergone chemical fractionation during the impact processes. Previously such a detailed classification has only been possible when near-intact particle fragments have been identified in hypervelocity impacts (HVIs) in space hardware, e.g. the Mg-rich olivine particulates from Solar Max (Rietmeijer and Blandford, 1988).

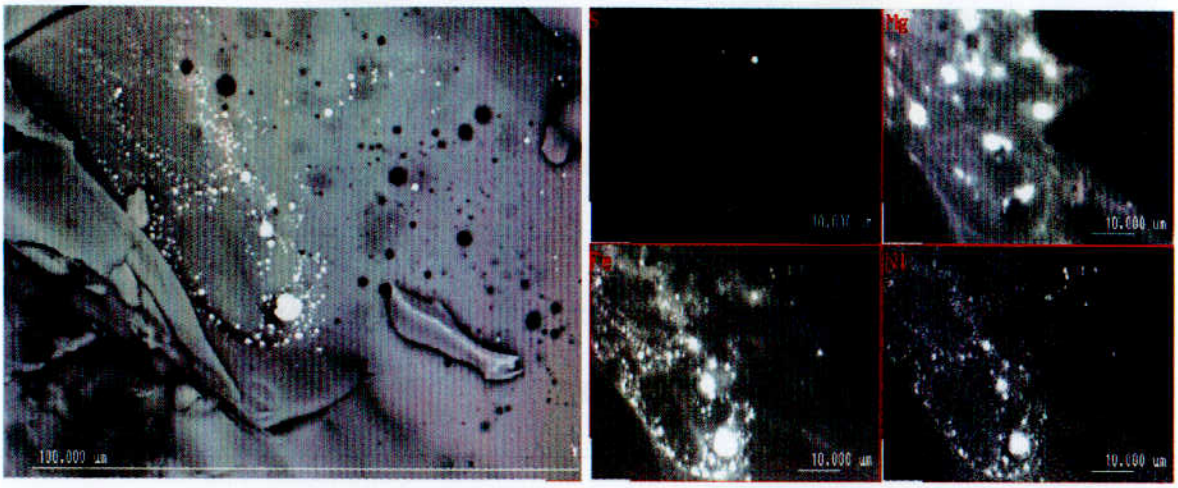

Figure 5.4 BEI of the impact crater identifies bright and dark areas in the melt-pit which correspond in the X-ray maps to Fe-Ni metal droplets and Fe-Ni sulphide droplet (bright areas) and Mg+Fe (dark areas).

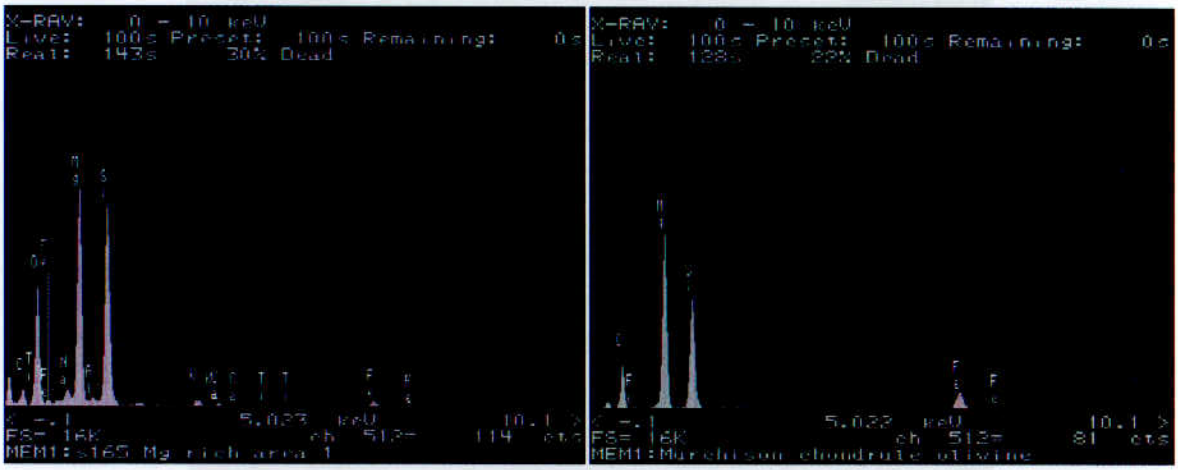

Figure 5.5 Shows the comparison of the EDS spectrum obtained from the Mg-rich residue component with a spectrum obtained from an olivine grain from a meteorite sample.

5.3.3 'Layered silicates' & Phyllosilicates

The identification of a residue that is predominately 'layered silicate' rather than mafic silicate in origin is problematic. HVI processes such as devolatisation and metamorphism are likely to remove water, or alter the mineralogy to such a degree that the resultant residue would probably be indistinguishable from that of a primary, anhydrous mafic particle (i.e. the dominant elemental components will be Mg and Fe). However, we suggest that notwithstanding such difficulties it might be possible to enable such identification by observing the textural morphology of the residue as well as the chemistry

(Graham et al., 1998). In figure 5.6, the BEI image identified a discrete dark area within the melt. The back-scattered electron intensity was lower than would be expected for a silicate of mafic origin. The darker area corresponded to Mg-rich and Fe-poor X-ray maps; the Si peak was also lower than generally associated with mafic residues. A similar observation in an LDEF residue led Zolensky et al. (1994) to conclude that the impactor was a 'layered silicate' in origin. Thus, using this as a guide it is proposed that the residue shown in figure 5.5 was also produced by the impact of a layered silicate.

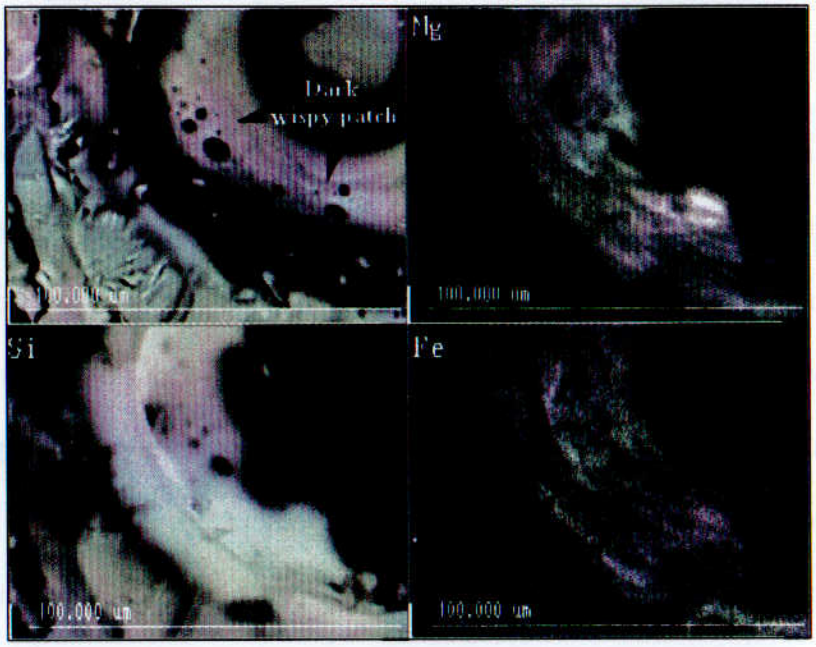

Figure 5.6 A residue of possible 'layered' silicate origin. The BEI image identifies dark wispy patches in the melt, which corresponds to the Mg and Fe X-ray elemental maps.

5.3.4 Metallic Components

The mafic residue shown in figure 5.4 also contained minor metallic phases, Fe-Ni sulfides, Fe-sulfides and Fe-Ni metal as surface immiscible melt droplets/globules. Such features were identified in the LDEF residues (Brownlee et al., 1993) and it is assumed that these droplets are the product of extremely rapid cooling as there appears to be no volatile loss of sulphur. The observation of such droplets in association with Mg+Fe components is not unexpected if the residue is of micrometeoroid origin as both mafic and 'layered'

silicate-dominated IDPs contain minor metallic phases (Klöck and Stadermann, 1994), as do AMMs (Genge and Grady, 1998). In two craters, the metal phase was identified as the sole component, where the melt pit was covered in nanometre to micron sized Fe-Ni metal globules (maximum diameter was 5μm). An artificial impactor could have generated the globules, but the Ni concentrations were distinctively within the range of meteoritic material (up 7.5 wt%), suggesting that the original impactor may be natural Fe-rich, non-chondritic micrometeoroids (this observation is discussed further in Chapter 6).

5.3.5 Refractory Components

Two craters contained abundant Ca-rich particles (<10μm in diameter) (Figure 5.7), whose EDS spectrum was remarkably similar to that of the carbonate mineral calcite. Although the micro-spot analysis showed a lack of silicon, such a signal is not unambiguously indicative of natural origin. It is possible that the Ca-rich particles could be remnants of urine, although in that case the EDS spectrum should contain other elements (e.g. Na and K). The lack of these volatile elements suggests that the Ca-rich particles are not a result of space debris or contamination. We tentatively suggest that these Ca-rich particles are in fact remnants of rare refractory phases such as: hibonite, gehlenite and perovskite that have all been identified previously in IDPs (Zolensky, 1987). This observation is further supported by the identification of Mg- and Al-rich oxides (possibly spinel), Mg- and Fe-bearing silicates with a low back-scattered electron intensity (possibly saponite) and a Mg- and Fe- non-silicate residue (possibly carbonate) in association with the Ca-particles. A mineral assemblage similar to this was identified in a chondrule in Murchison a carbonaceous chondrite meteorite, a group which has previously been suggested as parent body materials for IDPs and AMMs (e.g. Klöck and Stadermann, 1994). The preservation of near-intact particles may indicate a relatively low velocity oblique impact; previous

studies (e.g. Brownlee et al., 1993) suggested particles of asteroidal origin would have the orbital parameters to allow this.

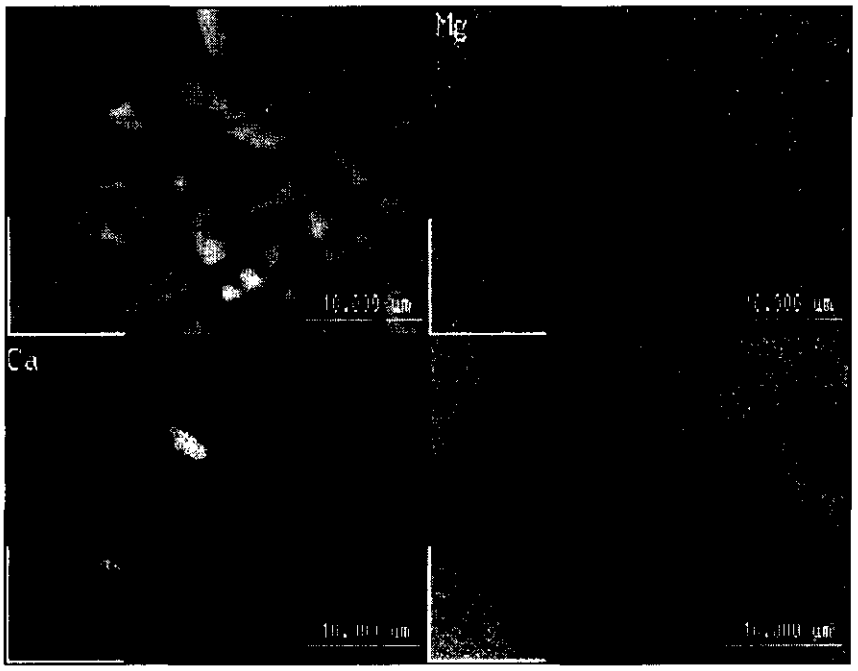

Figure 5.7 X-ray maps identifying the Ca-rich particles trapped in the spall zone of the impact crater.

5.4 Natural & Simulated Hypervelocity Impacts Into Solar Cells

(Extracted from Graham et al. (1999b))

5.4.1 Textural Observations Of Residues

The physical appearance of the impact residues identified within the craters (D_{CO} 100-1000μm) were highly variable in both quantity and composition; a similar conclusion was previously made in LDEF studies concentrating on micrometeoroid residues in Al and Au substrates (Brownlee et al., 1993). Our data however, especially that from the LGG (light gas gun) experiments, suggest that apart from the velocity dependent factors, there may also be a strong link between residue texture and the original mineralogy of the impactor. Although the processes of formation and retention of residues are undoubtedly extremely

complex, it is unlikely that the textural variations observed in our LEO HVI are due to differing types of interaction between a single composition of impactor particle and different components of the host substrate. It seems likely that variations in the degree of impactor vaporisation and fragmentation, the viscosity and miscibility of melt components (and therefore the intimacy of their mixing) together create residue textures that may be diagnostic of the impacting mineralogy. This may prove to be important in distinguishing silicates of differing crystal structure and volatile content (e.g. orthosilicates such as olivine, framework silicates such as pyroxene, and hydrous phyllosilicates such as saponite). EDS spectra of embedded particles sometimes clearly reveal (Mg+Fe)/Si ratios directly comparable to those of specific mafic silicates, however many residues show much greater mingling with the host melt and cannot be assigned so simply to mineral groups on chemistry alone. Combined chemical and textural distinction might allow direct comparison of impactors with the recognised classes of interplanetary dust particles (mafic silicates; phyllosilicate and refractory phases (e.g. Bradley, 1994)). The textural features of the 20 residues identified as MM in origin in the solar cell craters can be defined as: glasses (surface (2/20) and sub-surface (10/20)); surface globules (13/20) and near-intact particles (2/20). A typical residue would consist of more than one of the different textural variations. To allow comparisons between LDEF observations and those herein, LDEF terminology (Brownlee et al., 1993) is used where appropriate in the description of the glass residues.

5.4.2 Vesicular Glass Residues

Vesicular melt residues usually have a distinctive 'ropy' appearance in BEI. They appear as networks on the surface of the melt pit, and occasionally as detached strings in the shattered surroundings. In some cases these melts demonstrate a degree of volatile retention during their deposition, in the form of possible gas bubbles, (dark areas in BEI

see figure 5.8a). The residues are usually enriched significantly in Mg, Ca and Fe above the solar cell composition, an assemblage suggestive of an origin from a mafic silicate, such as pyroxene as previously suggested in the preliminary investigation of the solar cells (Graham et al., 1997b). Vesicular residues were previously identified in LDEF craters on pure Al and Au substrates by Brownlee et al. (1993) who also suggested that the vesicular nature was a product of the volatile content within the impactor. The HVI of soda-lime glass (Ca-bearing silicate), selected as a micrometeoroid analogue, in the LGG also showed a characteristic ropy texture (figure 5.8b) in the residue similar in appearance to those which we consider to be a result of impact by natural particles. It is noteworthy that the vesicular texture proved to be enriched in Ca and Na (i.e. high volatile content within the projectile).

Figure 5.8a BEI of a vesicular residue (black arrows highlight the area of interest) observed in a LEO derived impact crater generated by a micrometeoroid. **Figure 5.8b** A BEI of a vesicular residue (black arrows highlight the area of interest) observed in an impact crater generated in the laboratory using soda-lime projectiles.

5.4.3 Glass-embedded, Concentrated Residues

In figure 5.4 the Mg- and Si-rich residue from LEO is an embedded patch within the melt pit. Were the patch derived from thermal melting of the impactor, or a condensate from a

gas, it might be expected that such a residue would show a high degree of elemental mixing with the host substrate (essentially a boro-silicate, similar to fluxes used to dissolve silicates for bulk geochemical analysis). The ED X-ray spectrum from the residue was, however, very similar to those from a meteoritic silicate grain (olivine from the CM2 meteorite Murchison – figure 5.5). This suggests that the patch may be a concentrated Mg+Si glass within the melt glass of the host, with almost no elemental mixing (i.e. immiscibility), or it is a surviving, shocked, solid particle beneath the melt surface. It was not possible to be certain whether the spectra from the residue patch shows the pristine composition of an end-member olivine or whether some degree of elemental fractionation has occurred during the impact process, although the former seems more likely. If the residue is a shocked solid particle it is unlikely that significant fractionation would have occurred.

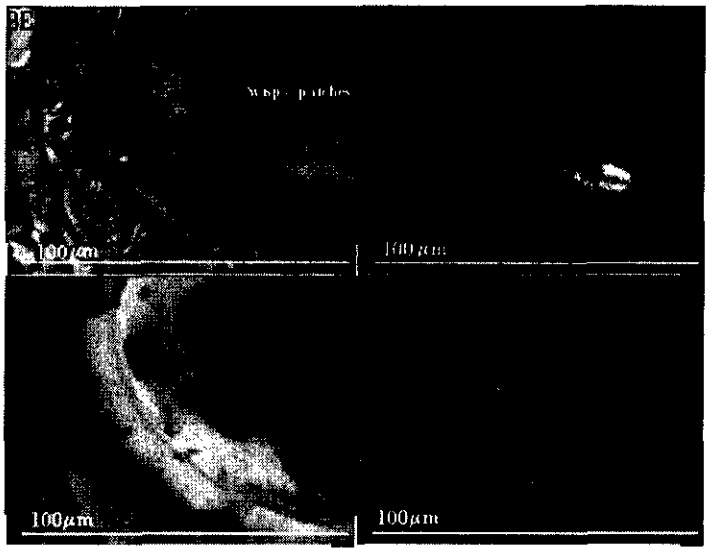

Figure 5.9 A BEI of a thin glass 'wispy' residue (highlighted by the black arrows) observed in a LEO generated crater. The discrete patches in the BEI correspond to enrichments in both the Mg and Fe elemental X-ray maps.

5.4.4 Thin Glass & 'Wispy' Residues

The textures described above show only limited interaction with the host melt during the impact process, indicated by the clear compositional contrast in BEI between vesicular or

embedded glass and the melted borosilicate substrate. The 'thin glass' residue in some LEO HVI is much more difficult to see, with only a slightly darker tone in BEI, and the texture could easily be overlooked. The texture is seen most easily in X-ray maps that enable the location of enrichment in Mg to be identified (figure 5.9). The lack of fluorine in these areas indicates the magnesium is not derived from the CMX layer of the cell. We tentatively suggest that this marked difference in texture (compared to vesicular and embedded residues) may be indicative of a different silicate mineralogy, probably a hydrous phyllosilicate component. If a LGG impactor of heterogeneous origin, e.g. Orgueil (CI carbonaceous chondrite meteorite) matrix (phyllosilicate-dominated) is added to the shot programme, it may well elucidate these preliminary findings.

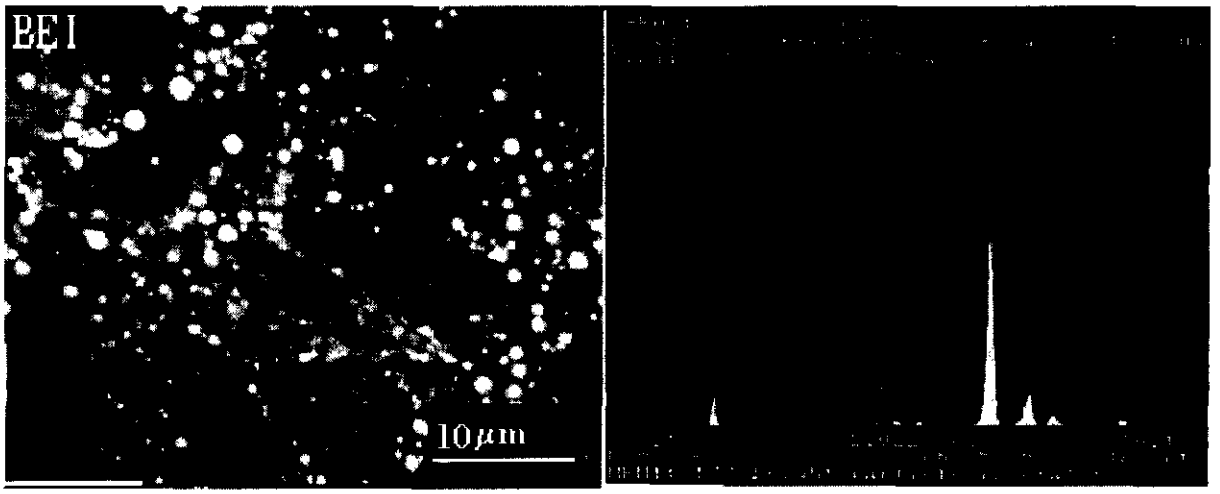

Figure 5.10 BEI of the metallic surface melt droplets observed in a LEO generated impact crater. The ED spectra obtained from the analysis of an individual droplet shows the enrichment in Fe and Ni.

5.4.5 Surface Globules

In low magnification BEI, several craters contained remarkably bright patches, showing strong compositional contrast between the host and the discrete residue chemistry (figure 5.4). At high magnification these patches reveal myriad separate, 1-10μm-sized hemispherical globules on the surface of the melt-pit or shallowly embedded within the melt glass (figure 5.10). X-ray maps showed that the residue had not mixed with host melt in the way that silicates sometimes did. The globules were composed of Fe-Ni metal

(kamacite ratios) and metal sulfides (Fe-Ni sulfides and Fe-sulfides); similar globules were identified in a crater on Al from LDEF (Brownlee et al., 1993) and it is assumed that they form by very rapid quenching. There appears to be no loss of volatile sulfur during the process, suggesting that the droplets were immiscible liquid melt droplets, rather than condensates from a gaseous phase. The pyrrhotite (FeS) impactor in the LGG produced very similar textural features (figure 5.11) on a variety of scales. There was, however, some variation of texture from the expected hemispherical globule form, some melt surfaces showed amalgamation of globules into broader surface patches or stretching of sulfide residue into streaks and curls. There was no evidence of mixing with the borosilicate melt.

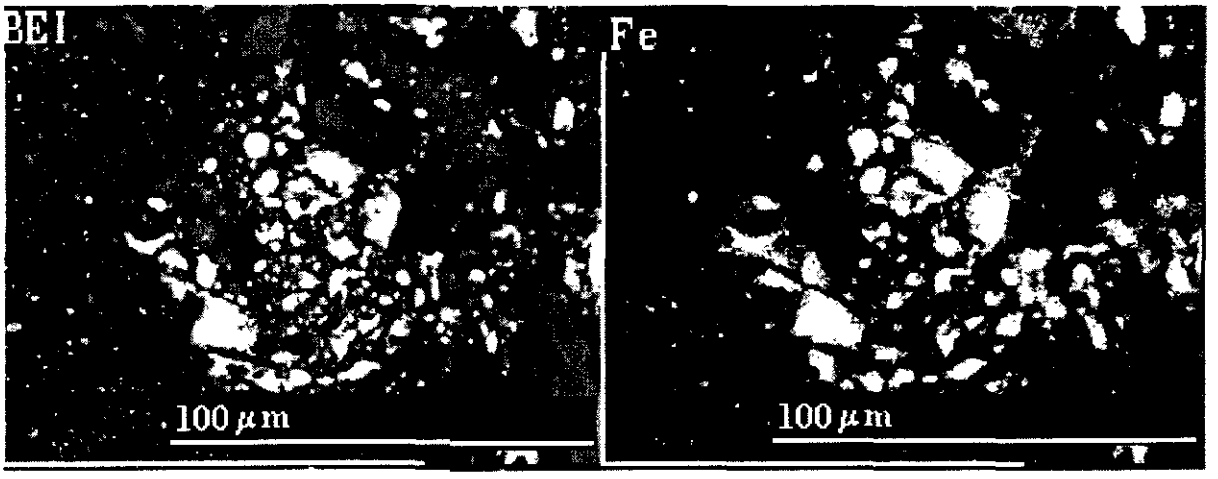

Figure 5.11 *BEI of the impact residue derived from the laboratory simulated pyrrhotite (FeS) LGG shot.* The melt droplets in the BEI correspond to the enrichments in the Fe elemental X-ray map.

5.4.6 Near-intact Particulate Residue Material

The preservation of near-pristine particles in HVIs is extremely rare (Rietmeijer and Blandford, 1988; Brownlee et al., 1993) yet the identification of such material clearly offers the best opportunity to classify impactor origin. The steel projectiles fired during the LGG program revealed that residue material is not only deposited in the melt-pit, but that it is also possible to locate material in both the conchoidal fractures and the underlying spall zone. Therefore, there exists the probability that certain craters, especially when the

zone of conchoidal fractures does not show complete detachment of fragments around the entire circumference of the crater, residue or even debris from the impactor may be retained. The re-evaluation of the LEO-exposed impact craters identified one with calcium-rich material (<8 μm diameter) as near-intact particles located in the spall zone and radial fractures (figure 5.12). These fragments appeared not to be simply contamination at some later stage, as they showed evidence of surface melting (figure 5.13). We conclude that such debris was emplaced explosively. EDS X-ray microanalysis showed abundance of calcium and lack of silicon, giving a spectrum remarkably like that of the carbonate mineral calcite. Calcite is a common constituent of altered refractory inclusions and veins in hydrated carbonaceous chondrite meteorites (e.g. Grossman, 1975). It might be expected that explosive fragmentation on emplacement would result in the complete destruction and loss of such volatile-rich compounds and not their retention.

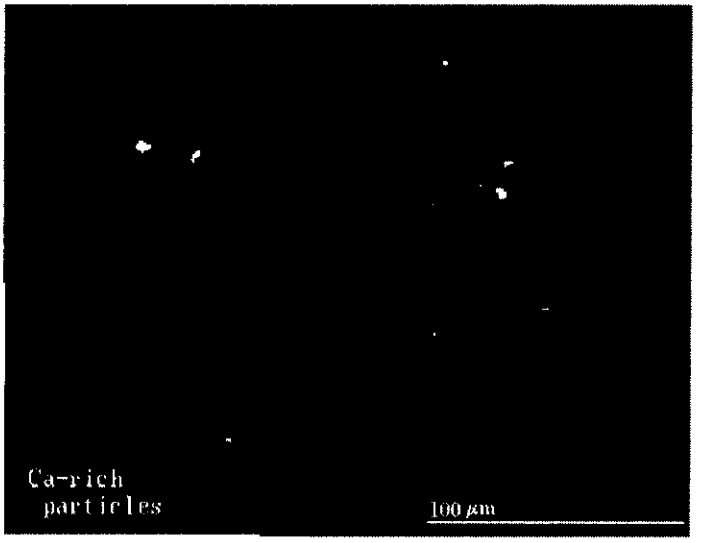

Figure 5.12 BEI of an impact crater generated in LEO, which contains Ca-rich particles in the spall zone. The lack of the particles in the surrounding area would suggest that they are not simply contamination products.

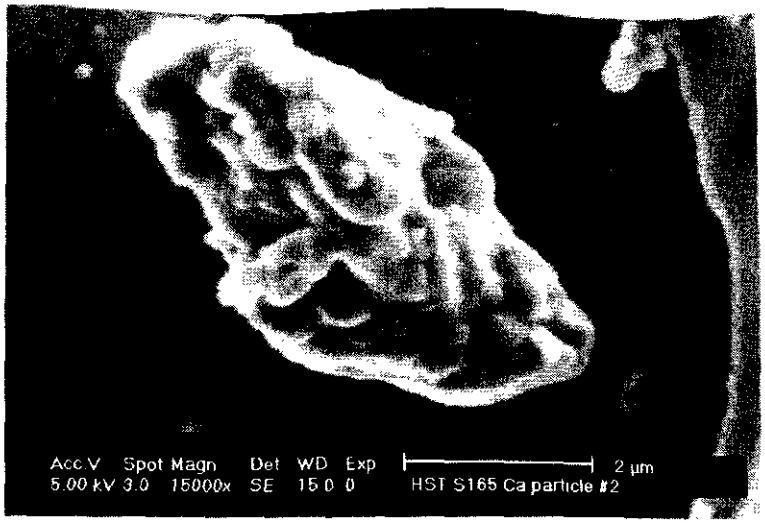

Figure 5.13 A secondary electron image (SEI) of a Ca-rich particle located in the LEO derived crater. The surface texture of the particle indicates that it has undergone a degree of melting that would suggest that it is not a contamination product.

To evaluate whether such a volatile chemistry would survive HVI, calcite grains were fired down the LGG. Subsequently, fragments were observed to be retained in the spall zone of several craters. These fragments (figure 5.14) were demonstrably not simply original mineral grains (i.e. artefacts of the experiment, accreted after formation of the craters), as they showed evidence of surface alteration and were mantled in a thin coat of borosilicate host glass melt. The LGG shot of $CaCO_3$ (at 5km/s) has indicated that calcite can survive HVI. It has been suggested that such EDS spectra of LEO impact particles could be ambiguous in distinction between minerals of micrometeoroid origin (calcite in this case) and space debris (Ca-rich particles from urine). It seems likely that were our fragments, remnants of urine solids, other volatile elements (e.g. Na and K) would be detected. Areas rich in sodium and chlorine have been found on the surface of some of the cells, probably as the result of contamination after recovery, but these are distinct in texture from impact residues. The techniques utilised in this study do not produce substantial volatile loss during analysis and the presence of some sodium or chlorine would be expected in urine-derived solids given the very substantial enrichment of these elements in urine when compared to calcium.

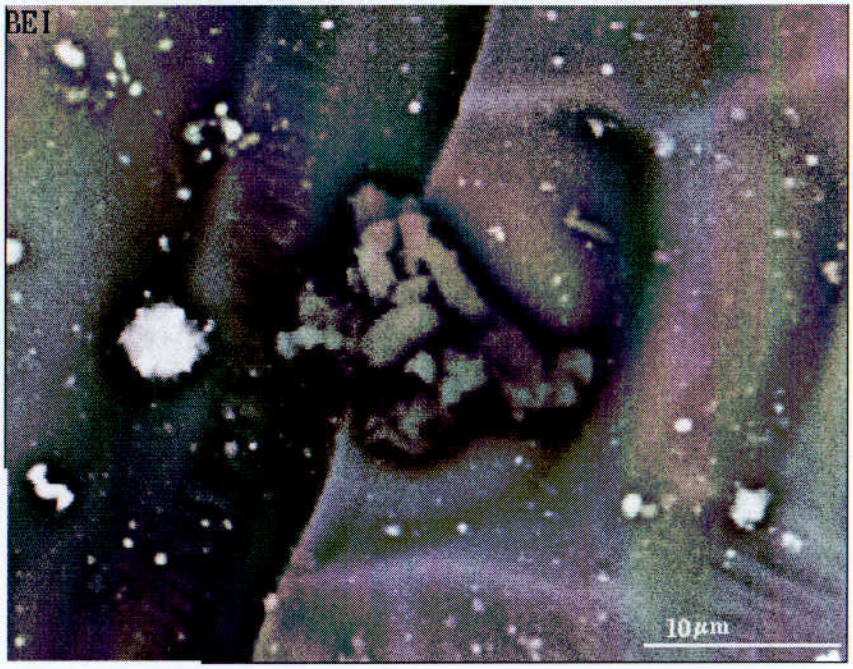

Figure 5.14 A BEI of Ca-rich fragments retained in the spall zone of a impact crater generated by the calcium carbonate LGG shot. The fragments are comparable to the fragments located in LEO impact craters (figure 5.13).

The scanning techniques employed in this investigation were not able to yield information on the crystallographic structure of the fragments. It is hoped that using the established techniques of residue extraction (Teetsov and Bradley, 1986) the larger particle (8μm diameter) can be removed, and any surviving crystal structure be determined by transmission electron microscopy.

5.5 Summary & Conclusions

Previous investigations into HVIs in space hardware have focused on ductile target surfaces, e.g. Al and Au (Bernhard et al., 1993b). The analysis of such surfaces highlighted the complexity of these studies, as the location of residue material was rare, (Brownlee et al., 1993). The investigation herein has focussed on solar cells (brittle surfaces) returned from the HST after 3.62 years of space exposure in LEO. Detailed analytical scanning electron microscopy has enabled the identification of extraneous

residue material in impact craters (D_{CO} = 100-1000μm). The residue material was initially classified in terms of either space debris or micrometeoroid in origin. The latter has been sub-classified using chemistry and textural observations e.g. embedded and vesicular glass melts identified as mafic silicates in origin.

Chapter 6

Iron-Nickel Metal Rich Micrometeoroid Residues & Interplanetary Dust Particles

6.1 Introduction

The residues that have been derived from micrometeoroid impactors are rarely composed of a single remnant mineral component (e.g. Fe-sulfides). Rather, they are generally an intimate mixture of the individual mineral components. This enables the use of the broad terminology of "chondritic", to describe polymineralic residues that have chemical compositions which are suggestive of those observed in IDPs (which in turn are similar to chondritic meteorites). Within the general term "chondritic" are included particles that contain remnants of anhydrous mafic silicates (i.e. olivines and or pyroxene) with minor components of Fe-Ni sulfides and Fe-Ni metal (figure 6.1) and particles with remnants of hydrous silicates (saponite and or serpentine) again with minor components (figure 6.2).

The broad classification used herein for residues found on space hardware allows comparison with studies of the extensive repository of cosmic dust particles collected from terrestrial locations, and particularly in those from the upper stratosphere (e.g. Warren and Zolensky, 1994). Also under the banner "chondritic" are residues that appear to be monomineralic metallic sulfides (figure.6.3). In detail these latter residues could have formed from particles of primary metallic sulphides (from some unknown source, but they could also come from non-chondritic meteorites e.g. irons (Buchward, (1975)), or they could represent a discrete portion of a chondritic meteoroid (which either fragmented to produce individual grains prior to impact or which became dissociated during the impact event).

Using Occam's razor the rotation of primary metallic sulfide particles is discounted because such materials have never been observed as conventional meteorites. However, within the collection of residues identified herein as micrometeoroid in origin, there are two Fe-Ni metal residues which appear to be monomineralic but which may be non-chondritic. If true, these would have been the first non-chondritic cosmic dust particles ever to have been identified.

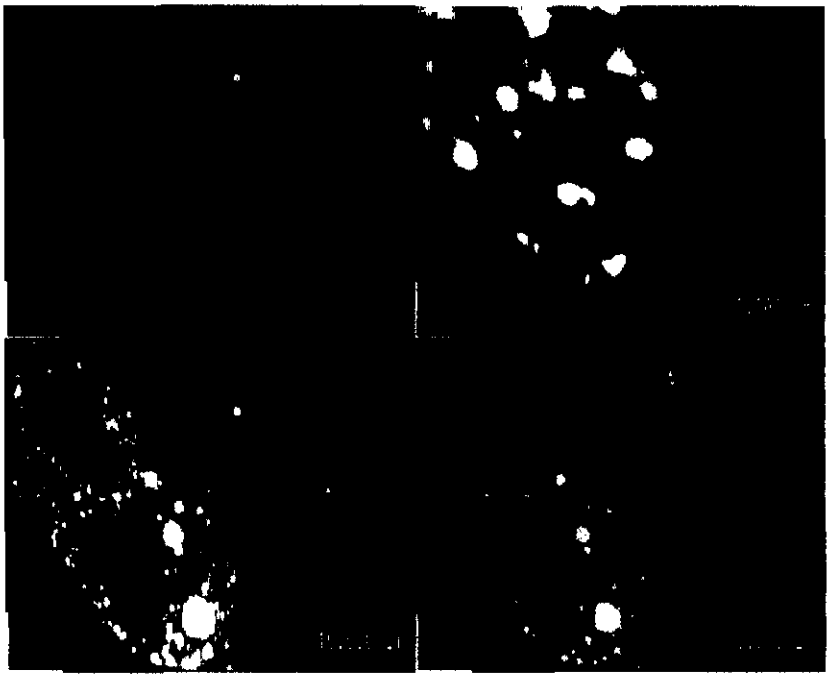

Figure 6.1 X-ray elemental maps showing residue materials which are enriched in Mg, Fe, Ni and S. This combination of elemental chemistries would be suggestive of an anhydrous (chondritic) origin for the impactor.

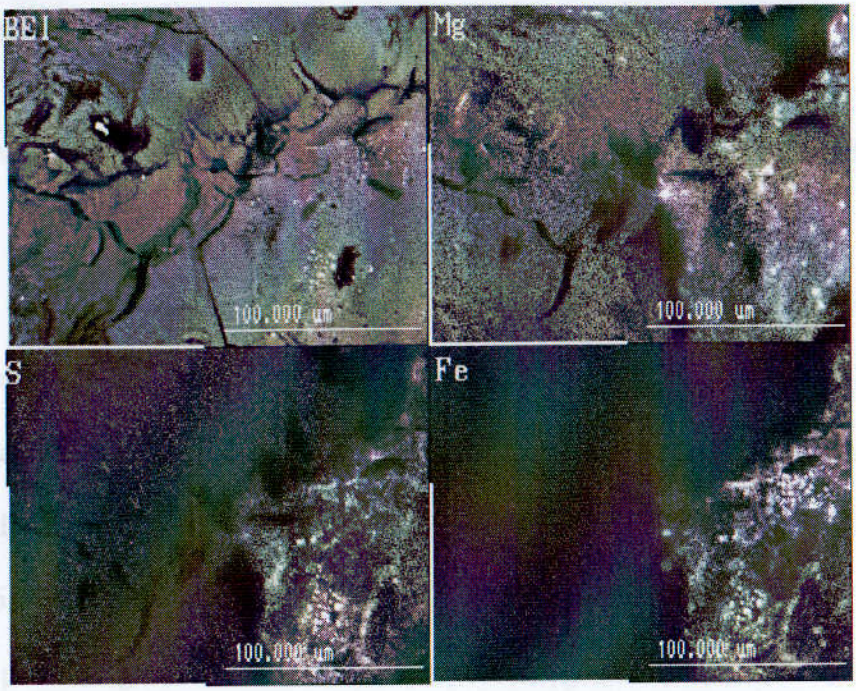

Figure 6.2 BE image of a impact residue which is suggestive of an hydrous (chondritic) origin for the impactor (see Chapter 5 for a detailed discussion of the possible distinguishing features in terms of chemistry and morphology which allow the classification in terms of hydrous and anhydrous origin). The X-ray elemental maps identify that the residue in enriched in Mg, Fe and S.

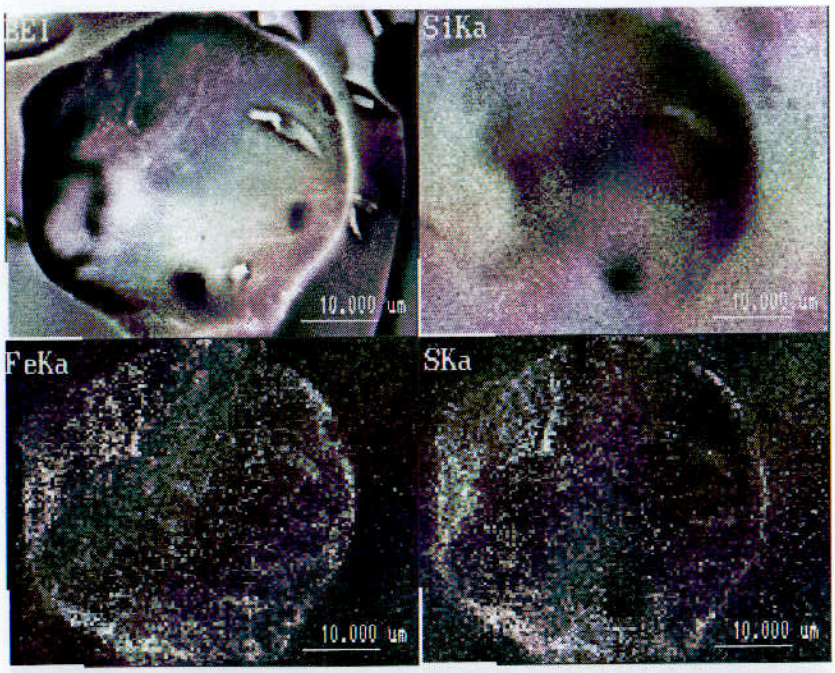

Figure 6.3 BE image of residue material which from the X-ray elemental maps is composed of Fe and S, suggestive of an Fe-sulfide impactor (most likely to be chondritic in nature).

6.2 A Detailed Analysis Of One Of The Fe-Ni Residues

6.2.1 Observations From Back-scattered Electron Imaging & X-ray Elemental Mapping

The optical analysis of the impact crater in HST solar cell s177 identified the black extraneous material that has been seen in several of the craters (see Chapter 3), yet in this crater the material appeared to be finely dispersed across the entire crater bowl. The BEI imaging of the crater at low magnification (x75) identified a bright mass covering the melt pit (figure 6.4). High magnification imaging of the melt pit identified this mass to be individual spherical globules attached to the surface and/or embedded within the melt surface (figure 6.5). The X-ray elemental maps of the melt pit identified these globules to be almost entirely composed of Fe and Ni (figure 6.5) compared to the analysis of the surrounding areas around the globules which were composed of the CMX melt from the solar cell itself.

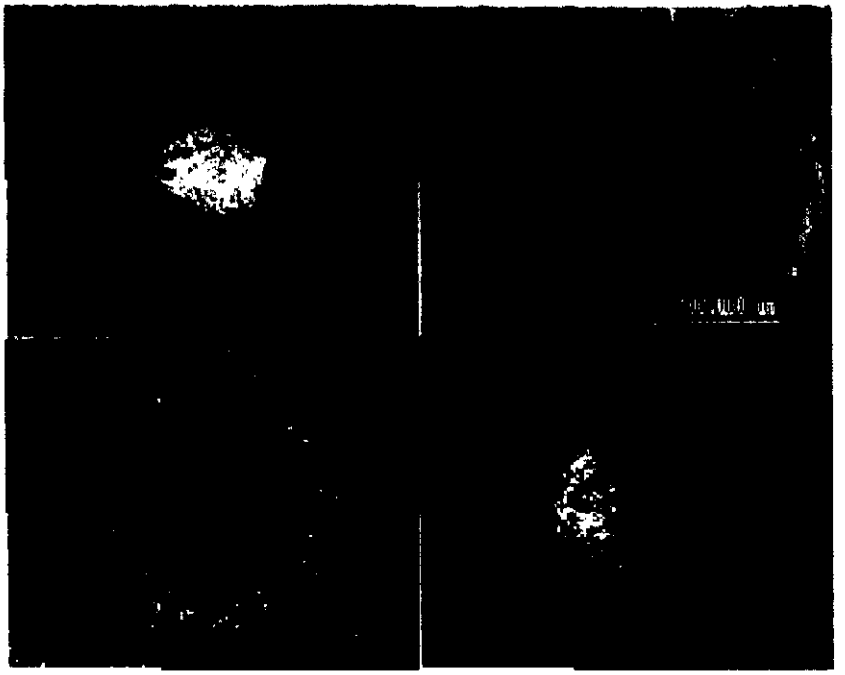

Figure 6.4 BEI of the impact crater in s177 (x75 magnification) and X-ray elemental maps that are suggestive of an Fe-rich impact residue.

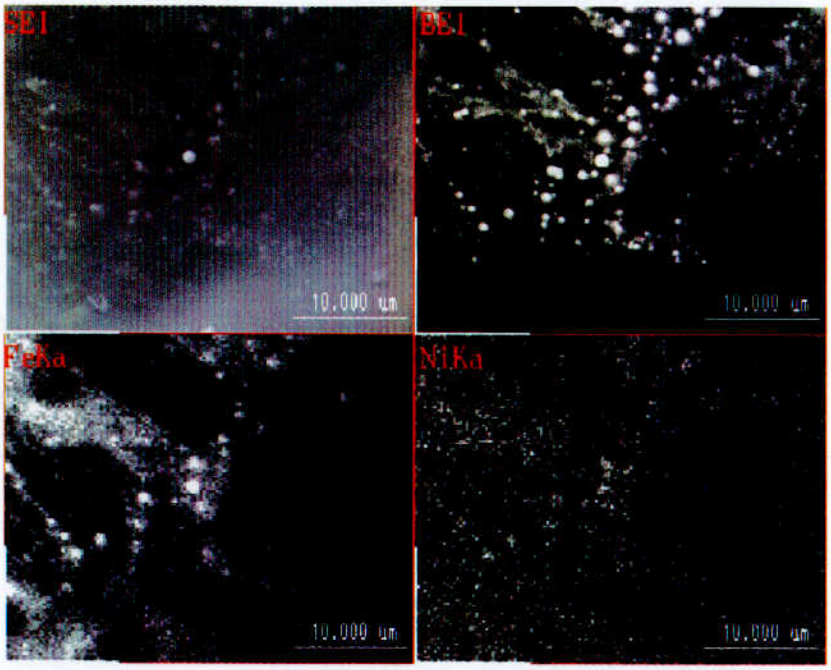

Figure 6.5 SE and BE imaging of the bright residue material within the crater pit that was identified in figure 6.4. The X-ray elemental maps indicate that the material is composed solely of Fe and Ni.

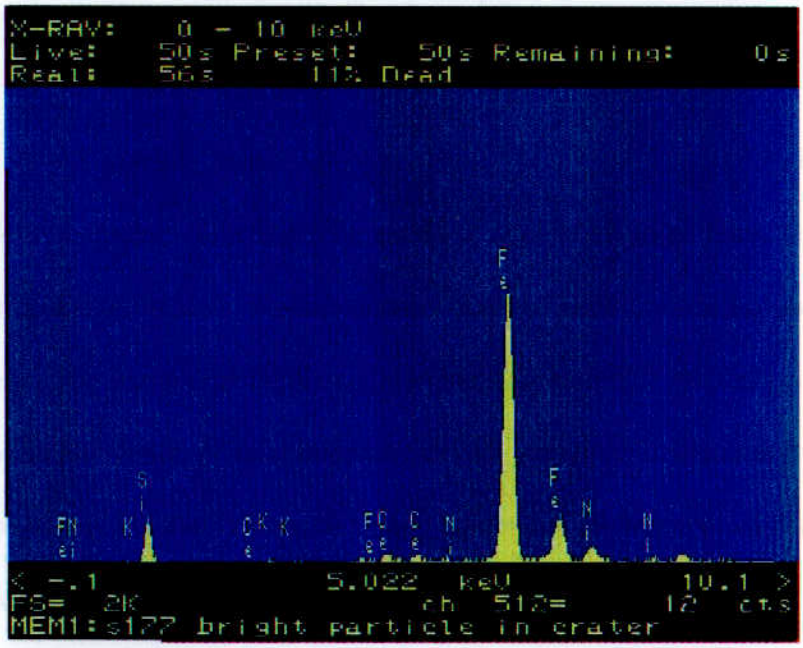

Figure 6.6 ED spectrum obtained from one of the Fe-Ni globules identified in figure 6.5 (the Si, K and Ce peaks are from the solar cell composition melt).

6.2.2 Detailed Quantitative Analysis Of The Bright Globules

In general the location of the melt residues did not allow quantitative elemental analysis because of analytical difficulties already discussed (see Chapter 2.5), however, plenty of

qualitative ED spectra were obtained (figure 6.6) which showed that each globule comprised only Fe and Ni. Never the less, it was decided that as the globules appear from the mapping to be comprised of Fe and Ni, an attempt at quantitative measurements was carried out. The deep position of the globules in the crater prevented the full use of analytical comparisons using the standard matrix "ZAF" (Z stands for atomic number effects; A for absorption effects and F for fluorescence effects).

Making the assumption that components other than Fe and Ni were contaminant components from the CMX glass, and applying quantitative corrections for the transition metals only, the composition of the globules turns out to be 93.4± 1.8% Fe by weight and 6.4± 1.8% Ni by weight, with trace Mn (data obtained from the mean and rmsd of 50 analyses of separate globules, 100 seconds each). At face value the data would suggest that the original impactor was a metallic Fe-Ni particle.

Of course an Fe-Ni particle could arise in similar ways to those considered above to explain the Fe-S residues. But there is an additional possibility here, namely that the particle has an association with another known class of (non-chondritic) meteorites – the iron meteorites. The elemental Fe/Ni ratio of the impactor are strongly suggestive of a composition of an Fe-Ni alloy found in practically all groups of iron meteorites (Buchwald, 1975). To confirm whether kamacite could generate an impact residue of the type observed, it was one of the monomineralic chemistries investigated with the laboratory shot program with the LGG. As expected the resultant residue produced the surface globules similar to those observed in S177 and the ED spectra of individual globules were also similar (figure 6.7) showing that Fe-Ni form an immiscible melt under HVI solar cells.

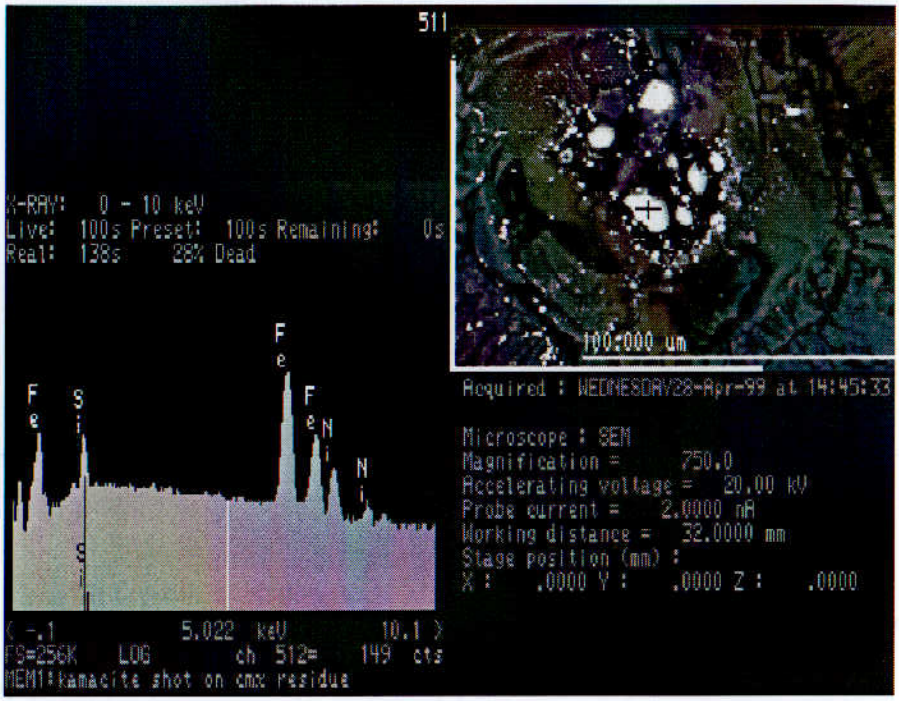

Figure 6.7 BEI and ED spectrum of the kamacite derived impact residue. The residue was generated by firing 125-150μm fragments of kamacite into a solar cell target using the light-gas-gun facility at the University of Kent.

6.2.3 Implications Of Metallic Impactors

There is always the possibility that the melt residues observed in craters are artefacts or contamination products generated during or after the return of the array. Since post-flight contamination will only be in the form of particulate material, rather than melt and it is quite obvious that the residue observed in S177 is melt, post-flight contamination can be ruled out.

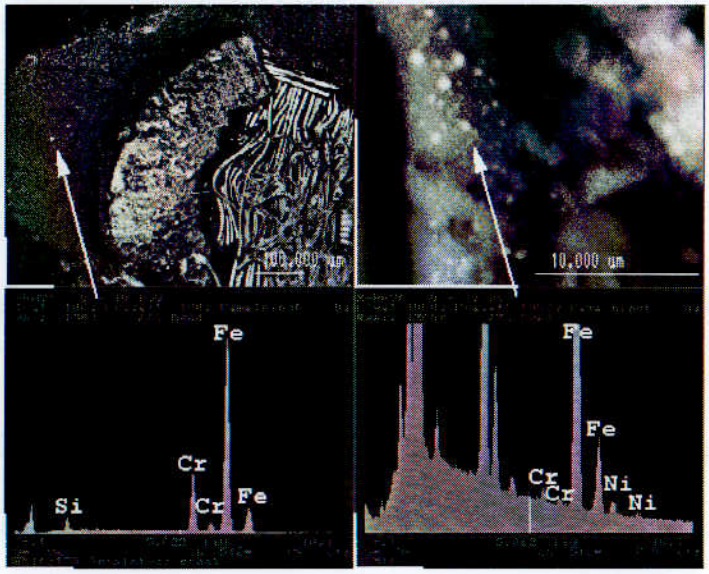

Figure 6.8 BE images and ED spectrum of the remnants of a space debris metallic impactor (only the elemental chemistries extraneous to the stiffener composition are shown).

It is entirely possible of course that the Fe-Ni globules were derived from space debris; For instance, there are many specialised metals used in the aerospace industry, from components on rockets and satellites for example. Impact craters derived from metallic particles of space debris have been located in returned spacecraft surfaces (e.g. Bernhard et al., 1993a and Christiansen et al., 1998). Yet many of these are complex metallic alloys, having a characteristic X-ray spectrum containing not only Fe and Ni but Cr and/or Al, V, Ti and Mo (e.g. alloys from LDEF surface, Bernhard et al., 1993a and b and shuttle surfaces Christiansen et al., 1998). The typical detailed composition of such stainless steels is > 70 wt % Fe; up to 14.5 wt % Cr and 6-8 wt % Ni (Gray, 1977). In this investigation (in solar cell 170) a residue apparently derived from a stainless impactor was also observed (figure 6.8).

From the spectrum obtained from this residue it is clearly possible to see the presence of both Ti and Cr. The globules analysed in S177 contained no Cr, Ti or Mo even in minor or trace amounts that are detectable by the ED detector. Also the quantitative analysis identified that the Fe content was (93.4 wt %) appreciably higher than that in most flight-

approved stainless steels. Collectively these observations were taken to suggest that the particles which produced the Fe-Ni globules during HVI are of natural origin rather than artificial.

Fe-Ni metal as a possible natural impactor had been identified in LDEF studies (e.g. Zolensky et al., 1994) but these globules were appreciably smaller in size (<50nm) compared to the larger structures observed herein and were only identified under the transmission electron microscope. Furthermore these droplets were associated with a ferromagnesian glass matrix (Zolensky et al., 1994) demonstrating that they were in fact inclusions or minor components within a more extensive, chondritic matrix. Similarly in this investigation Fe-Ni globules have been observed (figure 6.1) where they are associated *with a silicate component, and not as an individual isolated component.*

For the isolated Fe-Ni globules observed in s177 it could be argued that they represent extreme elemental fractionation during the impact event such that the silicate component has been lost by volatilisation. However this seems extremely unlikely since polymineralic residues of a chondritic nature have been observed in 8 out of the 20 impact residues in the solar cells classified as derived from micrometeoroid impactors (e.g. figure 6.1). It is therefore concluded that other mineral phases have not been observed because they were not there to start with; in other words the residue is a remnant of a monomineralic Fe-Ni particle. The problem which was manifest with this conclusion was, if true, that there should be examples of non-chondritic, Fe-Ni particles in the stratospheric IDP collectors.

It is well known that iron-rich spherules are represented in the ground-based collecting of micrometeorites, clearly if they do not exist in the stratospheric collections then the iron-rich spherules are probably formed during atmospheric heating and melting of chondritic materials (e.g. Brownlee, 1978). Since no one had ever reported any research on Fe-Ni

IDPs, the only way to be certain was to go through the cosmic dust catalogues and check every entry.

6.3 Analysis Of The Stratospheric Collections Of Interplanetary Dust Particles

To date the interplanetary dust particles collected in the stratosphere by NASA (e.g. Warren and Zolensky, 1994; Rietmeijer, 1999) is the most catalogued sampling of material. At present, IDPs can be classified as essentially mafic (olivine- and pyroxene-) silicates and layered- silicates (Klöck and Stadermann, 1994) although analysis of bulk chemistry of particles collected has also identified metallic sulfide (Mackinnon et al., 1982). What research has been carried out on metals in IDPs has focused on nanometre components within larger grains (e.g. Bradley, 1994). To put this into perspective note that the Fe-Ni globules discovered herein were typically 1μm in diameter.

It transpired during the search through the cosmic dust catalogues (section 6.3.1), along with extensive e-mail communication with M. Zolensky (curator of IDPs, NASA-JSC), that in fact Fe-Ni particles had been detected previously (e.g. Mackinnon et al., 1982). Now, if the make-up of the IDP collection was to mirror meteoritic fall statistics (using the number of meteorite falls up to 1992, Heide and Wlotzka, (1994)), it would be anticipated that 5.15% of IDPs ought to be Fe-Ni particles. That they are not requires some explanation.

Firstly particles collected in the stratosphere are subject to atmospheric entry selection effects (e.g. Flynn, 1989a&b) which may generate a collection and curation bias (Rietmeijer, 1999). In terms of collection there is a possibility that certain flights may collect only larger particles; alternatively particles with certain physical characteristics may

be favoured (Sutton, 1994; Rietmeijer, 1999). Concerns of such a problem can only be assessed if *every* particle collected from *every* flight is analysed. This is something which to date has not been carried out (Zolensky, personal communication).

However there is yet a further bias that may result from the preparation of the catalogue – this is because the cosmic dust community is currently interested in investigating the most primitive source of material in the Solar System, and that is the form most likely to be from comets, i.e. chondritic particles are the focus of most investigations (e.g. Bradley, 1994). As a result of this whilst the catalogues attempts to be representative of the material collected, there is nonetheless a degree of bias towards chondritic particles (Zolensky, personal communications). Therefore to assess the abundant Fe-Ni particles a review of the catalogues must be carried out.

6.3.1 Reviewing NASA's Cosmic Dust Catalogues

As a part of the collection and curation process, the Cosmic Dust Preliminary Examination Team (CAPET) compiles a series of catalogues which contains a secondary electron image of each particle recognised along with an X-ray elemental spectrum, and with a brief description and classification. At present there are a total of 15 catalogues which contain information on all the particles collected since 1981. To identify where Fe-Ni metal IDPs have been collected, a survey was carried out on the 15 catalogues essentially looking for particles with an ED spectra comprising of only Fe and Ni. From this survey a total of 24 particles were identified (table 6.1).

Cat No	Year	Collection Flag	Mount No	Particle No	Size(μm)
1:1	JAN 1982	W7017	W7017A	W7017A6	17
1:2	MAR 1982	W7017	W7017E	W7017E7	10
2:1	APR 1982	W7029	W7029A	W7029A9	2
2:1	APR 1982	W7029	W7029C	W7029C14	7
2:2	JUN 1982	W7029	W7029I	W7029I14	5
3:1	SEPT 1982	U2001	U2001D	U2001D10	9
4:2	SEPT 1983	W7027	W7027F	W7027F15	3
4:2	SEPT 1983	W7027	W7027I	W7027I6	7
6:1	NOV 1985	N/A	U2011C	U2011C8	12
7:1	NOV 1985	U2022	U2022G	U2022G19	10
8:1	NOV 1986	W7013	W7013A	W7013A4	7
11:1	JUN 1990	L2005	L2005J	L2005J2	8
11:1	JUN 1990	L2005	L2005J	L2005J8	8
11:1	JUN 1990	L2005	L2005J	L2005J15	9
11:1	JUN 1990	L2005	L2005J	L2005J22	8
11:1	JUN 1990	L2005	L2005Q	L2005Q3	15
12	JUN 1991	L2005	L2005T	L2005T3	10
12	JUN 1991	L2006	L2006J	L2006J1	12
12	JUN 1991	L2006	L2006L	L2006L1	10
12	JUN 1991	L2006	L2006L	L2006L11	13
12	JUN 1991	L2006	L2006G	L2006G11	10
13	SEPT 1992	L2005	L2005AC	L2005AC3	11
13	SEPT 1992	L2005	L2005AD	L2005AD6	11
14	JUNE 1994	L2008	L2008I	L2008I4	6

Table 6.1 Complete list of the 24 Fe-Ni rich particles that were identified in the 14 volumes of the Cosmic Dust Catalogue. The shaded areas are the samples were finally requested for this investigation.

As only a total of 24 particles were identified, it was not possible to request all the particles for analysis – the Cosmic Dust committee who allocate IDPs to research felt that as there was only a limited number of these particles the majority should remain in the cosmic dust collection at the NASA Johnson Space Center. Instead a total of 7 were requested, the selection criterion being that any particle below 7μm would be difficult to image or to analyse chemically (the particles requested are highlighted in table 6.1).

6.3.2 Experimental Handling

The small size of the stratospheric Fe-Ni IDPs made handling a complex problem. Ideally for a material, analysis would be carried out on a flat surface, i.e. each particle should be sectioned. For larger IDPs and micrometeorites this is not usually a problem and can be carried out using microtome techniques (e.g. Bradley and Brownlee, 1986) or the particles can be mounted in epoxy and polished flat. The size of the Fe-Ni IDPs (average diameter was 8μm) suggested that such microtoming would have resulted in the loss of the particle, thus it was decided to analyse the IDPs as intact whole particles.

The seven particles were mounted on to Beryllium substrates at the NASA JSC Cosmic Dust Facility (Houston, USA). Beryllium substrates rather than carbon substrates were used, as Beryllium is not within the detection range of the SEM at Brookes even when the ED detector is in ultra-thin window mode. This means that the only elements to be analysed will be those from the particles. As with the analysis of the HST solar cells, the investigation of the particle under the SEM was far from ideal conditions and it is likely that there will be edge effects generated by the spheres (see Chapter 2.5.3 for a discussion on edge effects).

6.3.3 Textural & Chemical Observations Of Fe-Ni Particles.

As expected the size of the particles (maximum diameter 12μm) proved problematic when imaging, as although a secondary electron (SE) image could be obtained this did not yield any topographic or compositional information on the particles below 7μm in diameter (see appendix 4 for SE images of all the particles). However on several of the larger particles successful SE imaging was carried out. The first significant feature to note about these Fe-Ni particles is the overall shape; apart from L2006L1 (which was unfortunately lost during the transportation from JSC to the Open University or preparation for analysis) they are all

spheres, compared to the irregular solids and aggregates which make up the bulk of the collection.

The spherical shape would suggest that the particles may have undergone melting during atmospheric alteration (discussed previously in Chapter 1). If so it might be anticipated that there would be a reaction rim around the particle where the Fe-Ni had been converted to magnetite. Indeed, in the extreme, entire particles may be oxidised during preliminary examination under the SEM. It became apparent that there was a thin discontinuous surface coat covering the particles, and beneath this there was a smoother surface (figure 6.9).

In order to study the structure in more detail, the thin surface coating was carefully removed from one of the particles, therefore exposing the core of the particle (figure 6.10). From the ED X-ray spectrum obtained from the particle it is clearly possible to see the chemical differences between the "rind" (figure 6.11a) and the particle (figure 6.11b). The "rind" is essentially composed of Fe and O and therefore it is highly likely that this is an Fe-oxide (probably magnetite). The observation of Fe-oxide coatings around the particles is not suprising as this has often been observed on both IDPs and micrometeorites (see Chapter 1.4). The Fe-oxide coat is associated with the alteration that occurs to the particles during atmospheric entry (e.g. Flynn, 1989a&b; Sandford and Bradley, 1989 and Genge et al., 1996). The core of the particle was comprised solely of Fe-Ni metal (figure 6.11b), which is in agreement with the other particles analysed. An intriguing question remaining unanswered is in what form did the Fe-Ni particles exist prior to atmospheric entry? Metallic fragments or spherules? (the latter being suggestive of asteroidal collection processes producing melt droplets).

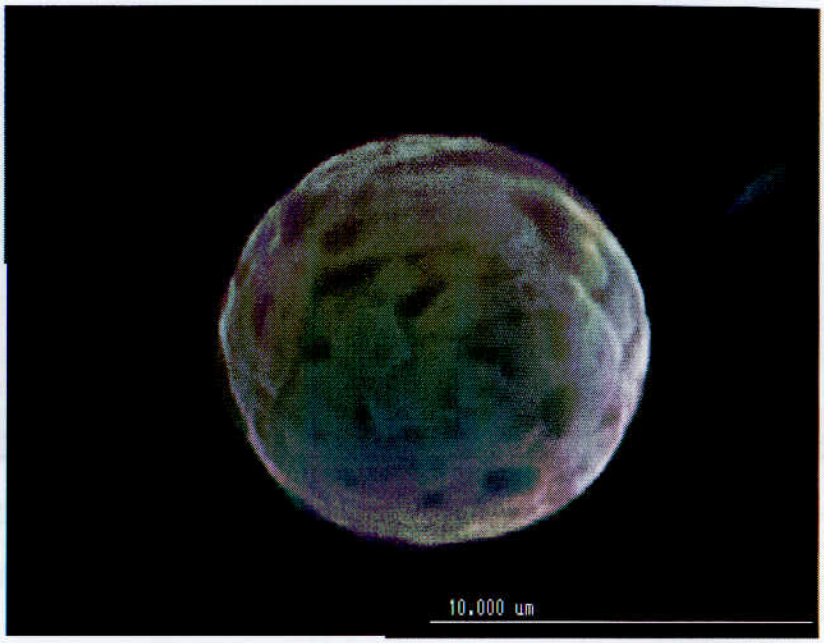

Figure 6.9 SE image of L2005t3. The particle appears composed of two layers, firstly a thin discontinuous coating on the outer part of the particle and then a smoother core. The discontinuous layer is likely to have been a result of processing the particle has undergone during atmospheric entry.

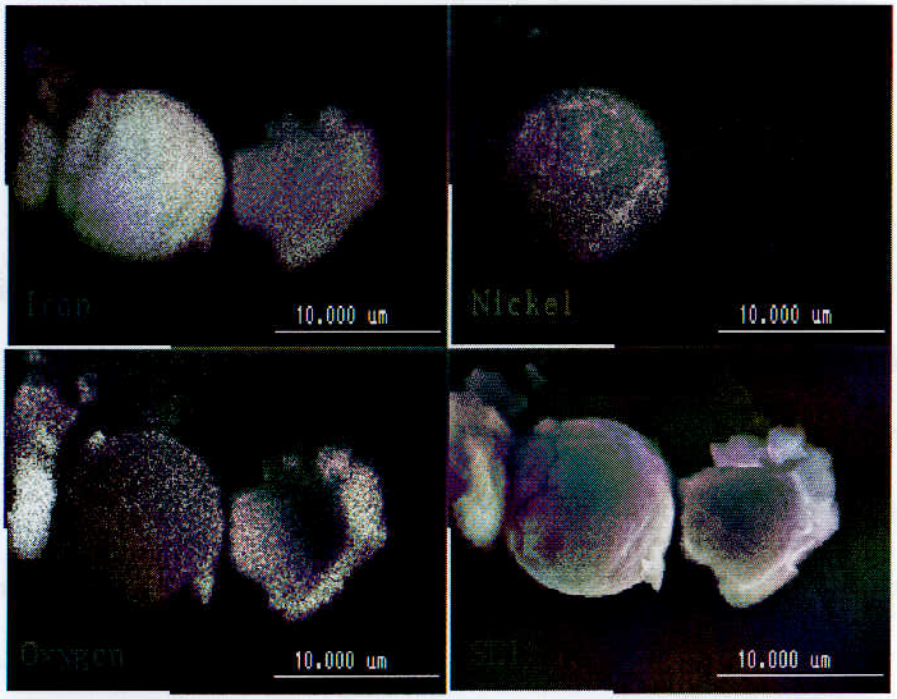

Figure 6.10 SE image and X-ray elemental maps for Fe, Ni and O for L2006j1. The "rind" or discontinuous outer layer which normally surrounds the particles is composed of Fe and O which is indicative of the magnetite rims which both IDPs and micrometeorites exhibit after atmospheric processing. The particle itself would appear to have metal core that is composed solely of Fe and Ni.

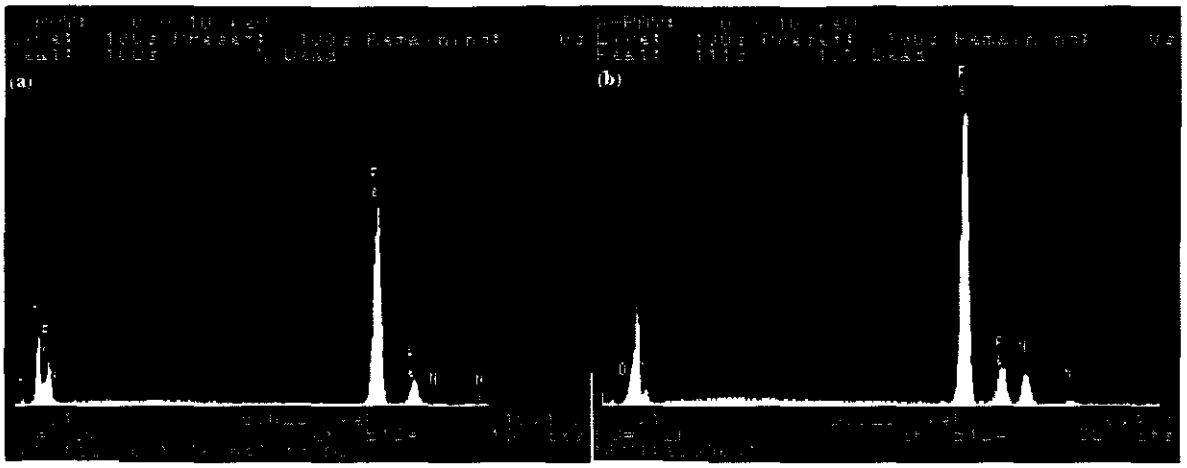

Figure 6.11a ED spectrum obtained from the "rind" of L2006j1. **Figure 6.11b** ED spectrum obtained from the metal core of L2006j1.

6.4 Origins Of The Fe-Ni Particles From The Stratosphere & Fe-Ni Residues Collected In The Solar Cells.

Previous work carried out on the iron spherules from deep-sea collections (e.g. Brownlee, 1978) has suggested that the particles were previously Fe-Ni sulfides, which during atmospheric entry have experienced elemental and mass loss. Therefore are the Fe-Ni rich IDPs collected since 1982 the result of similar process? Mackinnon and Mckay (1986) investigated IDPs collected from the stratosphere and observed that Fe-Ni particles were on average 4μm in diameter whilst Fe-Ni sulfides were on average 7.4μm in diameter. So the Fe-Ni rich IDPs are products of ablation processing, as they are smaller in diameter than the sulfides which have been modified to a lesser extent. Whilst this is an acceptable theory it should be noted that the Fe-Ni particles observed here in were approximately the same size as the Fe-Ni sulfides observed in previous studies (Brownlee, 1978; Mackinnon and MacKay 1986).

If Fe-Ni rich IDPs are the result of ablation effects, then it is still necessary to explain the observed residue in s177 solely comprised of Fe-Ni metal. Recall that the residue in s177

showed no evidence of the any sulfide-rich material. Whilst it could be argued that the sulfide component was lost during the impact event, this would seem unlikely as Fe-Ni sulfides and Fe-sulfides are frequently observed as the dominant residue chemistry in other impact features. Having made a case for the Fe-Ni metal residue in s177 being generated by a particle composed solely of Fe-Ni metal then it is logical to conclude that the Fe-Ni rich IDPs collected in the stratosphere have the same origin.

Along similar lines of reasoning note that it has been suggested that the Fe-Ni sulfide IDPs may be ablation debris from the fusion crusts that formed on meteorites during atmospheric entry (Rietmeijer and Mackinnon, 1984); however since Fe-S residues are observed in the LEO impacts, it is also possible that Fe-S IDPs could arise from primary Fe-S particles. The original impactors prior to collision have not encountered any ablation effects in LEO therefore it is highly unlikely that they are debris from a meteorite in that sense. That said, a meteorite or possibly larger body cannot be ruled out. It is possible that the Fe-Ni metal residues and Fe-Ni metal IDPs are ablation products from meteoroid or asteroidal collision. When metal cosmic spherules were identified from deep-sea sediment (Blanchard and Davis, 1978), it was suggested that these spherules were splash ejecta from asteroidal collision, which had spiralled to Earth under Poynting-Robertson drag (Parkin et al., 1983). Therefore it would be possible to suggest that the Fe-Ni residues and the Fe-Ni metal IDPs originated from collisions of this nature. Such a mechanism would have the potential to produce metal spherules in a range of diameters (i.e. from μm, as seen in type I deep sea spherules, to μm, as inferred from the HVI residues). To back this up note that there are meteorites, for example Vaca Muerta, which contain a range of metal droplets from millimetre to sub-micron in the matrix material (figure 6.12). An interesting consequence of collision processes is that silicate spherules would presumably be formed as well. In any case, such materials should be searched for in the cosmic catalogue.

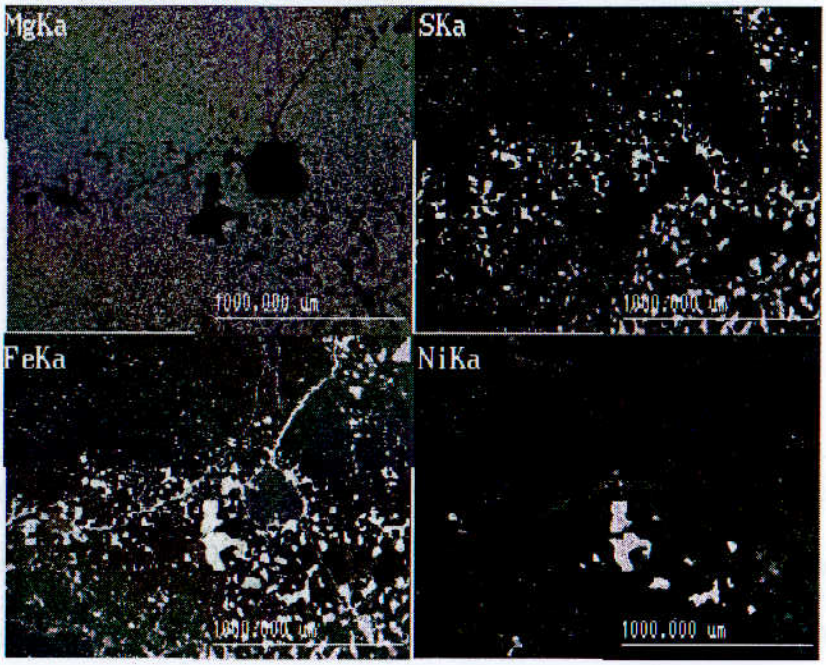

Figure 6.12 X-ray elemental maps for the distribution of Mg, Fe, Ni and S in the matrix material of Vaca Muerta (a stony-iron meteorite classified as a mesosiderite) (image courtesy of A.T. Kearsley).

Further work is required to constrain the possible origins of the Fe-Ni residues and Fe-Ni metal IDPs. Perhaps the most interesting finding from this study is the bias that is perhaps evident in terms of sampling of the IDPs catalogued from the stratospheric collections. Although arguments will always favour the stratospheric collection of IDPs as the primary resource with which to study cosmic dust, the significance of the micrometeoroid remnants in the spacecraft surface must not be underestimated. As a comment by C.G.Simon (1993), one of the LDEF scientists highlighted:

"*Future adjustments, resulting from better understanding of contamination issues and impactor deposition mechanisms, and from additional analyses of orbital impact sites, may alter the statistical distribution of manmade and natural impactor classifications deduced from the currently available data*".

Chapter 7

Overview & Future Work

7.1 Overview

The aim of this thesis was to investigate the mineralogy and chemistry of micrometeorites. Previous investigations (e.g. Wright et al., 1997 and Genge et al., 1997) have focused on intact particles which have been collected from terrestrial environments. These particles have been subject to selection and modification processes (e.g. Love and Brownlee, 1991) that occur during atmospheric transit.

Therefore, the investigation of particles collected in low Earth orbit (LEO) should in principle yield the best representation of micrometeoroids. Previous collections of LEO material have focused around dedicated *in-situ* collector experiments, e.g. "The chemistry of micrometeorites" experiment of LDEF (Zolensky et al., 1994), which are expensive and often only single-flight opportunities. Whilst the benefits and knowledge gained from such investigations are not in doubt, it is however questionable whether the maximum yield of information was obtained.

Essentially the problem with LEO collections is that it is inherently difficult to collect a particle intact when impact velocities can be 5-20km/s. At such velocities, particles are subjected to melting and devolatilization. Therefore the value of such studies to the cosmic dust community is questionable as intact pristine particles are rarely recovered (Rietmeijer and Blandford, 1988). However the advent of NASA's "Stardust" mission has led to the development of technologies to overcome the problems of collecting material (Hörz et al., 1998).

Not withstanding the investigation problems, the hypervelocity impact damage (μm to mm in scale) sustained by one of the Hubble Space Telescope (HST) solar arrays, returned to Earth after 3.62 years of exposure to LEO, has added an important repository to the collections available for laboratory post-flight investigations. As well as retaining remnants of micrometeoroid impactors, the array surface will also harbour remnants of a second population of material which is present in LEO. Space debris has been generated by the human utilisation of LEO in the latter part of the 20th century and are typically fragments of upper stages from rockets, solid condensates from rocket fuel and components from other space hardware.

Wright et al. (1995), as part of a detailed post-flight investigation (Carey, 1998) received 26 samples (20 solar cells and 6 buffer assemblies) from the HST array. In an attempt to characterise impact features and analyse meteoroid/space debris residues the samples were investigated by optical and scanning electron microscopy. The general findings of this study (Wright et al., 1995) were that HST solar cells were not ideal substrates upon which to search for micrometeoroid impact residues because of the complex compositional chemistry of the host substrate. In contrast, the identification of space debris-derived residues such as paint fragments and rocket propellant were more readily identified. Whilst the location of impact features was not difficult, the identification of substantial residue material proved difficult.

The time scale of the investigation meant that it was not possible to carry out detailed analytical examinations (under the SEM) of impact features. Therefore the goals of this thesis were: 1) To develop analytical protocols by which residues could be readily located and identified. 2) To classify residues in terms of space debris and micrometeoroid - if

possible the latter to be sub-classified in terms of mineralogy and chemistry that can be directly compared with the current terrestrial collections of dust.

7.2 Analytical Developments

Analytical scanning electron microscopy is a well established technique for this type of investigation. Therefore, the developments enhanced by this thesis are related to the analysis protocols rather than to hardware. The method of analysis carried out in Wright et al. (1995) used individual micro-spot analysis using energy-dispersive X-ray spectrometry, which is a typical approach along with obtaining secondary electron (SE) images. This thesis has used digitised back-scattered electron (BE) imaging and X-ray emission elemental mapping.

The digitised BE imaging enabled the manipulation of data (at pixel resolution) to clearly define compositional changes in the different layers of the solar cells and more importantly any extraneous material. This extraneous material when imaged in BE mode produced highly distinctive morphologies. The advantage of BE imaging over SE imaging was that extraneous material that was embedded beneath the surface of the melt zone (to a depth of approximately 1μm) was identified. The digitised X-ray elemental mapping again enabled the manipulation of data to distinguish between the various melt states that occurred within the crater. These states can be defined as: 1) Impactor melt residue; 2) impactor and cell host melt residue and 3) cell host melt residue.

The CMX cover glass of the solar cells contains a micron-thick layer composed of Mg and F that was removed during the impact process. By mapping for areas which showed depletion in Mg and F it was also possible to locate small impact features (10-50μm in diameter) which might not have been located in the preliminary optical investigation of the

cells. The use of both digitised BE imaging and X-ray emission elemental mapping has proved to be a powerful combination of scanning electron microscopy techniques for which the rapid identification protocol was derived.

The methodology of the rapid identification protocol (figure 7.1) was a preliminary optical survey that was carried out at x10, x20, x40 magnifications, and was used to locate impact features. The SEM investigations, initially used BE imaging of the impact crater at a low magnification (<x250) but at a high pixel resolution (512 x 512 point matrix with repeated Kalman frame averaging to increase signal-to-noise ratio). The impact pit was then examined at higher magnification (>x250) to identify any areas of melt that contained residual material from the impactor. Areas of interest were then mapped for 22 characteristic X-ray intervals at 128x128, 256x256 and 512x512 pixel resolutions.

The higher resolution maps were carried out with repeated frame averaging to yield high contract. For the purpose of identification between space debris and micrometeoroid residues the 128x128 pixel resolution maps were adequate in most cases. However higher resolution maps were essential for more detailed micrometeoroid research. The classification of material was obtained from semi-quantitative micro-spot analysis to obtain ED spectra. The spectra obtained for the residual material was always compared with a "clean" (i.e. away from the impact) spectra of the host.

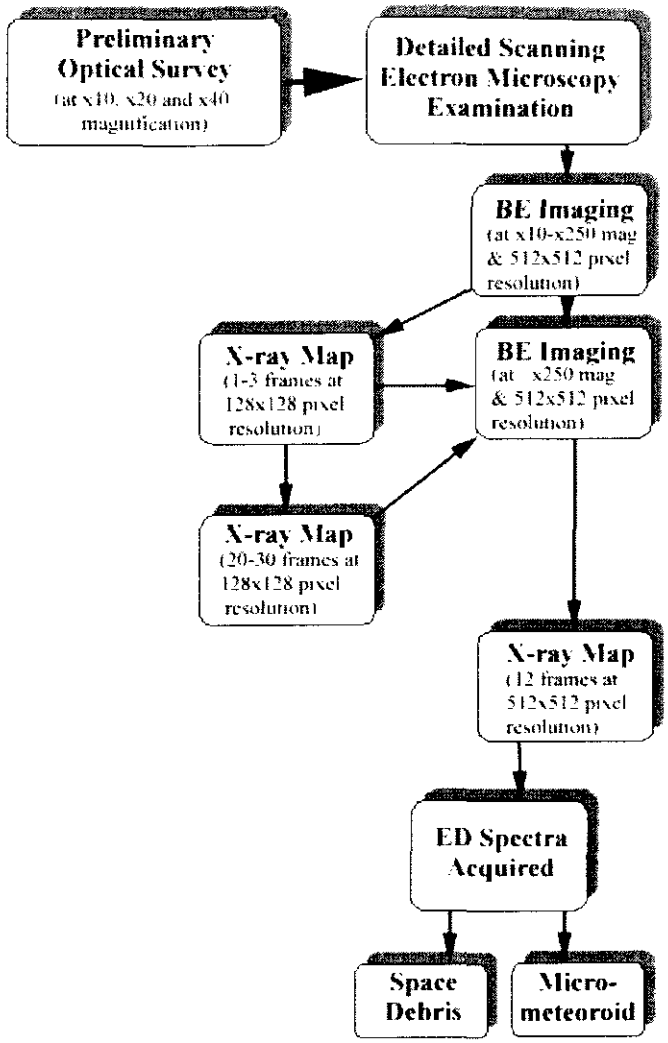

Figure 7.1 Flow diagram summarising the analytical protocol for the analysis of impact residues observed in HST solar cells used in this thesis.

The significance of this protocol was highlighted in Carey, (1998) which as part of ESA contract 1887/96/NL/JG (Meteoroid & Debris Flux & Ejecta Models) reviewed the protocol and concluded that it was a significant step forward in post-flight analysis investigations.

7.3 Hypervelocity Simulated Shot Program

7.3.1 Summary

The simulated impacts were undertaken using projectiles in the 125-250μm grain diameter to allow detailed examinations of residue textural morphologies. The projectiles were well-characterised in terms of mineral chemistry. The residues were produced by accelerating the projectiles individually into HST solar cells at velocities of approximately 5km/s using the light-gas-gun (LGG) facility at the University of Kent.

The textural morphologies produced were highly variable but comparable with those observed in LEO derived impact features investigated in this thesis and in previous simulated impact studies (Hörz et al., 1983). The simulated shot program has generated a suite of characteristic residue morphologies that in part appear to be due to the individual chemical properties of the projectiles. The program has as yet, failed to resolve the question of whether it is possible to unambiguously distinguish between residues derived from hydrous and anhydrous silicates.

7.3.2 Future Shots

The shot program, apart from the Orgueil matrix shot, has used single composition mineral powders. It is proposed that artificial micrometeoroid projectiles are made up and fired into HST solar cells. The composition of the artificial micrometeoroid projectiles would be based on known compositions of known micrometeorites. Therefore the projectiles would consist of: 1) Mafic-silicates mixed with Fe-sulfides and Fe-Ni metal as an analogue of anhydrous particles. 2) Phyllosilicates with Fe-sulfides and Mg-Fe carbonates as an analogue of hydrous particles.

7.4 Hypervelocity Impacts into HST Solar Cells: Micrometeoroid Versus Space Debris

7.4.1 Overall Summary

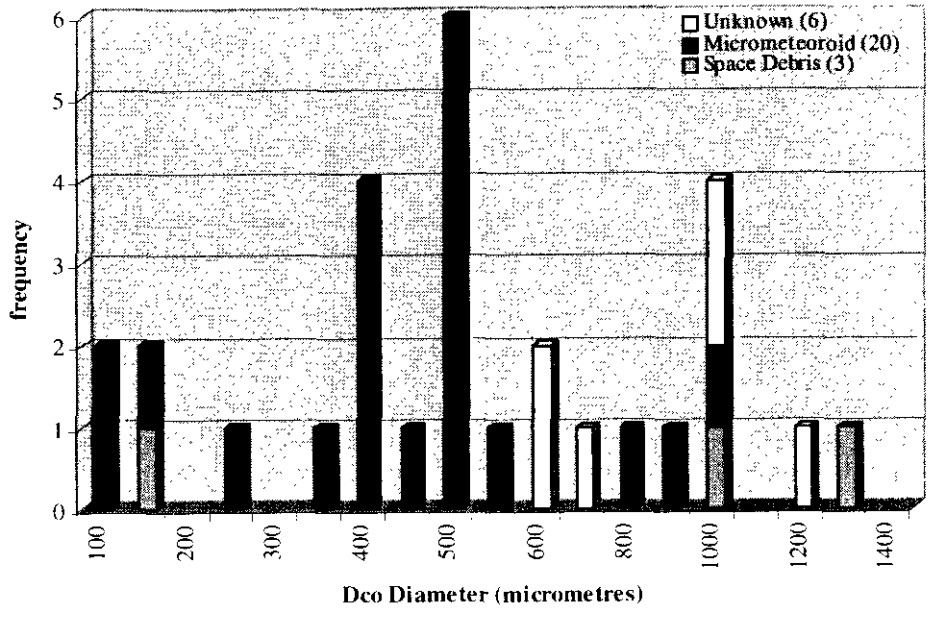

Figure 7.2 A distribution plot showing the frequency of impact residues in terms of chemistry for 1-1000μm craters.

For this thesis, 25 individual solar cells were specially selected on the basis that they contained impact craters (diameter 100-1000μm) which had the most potential to retain impactor residue chemistry. The solar cells were subjected to a detailed investigation using the protocol that was summarised in section 7.2 using the SEM. The detailed examination identified 29 impact craters within the 100-1000μm size range (figure 7.2) which were found to contain 3 residues which were space debris derived, 20 which were micrometeoroid derived and 6 which remained unclassified.

The number of craters which contained unclassified impact residue was much lower than similar previous investigations (e.g. Bernhard et al., 1993b) were up 72% were

unclassified. The data would suggest that the impact craters within the 100-1000μm range are dominated by micrometeoroid-derived residues (20 out of the 29 investigated).

As the samples were specially selected for this thesis in terms of yielding the highest potential for retaining residues, it has generated a sample bias. Therefore it is not possible to generate a flux plot directly from the data obtained, nor is it essentially accurate to compare and contrast the findings within this thesis with those obtained by Bernhard et al. (1993b), as they analysed over 600 impact features whereas only 29 were analysed and discussed herein.

Nevertheless, independent to the work carried out in this thesis, flux modelling has been carried out on previous and new HST data (not based on chemistry) which predicted that for the size range examined herein, micrometeoroids would be the expected dominating impactor (Unispace Kent, 1998). Equally significant was that the flux modelling predicted that space debris would become the dominant impactor origin at the higher crater size range. The 3 residues identified as space debris were all located in craters above 900μm diameters.

7.4.2 Residue Chemistry

In terms of residue chemistry the three residues which were identified as derived from space debris material were identified as remnants of paint fragments and printed circuit board component. The identification and subsequent classification of impact residues in terms of micrometeoroid origin has been aided by laboratory analogues generated by using the light-gas-gun facility at Kent. The micrometeoroid-derived residues can be interpreted in terms of simple mineralogical remnants: (1) mafic (olivine and/or pyroxene), it is rarely possible to give an unambiguous classification; (2) metallic sulfides; (3) hydrous or

volatile-rich silicates (probably phyllosilicates, saponite and/ or serpentine); (4) altered refractory mineralogies.

The identification of individual mineral component alone does not conclusively prove an origin for the impactors in terms that are comparable with micrometeorite compositions (Klöck and Stadermann, 1994). Yet the residues observed are rarely of a single composition being rather intimate mixtures of the remnants described above. The association of remnant phyllosilicates with mafic silicates and metallic sulfides within the residue would certainly indicate a carbonaceous chondrite affiliation (Bradley, 1994) in terms of parent bodies origin. Nevertheless, the majority of residues appear to be dominated by remnants of mafic silicates with metallic sulfides. Such chemistries do not simply fit the carbonaceous chondrite origin alone, but rather span almost the entire range of meteoritic classifications.

Previous studies (Flynn, 1990 and Brownlee et al., 1993) suggested that residues observed in LDEF with a similar composition to those identified herein were generated by relatively low oblique velocities that would indicate an asteroidal origin.

7.4.3 Concluding Remarks

The significance of the results discussed herein in terms of potential hazard to orbiting space hardware are ambiguous. Previous research (National Research Council, 1995) suggest that micrometeoroids did not represent a significant threat to space hardware yet the results herein would suggest that in the small size range of impact damage (100-1000μm) the predominant impactors were micrometeoroids. The underlying problem is that space hardware which fail in LEO are very rarely returned to Earth for post-flight analysis. Therefore it is impossible to conclude whether the failure might have been due to impact damage from either space debris or micrometeoroid hypervelocity collision.

Notwithstanding all the interpretation and classification problems involved with the analysis of impact residues, the work carried out in this thesis has proved that the HST solar cell surfaces can act as a substantial passive collector for micro-particles in LEO. Furthermore, the detailed analysis of impact craters has identified and classified residues in terms of space debris and micrometeoroid origin. The latter has been sub-classified in terms that were directly comparable with the terrestrial collections of cosmic dust.

7.5 Further Work

The obvious development of this thesis would be to examine a larger number of solar cells that are randomly selected to rule out the sample bias that may have been generated herein. This could be achieved by carrying out a similar investigation to that described in this thesis on an area containing 100 cells removed from the array stored at ESTEC. This new survey should include a search for impact features greater than 1000μm and smaller than 100μm, both of these size ranges according to the recent flux models (e.g. Unispace Kent, 1999) should contain a greater number of impacts generated by space debris.

Whilst the interpretation of impact residues that are presumably derived from micrometeoroids have been classified herein, it is not possible to unambiguously state that the interpretation is correct. The development of Nano-SIMS technology (Stadermann et al., 1999) may enable attempts to measure the isotopic composition of the micrometeoroid residue that might possibly reduce the ambiguity of the interpretation.

This thesis has only investigated the mineralogy and chemistry of micrometeoroids and space debris captured by the HST solar cells. There are, as was stated, a number of other surfaces (e.g. Al-clamps from LDEF) which have been exposed to LEO which could now

be re-examined using the techniques described herein. However whilst the improved detection and imaging capabilities of the SEM used in this thesis may well reduce the number of unknowns, the question remains - will it change the general finds of the LDEF investigation (e.g. Zolensky et al., 1994)?

The generation of impact residues using the LGG facility at the University of Kent has assisted in the interpretation of the residues preserved in the HST solar cells. That said, several of the selected minerals fired failed to produce abundant residues to investigate. This was particularly the case with the calcite shot, where fragments are disintegrating before they impact on the target material. Mixing the calcite with another mineral powder (diopside would be ideal as the residue generated by this mineral is very characteristic) might reduce this problem.

The composition, morphology and remnant impact mineral chemistry has been highly variable for the different individual mineral powders. In some cases the residue fragments give a near stoichiometric ED spectra when analysed under the SEM, whilst in others it is clearly possible to note the loss of volatiles (e.g. Na and K). It would be possible to assess this approximate loss of volatiles as the mineral powders for the shots were prepared from mineral standards. Quantitative analysis could be obtained for the pre-fired chemistry of the mineral projectile and this could be compared with the semi-quantitative analysis of the resultant impact derived chemistry, notwithstanding the technical problems which have been previously been discussed (section 2.5 and 6.2.2).

However individual mineral grains are not true analogues of the complex micrometeoroid chemistries. The next series of laboratory generated impacts to be fired should be polymineralic projectiles of known composition. It is possible that both IDPs and micrometeorites could be used for this purpose but the chemistry and mineralogy of these

would not be so well defined. Therefore it is suggested that 'artificial micrometeorites' are made up that would consist of mineral powders containing: 1) mafic silicates mixed with Fe-sulfides and Fe-Ni metal as an analogue of a anhydrous IDP and 2) phyllosilicates with mafic silicates, Fe-sulfides and Mg-Fe carbonates as an analogue of a hydrous IDP. These two mineral powders will hopefully resolve the problem of whether it is possible to distinguish between impact residues generated by hydrous and anhydrous micrometeoroids.

The use of "aerogel" to collect micrometeoroids in space (e.g. Brownlee et al., 1997 and Hörz et al., 1998) will revolutionise the study of such material as it is possible to capture material in a near-intact state. Therefore it is suggested that the mineral powders including the artificial micrometeorites also be accelerated into "aerogel" targets. This will allow preliminary assessment of the suitability of the current analytical techniques for the analysis of particles returned from the orbital debris collector on Mir (Hörz et al., 1998) and Stardust (Brownlee et al., 1997).

Appendix 1

BEI And X-ray Elemental Maps Of A Cross-Section Through A HST Solar Cell.

Appendix 1 contains the data obtained from an analysis of a cross-section made through an individual solar cell. The analysis was carried out at Oxford Brookes University using the Jeol 840 scanning electron microscope fitted with an Oxford Instruments e-XL X-ray Energy-Dispersive spectrometer. The analytical working conditions were an accelerating voltage of 20kV, beam current of 2nA and a working distance of 32mm.

Back-Scattered Electron Image of the HST Solar Cell and Support Stiffener Material.

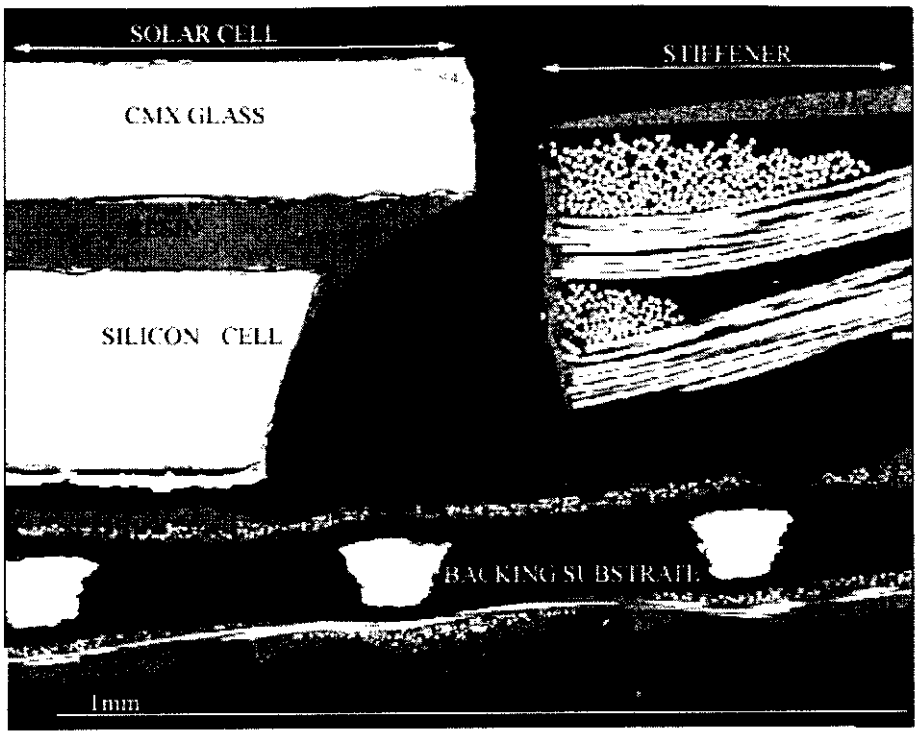

X-ray Elemental Maps Showing The Distribution Of C, Si, S And Ag Within The Solar Cell

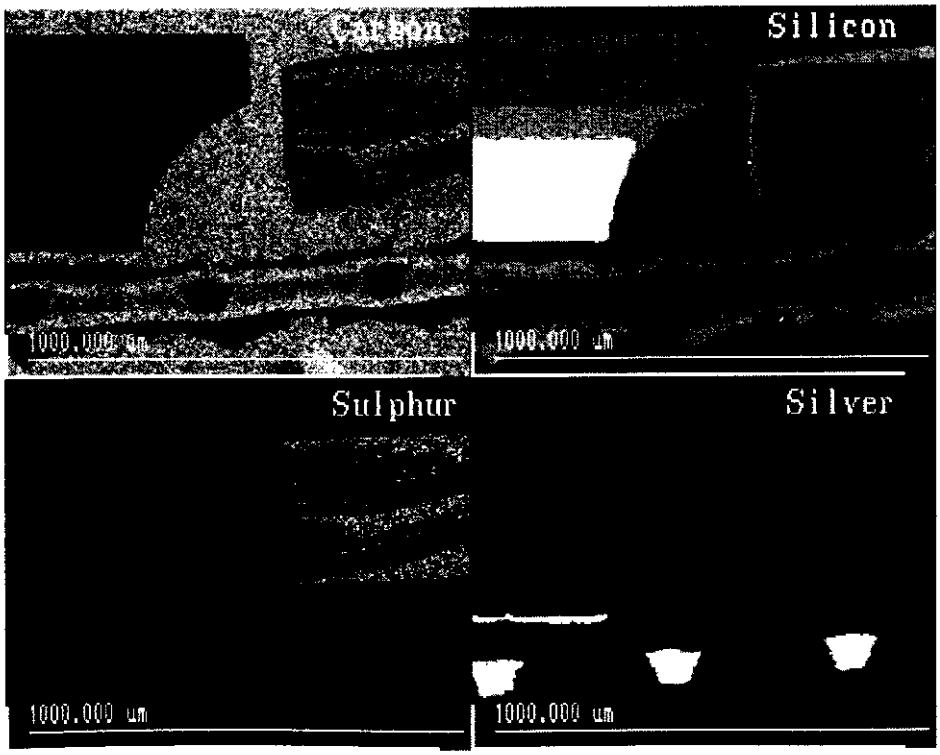

X-ray Elemental Maps Showing The Distribution Of C, O, S And Ca Within The Solar Cell.

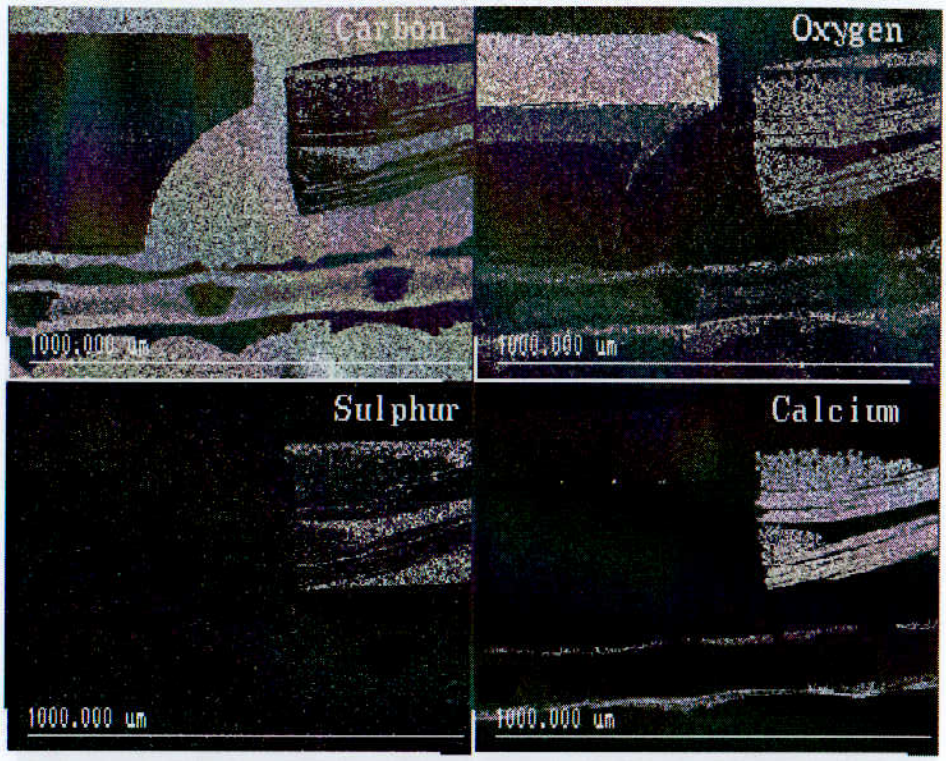

X-ray Elemental Maps Showing The Distribution Of Si, S And Ag Within The Solar Cell As individual Elements And As An Overlap.

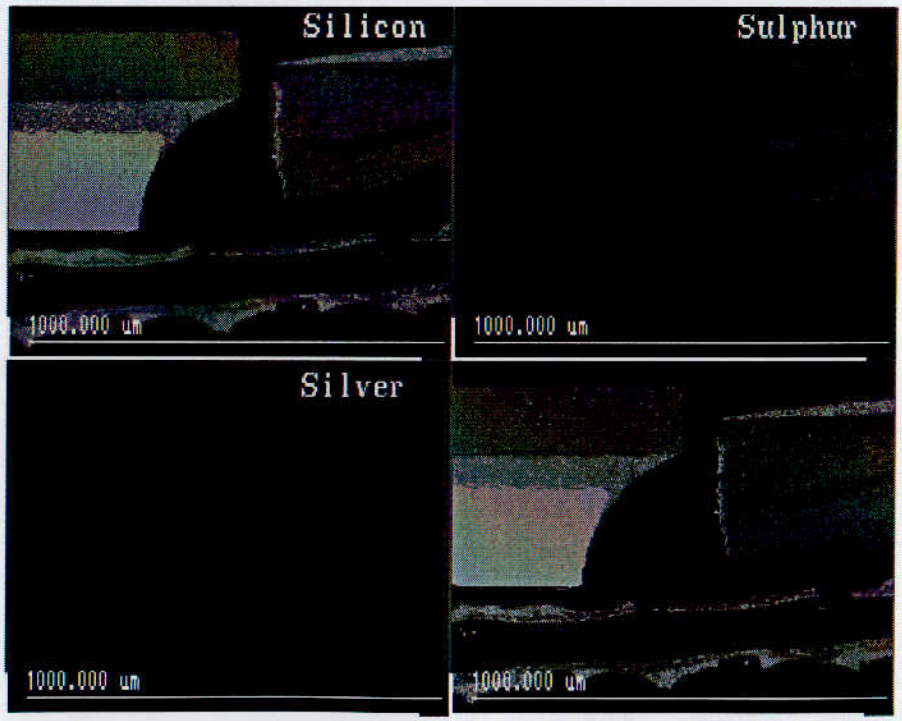

X-ray Elemental Maps Showing The Distribution Of Si, Ag, Ti And Al Within The Solar Cell. Due To Constraints Placed On This Work By ESA It Is Not Possible To Define the Position Of The Ti, Ag and Al layer Within The Solar Cell Composition

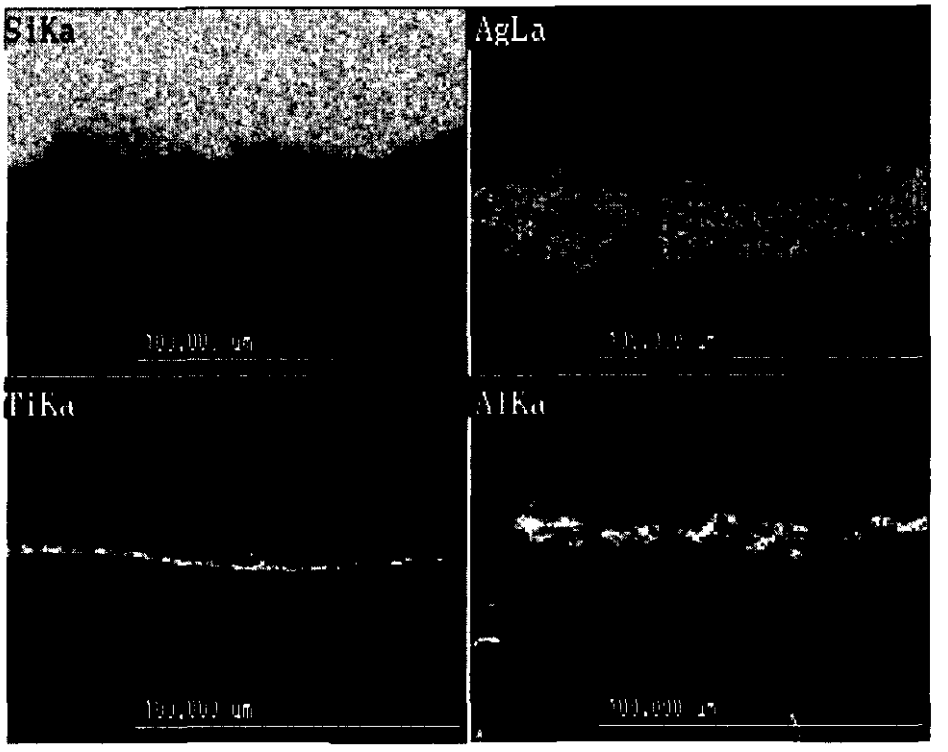

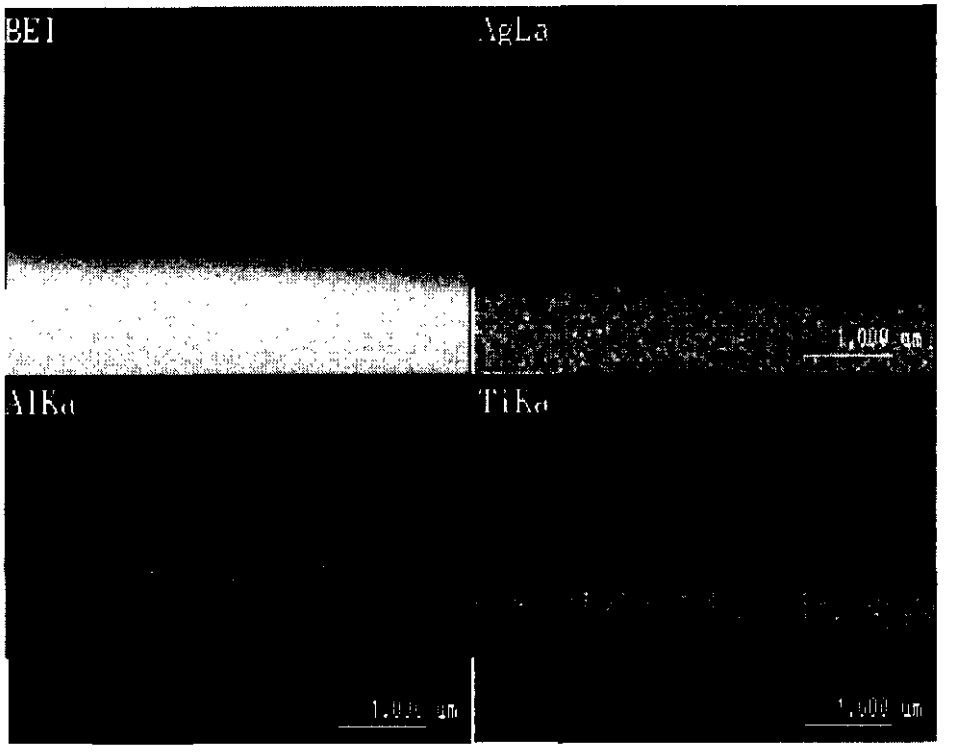

Appendix 2

Optical Images Of The Impact Craters Observed In HST Solar Cells

Appendix 2 contains the optical images of the impact craters observed in the HST solar cells used for this investigation. The images were taken at the Natural History Museum using a Leitz Wild M8 optical microscope fitted with a Sony DKC5000 digital camera. The microscope at the time the images were taken was not fitted with a calibration marker therefore the scale bars have been added to the images using detail obtained from the investigation using the scanning electron microscope.

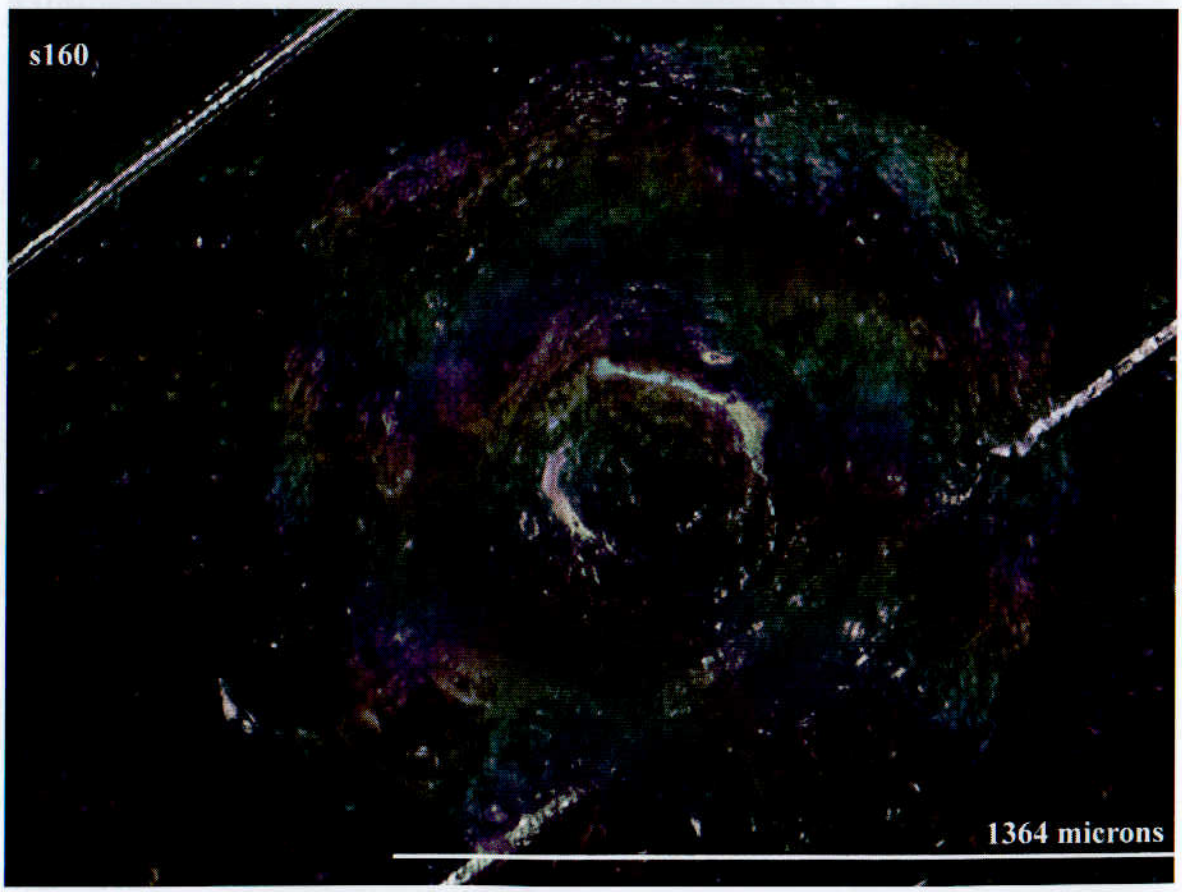

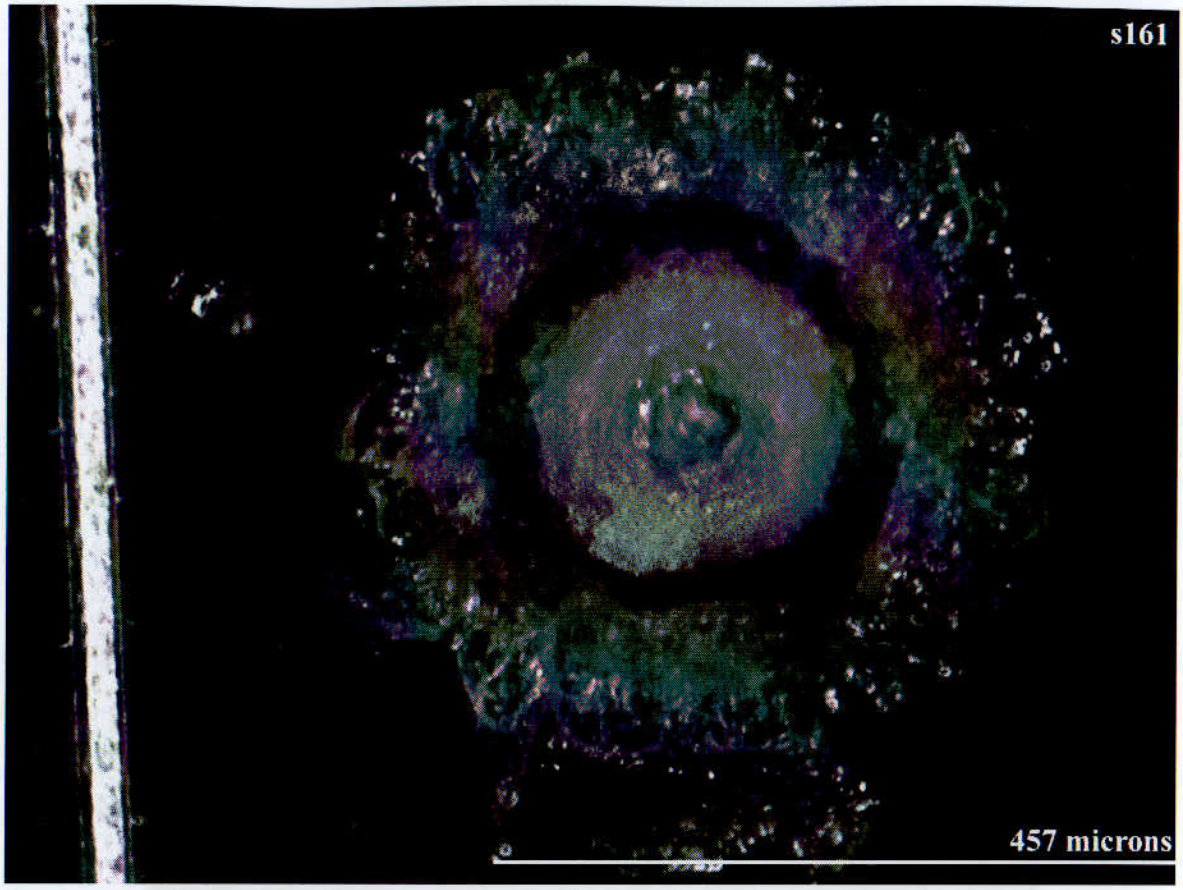
s161
457 microns

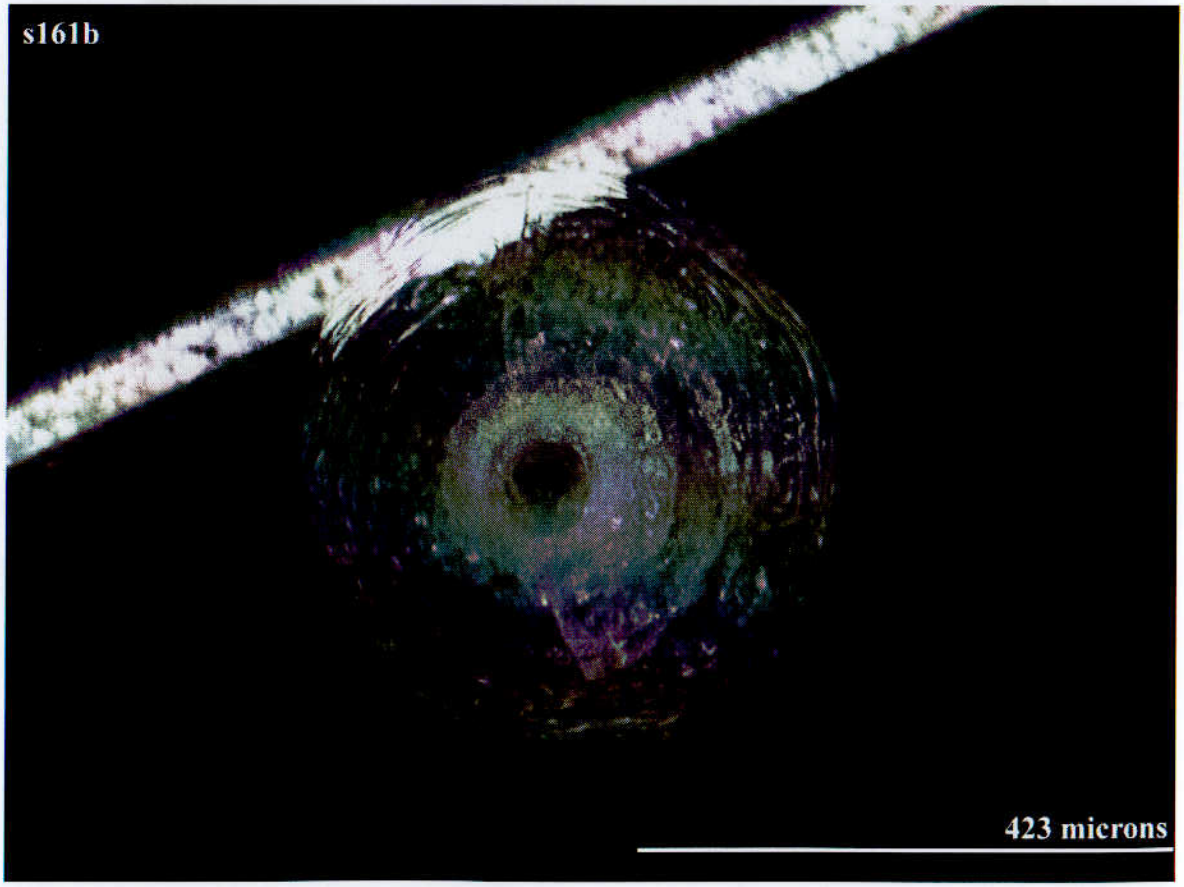
s161b
423 microns

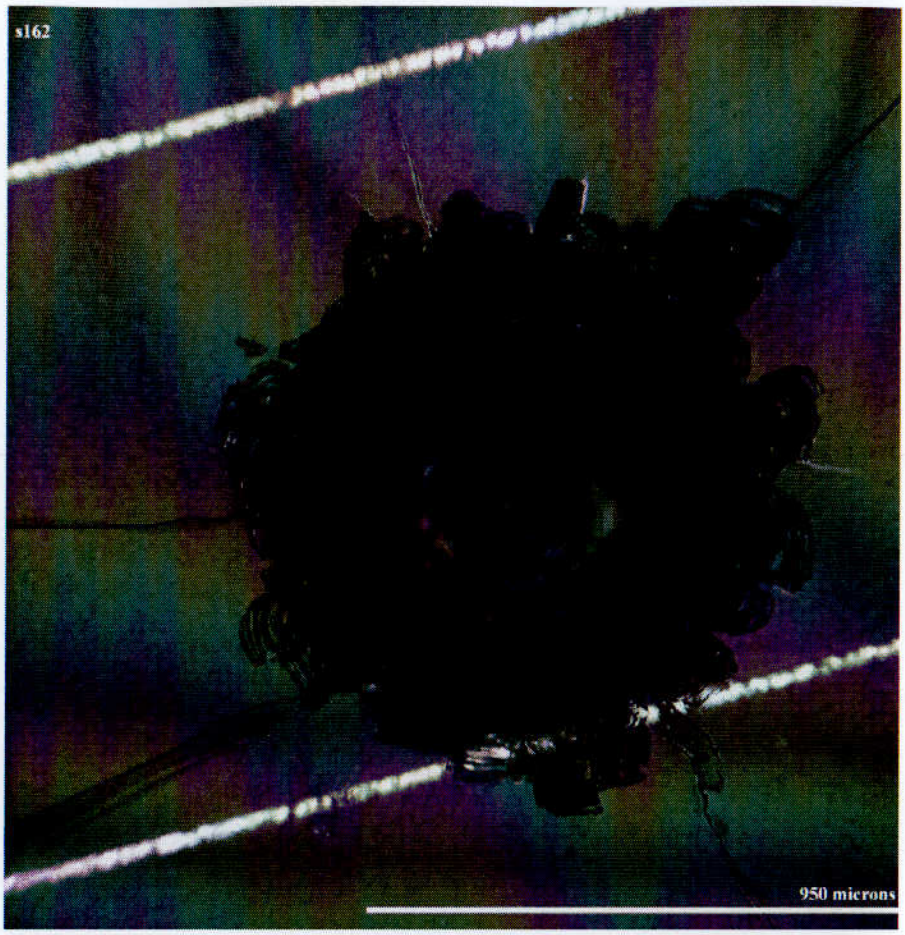
s162
950 microns

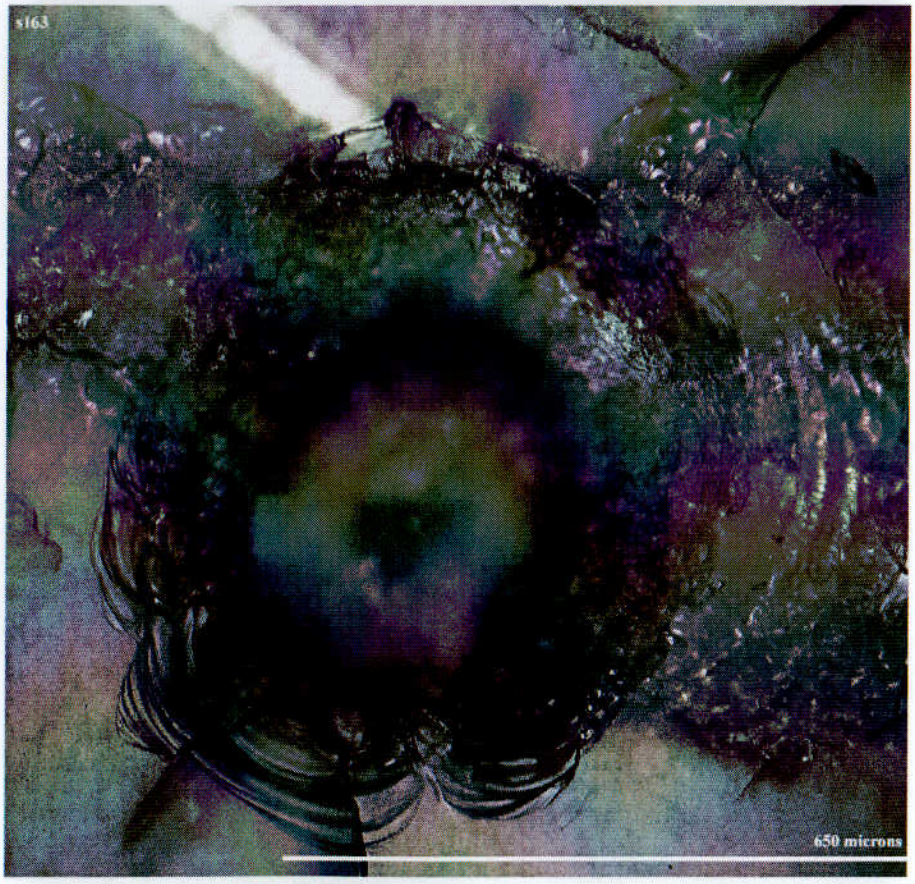
s163
650 microns

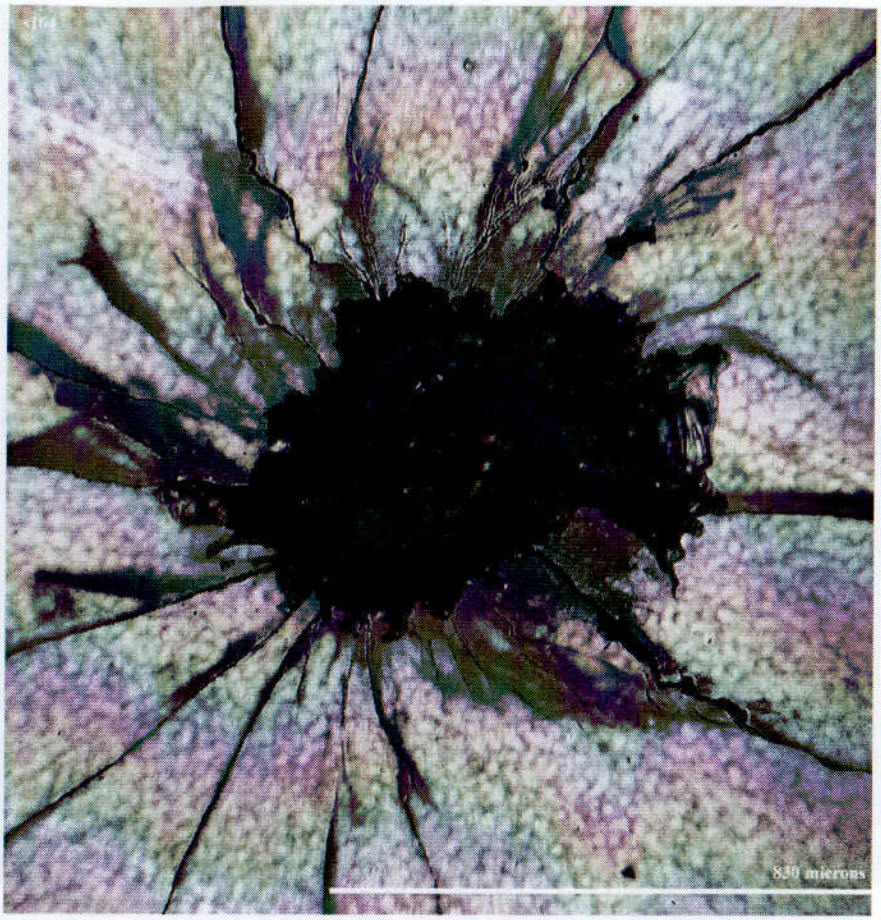
830 microns

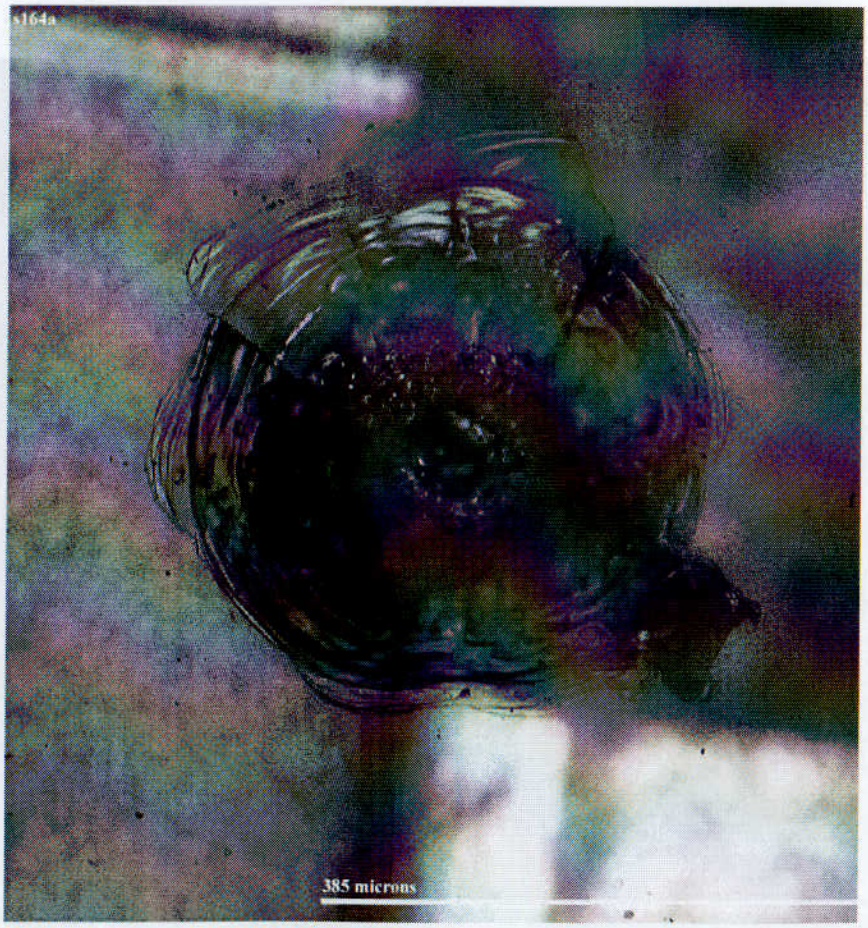
s164a
385 microns

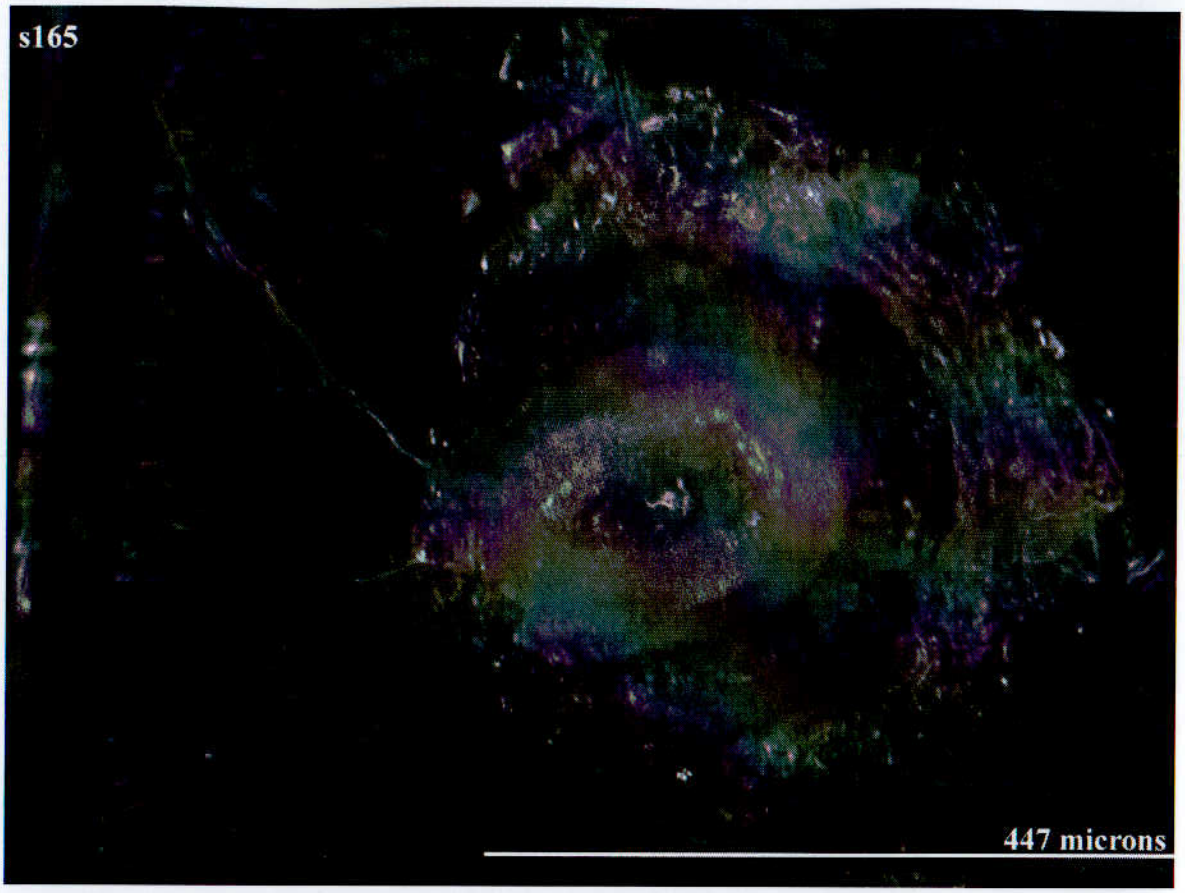
s165
447 microns

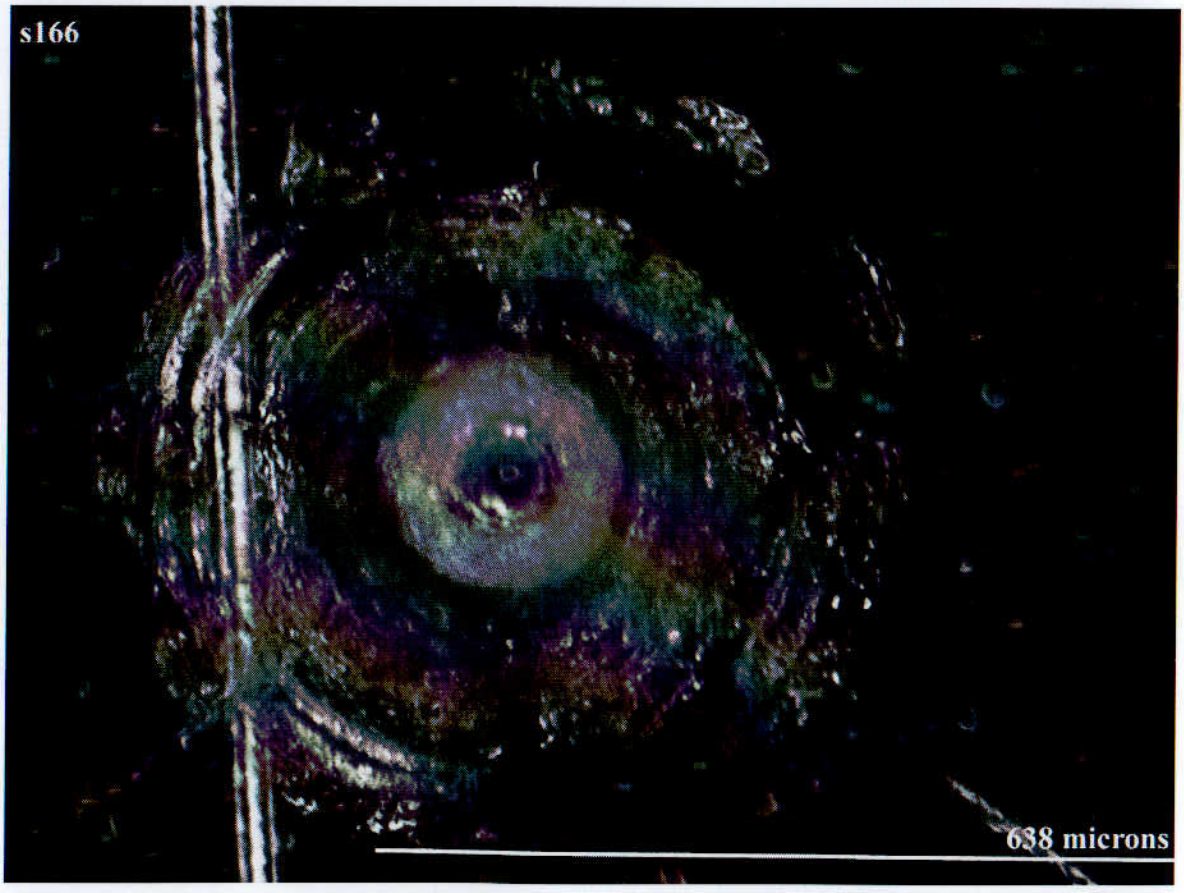
s166
638 microns

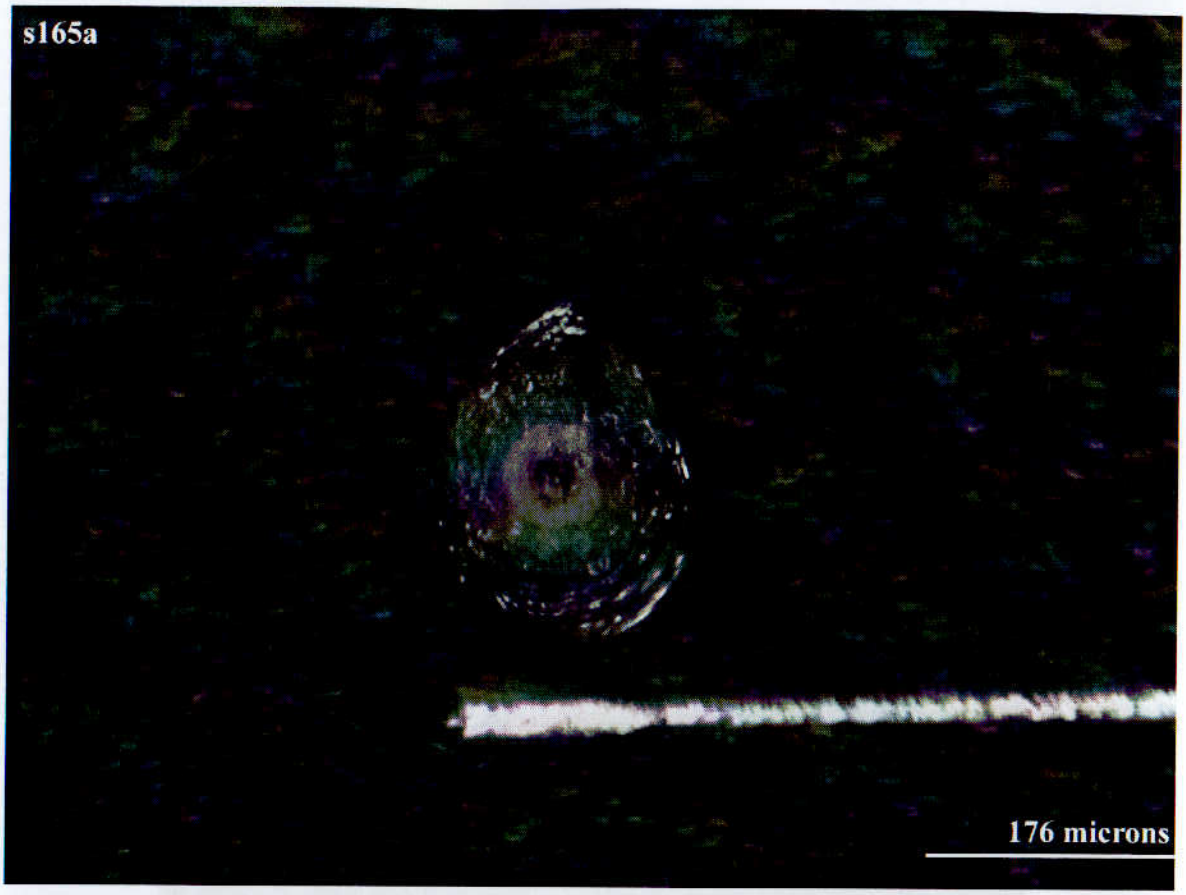
s165a
176 microns

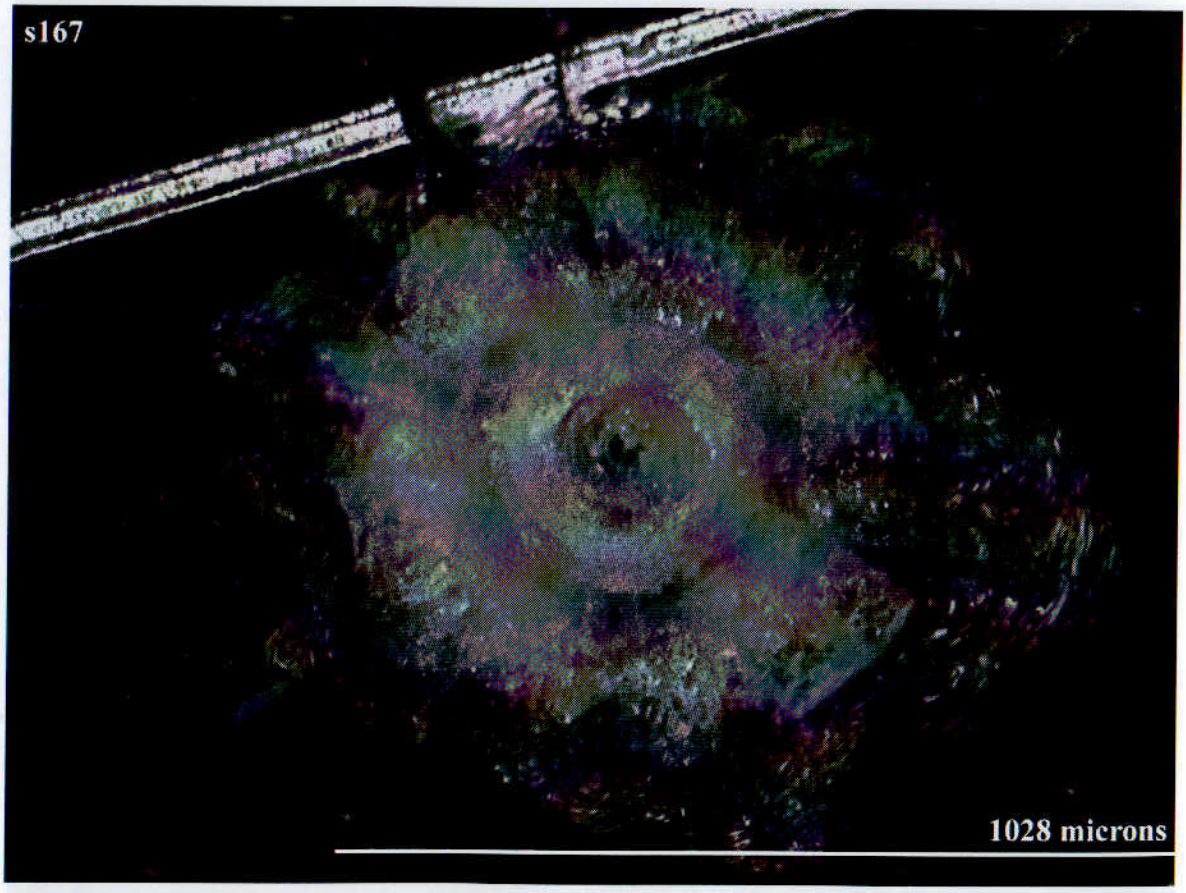
s167
1028 microns

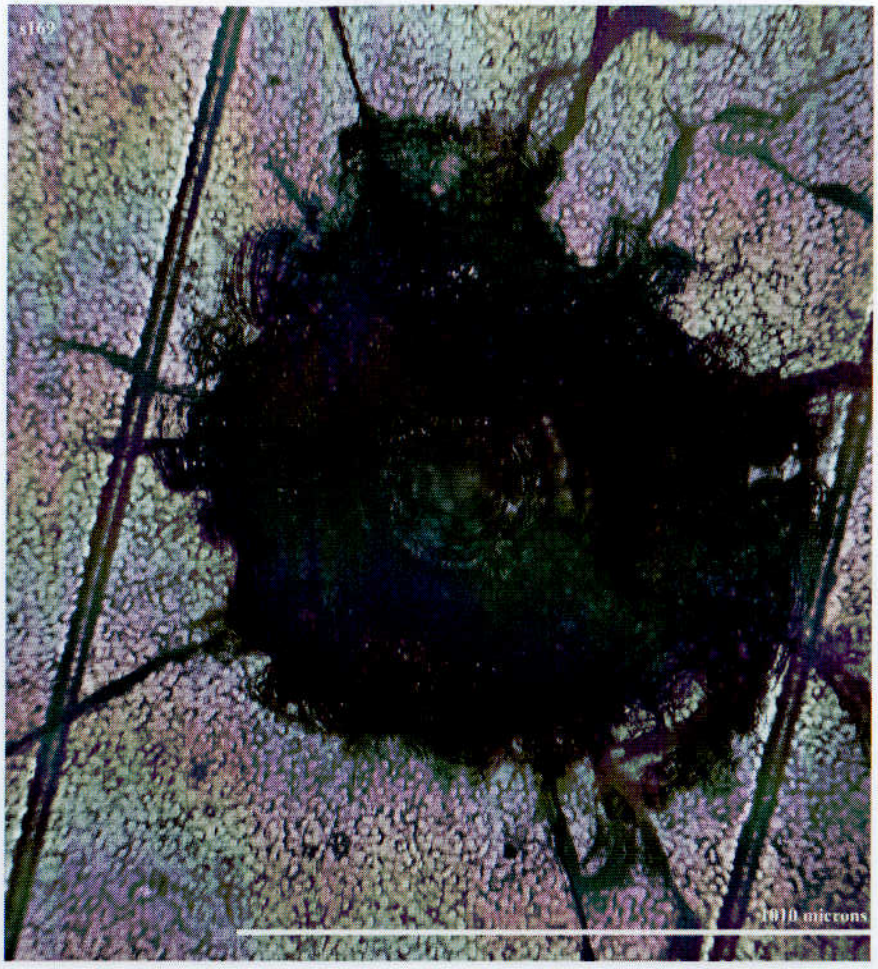
1030 microns

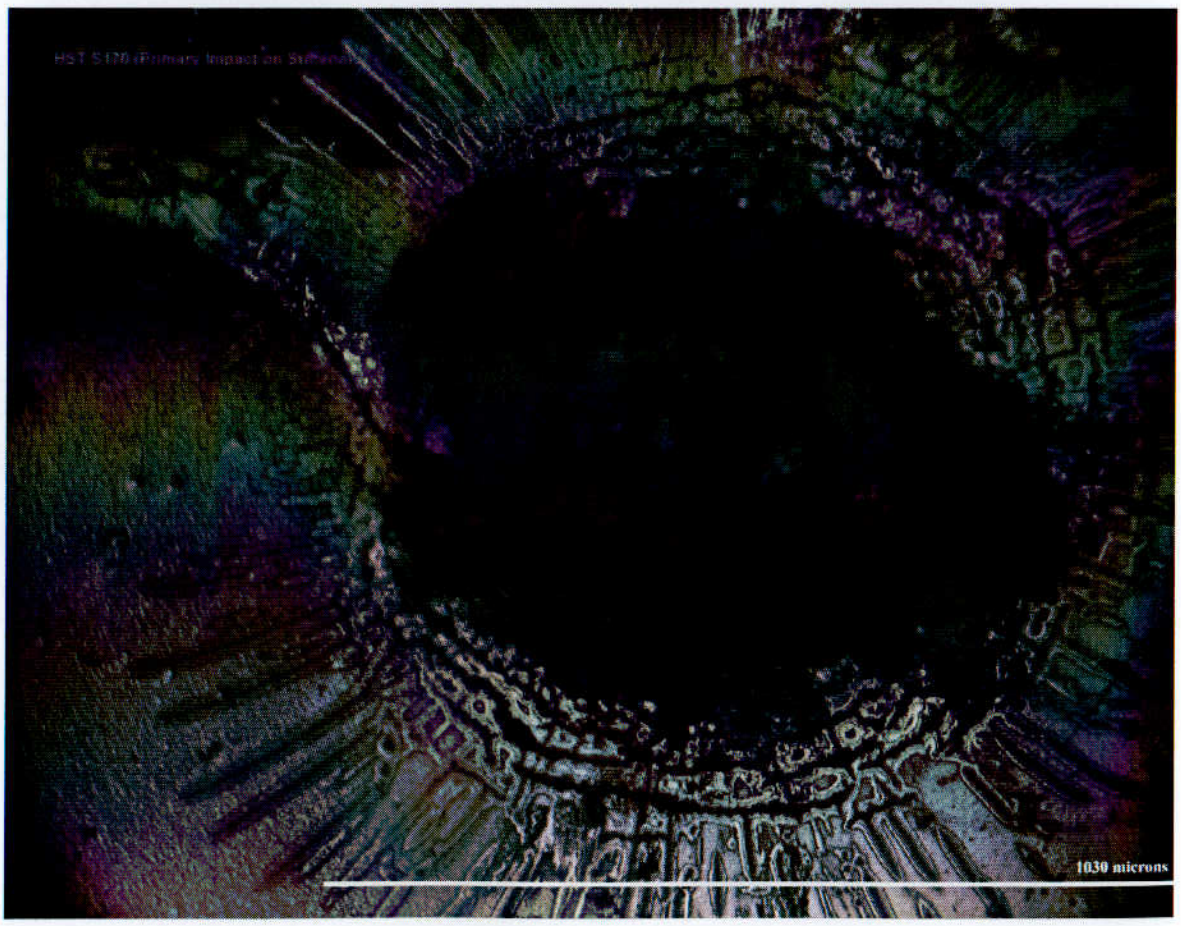
1030 microns

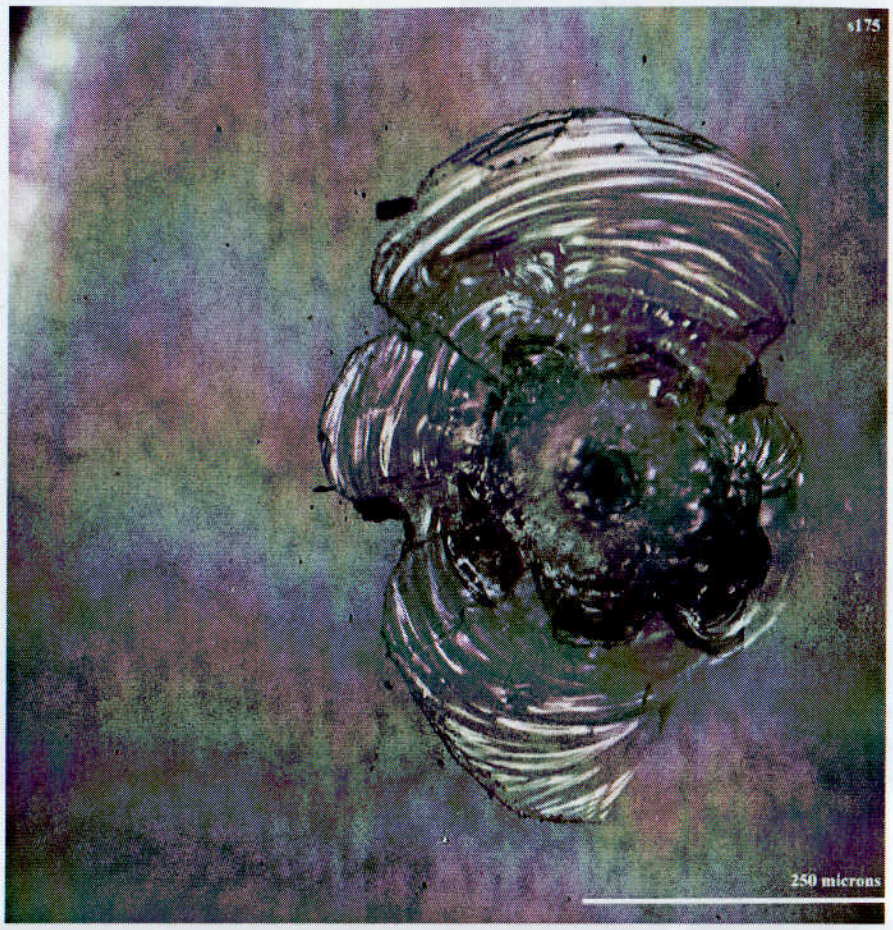
s175
250 microns

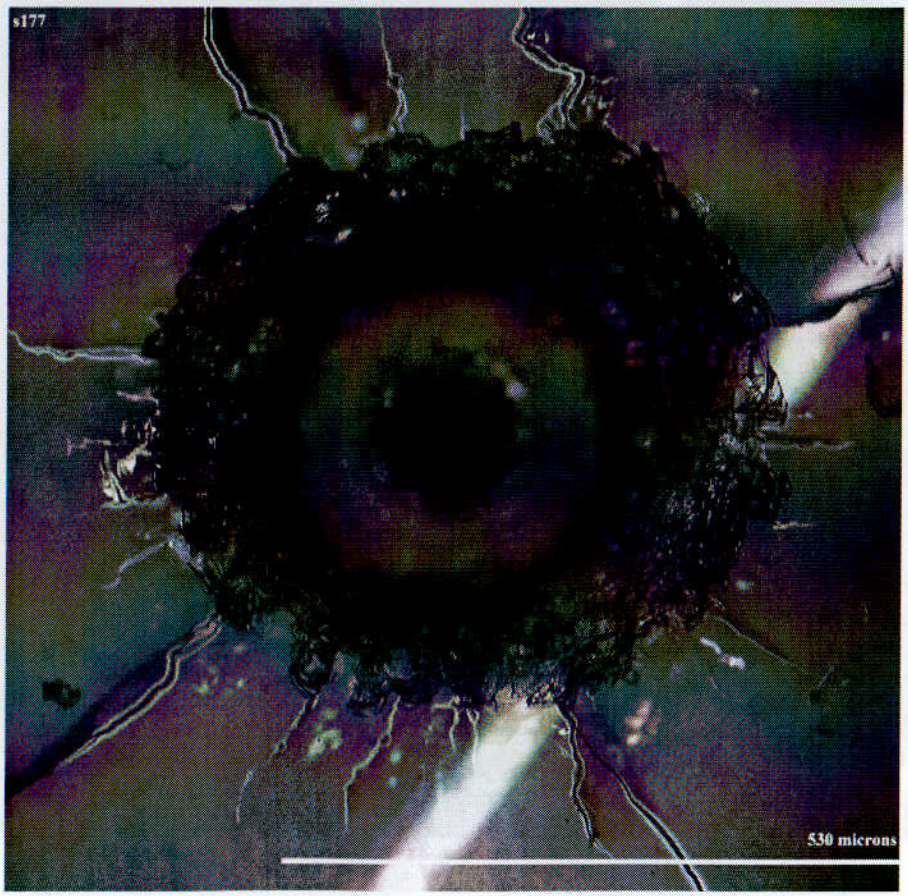
s177
530 microns

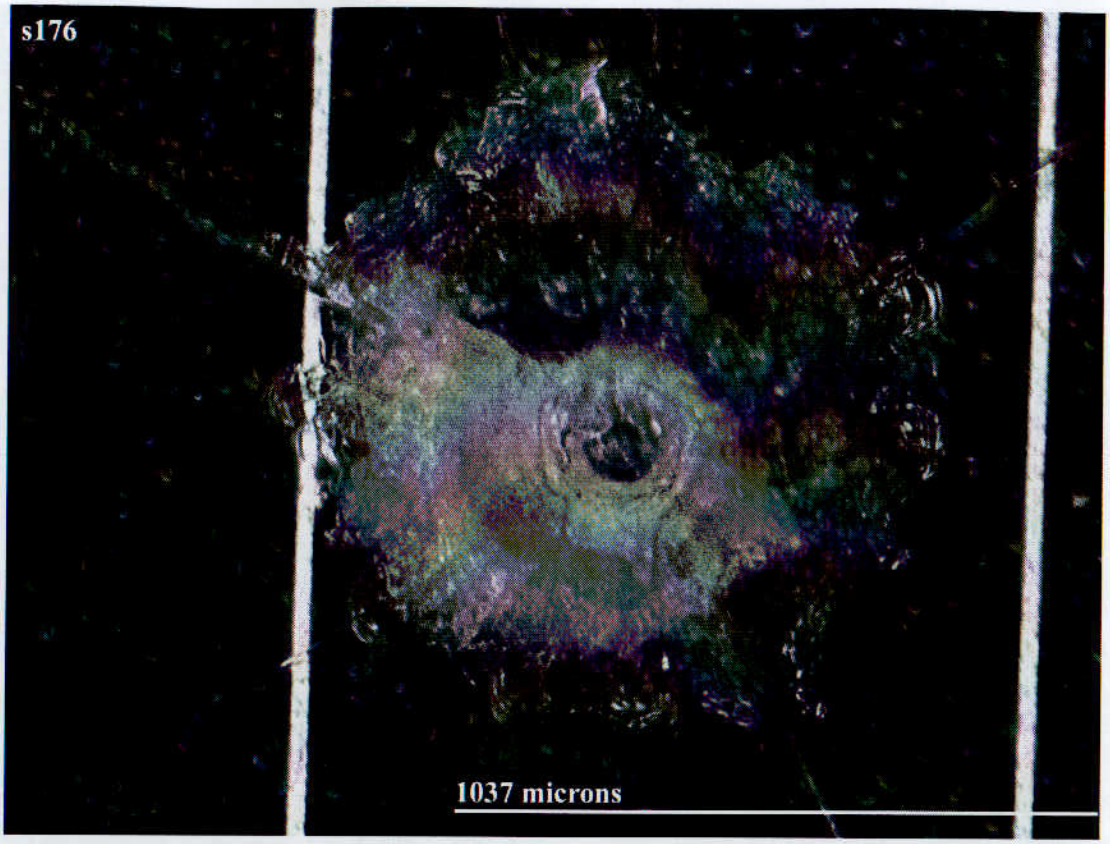
s176
1037 microns

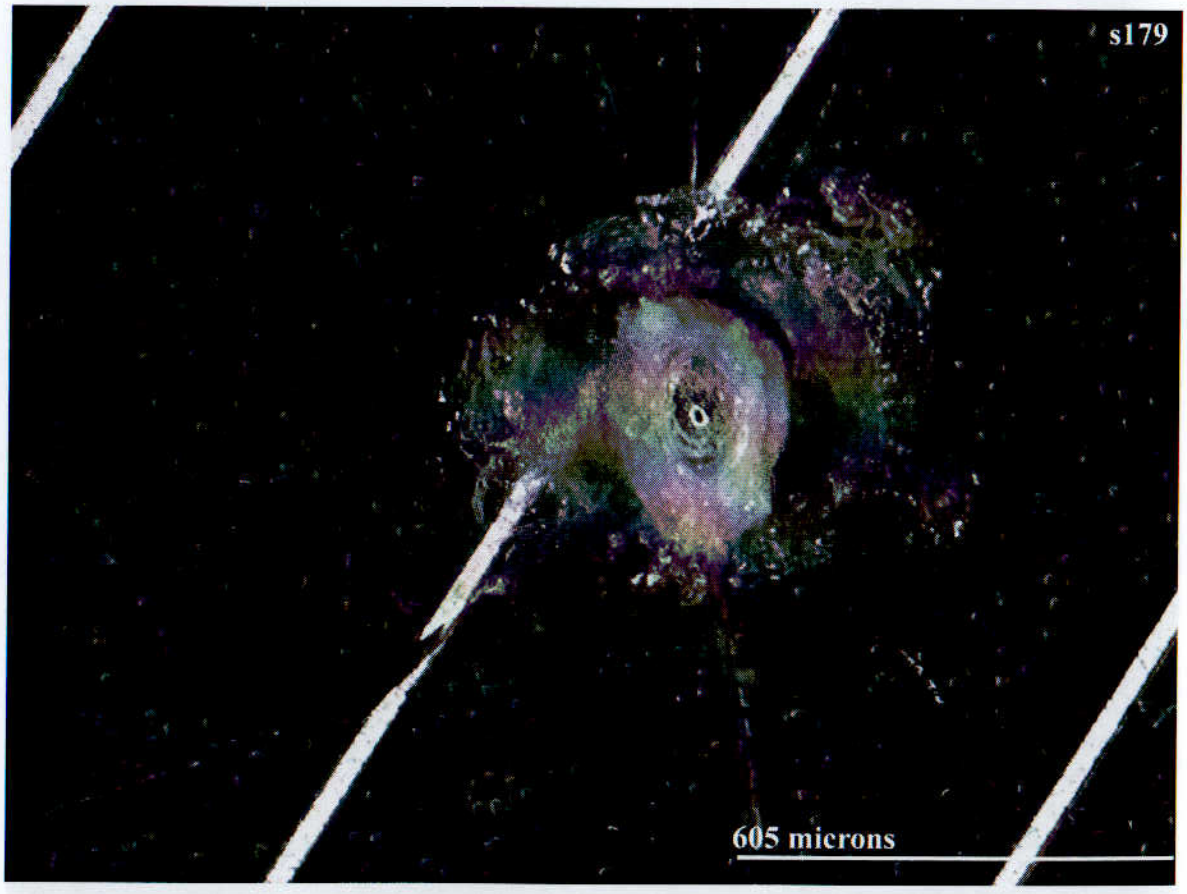
s179
605 microns

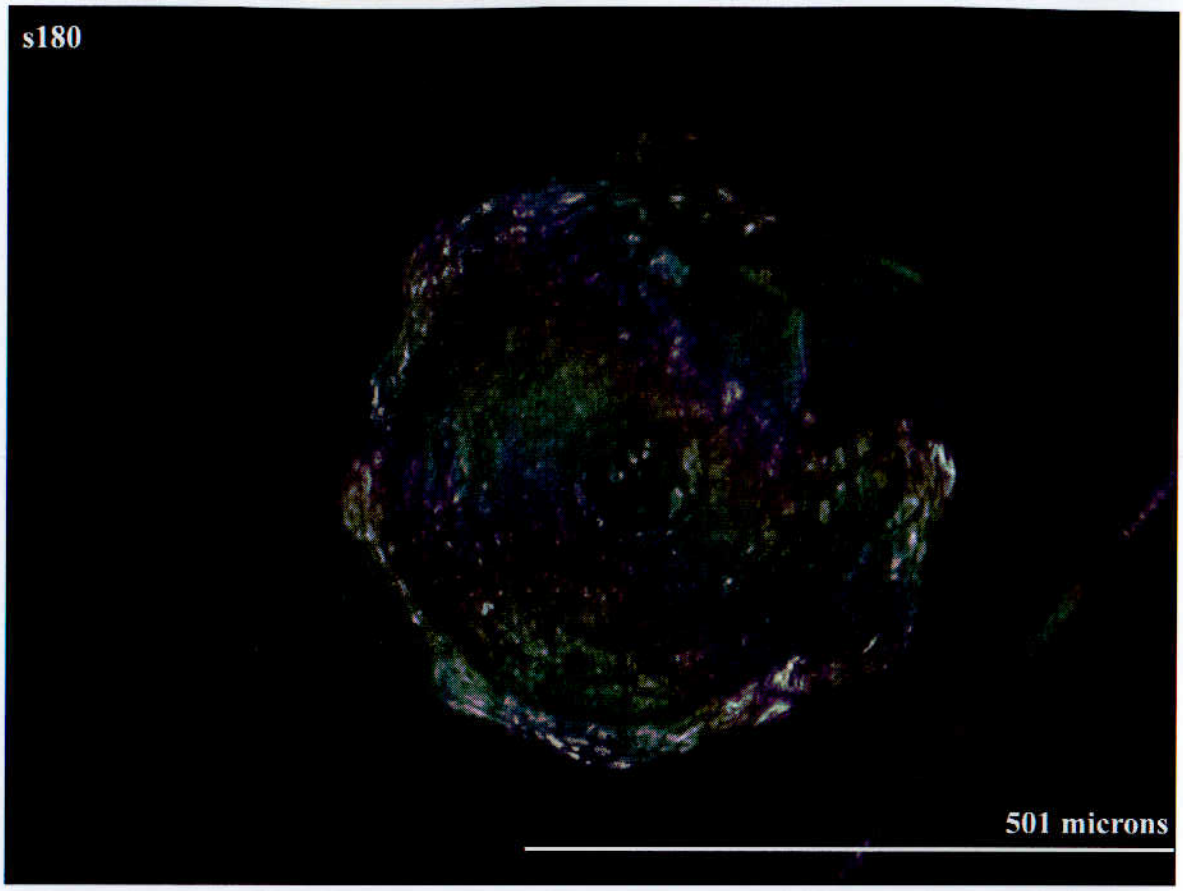
s180
501 microns

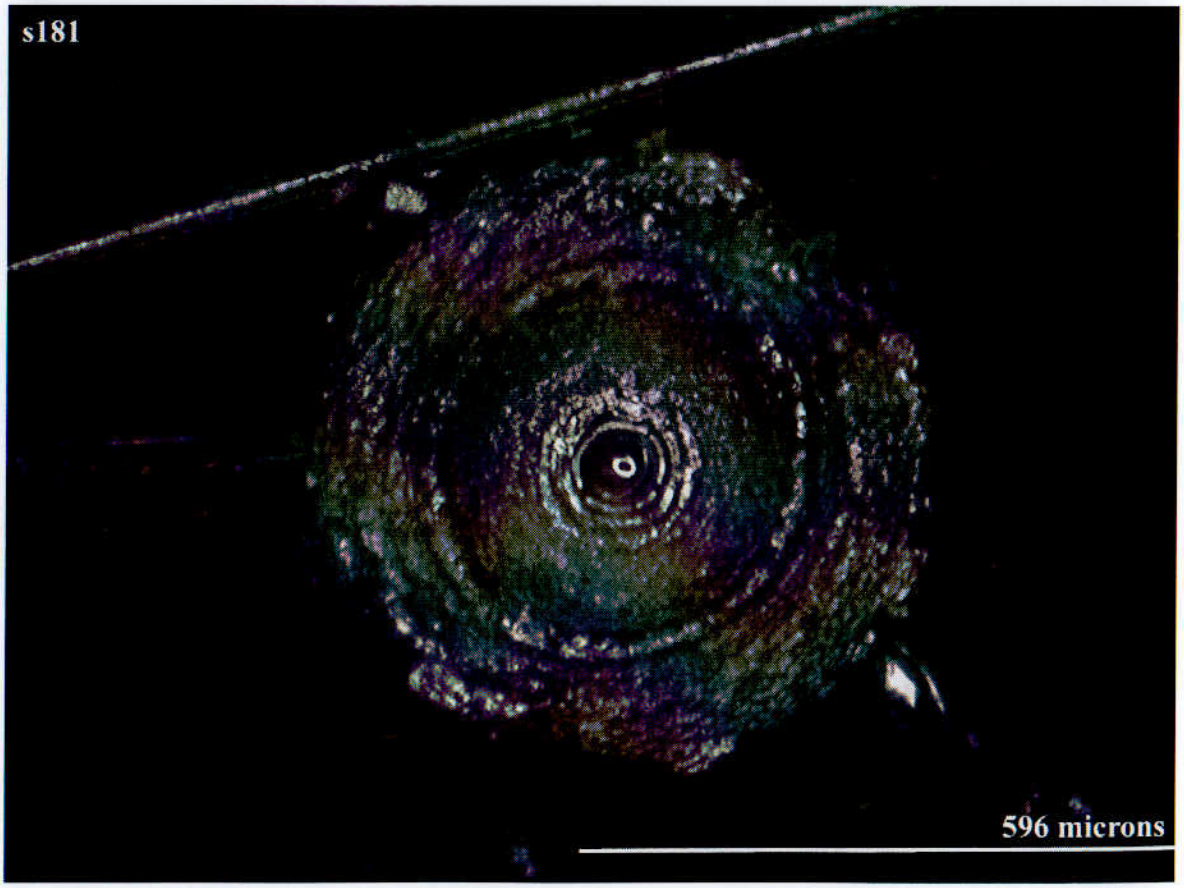
s181
596 microns

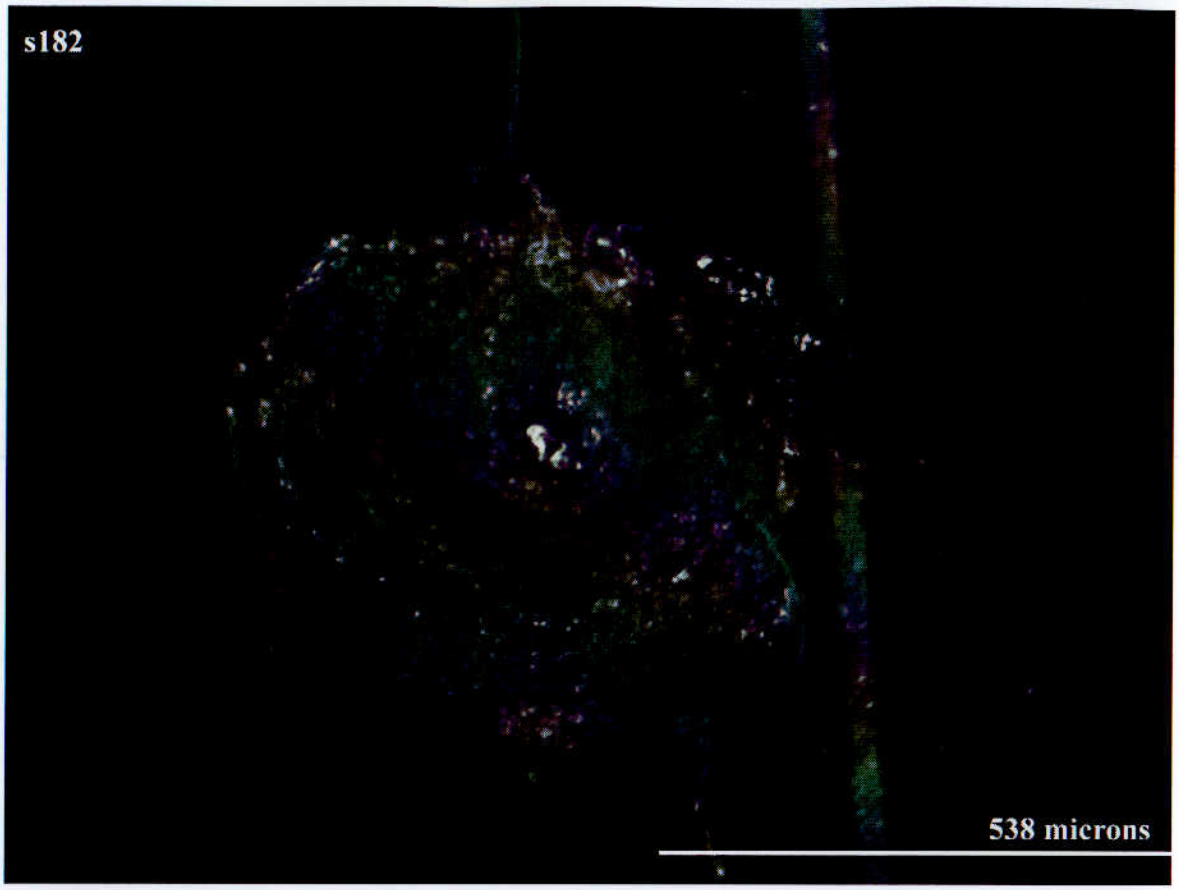
s182
538 microns

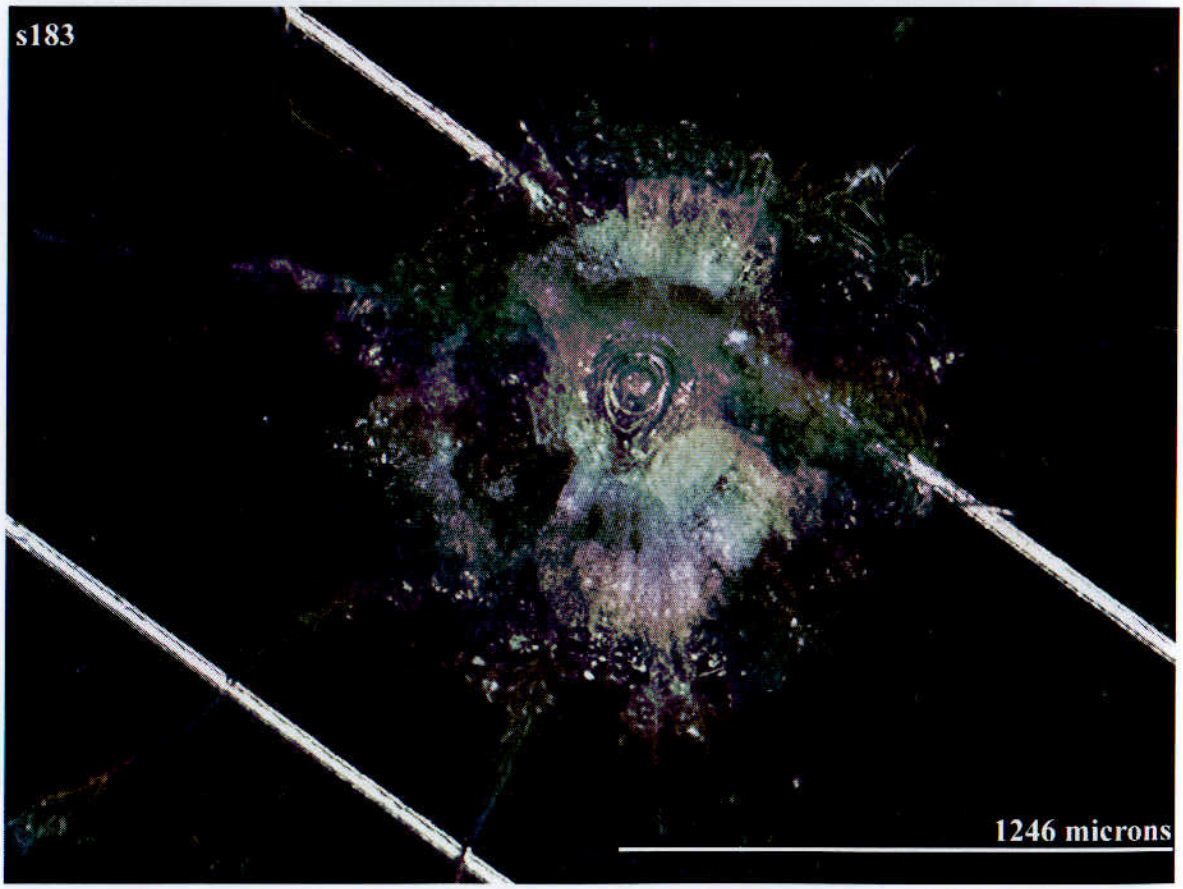
s183
1246 microns

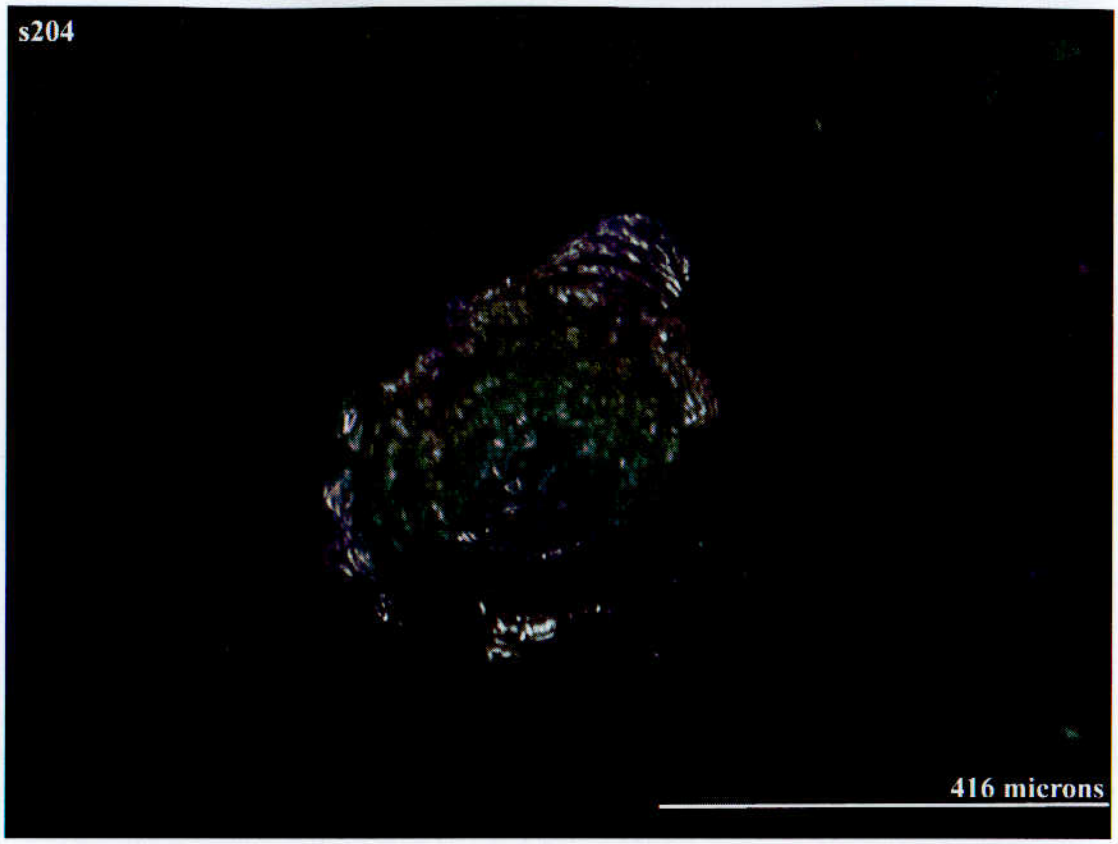
s204
416 microns

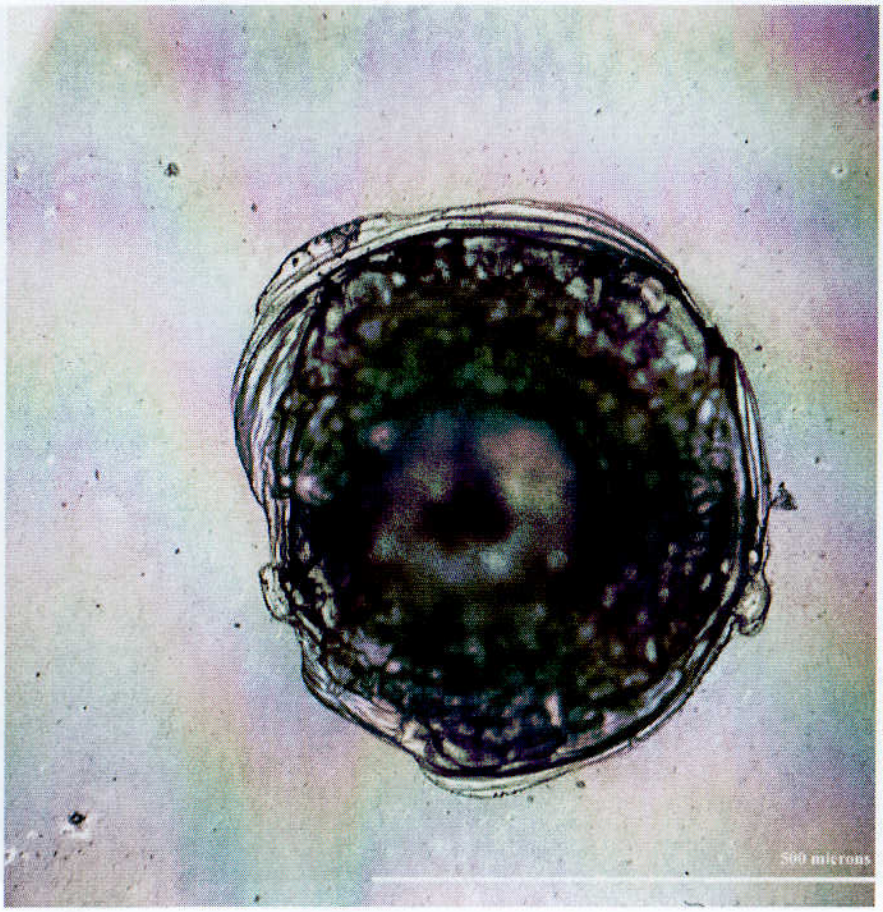
500 microns

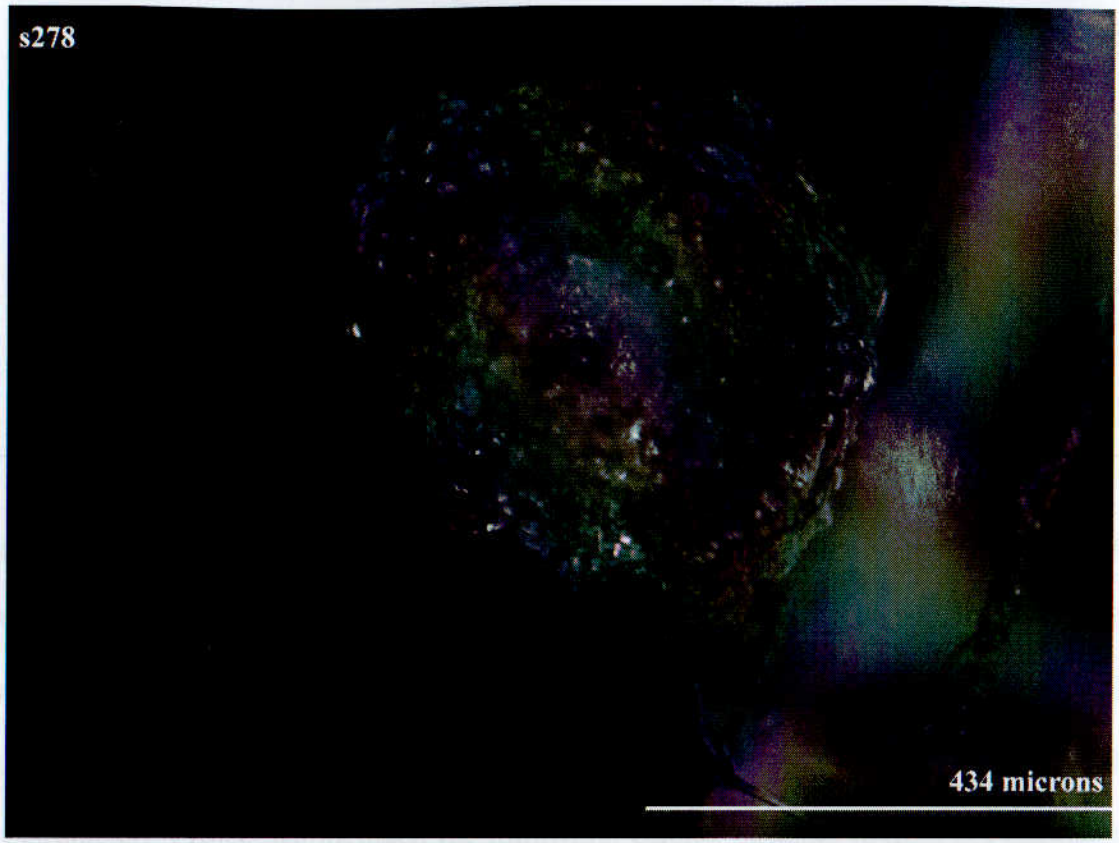
s278
434 microns

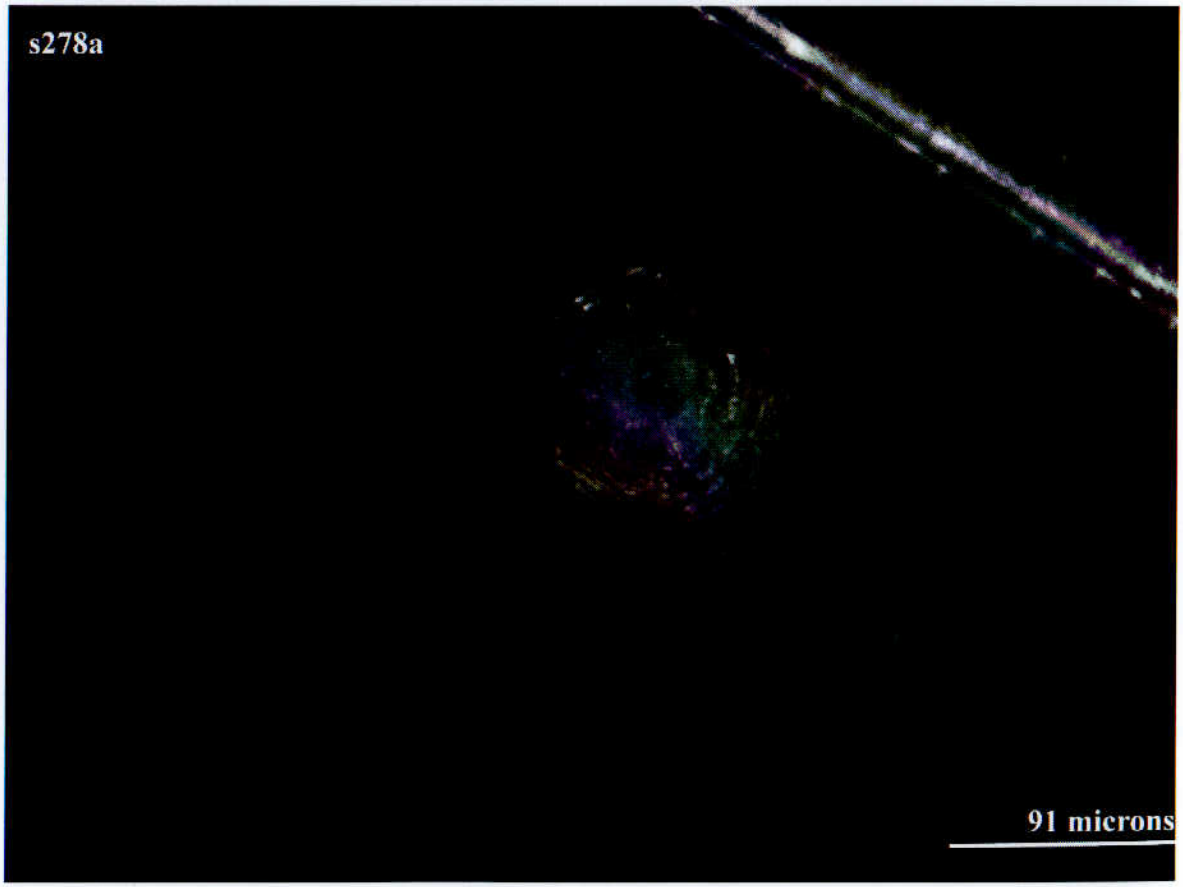
s278a
91 microns

Appendix 3

X-ray Elemental Maps Obtained For the Selected Mineral Shots Into HST Solar Cells

Appendix 3 contains the data obtained from the mineral shots into HST solar cells using the LGG facility at the University of Kent (Chapter 4.3). All the residues were investigated at Oxford Brookes University using the Jeol 840 scanning electron microscope fitted with an Oxford Instruments e-XL X-ray Energy-Dispersive spectrometer. Projectiles included the following: calcite, enstatite (pyroxene) (no residue found), diopside (pyroxene), olivine (from the Admire Meteorite), pyrrhotite, kamacite, nepheline, alumina, anorthite (feldspar), saponite (phyllosilicate) (no residue found), serpentine (phyllosilicate) (no residue found) and albite. A powdered meteorite sample (Orgueil matrix material) was also included in the shot program as this is a polymineralic mixture which includes phyllosilicates (i.e hydrous minerals) and should accurately reflect the nature of hydrous micrometeoroids.

Calcite

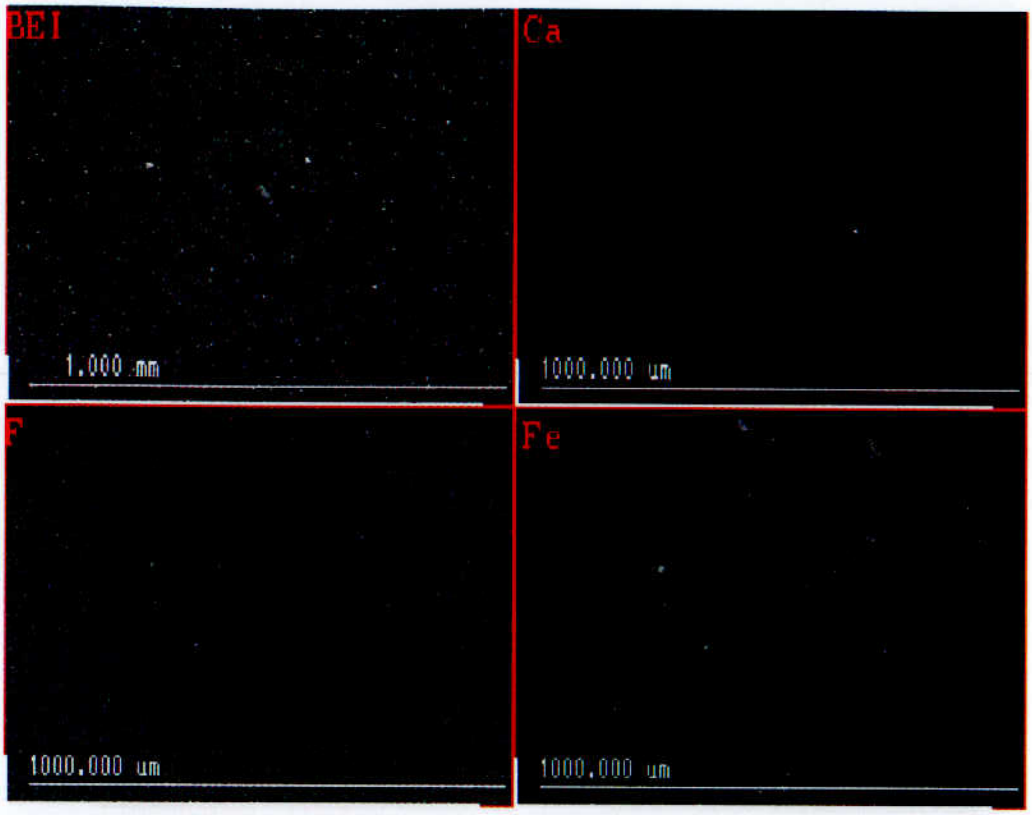
BEI
1.000 mm
Ca
1000.000 um
F
1000.000 um
Fe
1000.000 um

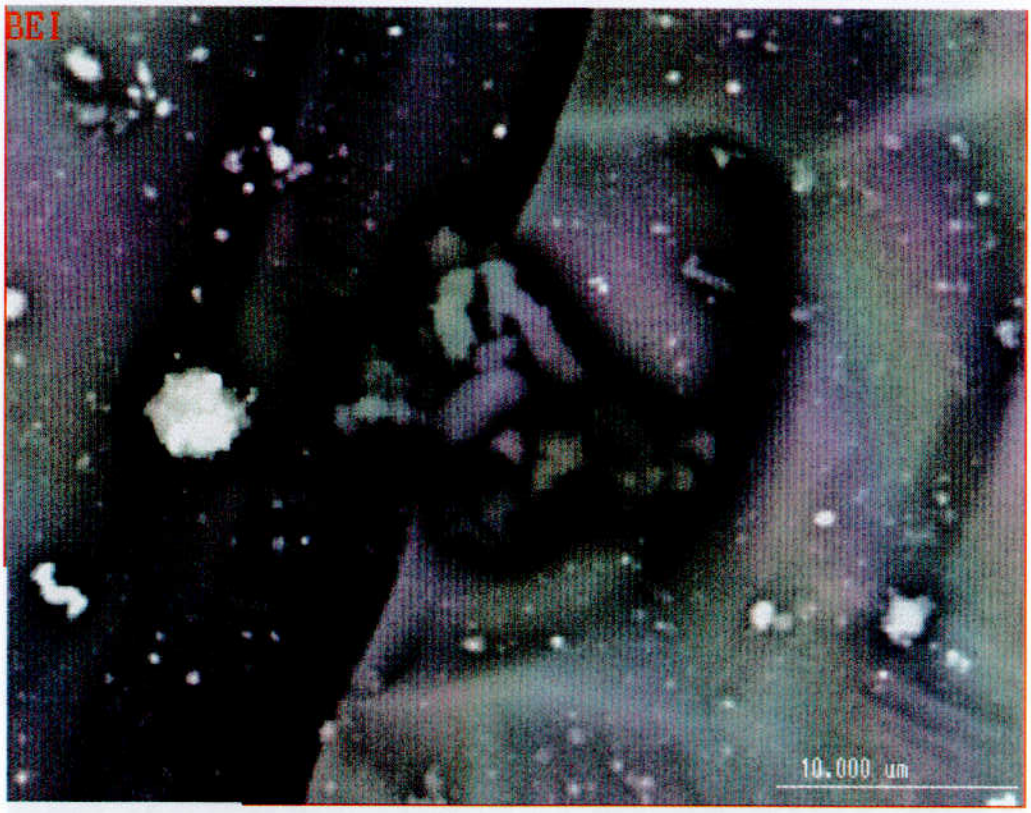
BEI
10.000 um

Olivine

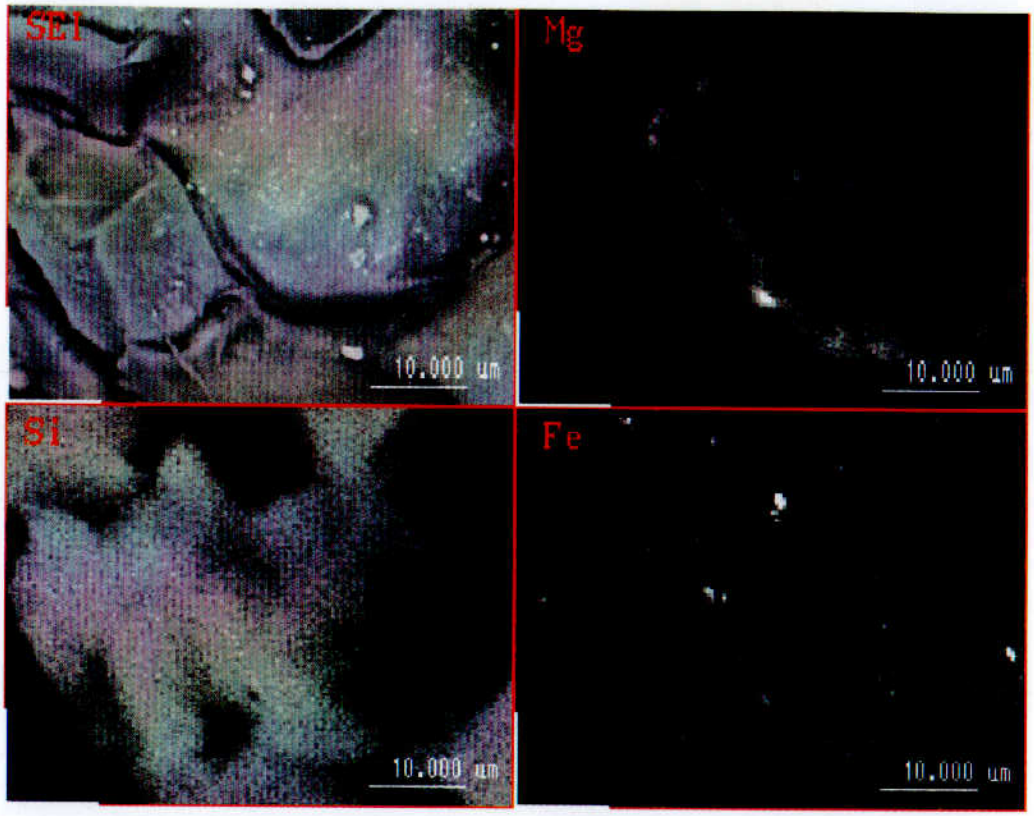

Pyroxene (diopside)

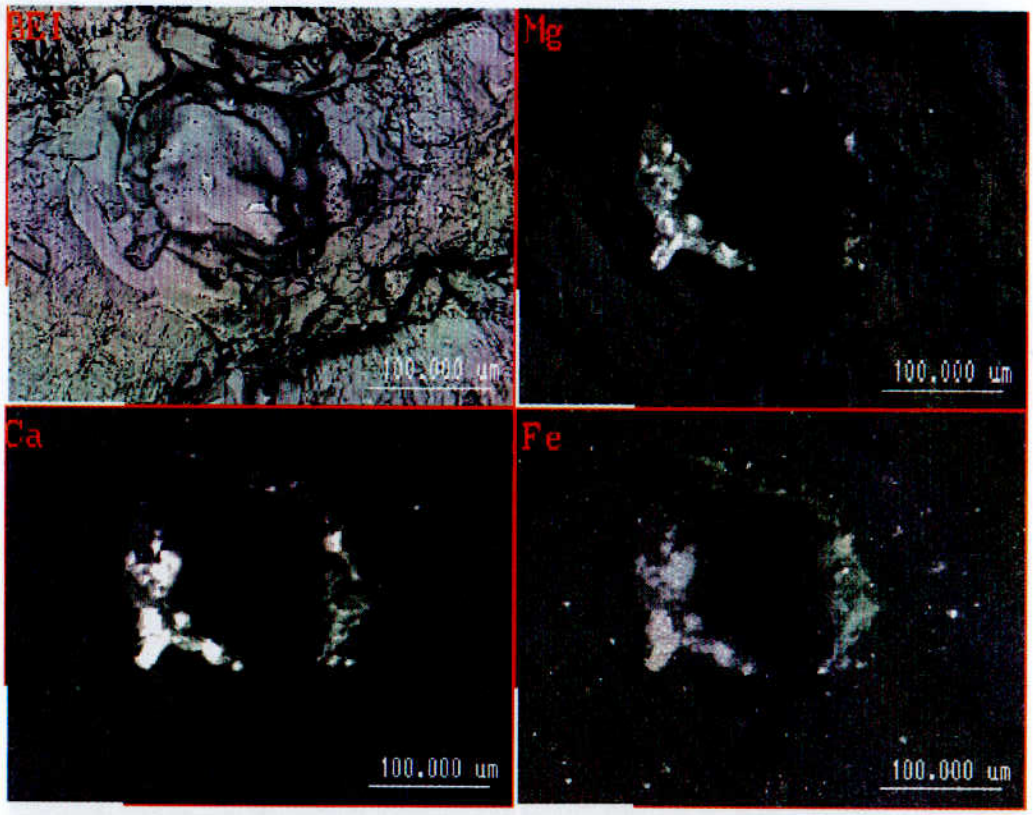

Nepheline

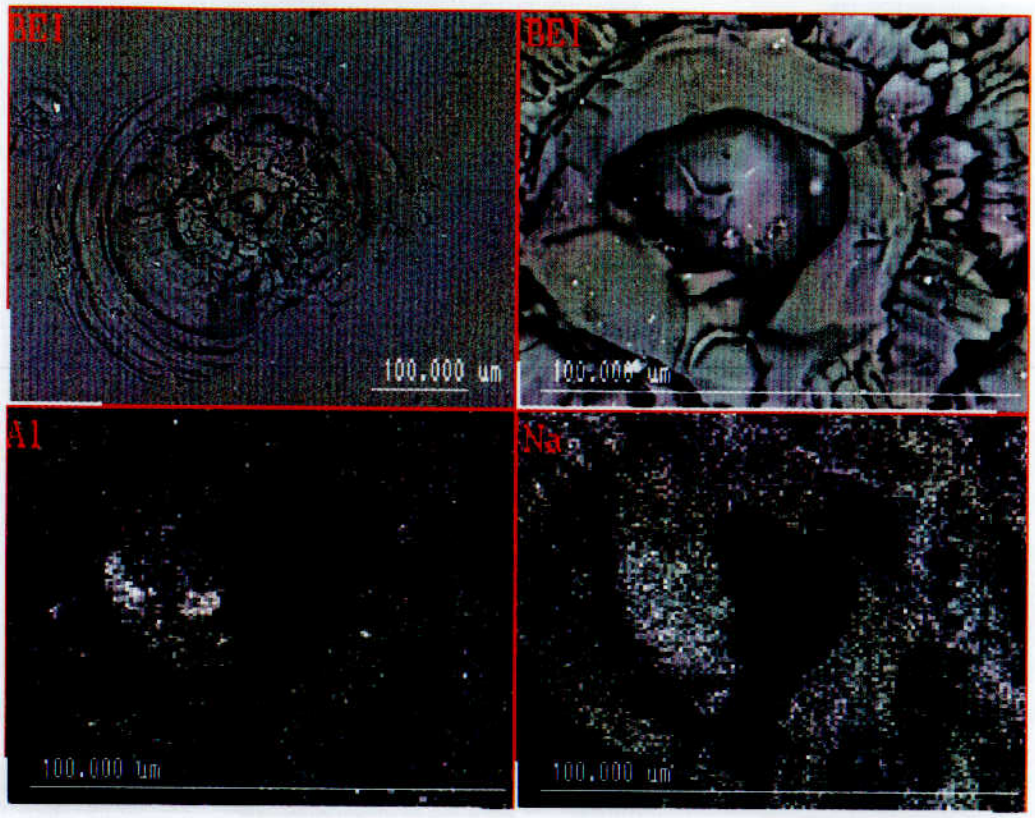

Albite

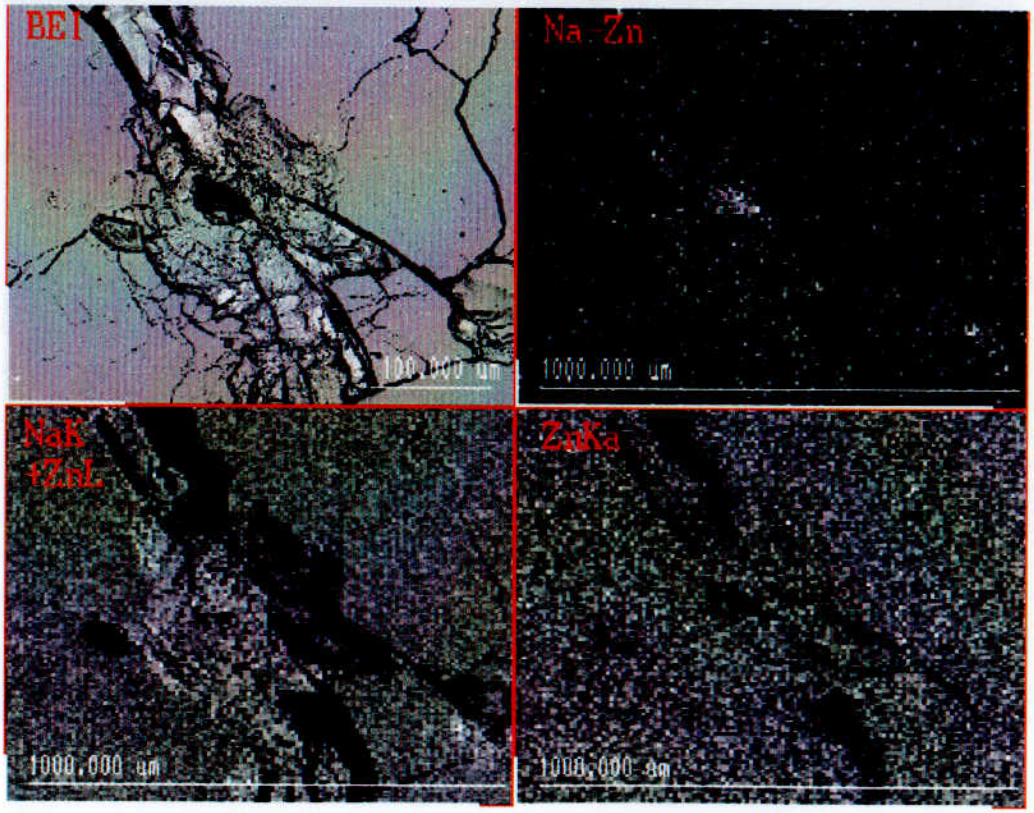

Pyrrhotite

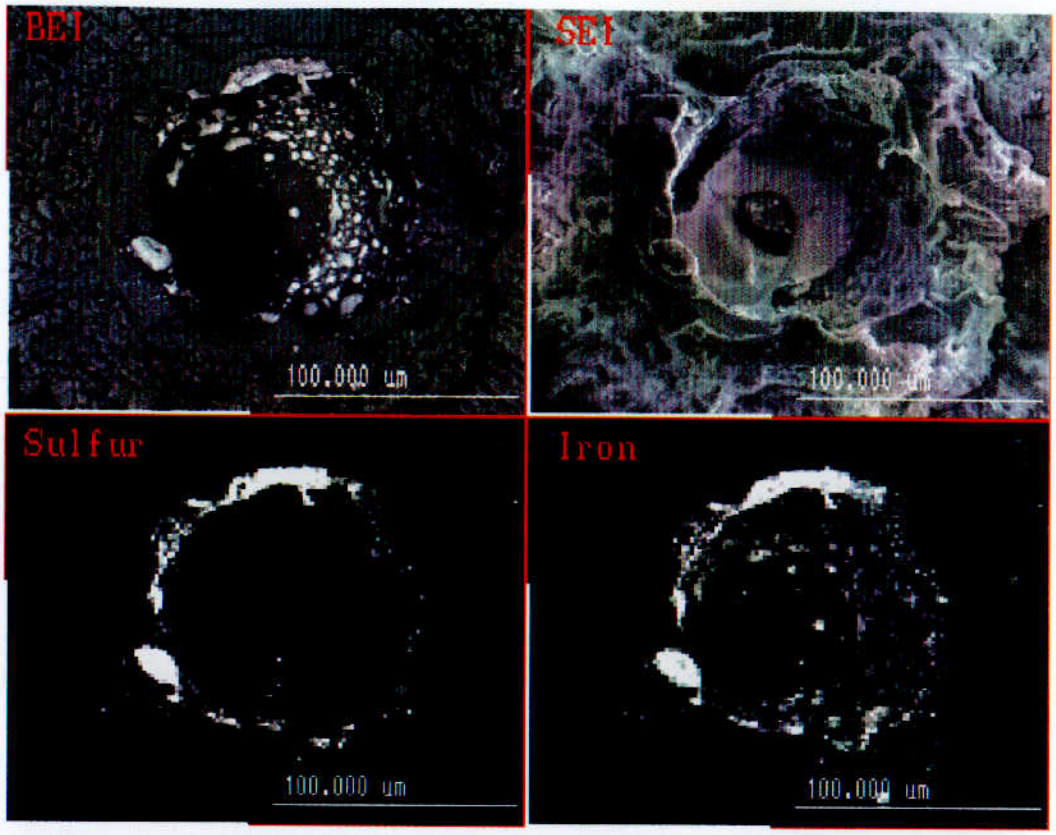

Kamacite

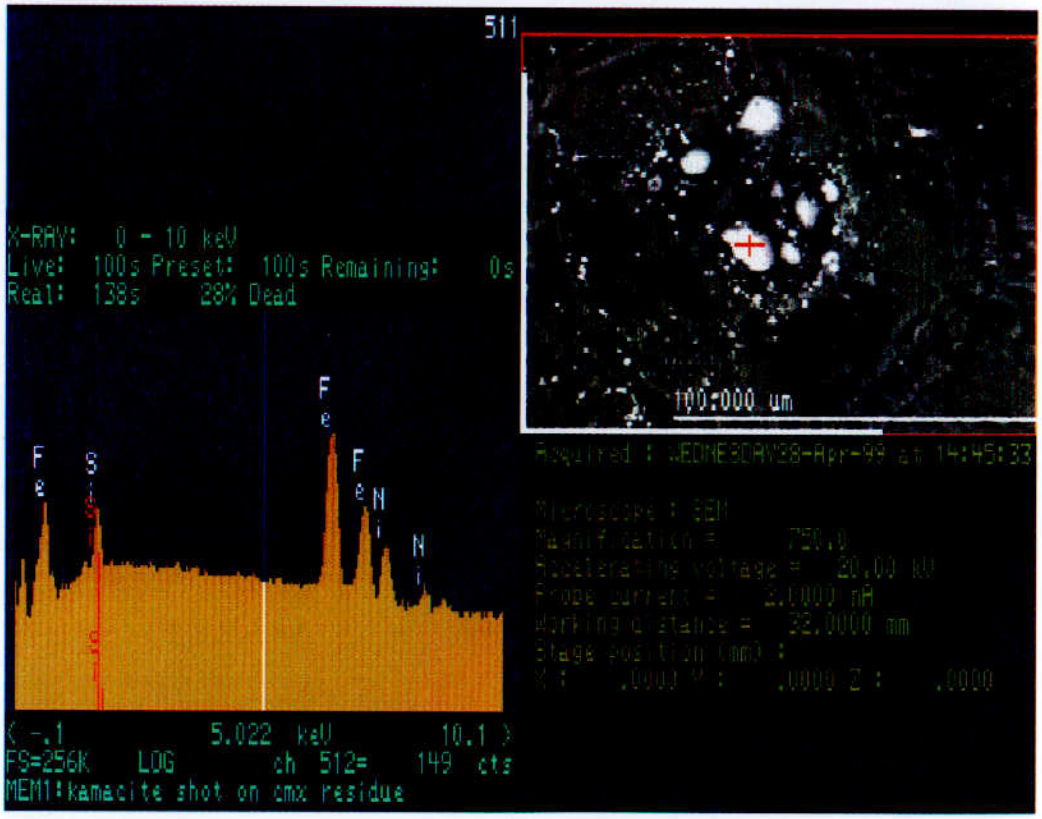

Meteorite Powder (Orgueil)

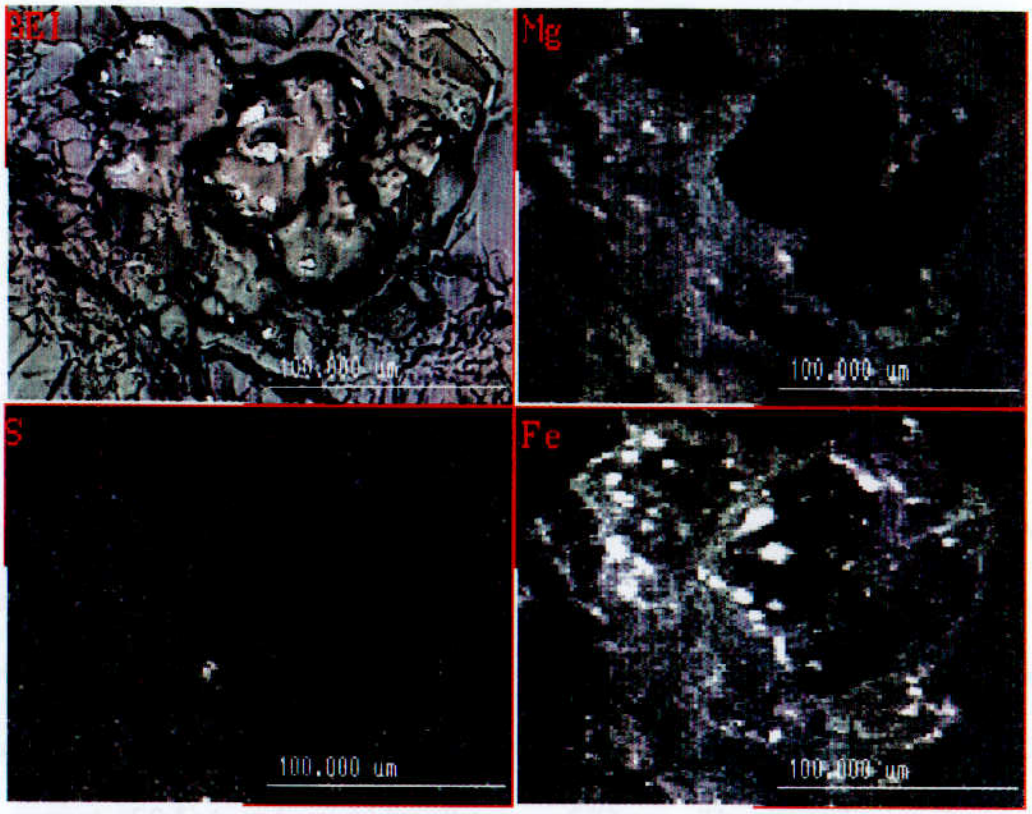

Appendix 4

Secondary Electron Images And Energy-Dispersive Spectrum Data For The Interplanetary Dust Particles

Appendix 4 contains the data obtained from the IDPs investigated in Chapter 6. All the particles were investigated at Oxford Brookes University using the Jeol 840 scanning electron microscope fitted with an Oxford Instruments e-XL X-ray Energy-Dispersive spectrometer. The analytical working conditions were an accelerating voltage of 20kV, beam current of 0.5nA and a working distance of 32mm. The appendix is set as follows: under each particle identification number and Cosmic Dust Catalogue (CDC) volume number there is a secondary electron image of the particle and a energy-dispersive spectrum obtained for that particle.

Particle W7027I6

(CDC Vol. 4:2 August 1983)

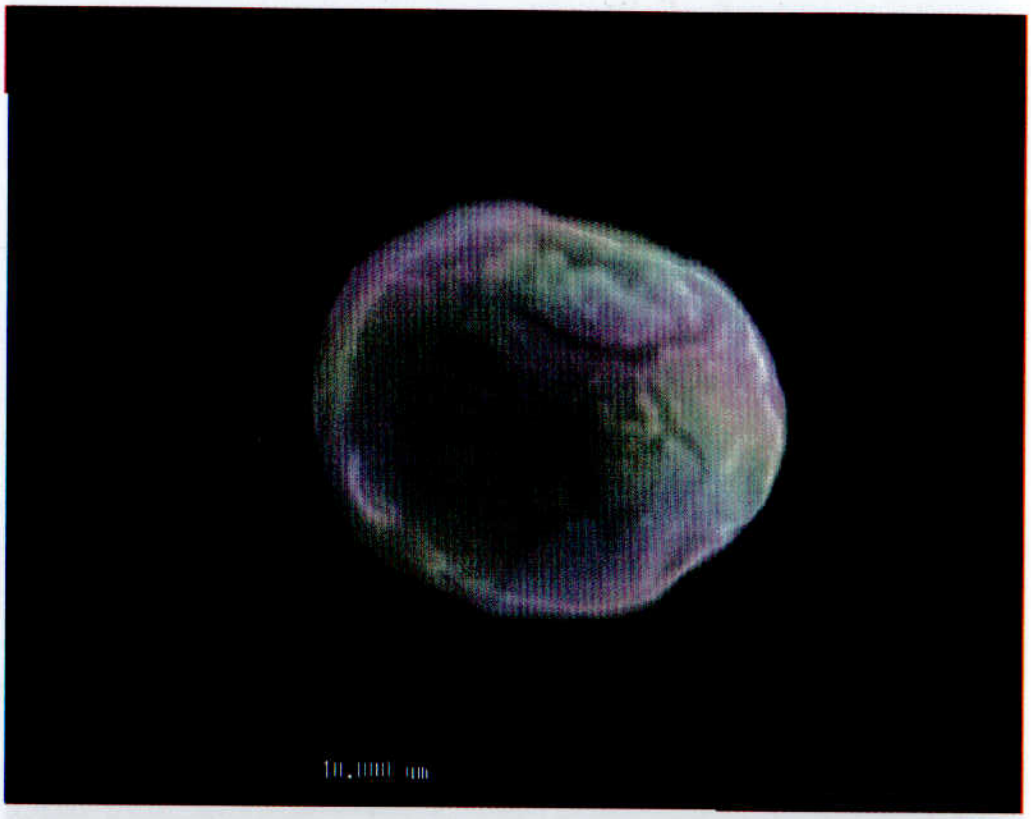

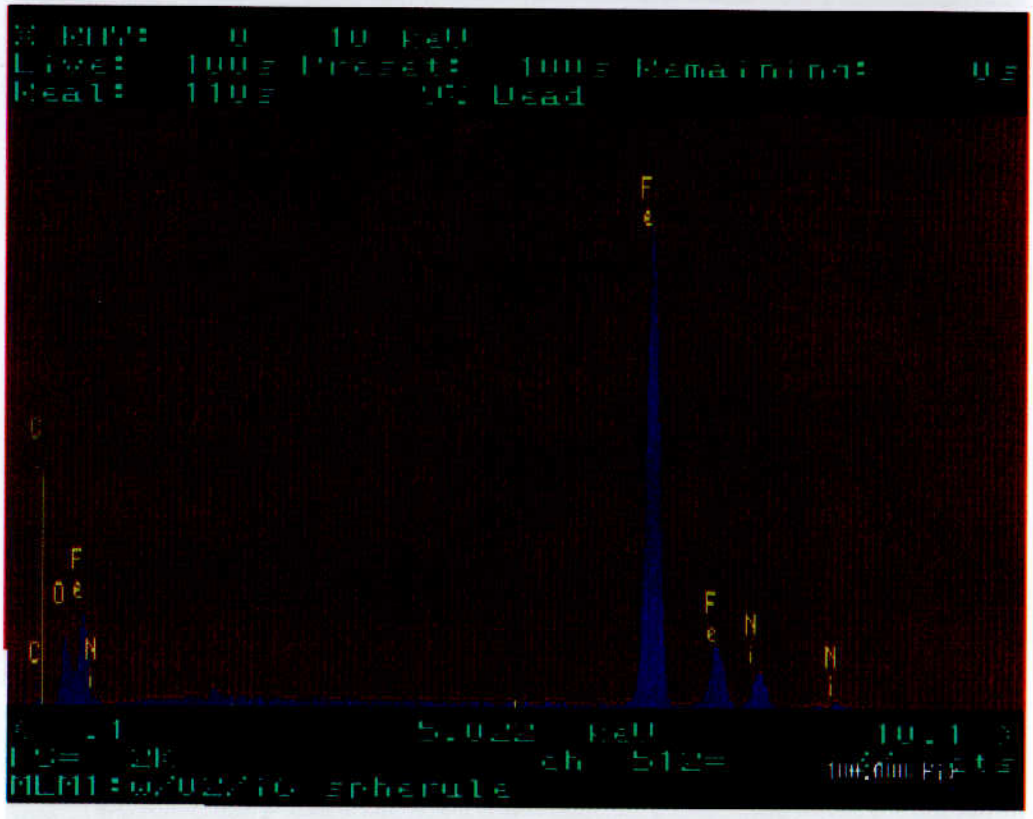

Particle W7013A4

(CDC Vol. 8:1 November 1986)

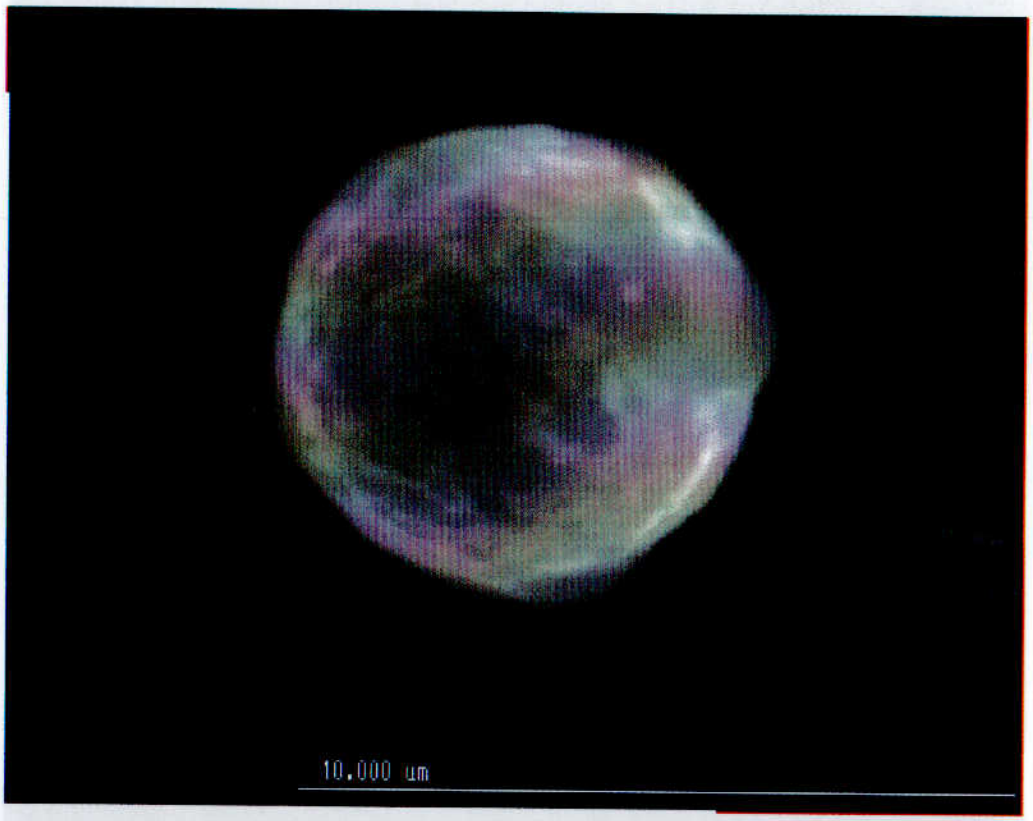

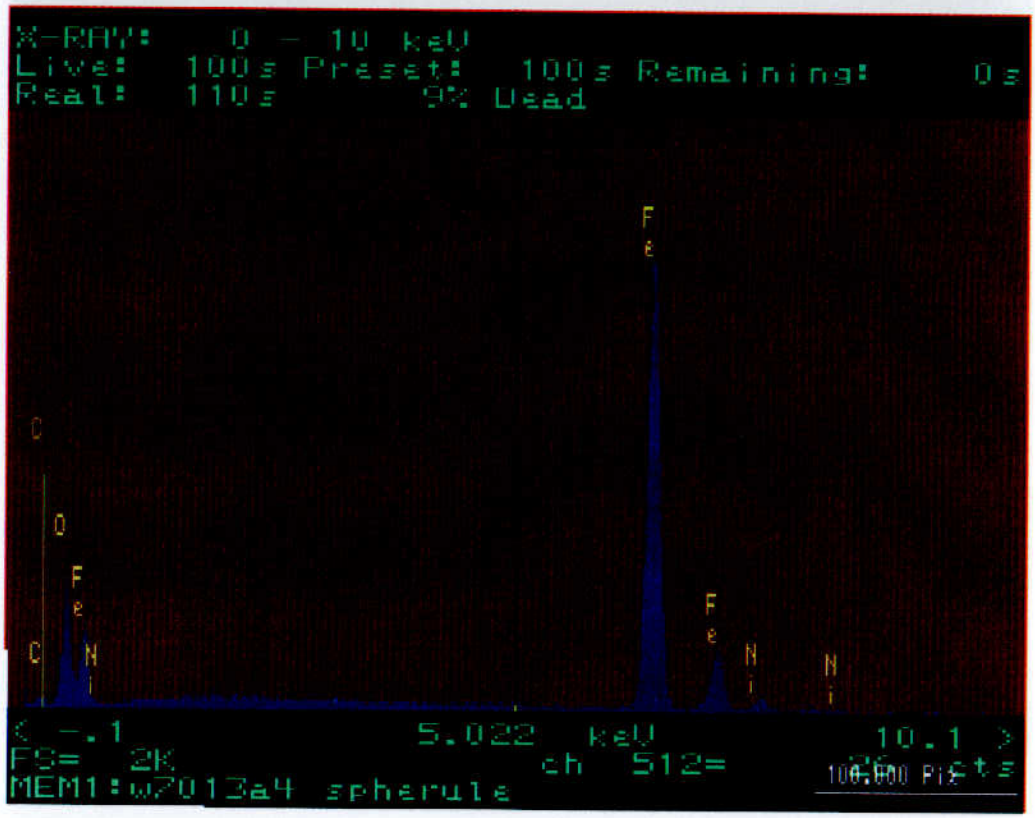

Particle L2005J15

(CDC Vol. 11:1 June 1990)

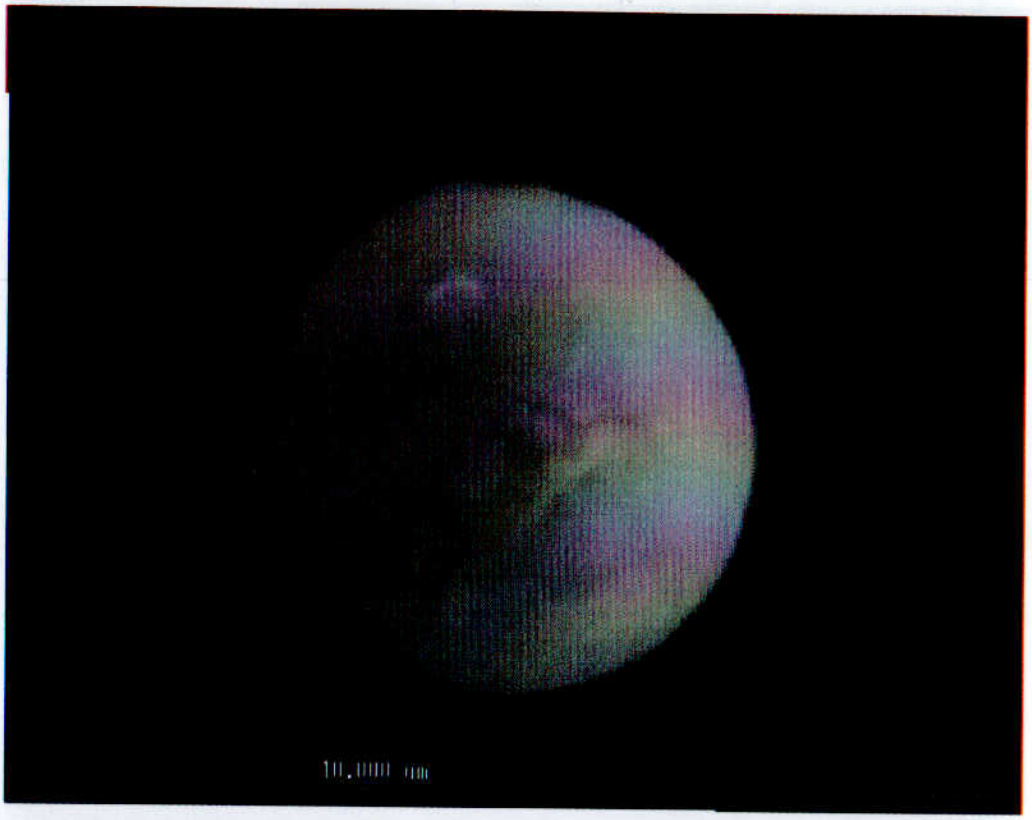

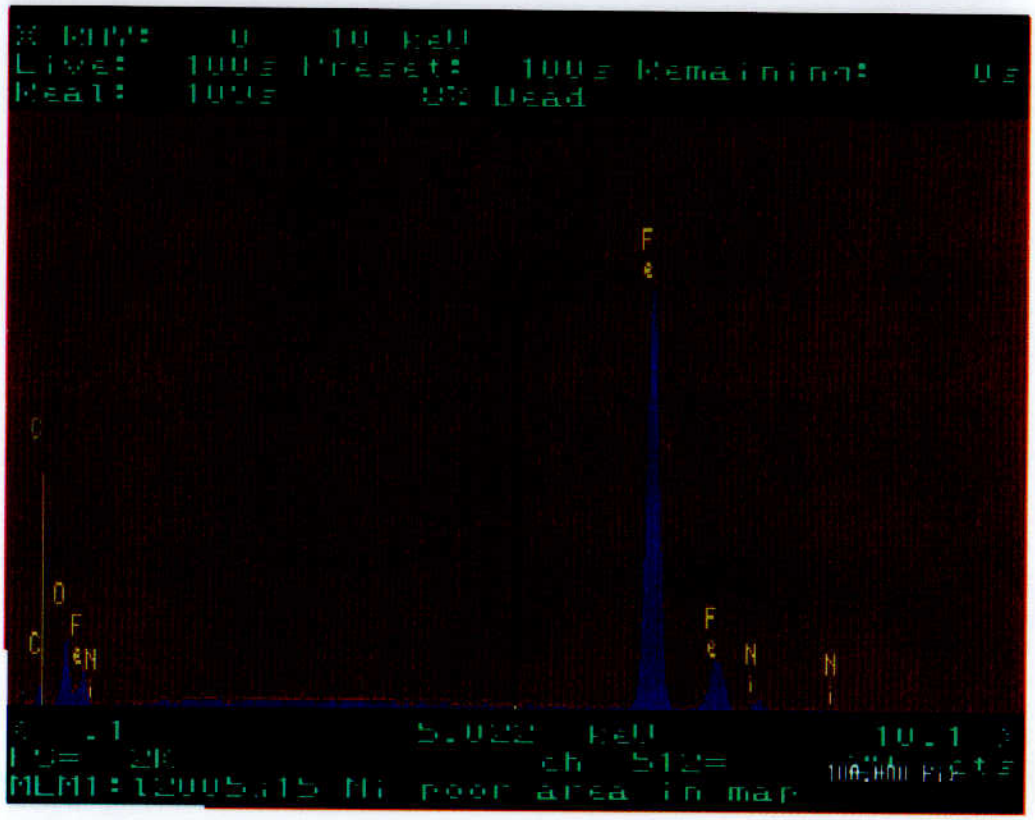

Particle L2006J1

(CDC Vol. 12 June 1991)

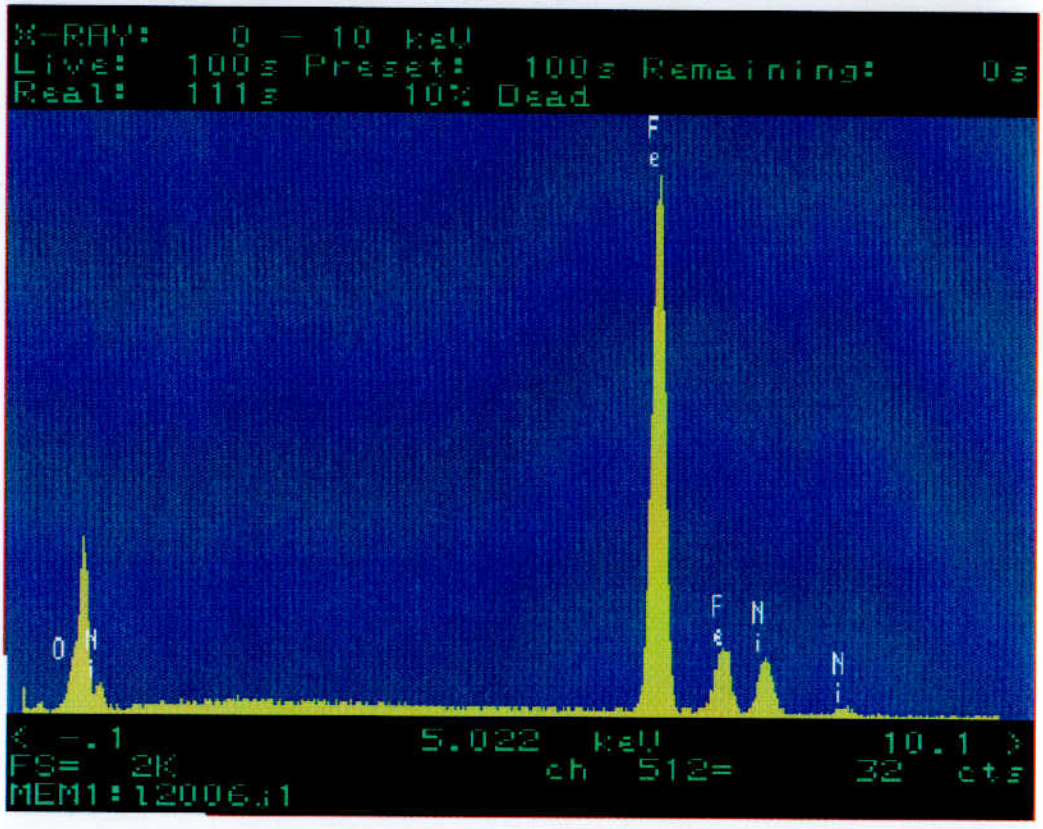

Particle L2006L1

(CDC Vol. 12 June 1991)

SAMPLE LOST DURING TRANSIT FROM NASA Johnson Space Centre (Houston Texas, USA) TO THE OPEN UNIVERSITY (Milton Keynes, UK)

Particle L2005T3

(CDC Vol. 12 June 1991)

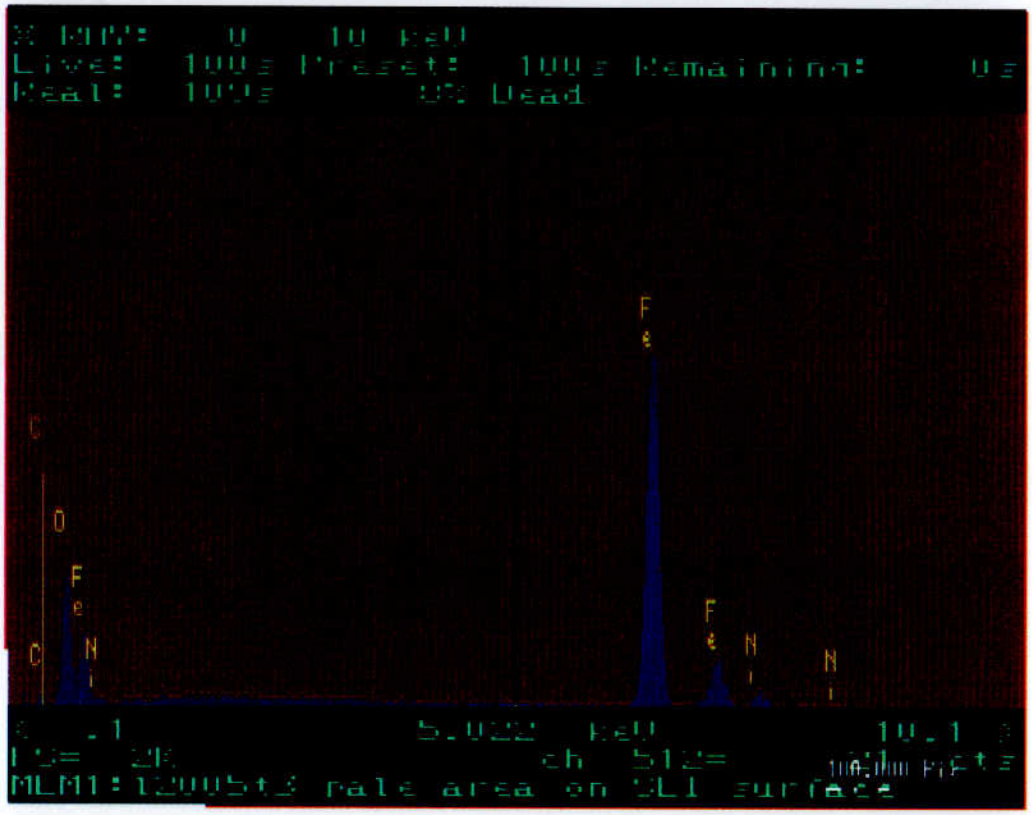

Particle L2008I4

(CDC Vol. 14 June 1994)

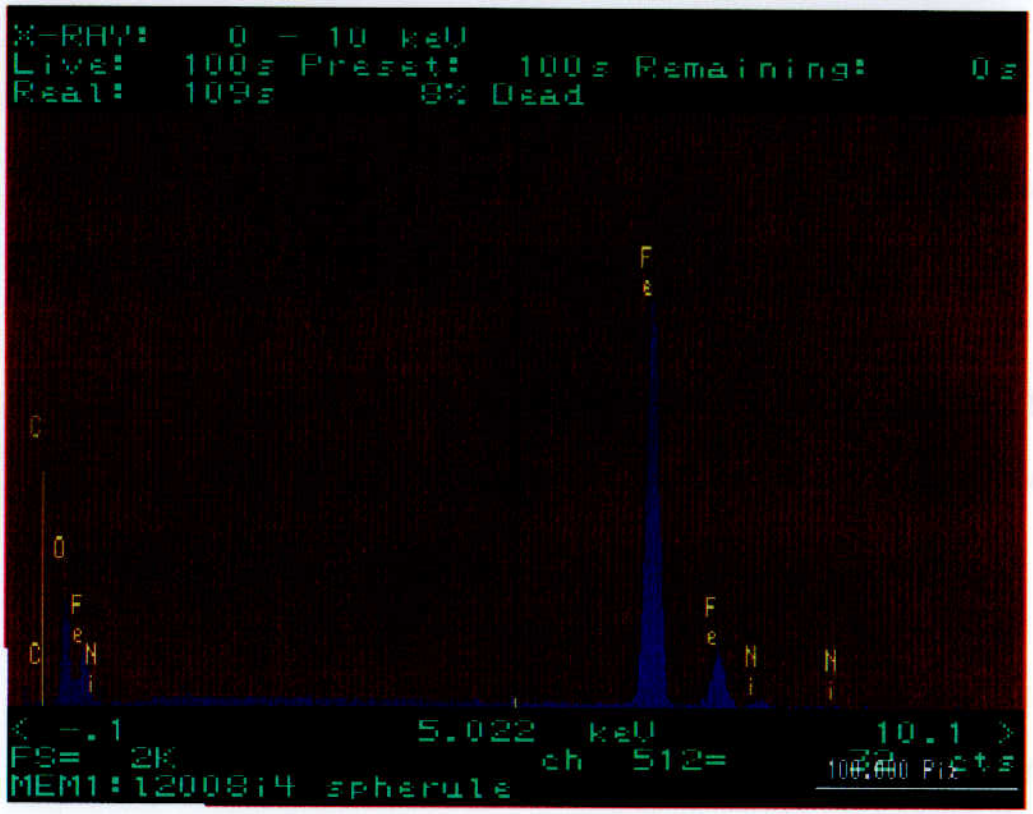

Appendix 5

Published Papers

Appendix 5 contains the "published" or "in press" papers that have been produced during the course of this thesis:

Graham.G.A, Sexton, A., Grady, M.M., & Wright, I.P., Further attempts to Constrain the nature of impact residues in the HST solar array panels, *Adv. Space Res.*, **20**, 8, 1461-1465, 1997a.

Graham.G.A, Kearsley, A.T., Grady, M.M., & Wright, I.P., The rapid identification of impact residues in the solar array panels of the HST by digitised back-scattered electron & X-ray elemental imaging, Proc. 2nd European Conf. On Space Debris, *ESA SP-395*, 183-187, 1997b.

Graham, G.A., Kearsley, A.T., Grady, M.M., Wright, I.P., Griffiths, A.D. and McDonnell, J.A.M., Hypervelocity impacts in Low Earth Orbit: Cosmic Dust versus Space Debris, *adv. Space Res.*, **23**, 1, 95-100, 1999a.

Graham, G.A., Kearsley, A.T., Grady, M.M., Wright, I.P. Herbert, M.K. and McDonnell, J.A.M., Natural and simulated hypervelocity impacts into solar cells. *Int. J. Impact Eng.*, **23**, 319-330, 1999b.

Graham, G.A., Kearsley, A.T., Grady, M.M., Wright, I.P. and McDonnell, J.A.M., The collection of micrometeoroid remnants from Low Earth Orbit. *Adv. Space Res.*, **25**, 2, 2000.

Pergamon

Adv. Space Res. Vol. 23, No. 1, pp. 95–100, 1999

Printed in Great Britain
0273-1177/99 $20.00 + 0.00

PII: S0273-1177(98)00235-X

HYPERVELOCITY IMPACTS IN LOW EARTH ORBIT: COSMIC DUST VERSUS SPACE DEBRIS

G. A. Graham [1], A. T. Kearsley [2], M. M. Grady [3], I. P. Wright [1], A. D. Griffiths [4] and J. A. M. McDonnell [4]

[1] *PSRI, The Open University, Milton Keynes MK7 6AA, U.K*
[2] *Geology, Oxford Brookes University, Oxford OX3 0BP, U.K*
[3] *Mineralogy Department, The Natural History Museum, London SW7 5BD, U.K*
[4] *USSA, The University of Kent at Canterbury, Canterbury CT2 7NR, U.K*

ABSTRACT

The understanding of the micron-sized populations of natural micrometeoroids and artificial space debris in low Earth orbit has benefited considerably from the post-flight investigations of retrieved surfaces from spacecraft, such as the Long Duration Exposure Facility. The returned solar array from the Hubble Space Telescope has added to this repository and has offered a further opportunity to document these particles. 25 individual solar cells were specially selected on the basis that they contained impact craters (diameter 100-1000 μm) which had the most potential to retain impactor residue chemistry. The solar cells were subject to a detailed investigation using analytical scanning electron microscopy which identified 29 impact craters, the analysis of which identified 3 residues as artificial in origin, 6 unclassified and 20 as natural in origin. The limited number of unclassified residues identified indicates that the methods of analysis employed in this investigation are a significant step forward for such studies and, if employed on a greater number of samples, will improve the calculations of the time-integrated flux rates for micrometeoroids and space debris in the low Earth orbit environment. Notwithstanding the small sample set examined, the observed chemical classification of the impact residues in terms of micrometeoroid to space debris (in the particle size range 8-80 μm) corresponds well to the flux model that predicts the dominance of natural particles.

NOMENCLATURE

Diameters and crater Classes as defined by Herbert and McDonnell (1997)
D_{CO} = conchoidal cracking diameter (μm)
D_P = Particle diameter (μm)

INTRODUCTION

The characterisation of low Earth orbit (LEO) micron-particle populations has benefited extensively from the post-flight investigations of retrieved surfaces from spacecraft, i.e. the Long Duration Exposure Facility (LDEF) (e.g. Zolensky *et al.*, 1994) and the European Retrievable Carrier (EuReCa) (e.g. McDonnell *et al.*, 1995). The micron-particle populations can essentially be sub-divided into two categories: 1) natural micrometeoroids (particles originating from comets, asteroids and possibly secondary ejecta from planetary impacts) (Brownlee, 1994), and 2) artificial space debris (fragments generated from spacecraft collisions, by-products of normal spacecraft operations etc). The returned solar array from the Hubble Space Telescope (HST) has offered a further opportunity to document the abundance of these particles, as prior to its retrieval the array was in LEO for 3.62 years at an orbital altitude of 600km, in essentially a sun-facing direction. The array was subject to a detailed post-flight investigation led by ESA, with micrometeoroid and debris studies focused upon the hypervelocity

The analyses conducted by the O.U/N.H.M were based on optical and scanning electron microscopy. The general findings of this study (Wright et al, 1995) were that 35% of the solar cells (7 out of the 20) had been completely penetrated by primary impacts. The main constituents of the solar cells are a borosilicate (BSiO) glass, which is a protective top layer for the underlying silicon (Si) solar cell, which is supported by an adhesive substrate (Si + minor Ca, Al & Mg), containing a fibre-glass backing tape. All the layers are held in place by silicon adhesive (Berthoud, 1995). These are not ideal substrate chemistries upon which to search for natural micrometeoroids, which contain the same chemical elements. In contrast recognition of material that is artificial in origin (i.e. space debris), such as rocket propellant, paint fragments etc. is somewhat easier. 65% of the solar cells contained impact features that showed evidence of material extraneous to the hosts, deemed to be associated with space debris. Only one impact event was throught to have been created by a natural micrometeoroid, but the findings were not conclusive.

In this study, we report on the attempts made to constrain further the nature and origin of extraneous material impacted on to the solar cells.

EXPERIMENTAL

Chemical compositions were determined qualitatively (O.U) using a Jeol JSM 820i scanning electron microscope (SEM) fitted with an integrated Kevex DELTA energy dispersive x-ray analyser (EDX). Quantitative analysis was carried out at the N.H.M using an Hitachi S2500 SEM fitted with a Link Analytical Systems AN10000 EDAX. The typical operating conditions for both SEMs were an accelerating voltage of 15 keV, a beam current of about 1 nA with a beam diameter of 1 μm and a working distance of 39 mm. The samples were carbon coated to reduce the effects of electrical charging during analysis

Preliminary EDS spot analyses were carried out on the primary impact craters on 6 solar cells; 1 was completely penetrated by the primary impact event, 3 contained impact events which had only penetrated the upper layers of the cell and 2 contained "punched" top surface impacts. It was difficult to find any material other than the host material on the cell which had been completely penetrated. The solar cells with "punched" top surface impacts were also difficult to analyse due to charging (the surface of the impacts made it impossible to coat the sample evenly). The best hope of finding a residue was therefore in the 3 partially-penetrated cells, of which two contained too much host debris from the upper layers of the cells. Thus the study concentrated on one of the partially-penetrated samples in more depth.

The selected sample had its flexible backing tape removed and spot analysis was carried out to confirm that the impact event had only partially penetrated the cell. The inner crater of the impact underwent spot analysis and was x-ray mapped for Si, Ti, Al, Fe, Ca, Mg, Ce and Na. After a residue had been detected by this way, the sample was subjected to a more detailed quantitative analysis. Quantitative analysis should normally be carried out on a flat substrate, but the nature of the impact made this impossible, so analysis of the residue was carried out until good repeatability resulted.

RESULTS

Figure 1a. shows a photomicrograph at x100 magnification of the primary impact crater in the selected solar cell; the diameter of the crater is 200μm. It can be seen that the crater comprises stepped surfaces that correspond to the different layers of the solar cell that have been ejected during the impact. Figure 1b. shows a view into the inner crater of the impact; in the bottom left hand corner of the image it is possible to see an area displaying textural differences to the surrounding surface.

Figure.1a

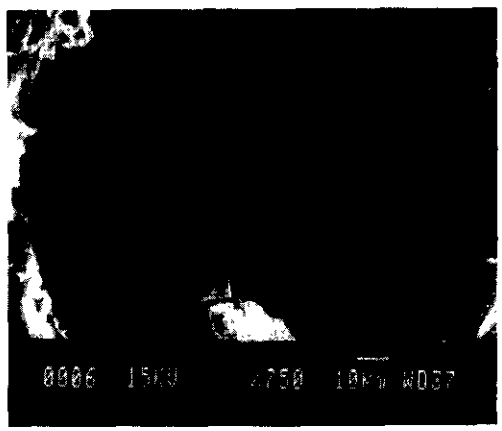

Figure.1b.

Figure 2a. and 2b show the results of chemical analyses obtained from silicon solar cell surrounding the residue (2.a) and the residue itself (2.b)

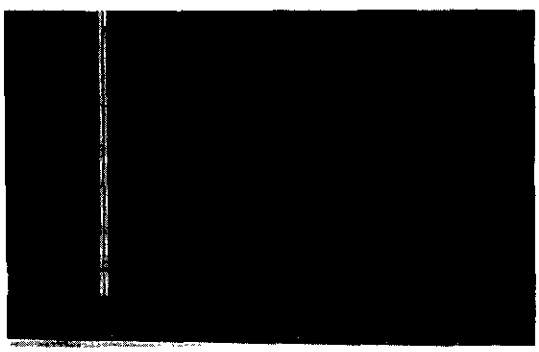

Figure.2a.

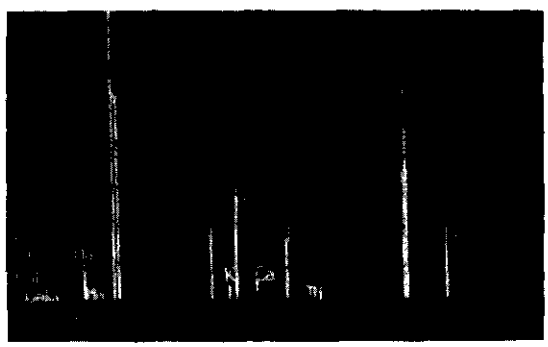

Figure.2b.

Table 1. shows the typical major element results for the quantitative analysis carried using the EDAX.

Element	%Element	Error ±	Oxide	%Oxide	Formula
Na	3.19	0.14	Na_2O	4.30	0.29
Mg	7.58	0.11	MgO	12.56	0.66
Al	2.11	0.08	Al_2O	4.00	0.17
Si	28.70	0.12	SiO_2	61.40	2.16
K	0.88	0.05	K_2O	1.05	0.05
Ca	1.66	0.06	CaO	2.33	0.09
Fe	10.47	0.22	FeO	13.82	0.41
Ba	1.37	0.19	BaO	1.53	0.02
Ti	0.29	0.09	TiO_2	0.49	0.01
O*	45.34	n.m		n.m	6.00
Total	101.59			101.48	

*Oxygen is not detected, and is thus calculated by difference

DISCUSSION

The impact craters in the HST solar array are a usual product of space exposure; what remains to be understood is the relative proportions formed by natural particles (micrometeoroids) and artificial materials such as paint fragments, rocket propellants etc. (space debris). Since all impacts have occurred at relatively high velocities, very little or none of the original impacting material survives, making identification difficult. The situation is complicated further by the fact that the host material (solar cells or buffer assembly) contain a number of elements also found in micrometeoroids and space debris. This problem has been highlighted by recent work (Bernhard et al, 1993a,b) on impacts recorded by the Long Duration Exposure Facility. It is from these observations that criteria have been established to distinguish between space debris and micrometeoroids (Zolensky et al, 1993). Chemical analysis of the possible residue (figure 2.b) shows a clear contrast to that obtained from the silicon solar cell (figure 2.a) Although the apparently high titanium (Ti) signal would seem to indicate a space debris origin for the impact residue. The Ti peak obtained in (figure 2.b) could be identified as a barium (Ba) signal, Ti and Ba are notorious for showing the effects of peak overlaps during EDAX qualitative analysis (Vaughan, 1983). In this example the K-lines of Ti overlap the L-lines of Ba. The suggestion that the Ti peak is a Ba peak is confirmed by the presence of a multiple peak pattern in the spectra after the peak labelled as Ti and the data obtained from the quantitative analysis for both Ti and Ba. Thus this signal is identifying the Ba which is present within the top layer of the cell. The major element chemistry particularly the identification of Fe suggest that the impact residue was of natural origin. The quantitative analysis in Table1 indicates that the mineral formula might correspond to that of a mafic silicate, e.g. a pyroxene ($(Mg,Fe)_2Si_2O_6$), with additional material from the substrate implying that the impacting particle in this sample was of natural origin.

In order to ascertain unambiguously the origin of the residue, it maybe necessary to make isotopic measurements. A key element to study here would be oxygen. Unfortunately in-situ techniques (e.g. ion microprobe) may not give results of sufficiently high precision, furthermore, removal of the residue for laser probe fluorination is practically impossible. It might be possible to measure rare earth elements (REE) in the residue by ion microprobe, a project we intend to investigate using the P7 / concept probe (Long et al, 1988).

Although partially-penetrated impacts are are a predominant in the solar cells studied (52% of the original O.U/N.H.M sample set where classified as such) (Wright et al, 1995), the feature described here is relatively rare (unique amongst the 6 impacts). The essential property of this feature is that the impact removed the upper layers of the solar cell leaving behind in the inner crater a flat area of underlying material, creating a trapping medium upon which the residue was deposited. If similar features could be identified, perhaps by a computerised optical survey, then there should be a good chance of determining the origin of the impacting particles in each case. This would then answer the original question of ascertaining the relative proportions of impacts from micrometeoroids and space debris.

ACKNOWLEDGEMENTS

This work was carried out as part of a PPARC/CASE research studentship awarded to G.A.Graham. Mrs Naomi Williams and Mr John Spratt are thanked for assistance and guidance with the SEM work.

REFERENCES

Bernhard,R.P., Durin,C. and Zolensky,M.E., Scanning electron microscope/energy dispersive x-ray analysis of impact residues in LDEF tray clamps, *LDEF-69 Months in Space 2nd Post Retrieval Symposium*, NASA CP 3194 Part 2, 541-550 (1993a).

Bernhard,R.P., See,T.H. and Hörz,F., Projectile compositions and modal frequencies on the "chemistry of micrometeorites" LDEF experiment, *LDEF-69 Months in Space 2nd Post Retrieval Symposium*, NASA CP 3194 Part 2, 551-574 (1993b).

Berthoud,L., Micro-impacts on HST Solar-array-1 surfaces, *Proc. HST Solar Array Workshop*, ESA-WPP-77, 477-492 (1995).

Eaton,D., The Hubble Space Telescope First Service Mission, *ESA Bulletin*, 76, 73-79 (1993).

Flam,F., Repairs rekindle 3-year-old dream, *Science*, 262, 1810 (1993).

Long, J.V.P. and Gravestock, D.C., An Ion Microprobe system for geological and other applications, In *Secondary Ion Mass Spectrometry SIMS VI* (eds Benningham,A., Huber,A.M. & Werner,H.W.), Wiley, 161-164 (1988).

Vaughan,D. (ed), *Energy-Dispersive X-ray micro-analysis - An Introduction*, Kevex Corporation, 52pp (1983).

Wright, I.P., Sexton,A. and Grady,M.M., Impacts into HST solar array panels: optical characterisation of impact damage and chemical analysis of residues, *Final Report ESA/ESTEC Contract No WMA/94-335/GD/HST*, 26pp (1995).

Zolensky,M.E., Zook,H.A., Hörz,F., Atkinson,D.R., Coombs, C.R., et al, Interim report of the meteoroid and debris special investigation group, *LDEF-69 Months in Space 2nd Post Retrieval Symposium*, NASA CP 3194 Part 2, 277-302 (1993).

THE RAPID IDENTIFICATION OF IMPACT RESIDUES IN THE SOLAR ARRAY PANELS OF THE HST BY DIGITISED BACK-SCATTERED ELECTRON & X-RAY ELEMENTAL IMAGING

G.A.Graham[1,3], A.T.Kearsley[2], M.M.Grady[3] & I.P.Wright[1]

[1]Planetary Sciences Research Institute, The Open University, Milton Keynes MK7 6AA, U.K.
[2]Geology, Oxford Brookes University, Headington, Oxford OX3 7AB, U.K.
[3]Department Of Mineralogy, The Natural History Museum, London SW7 5BD, U.K.
Correspondence author's e-mail address: g.a.graham@open.ac.uk

ABSTRACT

Spacecraft in low Earth Orbit are prone to hypervelocity impact damage from micrometeoroids and space debris. Preliminary optical surveys using a petrographic microscope and then a detailed scanning electron microscopy study using digitised back-scattered electron imaging and X-ray emission elemental mapping has lead to a simple and rapid identification method for impact residues. The methodology was developed using nine solar cell samples removed from the returned V-2 Solar Array Panel of the Hubble Space Telescope after 3.62 years of space exposure. The results suggest that maybe the majority of small impact craters (<100μm in diameter) are a consequence of micrometeoroids rather than space debris although a large data set would be required to substantiate this.

1.INTRODUCTION

Spacecraft which are in Low Earth Orbit (LEO) are particularly susceptible to impact damage from particles less than 1 mm in diameter travelling at speeds between 5-70 km/s (Ref.1). This hypervelocity material can be defined as either natural micrometeoroids (impact residues containing Mg, Fe, Ni, S etc.) or space debris, such as paint fragments or rocket propellant (impact residues containing Ti, Al etc.). Impact damage and ultimately the residue chemistry, can only be studied when LEO materials are returned to Earth and investigated as part of post-flight investigation. The scientific benefit of such studies was highlighted by the Long Duration Exposure Facility (LDEF) launched by NASA to study the effects of long term space exposure (LDEF was in a LEO for 5.7 years) (Ref.2). The Post-Flight investigation of LDEF included the effects of impact damage on all types of surfaces, including solar cells (Ref.2). The impact investigation primarily employed optical microscopy for sample surveys and crater measurements and then more advanced electron microscopy techniques (Ref.3), such as Field Emission Scanning Electron Microscopy (FESEM) (Ref.4). These techniques enabled the distinction between micrometeoroids and space debris and in some case more detailed classifications of the original impactor (Ref.3). LDEF findings also highlighted the fact that surfaces which were previously thought only to be susceptible to micrometeoroid impacts were also subject to collision with space debris as well (Ref.2). This increase could be directly attributable to the increase in the utilisation of LEO for communication satellites, etc (Ref.5).

The techniques and knowledge gained from LDEF and more recently post-flight studies of the ESA European Retrievable Carrier (EURECA) were used in an initial investigation of one of the retrieved solar array panels from the Hubble Space Telescope (HST) (Ref.7). Prior to retrieval, the array had been in a LEO (600km) for 1320 days (Ref.1). For the impact analysis, the array was cut up into individual solar cell samples and sent to several European institutes (Ref.7) The initial impact residue analyses of the solar cells suggested that the identification of extraneous impact material would be complicated by the complex nature of the solar cells (Ref.8). The collector cells are made of a top, protective layer (150μm thick) of CMX borosilicate glass, bonded by a layer of silicone resin (70μm thick) to the underlying silicon solar cell (250μm thick). This composite structure is supported by a fibre-glass backing tape, again held in place by resin (Fig.1) (Ref.9). The main chemical constituents of the cell are Si and Ca, elements which have in the past also been used as indicators of micrometeoroid residues, but which clearly cannot easily be reliably used to recognise impact residues in this context.

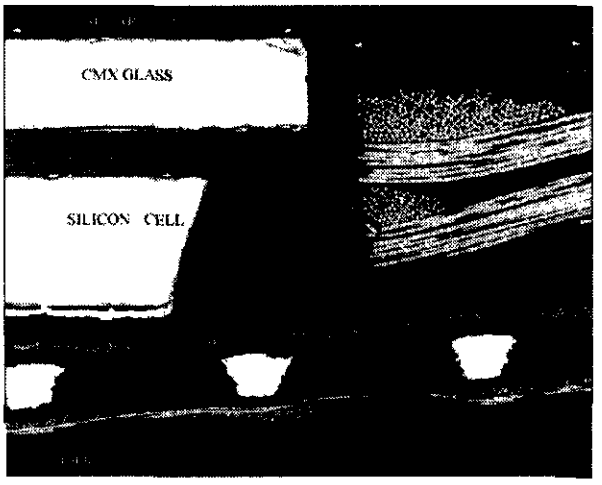

Figure 1. A cross-section through a typical solar cell and supporting resin stiffener.

Analysis was further complicated by the dilution of other potentially more reliable elemental "fingerprints" due to mixing during impact with the target cell

composition. This analytical difficulty had previously resulted in several of the intial investigations yielding inconclusive evidence of natural impactors (i.e. micrometeoroids, Ref.8). Nevertheless, a number of small (1-5mm) craters were attributed to micrometeoroids (Ref.10). Space debris residues proved somewhat easier to recognise due to their distinctive chemical signature (e.g. substantially higher Ti and Al than in the cell). The majority of impacts were thus attributed to space debris although a substantial number were unclassified. This was also in part due to time constraints of the post-flight investigation (Refs.8, 10)

Here we report on the further development of the techniques applied in previous studies (Refs.7, 10) and upon their improved utilisation in location and identification of impact residues. Recent work (Ref.11) has confirmed the tentative suggestion of the post-flight investigation that the best preservation of extraneous material should occur in samples where only the top layers of the cell have been penetrated and the uderlying layers have acted as a trapping medium. This observation has led to the selection criterion for the samples examined in the present study. Suitable craters are generally less than 100μm in diameter, smaller than many considered in earlier studies (e.g. diameters up to 1mm in Refs. 7, 8 & 10). Thus there is a samples bias towards small impactors and / or low impact velocities.

2. ANALYTICAL PROCEDURES

The nine solar cells used in this study were removed from the upper blanket of the Solar Panel Assembly (SPA), section B of the V-2 array. The sample numbers of the cells are: S162, 163, 164, 169, 170, 175, 177, 275 and 276. Note that 275 and 276 were cut after the solar array had been removed from the clean room at ESTEC (Noordwijk) and therefore might be expected to show any effects of terrestrial contamination.

The samples were initially examined using a Zeiss-Axioplan Universal optical microscope. The optical survey was carried out at x10, x20, x40 magnification and was used to locate impact features. The samples were then carbon coated to prevent electrical charging during investigation by a JEOL JSM 840 SEM fitted with an Oxford Instruments e-XL X-ray Energy dispersive spectrometer (at Oxford Brookes University). The analytical work was carried out at an accelerating voltage of 20kV with a beam current of 2nA and a working distance of 32mm. The initial analysis involved the use of digitised back-scattered imaging (BEI) of the impact crater at a low magnification (<x250) but at a high pixel resolution (512 x 512 point matrix with repeated Kalman frame averaging to increase signal to noise ratio). The impact pit was then examined at high magnification (<x750) using BEI, but this often did not clearly show the presence of residue. X-ray emission mapping was therefore employed for 20 characteristic X-ray energy intervals (Fig.2).

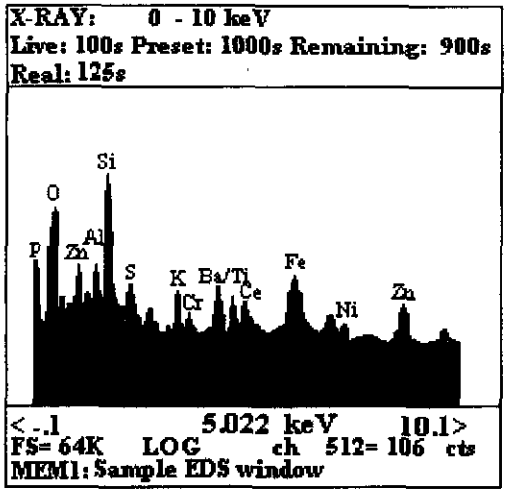

Figure 2. An example of the ED spectral windows used for X-ray mapping.

Areas of interest were located at low magnification and low resolution (128^2 pixels), then mapped at higher magnification and resolution and with repeated frame averaging to yield high contrast. The initial BEI and mapping investigations identified residues on a low detailed scheme (Ref.6) within 3 hours of analyse time. Selected spot micro-analyses of the located residue were then acquired and, after distinction of cell melt components by comparison with known cell composition, a classification based on elemental association in the impact was performed. The results are broadly comparable with the types of particle signature utilised in classification of LDEF impactors (Refs.3, 6), but we suggest that a more careful scrutiny of the elemental association and ratios may lead to a more specific evaluation of particle origins, whether natural or artificial.

3. RESULTS

The nine samples studied all contained small impact craters (diameter <100μm). A total of eleven impact craters was analysed (table. 1)

Sample No.	Findings	Conclusion
162	Mg, Fe, S	Micrometeoroid
163	Spalled melt	Unknown
164	Fe, S, Ni, Mg	Micrometeoroid
164	Fe, S	Micrometeoroid
169	-	Unclassified
170	Fe, S	Micrometeoroid
Stiffener (170)	Fe,Ni,Cr,Ti,Mn	Space Debris
175	Fe, Ni, S, Mg	Micrometeoroid
177	Fe, Ni, Mn	Micrometeoroid
275	Na, Cl, C,N, O	Space Debris
276	Fe, S	Micrometeoroid

Table 1. Summary of impact residue results

Cells 164 and 170 both contained two impact craters, both of which were analysed, although it is not possible to attain whether these craters are associated with one or different impact events on the same cell. Although only the major impact features were studied, all of the samples contained evidence of multiple impact deformation to varying degrees (e.g. from shallow surface cracks on the CMX glass to 10μm or larger impact crater).

4. DISCUSSION

4.1 Methodology

The preliminary optical survey made it possible to select the most promising samples likely to contain residue material, for additional study by electron microscopy. At higher magnification (>x20) it was possible to locate debris and melt material within the crater pit, although it was not possible (using the optical microscope) to infer an origin for such material. It nevertheless suggested that the sample would be worth a detailed investigation. The material located by optical microscopy often appeared as black, metallic, fibrous particles above the underlying substrate of the solar cell. The repeated discovery of such material strongly suggests that partially penetrated cells offer the best preservation of impacting material (as suggested by previous work, Refs.10, 11).

When a solar panel experiences an impact event the cell itself undergoes extensive damage which often results in the partial detachment (i.e. spall zone) of the CMX glass and localised fusion of the underlying layers. The crater pits often exhibit melt features of both the cell and the impactor. This means that the preserved debris is often of complex chemical composition, e.g. the residue can consist of at least four components: impactor fragments and melt, impactor and cell melt (this can be composed of several different cell substrates), and cell fragments and melt.

The digitised BE images (BEI) show the compositional constrast between pixels and may define the chemical changes within the different layers of the cell and more importantly the compositional differences between the cell and any extraneous matter. Most impact residues under BEI have a distinctive, ropy vesicular appearance when compared to the surrounding host area (Fig.3). In some case these melts demonstrate possible volatile retention during rapid cooling. This is indicated by the structures in Fig.3: within the residue there are small areas (dark in the BEI) which could be gas bubbles.

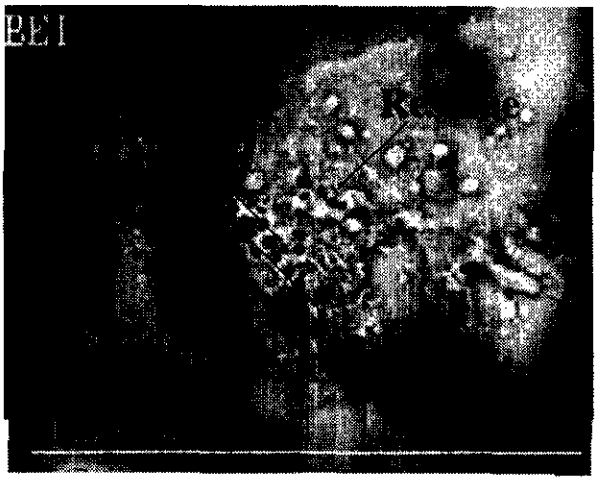

Figure 3 A BEI of a vesicular residue within a melt.

In previous studies (Refs.8 & 10) impact features were investigated using secondary electron imaging (SEI), which produced highly detailed images of the impact crater. These were not always useful when attempting to locate residues, since SEI is primarily a topographic imaging method and in a number of cases the impactor and the cell have fused, resulting in a complex melt where the residue of the impactor maybe embedded within the layers of the cell leaving little or no surface trace. BEI can locate compositional differences between a impactor residue and the cell melt to a depth of about 1μm below the surface of the crater pit (Fig.4).

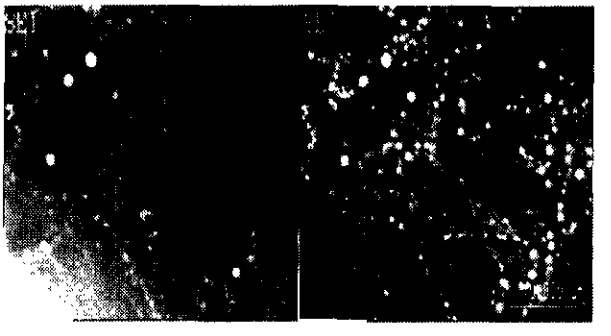

Figure 4. Comparison between SEI and BEI.

Previous work on the HST solar cells (Ref.10) had used BEI, but found it not to be particularly useful. It may be this was due to the samples being gold coated (instead of carbon). Although such a coat can be used for SEI work, it reduces the clarity of BEI and means that embedded features such as those in (Fig.4) would probably not be identified (Ref.12).

After the BEI has located the area containing the residue, the digitised X-ray maps distinguish between the elemental variations that occur within the melt and thus distinguish between the cell components and the impactor residue. It is possible from the maps to infer the origin of the impactor. For example Fig. 5, the maps identify four different compositions within the residue: a Mg-silicate, Fe-Ni sulfide, Fe-sulfide and

possibly Fe-Ni metal. Thus the impactor was probably a polymineralic micrometeoroid and is similar to the types of chondritic residues identified in LDEF (Refs.2, 3).

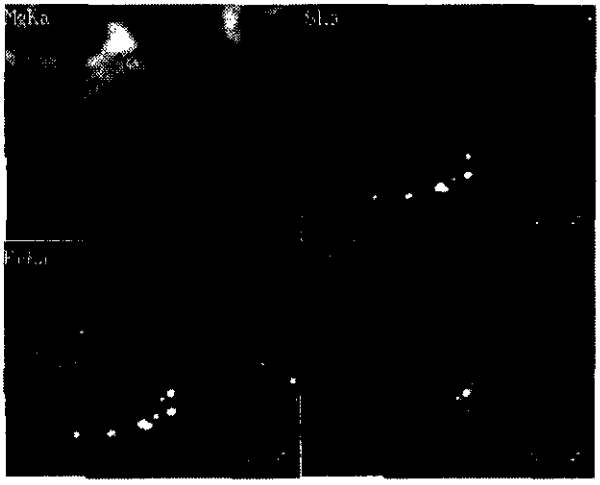

Figure 5. X-ray maps identifying the different elemental components within the residue.

The X-ray maps can also be used to identify embedded features, the benefit they have over BEI is that they can show elemental variations up to a depth of about 5 μm beneath the melt surface.

Again the reason why the X-ray mapping appears to be so successful in the identification of residues compared to previous work (Ref.10) may also be due to sample coating (i.e., carbon versus gold). A gold coat on a sample will greatly affect the maps, because not only does it prevent beam penetration, but it will also mask several important elements used for residue identification purposes (e.g. S, P and possibly Ni) (Ref.12).

The combination of BEI and X-ray mapping have proved highly successful in the location and identification of residues within the solar cells studied. The small number of samples specially selected as being the most likely to contain residues does create a sample bias. To prove that the techniques can be used on other types of cratering, a sample which had been completely penetrated was selected. This impact crater was probably one of the most difficult to study because it was in the stiffener substrate and not the solar cell itself (Fig.1). The stiffener is composed of several silicone and sulfone resin layers and a woven glass fibres.The glass fibres complicate imaging of the crater because they do not allow a high quality carbon coating, resulting in charging during SEM analysis, which meant that it was almost impossible to obtain an SEI of the crater and very difficult for BEI. The digitised BEI did allow the affect of the charging to be reduced and a high resolution image was produced (Fig.6a). This image showed bright particles on both the crater lip and on the glass fibres within the crater. The image also confirmed that the impactor had completely penetrated the cell, reflected by extensive damage to the glass fibres. A higher magnification image of individual fibres indicated that residue had been fused on to them (Fig.6b). X-ray maps of the crater, and the individual fibres within, showed the different compositions of the stiffener layers and areas slightly enriched in Fe, Ni and Cr (Fig.6c & 6d). The elemental composition (especially the high Cr) would suggest an impactor of artificial origin, i.e a metal alloy such as stainless steel. The size of the impact residues on the individual fibres (<1 μm) meant that even semi-quantitative analyses could not be carried out. The location and subsequent identification of a residue in such a complex substrate proved that the techniques employed in this study can be used on various types of substrate from the 'simple composition' of the solar cells to a composite glass-fibre stiffener.

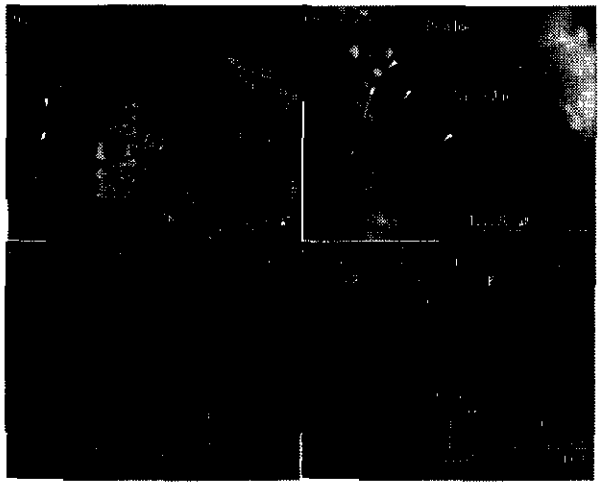

Figure 6a. The BEI of the impact into cell stiffener, 6b. The BEI of an individual glass fibre, 6c & 6d. EDS of the bright particles and residue identified in the crater

4.2 Micrometeoroid Impactors

Seven of the eleven impact craters studied contained natural micrometeoroid residues (Table.1). These were classified as: Fe-Ni sulfides or mafic silicates (e.g., olivines and pyroxenes). The mafic silicates which represent chondritic impactors are typical of those detected on LDEF [Refs.2-4]. The Fe-Ni metal residue, on the other hand may represent a micrometeoroid class not frequently identified in the collections of cosmic dust [Ref.13].

The fact that the majority of the impacts appear to be a consequence of micrometeoroids rather than space debris is interesting and worthy of further comment. Firstly, the HST solar arrays prior to removal were in a sun facing orbit 60% of the time (Ref.8) and may not, therefore present an unbaised random sample of impactors. Secondly, the low incidence of space debris could be associated with the orbital altitude of the HST (≈600 km). Compared to both EURECA (500km) and LDEF (320-450 km) the HST was in a higher orbit,

although the results for LDEF (Ref.3) are similar to the findings here.

The mafic silicates included the probable identification of an Mg-olivine, which LDEF studies [Ref.3] failed to observe. The frequent discovery of sulfides in residues highlights the fact that our technique is able to characterise residues which contain volatile elements which were thought to vaporise during the violent impact process. The reason why such volatile elements are not lost could be related to the type of impacts, i.e. because they have not completely penetrated the cell, there is an efficient trapping mechanism. Some volatiles including gases may also be retained in the melt glass because of rapid cooling.

Although it is possible to identify the natural micrometeoroids as extraterrestrial, it is not easy to classify them in terms of meteorite class using the present schemes [Refs.3, 6]. These previous schemes have classified residues as "chondritic", but the use of the term is ambiguous. Herein a number of Fe-Ni sulfides has been detected, which could be residues from chondritic particles. Alternatively, however, they may also arise from meteorites analogous to irons or stony-irons. It is therefore preferable to specify likely mineralogy rather than attempt detailed classification to meteorite type.

4.3 Space Debris Impactors

Only two of the impact residues studied (Table.1) were identified as space debris. These were classified as S-bearing organic matter and salt and a residue of Fe with accessory Ni and Cr. The presence of Cr implies that the impactor was some type of stainless steel (which has numerous space applications). Solar cell 162 contained impact crater caused by a natural impactor also contained a Ti-rich particle in a matrix rich in C, N and O, suggestive of a paint fragment and associated bonding polymer. This fragment was fused to the rim of the crater (Fig.7).

Figure.7 BEI of Ti-rich particle fused to crater lip.

This implies that it is possible for cells to collect low velocity "additions" which may or may not be the cause of the crater formation. This finding shows a complication to post-flight investigations, it is quite possible to wrongly identify which impactor generated the crater!

4.4 Further Applications

The X-ray maps can rapidly identify minor elemental variations across the surface solar cell substrate at low magnification (<x50). This could be used to locate rapidly the number of impact craters present on a sample. The best method of carrying out this type of work is to use a feature which was identified in previous studies (e.g Ref.8), that the solar cells are coated with an ultra-thin MgF_2 layer. When a cell has experienced an impact event this layer is removed, thus by mapping for either Mg or F, it is possible to locate area with low concentrations in these elements and thus locate craters (Fig.8).

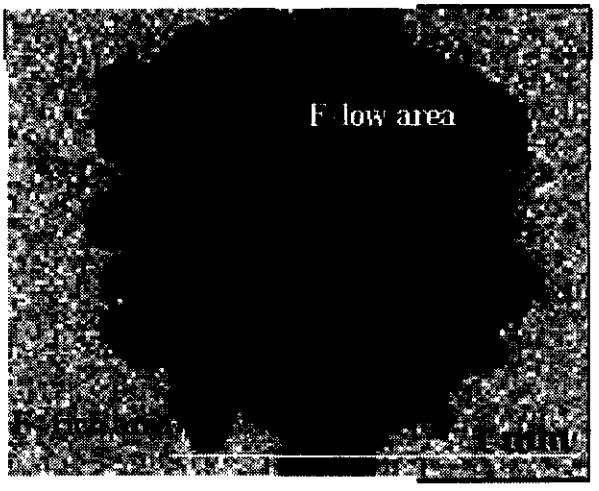

Figure.8 Elemental map for F over crater area.

The characteristic X-ray map showing the loss of an F-rich surface (Fig.8) where a impact has occurred, also clearly defines the extent of damage. Thus these maps could be used for the crater measurements carried out as apart of a post-flight investigation (Ref.7).

5. CONCLUSIONS

There is no simple technique which enables comprehensive identification of residues in very small impact craters on space hardware. However the combination of BEI and X-ray mapping appears to offer a systematic method by which residues can be located, identified and where possible classified by micro-spot analyses. These techniques could be employed in identifying new features when future samples (e.g. from EURECA II, or spacestation materials) are returned to Earth, as apart of the Post-Flight Investigations.

The results of this study indicate that 11 non-penetrating impacts (i.e. craters <100μm in diameter) in HST solar cells are a consequence of natural micrometeoroids and not space debris. Although a larger data set is required to substantiate whether this is a general feature on all impacted space hardware, it does supports the findings of LDEF [Ref.3] and previous HST impact residue studies [Ref.10].

ACKNOWLEDGMENTS

This study was carried out as part of a PPARC/CASE grant to G.A.Graham jointly within the Earth History, Materials and Processes theme of the Natural History Museum and the PSRI at the O.U. Dr G.Drolshagen (ESTEC/ESA) is thanked for supplying the nine HST solar cells samples used in the study. Dr P.Bland (O.U) is thanked for his assistance with the optical survey of the samples. Jon Wells (Oxford Brookes University) is thanked for the rapid production of the solar cell polished section used in this study.

REFERENCES

1. Herbert, M.K., Hubble Space Telescope Solar Array #1 Impact damage - The First Post Flight Survey, *Proc. Hubble Space Telescope Solar Array Workshop*, ESA WPP-77, 301-308, 1995.

2. Zolensky, M.E., et al., Meteoroid Investigations Using The Long Duration Exposure Facility, In *Analysis Of Interplanetary Dust Particles* (eds M.E. Zolensky, T.L. Wilson, F.J.M. Rietmeijer and G.Flynn), AIP Conf. Proc 310, AIP Press, 291-304, 1994.

3. Bernhard, R.P., Durin, C. & Zolensky, M.E., Scanning Electron Microscope/Energy Dispersive X-Ray Analysis Of Impact Residue In LDEF Tray Clamps, *LDEF 2nd Post-Retrieval Symp.*, 551-573, 1993.

4. Borg, J., Bunch, T.E.,Brozolo, F.R. & Mandeville, J.C., Further Analysis Of LDEF FRECOPA Micrometeoroid Remnants, *LDEF 2nd Post-Retrieval Symp*, 347-356, 1993.

5. Zolensky, M.E., McKay, D.S., Kaczor, L.A, *J.Geophys. Res.*,vol 94,No D1, 1047-1056,1989.

6. Zolensky, M.E., et al., Interim Report Of Meteoroid and Debris Special Investigation Group, *LDEF 2nd Post-Retrieval Symp*, 277-302, 1993.

7. Drolshagen, G., HST Meteoroid And Debris Impact Analysis: Overview, *Proc. Hubble Space Telescope Solar Array Workshop*, ESA WPP-77,295-300, 1995.

8. Wright, I.P., Sexton, A., & Grady, M.M., Impacts In The HST Solar Array Panels: Optical Characteristion Of Impact Damage And Chemical Analyses Of Residues, *Final Report ESA/ESTEC Contract No WMA/94-335/GD/HST*, 1-26, 1995.

9. Berthoud, L., & Paul, K., Micro-Impacts On HST Solar - Array - 1 Surfaces, *Proc. Hubble Space Telescope Solar Array Workshop*, ESA WPP-77 , 477-492, 1995

10. Mandeville, J.C., Rival, M., & Durin, Ch., Small Craters And X-ray Analysis On HST Solar Cells: Preliminary Results, *Proc. Hubble Space Telescope Solar Array Workshop*, ESA WPP-77, 513-525, 1995.

11. Graham, G.A., Sexton, A., Grady, M.M., & Wright, I.P., Further Attempts To Constrain The Nature Of Impact Residues In The HST Solar array Panels, *Adv Space Res* (In Press), 1997.

12. Reed, S.J.B., Electron Microprobe Analysis And Scanning Electron Microscopy In Geology, Cambridge Univ Press, 1996.

13. Graham, G.A., Kearsley, A.T., Grady, M.M., & Wright, I.P., An Fe-Ni Melt Residue Deposited in Space: A New Class Of Micrometeoroid, *Lunar Planet. Sci. XXVIII*, (In Press), 1997

Pergamon

Adv. Space Res. Vol. 23, No. 1, pp. 95–100, 1999

Printed in Great Britain
0273-1177/99 $20.00 + 0.00

PII: S0273-1177(98)00235-X

HYPERVELOCITY IMPACTS IN LOW EARTH ORBIT: COSMIC DUST VERSUS SPACE DEBRIS

G. A. Graham [1], A. T. Kearsley [2], M. M. Grady [3], I. P. Wright [1], A. D. Griffiths [4] and J. A. M. McDonnell [4]

[1] *PSRI, The Open University, Milton Keynes MK7 6AA, U.K*
[2] *Geology, Oxford Brookes University, Oxford OX3 0BP, U.K*
[3] *Mineralogy Department, The Natural History Museum, London SW7 5BD, U.K*
[4] *USSA, The University of Kent at Canterbury, Canterbury CT2 7NR, U.K*

ABSTRACT

The understanding of the micron-sized populations of natural micrometeoroids and artificial space debris in low Earth orbit has benefited considerably from the post-flight investigations of retrieved surfaces from spacecraft, such as the Long Duration Exposure Facility. The returned solar array from the Hubble Space Telescope has added to this repository and has offered a further opportunity to document these particles. 25 individual solar cells were specially selected on the basis that they contained impact craters (diameter 100-1000 μm) which had the most potential to retain impactor residue chemistry. The solar cells were subject to a detailed investigation using analytical scanning electron microscopy which identified 29 impact craters, the analysis of which identified 3 residues as artificial in origin, 6 unclassified and 20 as natural in origin. The limited number of unclassified residues identified indicates that the methods of analysis employed in this investigation are a significant step forward for such studies and, if employed on a greater number of samples, will improve the calculations of the time-integrated flux rates for micrometeoroids and space debris in the low Earth orbit environment. Notwithstanding the small sample set examined, the observed chemical classification of the impact residues in terms of micrometeoroid to space debris (in the particle size range 8-80 μm) corresponds well to the flux model that predicts the dominance of natural particles.

NOMENCLATURE

Diameters and crater Classes as defined by Herbert and McDonnell (1997)
D_{CO} = conchoidal cracking diameter (μm)
D_P = Particle diameter (μm)

INTRODUCTION

The characterisation of low Earth orbit (LEO) micron-particle populations has benefited extensively from the post-flight investigations of retrieved surfaces from spacecraft, i.e. the Long Duration Exposure Facility (LDEF) (e.g. Zolensky *et al.*, 1994) and the European Retrievable Carrier (EuReCa) (e.g. McDonnell *et al.*, 1995). The micron-particle populations can essentially be sub-divided into two categories: 1) natural micrometeoroids (particles originating from comets, asteroids and possibly secondary ejecta from planetary impacts) (Brownlee, 1994), and 2) artificial space debris (fragments generated from spacecraft collisions, by-products of normal spacecraft operations etc). The returned solar array from the Hubble Space Telescope (HST) has offered a further opportunity to document the abundance of these particles, as prior to its retrieval the array was in LEO for 3.62 years at an orbital altitude of 600km, in essentially a sun-facing direction. The array was subject to a detailed post-flight investigation led by ESA, with micrometeoroid and debris studies focused upon the hypervelocity

impact damage which the array had sustained (Drolshagen, 1995). These studies investigated the crater morphology generated by particles impacting onto individual solar cells (McDonnell *et al.*, 1995), and residue chemistry from the impactor if retained (e.g. Wright *et al.*, 1995). The chemical investigations proved variable in success, it was often not possible to identify residue in the large craters (crater diameter >1 mm). Residue in the smaller craters (crater diameter <1 mm) was too small to identify, a complex mixture of the cell and impactor, or had been removed by the impact event (Rival *et al.*, 1997).

Recent work (Graham *et al.*, 1997a) has shown that the smaller craters (crater diameter 100-1000 μm) offer the best potential for the retention of residue, as they tend to penetrate only the top layers of the cell. Chemical analysis of residues has been enhanced by the development of a rapid technique using scanning electron microscopy (Graham *et al.*, 1997b). Herein we report on the analysis of 25 solar cells containing a total of 29 impact craters of morphological Classes I – II, as defined by Herbert and McDonnell (1997).

EXPERIMENTAL PROTOCOL

Solar Cells

The ability to identify and classify extraneous material is dependent upon a clear understanding of the composition of host material, as the impact melt is often a complex mixture of both the impactor and the cell. HST cells are composed of a top protective layer (150 μm thick) of CMX borosilicate glass, coated with a MgF_2 layer. A layer of silicone resin (70 μm thick) bonds the CMX to the underlying silicon solar cell (250 μm thick), beneath which is a silver connector strip. This composite structure is supported by backing-tape containing glass-fibre reinforcement, Figure 1.

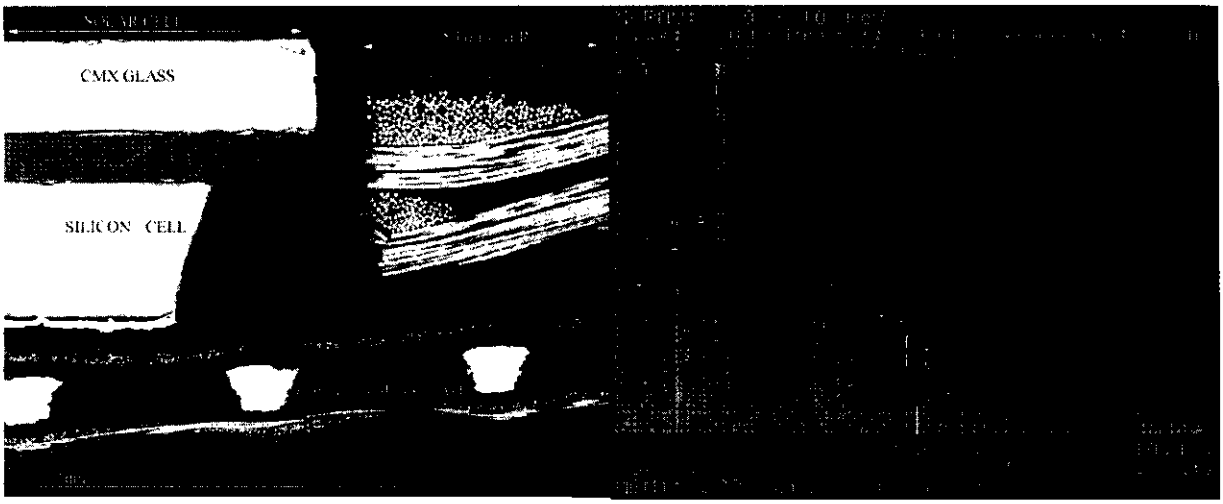

Fig. 1. BEI of a section through a solar cell with supporting stiffener, and EDS spectrum of the CMX glass layer.

Scanning Techniques

The 29 impact features were selected after optical analysis using a Leitz Wild M8 microscope with Sony DKC 5000 digital photo camera. Individual solar cells were then carbon-coated and examined using a JEOL JSM-840 scanning electron microscope (SEM) and Oxford Instruments eXL energy-dispersive X-ray spectrometer (EDS). Our eXL has a light element detector that can detect C, N, O, and F and can, for example, distinguish metals from their oxides. Analytical work was carried out at an accelerating voltage of 20 kV, a beam current of 2 nA and working-distance of 32 mm. Digitised back-scattered electron imaging (BEI) and X-ray elemental mapping employed the protocols described in Graham *et al.* (1997b).

Classification

Our classification of impact-derived residues, in terms of micrometeoroid or space debris, was based on the schemes used during the post-flight analyses of LDEF experiments (Bernhard *et al.*, 1993a). Identification of extraneous material is complicated by "mixing" between the melted host and the impactor, thus the derived melt may show only minor increases in certain elemental abundance above the original composition of the host. Notwithstanding such difficulties, it has proved possible to classify residues successfully.

Space Debris. The presence of Ti and Al within the solar cell complicates the identification of some residues. Ti-rich residue associated with both Al and O may have an origin in the host cell, rather than from an extraneous impactor. EDS spectra and X-ray elemental maps that contain the following elemental signatures may be used as indicators of an artificial origin:

- Mainly Ti + possible minor C,N,O (paint fragments)
- *Mainly Fe + Cr (in variable concentrations), Mn + possible trace Ni (specialised steels)*
- Mainly Al + minor Cl, O, Cr (Solid-Rocket Motor ablation products)
- Mainly Sn + Cu (Printed Circuit Board (PCB) components)
- Na, Ca, K, Cl (salt water contamination / human waste).

It is also possible that secondary craters could be generated by fragments of arrays (or other components) of the HST. CMX impacts onto other substrates might be identified by residue enrichment in Mg, Si, Ce, Ca, K, Al, Ti and Zn, but would be very difficult to distinguish upon a solar cell.

Micrometeoroids. The micrometeoroid residues may not retain the stoichiometric chemical signature of their parent mineral and may give analyses that cannot easily be compared to those of mineral standards. Nevertheless EDS spectra and X-ray elemental maps that contain the following signatures may be used as indicators of micrometeoroid origin:

- Mg & Si enrichments + Fe (mafic silicate / phyllosilicates)
- Fe + S (Fe-sulfides)
- Fe + Ni + S (Fe-Ni sulfides)
- *Fe + Ni metal (Ni concentration at meteoritic ratios).*

RESULTS

A total of 29 impact craters were analysed for the presence of residue material.

Table 1. Summary of Impact Residue Analysis

Description	Number	% of Total
Unknown	6	21
Space Debris	3	10
Micrometeoroid	20	69
Total	29	100

Chemical Analysis

Table 1 shows that there was abundant residue in the 29 impact craters analysed. Residues of micrometeoroid origin were identified as Mg-silicates (possibly olivine or pyroxene), Mg-Fe silicates (possibly phyllosilicates); Fe-sulfides; Fe-Ni-sulfides; Fe-Ni metal and calcite fragments associated with Mg-Fe non-silicates (possibly Mg-Fe carbonates). These components were identified as either single or multi- component residues, their detailed chemistry is discussed in Graham *et al.* (1998). The space debris residues were identified as derived from paint

(EDS spectra with Ti, C, N and O); metallic fragments (EDS spectra with Fe, Cr, Mn and trace Ni in sensible ratios for stainless steel) and printed circuit board (PCB) components, Figure 2.

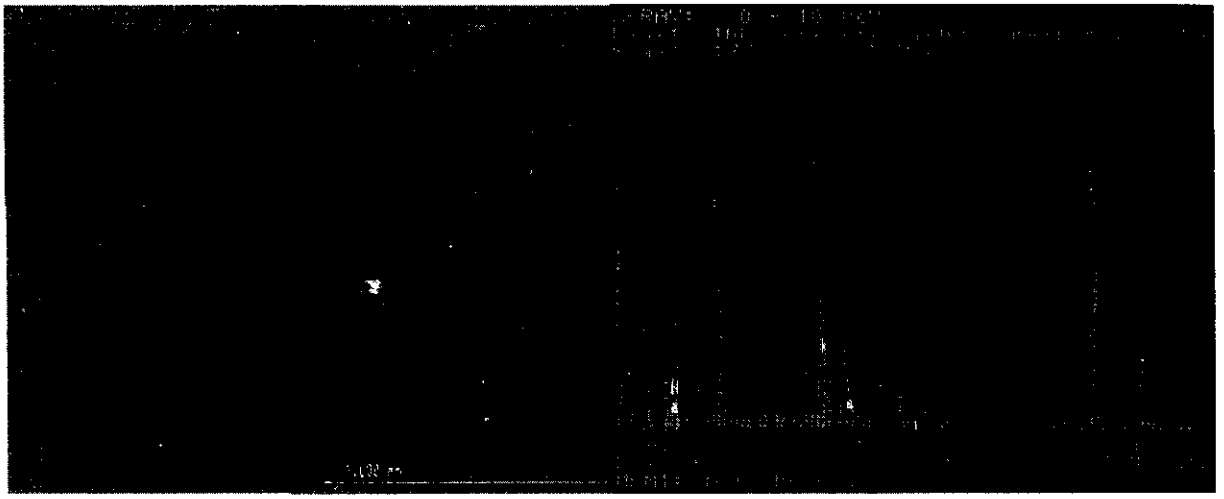

Fig. 2. BEI image of an impact crater with bright particles in the crater pit. EDS spectrum containing Sn and Cu suggesting an artificial origin (possibly PCB fragments).

Crater Analysis

The 29 craters are Class I – II impacts, with D_{CO} = 100 – 1000 μm (Figure 3). Calibration of the D_{CO} measurements indicates that the impacting particle size range was 8- 80 μm diameter.

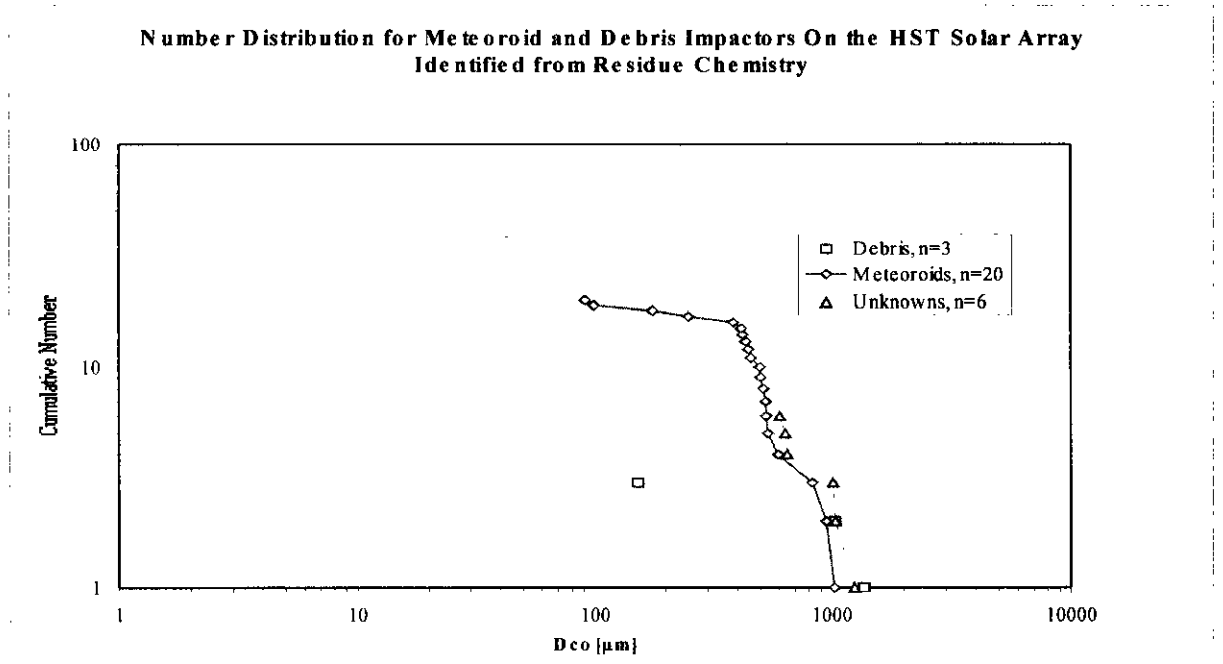

Fig. 3. Number Distribution for Micrometeoroid and Debris Impactors Vs Conchoidal Diameter.

DISCUSSION

The proportion of identified residue is in marked contrast to previous studies of LDEF and HST solar cells, in which up to 75% of the impact craters were 'unclassified'. This increase in identified residues may be due to a number of factors apart from use of digitised BEI and X-ray mapping. The earlier investigations (Wright *et al.*, 1995) used larger Class III-IV impact craters (as defined by Herbert and McDonnell, 1997), with D_{CO} up to 2 mm. Such craters show substantial impact damage to the cell, and there is no trapping mechanism for residue material comparable to that seen in the smaller Class I-II craters of this investigation. Earlier studies (e.g. Rival *et al.*, 1997) also found that the complex cell composition made interpretation of residues extremely difficult, particularly for micrometeoroid residues. The problems of complex cell chemistry have been overcome by detailed analyses of cell cross-sections, enabling recognition of minor variations in the chemistry of the melt, and thus distinction between host and extraneous material.

The reduced number of 'unclassifieds' in comparison to the specific micrometeoroid experiments on LDEF (Bernhard *et al.*, 1993b, Brownlee *et al.*, 1993) may be attributable to a number of factors. Our new methods are now sufficiently sensitive to resolve tiny (sub-micron) residues and to detect the light elements (C, N, O) that enable distinction between the chemistry of the host and the impactor (for example Al–foils of a collector, and Al-oxides from space debris). The exhaustive work of Bernhard *et al.* (1993b) discussed over 600 impact craters on LDEF, substantially more than the 29 impacts discussed herein. Nevertheless our sample, specifically selected to be within the D_{CO} range of 100 – 1000 μm but otherwise unbiased, clearly shows great potential for rapid and thorough interpretation of large numbers of craters. The same technique can be successfully employed on craters of diameters between 2 and 1000 μm on aluminium.

Our data suggest that the Class I-II impact craters on HST are dominated by micrometeoroid-derived residues (69%), possibly from relatively low, oblique impact velocities. Previous studies (Flynn, 1990 and Brownlee *et al.*, 1993) suggest that particles of asteroidal origin might have orbital parameters of this nature. The dominance of natural residues raises the possibility that LEO may harbour a previously under-estimated population of micrometeoroids, although the nature of the HST orbit (all of the array surfaces were exposed to earth- and sun-facing environments) means that it is not possible to confirm this hypothesis. However, re-examination of known orbital-orientation surfaces of LDEF using our techniques might well resolve whether such findings are significant in number on earth-facing surfaces.

ACKNOWLEDGEMENTS

This work was carried out as part of a PPARC/CASE (The Natural History Museum) studentship to G.A.G. J.A.M.M. was supported by ESA contract – ESTEC No. 11887/96/NL/JG.

REFERENCES

Bernhard, R. P., C. Durin, and M. E. Zolensky, Scanning Electron Microscope / Energy Dispersive X-ray Analysis of Impact Residues in LDEF Tray Clamps, *LDEF 69 Months in Space - 2nd Post-Retrieval Symp.*, 541-550 (1993a).

Bernhard, R. P., T. H. See, and F. Hörz, Projectile Compositions and Modal Frequencies on the "Chemistry Of Micrometeorites" LDEF Experiment, *LDEF 69 Months in Space - 2nd Post-Retrieval Symp.*, 551-574 (1993b).

Brownlee, D. E., D. Joswiak, J. P. Bradley and F. Hörz, Interplanetary Meteoroid Debris in LDEF Metal Craters, *LDEF 69 Months in Space - 2nd Post-Retrieval Symp.*, 577-584 (1993).

Brownlee, D. E., The Origin and Role of Dust in the Early Solar System, In *Analysis of Interplanetary Dust Particles* (eds. M. E. Zolensky, T. L. Wilson, F. J. M. Rietmeijer and G. Flynn), AIP Conf. Proc. 310, AIP Press, Woodbury New York, 291-304 (1994).

Drolshagen, G., HST meteoroid and debris impact analysis: Overview, *Proc. Hubble Space Telescope Array Workshop*, ESA WPP-77, 295-300 (1995).

Flynn, G. J., The Near-Earth Enhancement of Asteroidal over Cometary Dust, *Proc 20th Lunar Planet. Sci. Conf.*, 363-371 (1990).

Graham, G. A., A. Sexton, M. M. Grady and I. P. Wright, Further Attempts to Constrain the Nature of the Impact Residues in the HST Solar Array Panels, *Adv. Space Res.*, **20**, 8, 1461-1465 (1997a).

Graham, G. A., A. T. Kearsley, M. M. Grady and I. P. Wright, The Rapid Identification of Impact Residues in Solar Array Panels of the HST by Digitised Back-Scattered Electron and X-ray Elemental Imaging, *Proc.2nd European Conf. on Space Debris*, ESA SP-393, 183-189 (1997b).

Graham, G. A., A. T Kearsley, M. M. Grady, I. P. Wright and J. A. M. McDonnell, The Collection of Micrometeoroid Remnants From Low Earth Orbit, *Adv. Space Res.*, submitted (1998).

Herbert, M. K. and J. A. M McDonnell, Morphological Classification of Impacts on the EURECA & Hubble Space Telescope Solar Arrays, *Proc.2nd European Conf. on Space Debris*, ESA SP-393, 169-176 (1997).

McDonnell, J. A. M., G. Drolshagen, D. J. Gardner, R. Aceti and I. Collier, EURECA's Exposure in the Near Earth Space Environment. Hypervelocity Impact Cratering Distribution at a Time of Space Debris Growth, *Adv. Space Res.*, **16**, 11, (11)73-(11)83 (1995).

Rival, M., J. C. Mandeville and C. Durin, Impact Phenomena on Brittle Materials: Analysis of 1μm to 1mm Impact Features on Solar Arrays, *Adv. Space Res.*, in press (1997).

Wright, I. P., A. Sexton and M. M. Grady, Impacts into HST solar array panels: Optical Characterisation of Impact Damage and Chemical Analysis of Residues, Final Report ESA/ESTEC Contract No. WMA/94 – 335/GD/HST, 26 (1995).

Zolensky, M. E., F. Hörz, T. H. See, R. P. Bernhard., C. Dardano, R. A. Barrett, *et al.*, Meteoroid Investigations Using The Long Duration Exposure Facility, In *Analysis of Interplanetary Dust Particles* (eds. M. E. Zolensky, T. L. Wilson, F. J. M. Rietmeijer and G. Flynn), AIP Conf. Proc. 310, AIP Press, Woodbury New York, 291- 304 (1994).

PERGAMON International Journal of Impact Engineering 23 (1999) 319–330

INTERNATIONAL JOURNAL OF IMPACT ENGINEERING

www.elsevier.com/locate/ijimpeng

NATURAL AND SIMULATED HYPERVELOCITY IMPACTS INTO SOLAR CELLS.

G.A.Graham[*,*], A.T.Kearsley[**], M.M.Grady[***], I.P.Wright[*], M.K.Herbert[****], and J.A.M.McDonnell[****].**

[*]Planetary Sciences Research Institute, The Open University, Walton Hall, Milton Keynes MK7 6AA, U.K., [**]Geology, Oxford Brookes University, Headington, Oxford OX3 7AB, U.K., [***]Mineralogy Department, The Natural History Museum, Cromwell Road, London SW7 5BD, U.K., [****]Unit For Space Sciences and Astrophysics, The University Of Kent at Canterbury, Canterbury CT2 7NR, U.K.

Summary–The solar array which was returned to Earth from the Hubble Space Telescope (HST) in 1993, after 3.62 years of space exposure in low Earth orbit (LEO), has offered the opportunity to document populations of natural micrometeoroids and artificial "space debris". Residues from the hypervelocity impact (HVI) of material deposited in 25 individual solar cells from the array have been investigated herein by scanning electron microscopy. The observations have been compared with the results of simulated HVIs into solar cells using known meteorite mineralogies. This has permitted assessment of the probability of retention for residue materials derived from HVI by well-characterised mineral species. The simulation experiments have thus far suggested that some of the textural features observed in impact residues are dependent on the nature of the individual mineral components within the original impactor. Furthermore it transpires that compounds containing volatile elements, such as Ca (from calcium carbonate), can be preserved as near-intact fragments explosively emplaced in an impact crater. Such unusual particles should not always be dismissed as simply contamination products if observed in LEO-derived HVIs. © 1999 Elsevier Science Ltd. All rights reserved.

INTRODUCTION

The presence of hypervelocity micro-particles in low earth orbit (LEO) has been a long standing concern, due to the impact damage hazard these particles present to space hardware such as satellites, e.g. Drolshagen [1]. The particles can be divided into two populations: natural micrometeoroids, e.g. Laurance and Brownlee [2] and artificial 'space debris', e.g. Bernhard *et al* [3]. The hypervelocity impact (HVI) of particles from either population leaves little evidence of the original impactor, although occasionally near pristine materials are observed, Rietmeijer and Blandford [4]; Hörz *et al.* [5]. As such while it is relatively easy to constrain the physical nature of the impact damage in space hardware, it is usually difficult to assess exactly what caused it. As only traces of material, usually a complex melt derived from residues of the impactor and the target material are identified, e.g. Zolensky *et al.* [6]. Much of the previous work on HVI onto space hardware was focussed upon the returned Solar Maximum Mission spacecraft, e.g. Warren *et al.* [7], and the Long Duration Exposure Facility (LDEF), e.g. McDonnell *et al.* [8]. Much of the investigation centred on impacts into ductile surfaces such as Al-clamps and Au-foils, Rose *et al.* [9]; Hörz *et al.* [10], which generated simple, bowl-shaped crater morphologies, Melosh [11]; Hörz *et al.* [10]. The chemical analysis of residual material from the impactor deposited in the craters was difficult since in most cases the material was vaporised and lost during the impact process, e.g. Brownlee *et al.* [12].

The Hubble Space Telescope (HST) solar array which was returned to Earth in 1993, after 3.62 years of space exposure, has offered an opportunity to document further the LEO environment and gain a better understanding of HVIs upon space-hardware. The surfaces

PII: S0734-743X(99)00083-4

returned from the solar array, unlike many of the previous studies already mentioned, are brittle in nature. Thus, instead of simple crater morphologies, they produce complex radial and conchoidal fractures with extensive spallation zones (Fig.1) during the crater forming process, Rival *et al.* [13]. The previous investigations of impacts into brittle targets have focussed on the crater morphologies, e.g. Mandeville [14] and impact dynamics, e.g. Taylor *et al.* [15]. The possible retention of impactor material has not been assessed extensively, as it has been presumed that, as with LDEF craters, much of the material would be lost. Recent work employing analytical microscopy techniques has been successful in both the location and identification of residue material in the solar cells, Graham *et al.* [16]. A programme of light-gas-gun shots that have produced similar impact features in the laboratory has now extended this work. Although many craters from LEO exposure have proved to contain very distinctive residue 'fingerprints' of the impactor mineralogy, some are not so easy to tie unambiguously to original mineralogy, and some were clearly due to polymineralic grains. The laboratory experiments were thus designed to discover what happens to impactors of well-characterised mineralogy during HVI in terms of chemistry and the amount of material retained. Herein we discuss the observations made on both simulated and LEO micro-particle impacts, and their implications for the ability of solar cells to retain residue material.

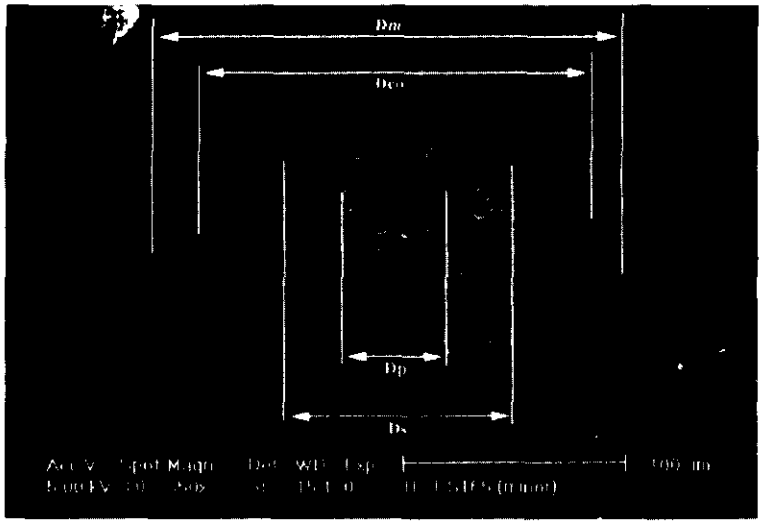

Fig.1 Secondary electron images (SEI) of an impact crater. The crater terminology can be described as the following: D_p = central pit (melt pit), this may contain debris in the form of melt residues; D_s = Shatter zone, this area is highly fragmented; D_{co} = Conchoidal spallation; D_m =Maximum damage detected at an impact site.

SAMPLES AND METHODS

Solar Cells

The samples of flight hardware from LEO used in this study were individual solar cells removed from the upper blanket of the solar array assembly from the HST, which was returned to Earth after the 1993 service mission. Prior to recovery, the array had been exposed to LEO for 3.62 years, at an operational altitude of approximately 600km, Drolshagen [1]. Upon return and de-integration the array was transported to a clean-room facility at ESTEC (the Netherlands), where it underwent post-flight investigation, Drolshagen [1].

The 25 individual solar cells (Fig.2) requested for the residue studies were specially selected on the basis that they contained class I and II impact craters, as defined by Herbert and

McDonnell [17], rather than holes (class V). The analysis of the impact holes had shown that little or no impactor material is retained, whereas class I and II craters appear to offer the potential to retain material as the impact had only penetrated the upper layers of the cell and a melt pit is generated.

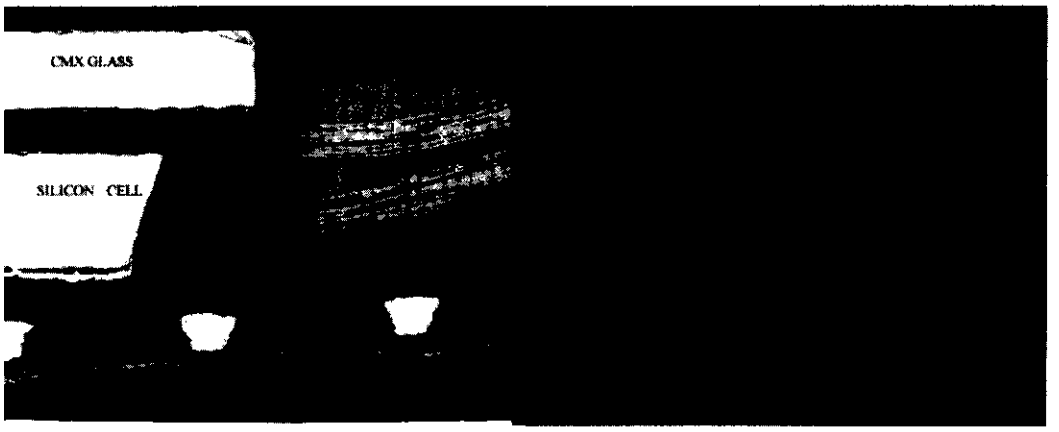

Fig.2 A cross-section of a solar cell and supporting stiffener and EDS spectra of the CMX glass. The solar cells are composed of a top protective layer (150μm thick) of CMX borosilicate glass coated with a Mg + F layer. A layer of silicone resin (70μm thick) on the underlying silicon solar cell (250μm thick) bonds the CMX layer. Below the silicon cell is a silver connector strip running through the cell (approximately 900 nm thick). Under the connector is a second layer of silicon resin (70μm thick). This composite structure is supported by a fibre-glass backing tape (100μm thick).

Scanning Techniques

The analytical protocols are described more fully in Graham *et al.* [16]. The chemical compositions and debris morphology associated with the impact features were determined using a JEOL JSM 840 SEM fitted with an Oxford Instruments e-XL X-ray energy dispersive spectrometer. The analytical work was carried out at an accelerating voltage of 20kV with a beam current of 2nA at a working distance of 32mm. Back-scattered electron images (BEI) and X-ray maps were digitised for analysis and storage. High-resolution imaging of selected craters was carried out on a Philips XL FEG-SEM fitted with a Robinson back-scattered electron detector, using an accelerating voltage of 5kV and a working distance of 15mm. All the samples were given an ultra-thin carbon coat to reduce the effects of charging during analysis.

Simulated Shots Program

Sabot-mounted impactor samples were individually accelerated in a light-gas-gun (LGG) at the University of Kent (U.K.), using the buck-shot technique described in Taylor *et al.* [18]. Grains were impacted on solar cell targets at velocities around 5 km/s (calculated from time-of-flight measurements using piezo-electric transducer sensors).

The first laboratory HVI were designed to demonstrate whether or not it is relatively easy to find and characterise different residues from LGG impacts, as had already been demonstrated for LEO-exposed materials, Graham *et al.* [16]. The first projectiles (up to 400μm in diameter) were composed of soda-lime glass (as an analogue of natural silicates) and stainless steel AISI 420 ball-bearings (as an analogue of space debris). Distinctive, unambiguous residues were found in a number of craters in each case.

Following this success, the programme was extended to a suite of high purity natural minerals (determined to be homogeneous in composition by examination under the SEM). The selected minerals included olivine (Mg-silicate); calcite (Ca-carbonate); pyrrhotite (Fe-sulfide); feldspar

(Ca-aluminosilicate) and pyroxene (Ca- + Mg- silicate). Projectiles of 125-250μm diameter were employed to provide simple, yet realistic, analogues of individual components of natural micrometeoroids. When a range of minerals may be intimately associated at the scale of micrometres, as seems to be the case in interplanetary dust particles (IDPs), e.g. Bradley [19] and probably in micrometeoroids, their impact may produce complex polymineralic residues that are difficult to assign to precise, individual mineral compositions. The use of well-characterised samples in a relatively simple experimental environment was therefore an essential first step to enable positive and unambiguous identification of impactor mineralogy before attempted interpretation of more complex, mixed-mineralogy HVI, such as those observed in polymineralic residues as seen by Graham *et al.* [16].

In particular, these impacts permitted an analysis of the degree to which samples undergo alteration during the impact process at 5 km/s, such as loss of volatile elements or chemical fractionation of the residue between different components such as the melt glasses and vapour. The textural characteristics of the residue were also noted as a further potential indicator of impactor mineralogy and were very similar to those seen on space exposed surfaces where impact velocities may range to 70 km/s, Hörz *et al.* [10].

In practice, LGG HVI residues needed to be interpreted with care, as the apparatus may create a number of contamination problems. It proved common place to identify finely-dispersed particles containing Fe, Al, S and Cu strewn across the surface of the target in every LGG shot. Energy-dispersive spectra (EDS) micro-spot analysis of gun components revealed that these contaminant elements are almost certainly derived from parts of the gun and chamber, including the Fe particle-bearing, Al-Cu alloy 'burst-disk'. The contaminants do not, however, resemble true impact residues in texture or grain size, and it can be easily demonstrated that they are not mixed with the solar cell glass melt. They can, therefore be reliably distinguished from impact residue. Previously the LGG has been used to model crater morphologies and impact processes, e.g. Taylor *et al.* [18], not to investigate chemical variations of residues, and the presence of such contaminants has been relatively unimportant.

OBSERVATIONS

Chemical Analysis

Experience suggests that morphological studies of craters, e.g. McDonnell *et al.* [8], are unlikely to yield sufficient information on the origin of an impactor to allow the broad classification in terms of space debris (SD) versus micrometeoroid (MM). Such a classification can only be achieved through chemical studies. Herein the residues identified in the HST solar cells have been classified as SD or MM using the previous schemes of Graham *et al.* [16] and those which arose during the post-flight studies of LDEF hardware, e.g. Zolensky *et al.* [20]; Bernhard *et al.* [3].

SD material is basically considered to be anything that is not from a natural MM source. SD-derived residues are classified based upon energy dispersive spectra (EDS) of characteristic X-ray emission, showing combinations of elements such as: Ti, C, N and O (possible paint fragments); Fe, Cr, Mn and possibly Ni (in the correct ratio for specialised steels); Sn and Cu (printed circuit board electronics); Al, Cl, O, Cr (possibly solid rocket motor components); C, Na, K, Cl, Ca (urine). The MM-derived residues may not retain the stoichiometric chemical signature of their parent mineral compositions. It is nevertheless possible from EDS spectra to assume that the following indicate MM origins: Mg, Fe, Ca, Si (olivine or pyroxene mafic silicates); Fe, S (Fe-sulfides); Fe, Ni, S (Fe-Ni sulfides); Fe-Ni metal (in the range of kamacite, a metal identified in meteorites); further more complicated elemental chemistries indicative of MM origins are also possible.

The analysis of 29 residues in the 25 solar cells exposed to LEO indicated 3 of the residues

were artificial in origin, 20 were natural in origin and 6 were unclassified (due to spalled melts, where it is assumed the residue was lost during the impact process). The amount of residue material identified in the solar cell craters is in stark contrast to LDEF studies where up to 73% of the impact craters into the Al and Au targets from various experiments on LDEF were unclassified, e.g. Brownlee *et al.* [12]; Zolensky *et al.* [6]. This contrast in residue abundance could be due to a number of reasons: 1) the analytical methods and detectors employed in the LDEF studies were insufficiently sensitive to identify discrete residues within the craters; 2) the impact process into Al and Au surfaces caused much of the material to be lost; 3) sample bias: the number of impact craters investigated was much higher for LDEF than HST (e.g. in the micrometeoroid chemistry experiment of LDEF, the number of impacts in the high-purity Au-targets was 199 and 415 impacts in the high-purity Al-targets, Bernhard *et al.* [21]); (this is substantially more than the 29 impacts observed herein); 4) the impact features identified in craters on LDEF do not represent average conditions, i.e. we might expect different features on different space hardware, Bernhard *et al.* [21].

Notwithstanding the high number of unclassified impacts (48%), for the trailing and leading edge surfaces of LDEF in the dedicated chemistry experiment, Bernhard *et al.* [21], the majority of impacts identified were classified as natural (39%) compared to artificial (13%). In the HST solar cell impacts, the number of unclassifed impacts are considerably lower, 6 out of 29 (21%); the rest are dominated by MM-derived residue (68%) (their detailed classification was discussed in Graham *et al.* [22]). This observation raises the possibility that LEO may harbour a previously under-estimated population of micrometeoroids, Graham *et al.* [23], as well as space debris. Further work is required to substantiate this observation.

Textural Observations Of Residues

The physical appearance of the impact residues identified within the craters (D_{CO} 100-1000μm) were highly variable in both concentration and composition; a similar conclusion was previously made in LDEF studies concentrating on micrometeoroid residues in Al and Au substrates, Brownlee *et al.* [12]. Our data however, especially that from the LGG experiments, suggest that apart from the velocity dependent factors, there may also be a strong link between residue texture and the original mineralogy of the impactor. Although the processes of formation and retention of residues are undoubtedly extremely complex, it is unlikely that the textural variations observed in our LEO HVI are due to differing types of interaction between a single composition of impactor particle and different components of the host substrate. It seems likely that variations in the degree of impactor vaporisation and fragmentation, the viscosity and miscibility of melt components (and therefore the intimacy of their mixing) together create residue textures that may be diagnostic of the impacting mineralogy. This may prove to be important in distinguishing silicates of differing crystal structure and volatile content (e.g. orthosilicates such as olivine, framework silicates such as pyroxene, and hydrous phyllosilicates such as saponite). EDS spectra of embedded particles sometimes clearly revealed Mg+Fe to Si ratios directly comparable to those of specific mafic silicates; however, many residues showed much greater interaction with the host melt and cannot be assigned so simply to mineral groups on chemistry alone. Combined chemical and textural distinction might allow direct comparison of impactors with the recognised classes of interplanetary dust particles (mafic silicates; phyllosilicate and refractory phases, e.g. Bradley [19]). The textural features of the 20 residues identified as MM in origin in the solar cell craters can be defined as: surface glass (2), sub-surface glass (10); surface globules (13) and near-intact particles (2). The impact residues rarely contained only the individual textures, a typical residue would consist of more than one of the different textural variations. To allow comparisons between LDEF observations and those herein, LDEF terminology, Brownlee *et al.* [12] is used where appropriate in the description of the glass residues.

Vesicular Glass Residues. Vesicular melt residues usually have a distinctive 'ropy' appearance in BEI. They appear as networks on the surface of the melt pit, and occasionally as detached strings in the shattered surroundings. In some cases these melts demonstrate a degree of volatile retention during their deposition, in the form of possible gas bubbles, (dark areas in BEI, Fig.3a). The residues are usually enriched significantly in Mg, Ca and Fe above the solar cell composition, an assemblage suggestive of origin from a mafic silicate, such as pyroxene as previously suggested in the preliminary investigation of the solar cells, Graham *et al.* [24]. Vesicular residues were previously identified in LDEF craters on pure Al and Au substrates by Brownlee *et al.* [12], who also suggested that the vesicular nature was a product of the volatile content within the impactor. The HVI residues of soda-lime glass (Ca-bearing silicate), selected as a micrometeoroid analogue, also showed a characteristic ropy texture (Fig.3b) similar in appearance to those which we consider to be a result of impact by natural particles. It is noteworthy that the vesicular texture was enriched in Ca and Na (i.e. high volatile content within the projectile).

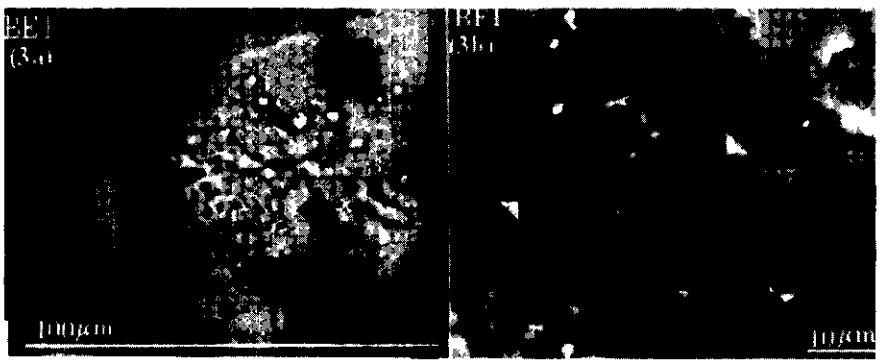

Fig.3a A BEI of a vesicular residue (black arrows highlight the area of interest) observed in LEO-derived impact crater generated by a micrometeoroid. **Fig.3b** A BEI of a vesicular residue (white arrows highlight the area of interest) observed in impact crater generated in the laboratory using soda-lime projectiles.

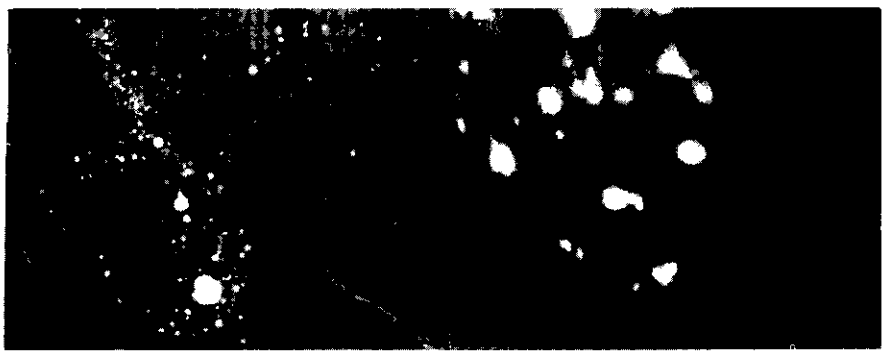

Fig.4a A BEI of an embedded residue observed in a LEO-derived impact crater. The residue is identified by the dark grey patches within the melt glass (the black arrows highlight the patches). The melt also contains bright globules, which are Fe-Ni metal melt droplets. The impact melt has been generated by a polymineralic micrometeoroid impactor. **Fig.4b** Shows the Mg elemental x-ray map for the melt glass. The Mg concentration directly corresponds to the embedded patches in the BEI.

Glass-embedded, concentrated residues. In Fig.4 the Mg- and Si-rich residue from a LEO impactor is an embedded patch within the melt pit. Where the patch derived from thermal melting of the impactor, or a condensate from gas, it might be expected that such residue would show a high degree of elemental mixing with the solar cell substrate. The ED X-ray spectra from

the residue (Fig.5a) were, however, very similar to those from a meteoritic silicate grain (olivine from CM2 Murchison - Fig.5b). This suggests that the patch may be a concentrated Mg+Si glass within the melt glass of the host, with almost no elemental mixing (i.e. immiscibility), or it is a surviving, shocked, solid particle beneath the melt surface. It was not possible to be certain whether the spectra from the residue patch showed the pristine composition of an end-member olivine or whether some degree of elemental fractionation had occurred during the impact process, although the former seems more likely. If the residue is a shocked solid particle it is unlikely that significant elemental fractionation would have occurred.

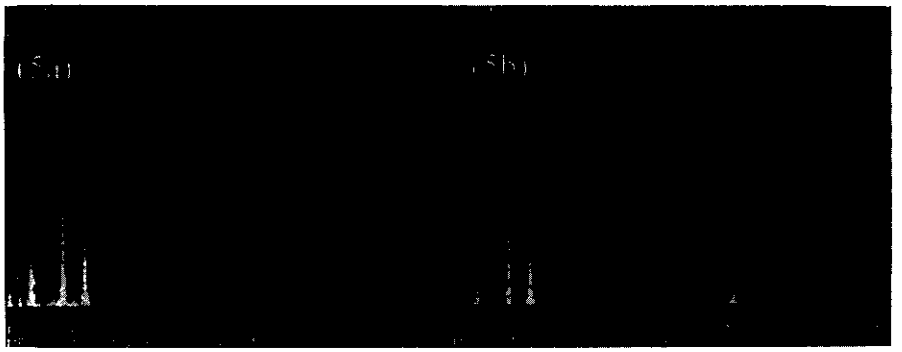

Fig.5a ED spectrum obtained from the analysis of the embedded residue. **Fig.5b** ED spectrum obtained from the analysis of an olivine grain in the Murchison meteorite. Although the ED spectrum for the residue is enriched in Si compared to the olivine from the meteorite the general pattern is comparable.

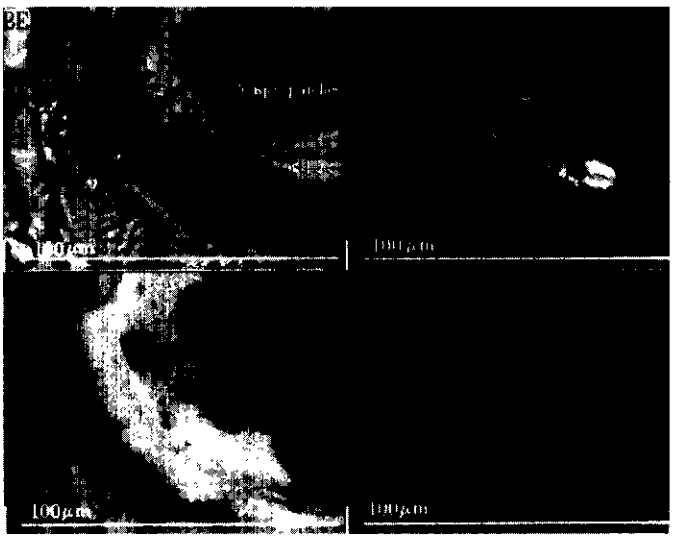

Fig.6 A BEI of a thin glass 'wispy' residue (highlighted by the black arrows) observed in a LEO generated crater. The discrete patches in the BEI correspond to enrichments in both the Mg and Fe elemental x-ray maps.

Thin Glass And 'Wispy' Residues. The textures described above show only limited interaction with the host melt during the impact process, indicated by the clear compositional contrast in BEI between vesicular or embedded glass and the melted borosilicate substrate. The 'thin glass' residue in some LEO HVIs is much more difficult to see, with only a slightly darker tone in BEI, and the texture could easily be overlooked. The texture is seen most easily in X-ray maps that enable the location of enrichment in Mg to be identified (Fig.6). The lack of fluorine in these areas indicates the magnesium is not derived from the CMX layer of the cell. We tentatively

suggest that this marked difference in texture (compared to vesicular and embedded residues) may be indicative of different silicate mineralogy, probably a hydrous phyllosilicate component. If a LGG impactor of heterogeneous origin, e.g. Orgeuil (CI carbonaceous chondrite meteorite) matrix (phyllosilicate dominated) is added to the shot program above, it may well elucidate these preliminary findings.

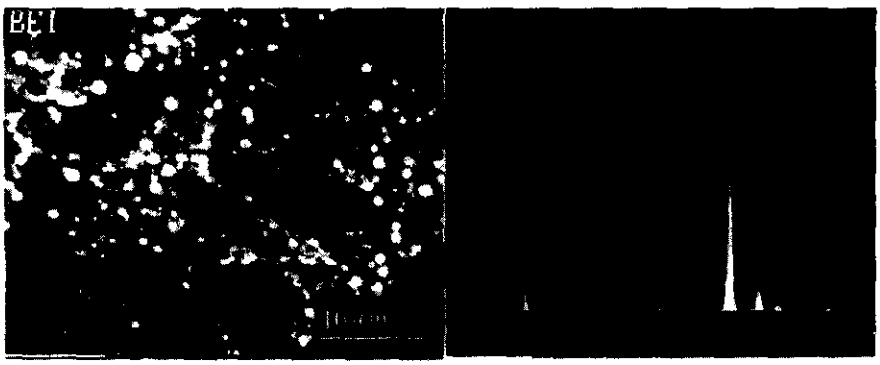

Fig.7 A BEI of the metallic surface melt droplets observed in a LEO-generated impact crater. The ED spectra obtained from the analysis of an individual droplet shows the enrichment in Fe and Ni.

Surface Globules. In low magnification BEI, several craters contained remarkably bright patches, showing strong compositional contrast between the host and the discrete residue chemistry (Fig.4a). At high magnification these patches reveal myriad separate, 1 - 10μm-sized hemispherical globules on the surface of the melt-pit or shallowly embedded within the melt glass (Fig.7). X-ray maps showed that the residue had not mixed with host melt in the way that silicates sometimes did mix. The globules were composed of Fe-Ni metal (Ni = 5-7.5 weight %, i.e. kamacite ratios) and metal sulfides (Fe-Ni sulfides and Fe-sulfides); similar globules were identified in a crater on Al from LDEF, Brownlee *et al.* [12] and it is assumed that they form by very rapid quenching. There appears to be no loss of volatile sulfur during the process, suggesting that the droplets were immiscible liquid melt droplets, rather than condensates from a gaseous phase. The pyrrhotite (FeS) impactor in the LGG produced very similar textural features (Fig.8) on a variety of scales although, some melt surfaces showed amalgamation of globules into broader surface patches or stretching of sulfide residue into streaks and curls. There was no evidence of mixing with the borosilicate melt.

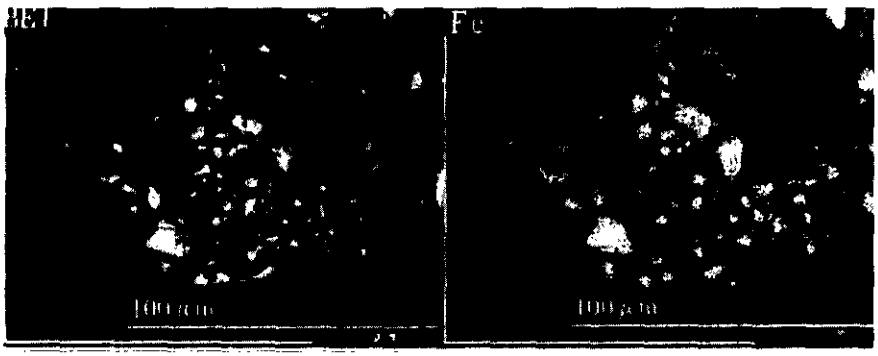

Fig.8 A BEI of the impact residue derived from an LGG-generated shot using pyrrhotite (FeS). The melt droplets in the BEI correspond to the enrichments in the Fe elemental x-ray map.

Near-intact Particulate Residue Material. The preservation of near-pristine particles in HVIs is extremely rare, Rietmeijer and Blandford [4]; Brownlee *et al.* [12], yet the identification of

such material clearly offers the best opportunity to classify impactor origin. The steel projectiles fired during the LGG program revealed that residue material is not only deposited in the melt-pit, but that it is also possible to locate material in both the conchoidal fractures and the underlying spall zone. Therefore, there exists the probability that in certain craters, especially when the zone of conchoidal fractures does not show complete detachment of fragments around the entire circumference of the crater, residue or even debris from the impactor may be retained. The evaluation of the LEO-exposed impact craters identified one with calcium-rich material (<8μm diameter) as near-intact particles located in the spall zone and radial fractures (Fig.9a).

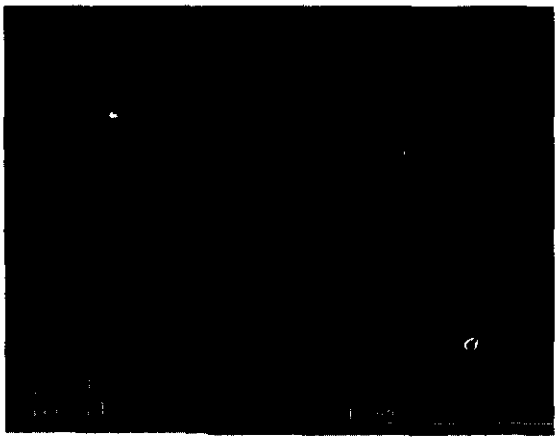

Fig.9a A BEI of an impact crater generated in LEO, which contains Ca-rich particles in the spall zone. The lack of the particles in the surrounding area would suggest that they are not simply contamination products.

Fig.9b *A secondary electron image (SEI) of a Ca-rich particle located in the LEO derived crater. The surface texture* of the particle indicates that it has undergone a degree of melting that would suggest that it is not contamination.

These fragments appeared not to be simply contamination at some later stage, as they showed evidence of surface melting (Fig.9b). We conclude that such debris was emplaced explosively. EDS X-ray microanalysis showed abundance of mainly calcium with no silicon, giving a spectrum remarkably like that of the carbonate mineral calcite. Calcite is a common constituent of altered refractory inclusions and veins in hydrated carbonaceous chondrite meteorites, e.g. Grossman [25]. It might be expected that explosive fragmentation on emplacement would result in the complete destruction and loss of such volatile-rich compounds rather than retention.

To evaluate whether such a volatile chemistry would survive HVI, calcite grains (125-250μm in diameter) were fired into a solar cell target using the LGG. Subsequently, fragments were

observed to be retained in the spall zone of several craters.

Fig.10 A BEI of Ca-rich fragments retained in the spall zone of a impact crater generated by the calcium carbonate LGG shot. The fragments are comparable to those observed LEO impact craters (Fig.9b).

These fragments (Fig.10) were demonstrably not simply original mineral grains (i.e. artefacts of the experiment, accreted after formation of the craters), as they showed evidence of surface alteration and were mantled in a thin coat of borosilicate host glass melt. The LGG shot of $CaCO_3$ has indicated that calcite can survive HVI.

It is clear that an EDS spectrum from a LEO-generated particle could be ambiguous if only Ca is observed since this could either be due to minerals of micrometeoroid origin (calcite in this case) or space debris (Ca-rich particles from urine). However we contest that, remnants of urine solids would be accompanied by other volatile elements (e.g. Na and K). Areas rich in sodium and chlorine have been found on the surface of some of the cells, probably as the result of contamination after recovery, but these are distinct in texture from impact residues. The techniques utilised in this study do not produce substantial volatile loss during analysis and the presence of some sodium or chlorine would be expected in urine-derived solids given the very substantial enrichment of these elements in urine when compared to calcium.

The scanning techniques employed in this investigation were not able to yield information on the crystallographic structure of the fragments. It is hoped that using the established techniques of residue extraction, Teetsov and Bradley [26], appropriate particles can be removed, and any surviving crystal structure be determined by transmission electron microscopy.

Debris Retention in HVI craters

The rigorous interpretation of HVI-derived residues in space hardware is a complex task. Crater size, penetration depth and accompanying degree of damage to the host can vary to a great extent (e.g. for the HST sample, crater diameters range from approximately 50 to 3000μm D_{CO}). There is potentially a strong bias to the population of impacting particles that can be recognised by residue studies, particularly if the host is only efficient at collecting the smaller particles, Graham *et al.* [24]. To date we have not yet seen a sufficiently large number of craters on solar cells to be able to assess whether residue can be routinely found in craters greater than 1500 μm in diameter. In this study a further limitation lies in the relatively small number of individual samples yet examined, and it is therefore very important to establish an efficient sampling method for a larger survey. To yield the maximum information on the LEO environment, it is essential to understand the likelihood of debris retention within a given crater size.

The pyrrhotite (FeS) LGG experiment, due in part to the buck-shot technique used in firing,

produced a large number of impact craters. Approximately 200 were of diameters comparable to those common in HVI from LEO (D_{CO} 100-2000 μm). The large number of craters, and the appropriate variation in crater diameter, offered the opportunity to quantify retention of residue in the crater size range that previous work, Graham *et al.* [24] had suggested would be the most effective at trapping material in brittle targets. 116 craters (D_{CO} 100-1700μm) were examined for residue: 111 (96%) contained FeS residue, 3 were unclassified (spalled melt) and 2 were contamination from the LGG. The results indicate that FeS is highly likely to survive HVI into a brittle target and should be adequately represented in a sample of natural impactors. This supports the observation that in the HVIs identified in solar cells from LEO as natural, 13 out of the 20 (65%) retained metal sulfide residues. Clearly we would like to extend this work to residue material from all of the other types of mineral shots employed herein. Furthermore to allow direct comparison with the retention of debris in LDEF craters, e.g. Bernhard *et al.* [21] laboratory HVI must use similar ductile targets (e.g. Al-blocks). Such experiments would form a logical extension of the present study, to be followed by a similar SEM survey of the craters.

SUMMARY AND CONCLUSIONS

Previous investigations of HVIs in space hardware have focused on ductile target surfaces, e.g. Al and Au, Bernhard *et al.* [21]. The analysis of such surfaces highlighted the complexity of these studies, as the location of residue material was rare, Brownlee *et al.* [12]. The investigation herein has focussed on solar cells (brittle surfaces) returned from the HST after 3.62 years of space exposure in LEO. Detailed analytical scanning electron microscopy has enabled the identification of extraneous residue material in impact craters (D_{CO} = 100-1000μm). The residue material was initially classified in terms of either space debris or micrometeoroid in origin. The latter has been sub-classified using chemistry and textural observations, e.g. embedded and vesicular glass melts identified as mafic silicates in origin.

The use of a LGG to simulate similar impacts has enabled critical evaluation of the nature of the LEO HVI derived-residues. Although the simulated residues are produced at lower velocities (~5 km/s) than compared to LEO derived residues (11-68 km/s for micrometeoroids) it appears that similar textures and chemical effects are produced.

Acknowledgements—This work was carried out as part of PPARC /CASE studentship to Giles Graham jointly within the 'Earth History, Materials and Processes theme' of the Natural History Museum (U.K.) and the Planetary Sciences Research Institute at the Open University (U.K.). Dr G.Drolshagen (ESTEC/ESA) is thanked for supplying the HST solar cells used in the work. The simulated shot program was carried as a part of ESA contract ESTEC No 11887/96/NL/JG. The authors thank the anonymous reviewers for their comments, which enhanced the manuscript. J.P.Bradley, R.M.Hough, M.E.Zolensky and F.J.M.Rietmeijer all provided useful discussion regarding this research.

REFERENCES

1. Drolshagen, G., HST meteoroid and debris impact analysis: Overview, *Proc. Hubble Space Telescope Array Workshop*, ESA WPP-77, 295-300 (1995).
2. Laurance, M.R. and Brownlee, D.E., The flux of meteoroids and orbital space debris striking satellites in low Earth orbit, *Nature*, **323**, 136-138 (1986).
3. Bernhard, R.P., Durin, C. and Zolensky, M.E., Scanning electron microscope / energy dispersive x-ray analysis of impact residues in LDEF Tray clamps, *LDEF 69 Months in Space - 2nd Post-Retrieval Symp.*, 541-550 (1993).
4. Rietmeijer, F.J.M. and Blandford, G.E., Capture of an olivine micrometeoroid by spacecraft in low Earth Orbit, *J. Geophys. Res.*, **93**, 11943-11948 (1988).
5. Hörz, F., Zolensky, M.E., Cress, G., Bernhard, R.P., See, T.H., et al., ODC: Aerogel particle capture during 18 months exposure on Mir, *Lunar Planet. Sci* XXIX, (CD-ROM abstr.), (1998).
6. Zolensky, M.E., Hörz, F., See, T.H., Bernhard, R.P., Dardano, C., Barrett, R.A., Mack, K., et al., Meteoroid Investigations Using The Long Duration Exposure Facility, In *Analysis Of Interplanetary Dust Particles* (eds M.E. Zolensky, T.L. Wilson, F.J.M. Rietmeijer and G.Flynn), AIP Conf. Proc. 310, AIP Press, Woodbury New

York, 291-304 (1994).
7. Warren, J.L., Zook, H.A., Allton, J.H, Clanton, U.S., Dardano, C.B., Holder, J.A., et al., The detection and observation of meteoroid and space debris impact features on the solar max satellite, *Proc. 19th Lunar and Planet. Sci. Conf.*, 641-657 (1989).
8. McDonnell, J.A.M., and the Canterbury LDEF MAP TEAM, Impact cratering from LDEF's 5.75 year exposure: decoding of the interplanetary and earth-orbital populations, *Proc. 22nd Lunar and Planet. Sci.*,, 185-193 (1992).
9. Rose, M.F., Best, S., Chaloupka, T., Stephens, B. and Crawford, G., Hypervelocity impact facility for simulating materials exposure to impact by space debris, *LDEF 69 Months in Space - 2nd Post-Retrieval Symp.*, 479-492 (1993).
10. Hörz, F., Cintala, M., Bernhard, R.P., and See, T.H., Penetration experiments in aluminum and teflon targets of widely variable thickness, In *Analysis of Interplanetary Dust Particles* (eds. M.E.Zolensky, T.L.Wilson, F.J.M.Rietmeijer and G.Flynn), AIP Conf. Proc. 310, AIP Press, Woodbury New York, 329-344 (1994).
11. Melosh, H.J., *Impact cratering. A geologic process*, Oxford University Press, Oxford 1996.
12. Brownlee, D.E., Joswiak, D., Bradley, J.P. And Hörz, F., Interplanetary meteoroid debris in LDEF metal craters, *LDEF 69 Months in Space - 2nd Post-Retrieval Symp.*, 577-584 (1993).
13. Rival, M., Mandeville, J.C. and Durin, C., Impact phenomena on brittle materials: analysis of 1μm to 1mm impact features on solar arrays, *Adv. Space Res.*, (In press) 1998.
14. Mandeville, J.C., Profile and depth of microcraters formed in glass, *Earth and Planet Sci. Lett.*, **15**, 110-112 (1972).
15. Taylor, E.A., Hayhurst, C.J. and Tsembelis, K., Hydrocode modelling of space debris - Hypervelocity impact on soda-lime glass using the Johnson-Holmquist Brittle Material Model, *Proc. 2nd European Conf. On Space Debris*, ESA SP-393, 449-454 (1997).
16. Graham, G.A., Kearsley, A.T., Grady, M.M. and Wright, I.P., The rapid identification of impact residues in solar array panels of the HST by digitised back-scattered electron and x-ray elemental imaging, *Proc. 2nd European Conf. On Space Debris*, ESA SP-393, 183-189 (1997).
17. Herbert, M.K. and McDonnell, J.A.M., Morphological classification on the EuReCa and Hubble Space Telescope solar arrays, *Proc. 2nd European Conf. On Space Debris*, ESA SP-393, 169-175 (1997).
18. Taylor, E.A., Kay, L., and Shrine, N.R.G., Hypervelocity impact on semi-infinite brittle materials: fracture morphology related to projectile diameter, *Adv. Space Res.*, (In press) (1998).
19. Bradley, J.P., Mechanisms of grain formation, post-accretional alteration, and likely parent body environments of interplanetary dust particles (IDPs), In *Analysis of Interplanetary Dust Particles* (eds. M.E.Zolensky, T.L.Wilson, F.J.M.Rietmeijer and G.Flynn), AIP Conf. Proc. 310, AIP Press, Woodbury New York, 291-304 (1994).
20. Zolensky, M.E., Zook, H.A., Hörz, F., Atkinson, D.R., Coombs, C.R., Watts, A.J et al., Interim Report Of Meteoroid and Debris Special Investigation Group, *LDEF 69 Months in Space - 2nd Post-Retrieval Symp*, 277-302 (1993).
21. Bernhard, R.P., See, T.H. and Hörz, F., Projectile compositions and modal frequencies on the "Chemistry of micrometeorites" LDEF experiment, *LDEF 69 Months in Space - 2nd Post-Retrieval Symp.*, 551-574 (1993).
22. Graham, G.A., Kearsley, A.T., Grady, M.M., Wright, I.P. And McDonnell, J.A.M., Micrometeoroid residue collected in low earth orbit, *Lunar Planet. Sci.*, XXIX, (CD-ROM abstr.) (1998).
23. Graham, G.A., Kearsley, A.T., Grady, M.M., Hough, R.M., Wright, I.P. and McDonnell, J.A.M., Populations of low earth particles: Significant other or simply space junk?, *Meteoritics Planet Sci.*, **33**(4), A61 (abstr. suppl.), (1998).
24. Graham, G.A., Sexton, A., Grady, M.M. And Wright, I.P., Further attempts to constrain the nature of the impact residues in the HST solar array panels, *Adv. Space Res.*, **20**(8), 1461-1465 (1997).
25. Grossman, L. Petrography and mineral chemistry of Ca-rich inclusions in the Allende meteorite, *Geochim. Cosmochim. Acta*, **39**, 433-454 (1975).
26. Teetsov, A. and Bradley, J.P., Micromanipulation of extraterrestrial particles, *Lunar Planet. Sci.* XVII, 883-884 (Abstr.) (1986).

Pergamon
www.elsevier.nl/locate/asr

Adv. Space Res. Vol. 25, No. 2. pp. 303–307, 2000

Printed in Great Britain
0273-1177/00 $20.00 + 0.00

PII: S0273-1177(99)00948-5

THE COLLECTION OF MICROMETEOROID REMNANTS FROM LOW EARTH ORBIT

G.A.Graham[1, 2, 3], A.T.Kearsley[2], M.M.Grady[3], I.P.Wright[1] and J.A.M.McDonnell[4]

[1]*PSRI, The Open University, Milton Keynes MK7 6AA, U.K*
[2]*Geology, BMS, Oxford Brookes University, Oxford OX3 7AB, U.K*
[3]*Mineralogy Department, The Natural History Museum, London SW7 5BD, U.K*
[4]*USSA, The University of Kent at Canterbury, Canterbury CT2 7NR, U.K*

ABSTRACT

The solar array panel returned from the Hubble Space Telescope after 3.62 years of space exposure offered the opportunity to study individual solar cells for hypervelocity impact damage and residue. A detailed electron microscope investigation of impact craters (100-1000μm diameters) has identified that most are residue-rich and by digitised x-ray elemental mapping and semi-quantitative micro-spot analysis the original precursor composition of the impactor can almost unambiguously be identified. The residues contain diverse elemental compositions that can be associated with known meteorite mineralogies and directly compared with interplanetary dust particles and micrometeorites, possibly the most likely source object. The observation of a magnesium-rich residue with (Mg+Fe) / Si ratio similar to that of forsterite (end-member Mg-olivine identified in meteorites), indicates that it is possible in favourable conditions to define clearly the compositional nature of the impactor. The identification of near-intact calcium-rich fragments, that are neither artefacts nor contamination, indicates that volatile chemistries can survive hypervelocity impacts in brittle glass substrates. The abundance of micrometeoroid residues in the individual solar cells has highlighted that valuable information can be retained from impact craters in returned space hardware which are essentially not designed as a dust collectors.

INTRODUCTION

Since over 90% of extraterrestrial material which bombards the Earth each year is less than 1mm in size, the study of this material is therefore fundamental to the understanding of small bodies within the solar system (Brownlee, 1994). Most of the work thus far has been carried out on terrestrial collections, e.g. interplanetary dust particles (IDPs) collected in the stratosphere, (Klöck and Stadermann, 1994) and micrometeorites (AMMs) collected in Antarctica (e.g. Genge and Grady, 1998). Much knowledge has been gained from such studies, yet these particles are subject to modification and selection effects during atmospheric entry (e.g. Genge *et al.*, 1997). Thus the best environment for the collection and subsequent investigations of cosmic dust might be above the stratosphere in low Earth orbit (LEO). Attempts at dust collection in this environment have focused on: 1) trapping intact particles using low density collector cells, made of silica-aerogel (Hörz *et al.*, 1998); 2) dedicated in-situ collectors, e.g. the "Long Duration Exposure Facility" (LDEF) (e.g. Bernhard *et al.*, 1993a), which was exposed to the prolonged effects of space exposure (69 months); 3) passive collectors, e.g. satellites (Bradley *et al.* 1986) which have been impacted by these particles. Passive collectors do not have dedicated collection surfaces such as the high purity Al and Au blocks which were used in LDEF experiments (e.g. Bernhard *et al.*, 1993a), but are piece of hardware which have been returned to Earth.

The characterisation of LEO particles is complicated by the fact that most of the particles are collected as a result of hypervelocity impact (11-68km/s, (Hörz, 1986)) onto the target material. The impact-generated crater leaves little trace of the original impactor apart from a complex melt-derived residue comprised of both impactor and host (e.g. Bradley *et al.*, 1986; Brownlee et al., 1993), although rare near-pristine material has been captured and investigated (Reitmeijer and Blandford, 1988). A further complication is the presence of a second orbital population of particles comprising artificial space debris, which includes paint fragments, solid rocket exhaust fragments and human waste (astronaut urine) (Zolensky *et al.*, 1993).

The '-V2' solar array panel returned to Earth from the Hubble Space Telescope (HST) in 1993, after 3.62 years of LEO exposure at approximately 600km altitude, has offered the opportunity to investigate further the constitution of micrometeoroids and space debris, (e.g. Drolshagen, 1995). Herein we report on the continuing attempts to distinguish between artificial and natural residues deposited in individual solar cells, in terms of chemistry, with the objective that the latter will be sub-divided into residues that have an affinity with IDPs and AMMs. We have previously reported on the identification of a

residue of mafic origin and the potential for the retention of impactor material (Graham *et al.*, 1997a) in classes I and II impact craters in individual solar cells (Herbert and McDonnell, 1997). The development of the rapid identification technique of impact residues in the solar cells (Graham *et al.*, 1997b) has further developed the study and enabled the classification of natural impact residue to be constrained further.

EXPERIMENTAL

Methods

A preliminary optical survey of 25 individual solar cells was undertaken using a Leitz Wild M8 microscope fitted with a Sony DKC 5000 digital photo camera to locate the impact features; 29 class I and II impact craters were recorded. The samples were subsequently carbon coated and examined on a Jeol JSM 840 scanning electron microscope (SEM) fitted with an Oxford Instruments e-XL X-ray energy dispersive spectrometer, operated at 20keV, 2nA beam current and a working distance of 32mm (the detailed analytical protocols are described in Graham *et al.*, 1997b).

Classification Scheme

The identification and classification of impact residues in terms of chemical composition is based on the scheme used in the LDEF studies (Zolensky *et al.*, 1993; Bernhard *et al.*, 1993b). Unlike the ductile surfaces of high purity Al and Au (essentially simple compositions) targets used on LDEF (Bernhard *et al.*, 1993a), the HST solar cells are a brittle substrate composed of a complex elemental composition (Berthoud and Paul, 1995; Graham *et al.*, 1997b). This initially caused difficulties in classification as those elements which have previously been used as "key fingerprints" (Si, Ca and Mg) for an indication of micrometeoroid residues, are fundamental constituents of the solar cells. Notwithstanding this problem and after detailed analysis of a cell, it is possible to distinguish minor compositional variations. A further complication to the classification is that most of the residue exhibit textural evidence of melting and possibly even condensation from a gaseous state. Thus they may not retain the stoichometric chemical signature of their parent mineral. Nevertheless, it is still possible to compare the energy spectrum obtained by electron microscopy of the residues with known meteorite mineralogies and therefore produce almost unambiguous classifications.

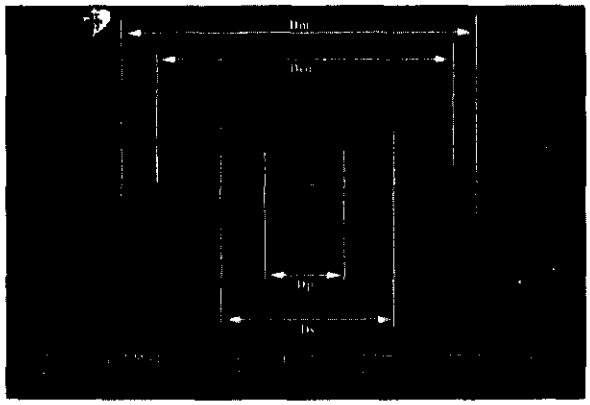

Fig. 1. A SEI image of a typical impact crater. The crater terminology can be described as the following: Dp = central pit (melt pit); Ds = Shatter zone, this area is highly fragmented; D_{CO} = Conchoidal spallation; Dm =Maximum damage detected at an impact site

RESULTS AND DISCUSSION

The 29 impact craters investigated were in the 100-1000μm crater diameter size range, Figure 1, based on measurements taken from maximum conchoidal damage (D_{CO}) as defined in (Herbert and McDonnell, 1997). The residues were identified as: 3 of artificial origin, 20 of natural origin and 6 were unclassified (spalled melts, where it is assumed the residue was lost during the impact process). The residue material identified was present in varying degrees of abundance and textural appearances within the central melt pit, the spall zone and the fracture cracks of the impact craters. The craters are essentially located in the top layers of the solar cell composite, Figure 1, which means that the host composition in the melt mixture containing the residue is that of the borosilicate glass. Thus the residue textures appear as: vesicular glasses, embedded concentrate glasses, thin 'wispy', glasses, surface immiscible globules and near-intact particles, these are discussed further in Graham *et al.*, (1998). Due to the limited number (29) of samples analysed and the possible bias present in the selection of a specific size range of craters, it is not possible to compare the significance of the results obtained here and those from specific LDEF experiments (Bernhard *et al.*, 1993a) where over 600 impact features were observed. However although quantitative comparisons are not possible, it is possible to compare the HST and LDEF results qualitatively, in terms of the impact chemistry.

Both IDPs and AMMs are identified in terms of the major mineralogical components (e.g. Klöck and Stadermann, 1994), thus to the natural impact residues must be sub-divided and classified in these terms so that direct comparison with IDPs and AMMs chemistry can be made. Thus to be able to make such comparisons, the residues must be classified in terms of mafic (olivine and pyroxene) silicates and layered silicates with phyllosilicates (e.g. saponite)

Mafic Origin

Elemental signatures of Mg, Si and Fe within a residue are an indication of possible mafic origin, although previous studies have highlighted that such an elemental combination without minor S or Ni, is not an unambiguous signal for meteoritic olivine and could be solid rock motor ablation debris (Laurance and Brownlee, 1986). The Mg-Fe- residues identified in the solar cells are components within a polycomposite residue, where the Mg-Fe component is the dominant chemistry, with minor associated Fe-Ni metal and Fe-Ni sulfides, Figure 2a. This combination of elemental components is strongly suggestive of mafic origin and similar residues were identified in the high purity Al/Au micrometeoroid collectors from LDEF (Brownlee *et al.*, 1993). The residue chemistries, if assumed to be mineralogical remnants, are typical of those of intact in IDPs or AMMs (Genge *et al.*, 1997). The mafic residues identified are observed as embedded and vesicular melt glass within the host melt (Graham *et al.*, 1998), therefore it is generally difficult to obtain a diagnostic signal that would enable the sub-classification of whether the residue is olivine or pyroxene dominated. However, one of the embedded glass residues contained (Mg+Fe) / Si ratios directly comparable with forsterite olivine (a specific mafic silicate identified in meteorites), Figure 2b. It is not possible to conclude that this is the original composition of the olivine or whether it had undergone chemical fractionation during the impact processes. Previously such a detailed classification has only been possible when near-intact particle fragments have been identified in hypervelocity impacts (HVIs) in space hardware, e.g. the Mg-rich olivine particulates from Solar Max (Rietmeijer and Blandford, 1988).

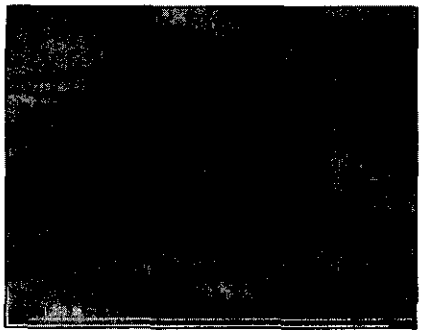

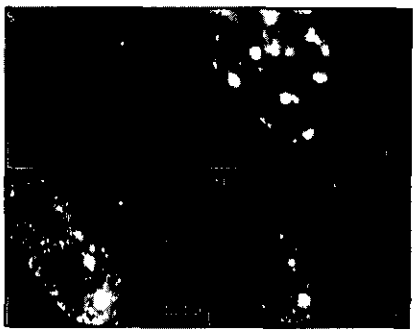

Fig.2a.

Fig.2b.

Fig.2a. A BEI of the impact crater identifies bright and dark areas in the melt-pit which correspond in the x-ray maps to Fe-Ni metal droplets and Fe-Ni sulphide droplet (bright areas) and Mg+Fe (dark areas). Fig.2b. shows the comparison of an EDS spectrum obtained from the Mg-rich residue component with a spectrum obtained from an olivine grain from a meteorite sample

'Layered silicates' and Phyllosilicates in Origin

The identification of a residue that is predominately 'layered silicate' rather than mafic silicate in origin is problematic. HVI processes such as devolatilisation and metamorphism are likely to remove water, or alter the mineralogy to such a degree that the resultant residue would be indistinguishable from a mafic residue (i.e. the dominated elemental components will be Mg and Fe). However we suggest that notwithstanding such difficulties it might be possible to enable such identification by observing the textural morphology of the residue as well as the chemistry (Graham *et al.*, 1998). In Figure 3., the BEI image identified a discreet dark area within the melt. The back-scatter electron intensity was lower than would be expected for a silicate of mafic

origin. The darker area corresponded to Mg-rich and Fe-poor x-ray maps; the Si peak was also lower than generally associated with mafic residues. A similar observation in an LDEF residue concluded that the impactor was a 'layered silicate' in origin (Zolensky *et al.*, 1994).

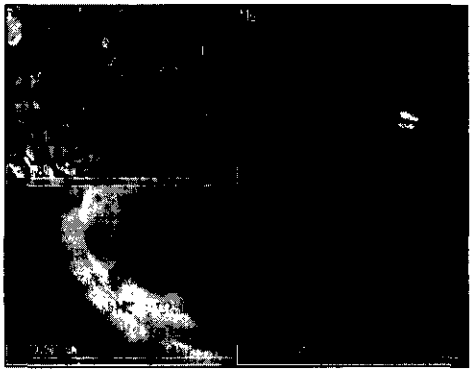

Fig.3. A residue possibly of indicating a 'layered' silicate origin. The BEI image identifies dark wispy patches in the melt, which corresponds to the Mg and Fe x-ray elemental maps.

Metallic Components

The Mg+Fe dominated residue also contained minor metallic phases, Fe-Ni sulfides, Fe-sulfides and Fe-Ni metal as surface immiscible melt droplets/globules, Figure 2. Such features were identified in the LDEF craters (Brownlee *et al.*, 1993) and it is assumed that these droplets are the product of extremely rapid cooling as there appears to be no volatile loss of sulphur. The observation of such droplets in association with Mg+Fe components is not unexpected if the residue is of micrometeoroid origin as both mafic and 'layered' silicate-dominated IDPs contain minor metallic phases (Klöck and Stadermann, 1994), as do AMMs (Genge and Grady, 1998). In two craters, the metal phase as was identified as the sole component, where the melt pit was covered in nanometer to micron sized Fe-Ni metal globules (maximum diameter was 5μm). An artificial impactor could have generated the globules, but the Ni concentrations were distinctively within the range of meteoritic material (up 7.5 wt%), suggesting that the original impactor may be natural Fe-rich non-chondritic micrometeoroids (Graham *et al.*, 1997c).

Refractory Components

Two craters contained abundant Ca-rich particles (<10μm in diameter), Figure 4., whose EDS spectrum was remarkably similar to that of a carbonate mineral calcite. Although the micro-spot analysis showed a lack of silicon, such a signal is not unambiguously indicative of natural origin. It is possible that the Ca rich particles could be remnants of urine, although in that case the EDS spectrum should contain other elements (e.g. Na and K). The lack of these volatile elements suggests that the Ca-rich particles are not a result of space debris or contamination due to evidence of surface melting on the individual particles. We tentatively suggest that these Ca-rich particles are in fact remnants of rare refractory phases which have been identified in IDPs (Zolensky, 1987). This observation is further supported by the identification of Mg- and Al-rich oxide (possibly spinel), Mg- and Fe-bearing silicate with a low back-scattered electron intensity (possibly saponite) and a Mg- and Fe- non-silicate residue (possibly carbonate) in association with the Ca-particles. A mineral assemblage similar to this was identified in a meteorite for the carbonaceous chondrite group. A group which have previously been suggested as parent body materials for IDPs and AMMs (e.g. Klöck and Stadermann, 1994). The preservation of near-intact particles may indicate a relatively low velocity oblique impact. Previous studies (e.g. Brownlee *et al.*, 1993) suggested particles of asteroidal origin would have the orbital parameters to allow this.

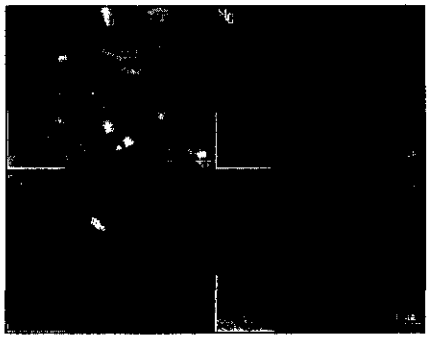

Fig.4. X-ray maps identifying the Ca-rich particles trapped in the spall zone of the impact crater

CONCLUSIONS

The ability to identify and classify residues within impacts in the HST solar cells in terms that can be directly compared with IDP chemistries (i.e. mafic silicates and layered silicates), suggest that returned space-hardware such as solar cells can act as excellent passive collectors for micrometeoroids.

ACKNOWLEDGEMENTS

This work was carried out as part of a PPARC/CASE studentship to G.A.G. J.A.M.M was supported by ESA contract - ESTEC No. 11887/96/NL/JG. A.T.K thanks UniSpace Kent for travel assistance to the 32nd COSPAR Assembly.

REFERENCES

Bernhard, R.P., See, T.H. and Hörz, F., Projectile Compositions and Modal Frequencies on the "Chemistry Of Micrometeorites LDEF Experiment, *LDEF 69 Months in Space - 2nd Post-Retrieval Symp.*, 551-574 (1993a).

Bernhard, R.P., Durin, C. and Zolensky, M.E., Scanning Elecron Microscope / Energy Dispersive X-ray Analysis Of Impact Residues in LDEF Tray Clamps, *LDEF 69 Months in Space - 2nd Post-Retrieval Symp.*, 541-550 (1993b).

Berthoud, L. and Paul, K., Micro-Impacts on HST Solar-Array-1 Surfaces, *Proc. Hubble Space Telescope Array Workshop*, ESA WPP-77, 477-492 (1995).

Bradley, J.P., Carey, W., and Walker, R.M., Solar Max Impact Particles: Perturbation of Captured Material, *Lunar Planet. Sci.*, **XVII**, 80-81 (abstr.) (1986).

Brownlee, D.E., Joswiak, D., Bradley, J.P. and Hörz, F., Interplanetary Meteoroid Debris in LDEF Metal craters, *LDEF 69 Months in Space - 2nd Post-Retrieval Symp.*, 577-584, (1993).

Brownlee, D.E., The Origin and Role of Dust in the Early Solar System, In *Analysis of Interplanetary Dust Particles* (eds. M.E.Zolensky, T.L.Wilson, F.J.M.Rietmeijer and G.Flynn), AIP Conf. Proc. 310, AIP Press, Woodbury New York, 291-304 (1994).

Drolshagen, G., HST meteoroid and debris impact analysis: Overview, *Proc. Hubble Space Telescope Array Workshop*, ESA WPP-77, 295-300 (1995).

Genge, M.J., Grady, M.M. and Hutchison, R., The Textures and Compositions of Fine-Grained Micrometeorites: Implications For comparisons with meteorites, *Geochim. Cosmochim. Acta*, **61**, in press (1997)

Genge, M.J. and Grady, M.M., Melted Micrometeorites from Antarctic Ice with evidence for the separation of immiscible Fe-Ni-S liquids during entry heating, Meteorit. Planet. Sci., **33**,425-434 (1998)

Graham, G.A., Sexton, A., Grady, M.M. and Wright, I.P., Further Attempts to Constrain the Nature of the Impact Residues in the HST Solar Array Panels, *Adv. Space Res.*, **20**, 8, 1461-1465 (1997a).

Graham, G.A., Kearsley, A.T., Grady, M.M. and Wright, I.P., The Rapid Identification of Impact Residues in Solar Array Panels of the HST by Digitised Back-Scattered Electron and X-ray Elemental Imaging, *Proc.2nd European Conf. On Space Debris*, ESA SP-393, 183-189 (1997b).

Graham, G.A., Kearsley, A.T., Grady, M.M. and Wright, I.P., An Fe-Ni Melt Residue deposited in Space: A New Class of Micrometeoroid?, *Lunar Planet. Sci.*, **XXVIII**,447-448 (Abstr.) (1997c).

Graham, G.A., Kearsley, A.T., Grady, M.M., Wright, I.P., Herbert, M.K. and McDonnell, J.A.M., Natural and Simulated Hypervelocity Impacts into Solar Cells, *Intl. J.Impact Eng.*, Submitted (1998).

Herbert, M.K. and McDonnell, J.A.M., Morphological Classification of Impacts on the EURECA & Hubble Space Telescope Solar Arrays, *Proc.2nd European Conf. On Space Debris*, ESA SP-393 ,169-176 (1997).

Hörz, F., Trajectory Determinations and Collections of Micrometeoroids on the Space Station, *LPI Tech Report 86-05*, Lunar and Planet. Inst., Houston Tex., pp102 (1986).

Hörz, F., Zolensky, M.E., Cress, G., Bernhard, R.P., See, T.H., Warren, J.H., *et al.*, ODC: Aerogel particle capture during 18 months exposure on mir, *Lunar Planet. Sci.*, **XXIX**, (CD-ROM abstr.), (1998).

Klöck, W. And Stadermann, F.J., Mineralogical and Chemical Relationships of Interplanetary Dust Particles, Micrometeorites and Meteorites, In *Analysis of Interplanetary Dust Particles* (eds. M.E.Zolensky, T.L.Wilson, F.J.M.Rietmeijer and G.Flynn), AIP Conf. Proc. 310, AIP Press, Woodbury New York, 51-88 (1994).

Laurance, M.R. and Brownlee, D.E., The Flux of Meteoroids and Orbital Space Debris Striking Satellites in Low Earth Orbit, *Nature*, **323**, 136-138 (1986).

Rietmeijer, F.J.M. and Blandford, G.E., Capture of an Olivine Micrometeoroid by Spacecraft in Low Earth Orbit, *J. Geophys. Res.*, **93**, 11943-11948 (1988)

Zolensky, M.E., Refractory Interplanetary Dust Particles, *Science*, 237, 1466-1468 (1987).

Zolensky, M.E., Zook, H.A., Hörz, F., See, T.H., Atkinson, D.R., Coombs, C.R., Watts, A.J., *et al.*, Interim Report Of M&D SIG, *LDEF 69 Months in Space - 2nd Post-Retrieval Symp*, 277-302 (1993).

Zolensky, M.E., Hörz, F., See, T.H., Bernhard, R.P., Dardano, C., Barrett, R.A., *et al.*, Meteoroid Investigations Using The Long Duration Exposure Facility, In *Analysis Of Interplanetary Dust Particles* (eds M.E. Zolensky, T.L. Wilson, F.J.M.

References

Aceti, R., Drolshagen, G., McDonnell, J.A.M. and Stevenson, T., Micrometeoroids and space debris – the EURECA post-flight analysis, *ESA Bulletin*, **80**, 21-26, (1994).

Aeritalia Space Systems Group, EURECA flight thermal analysis report, *EC-RP-AI-058*, 1, (1989).

Atkins, P.W., Physical Chemistry - 4th Edition, Oxford University Press, pp995, (1990).

Amari, S., Lewis, R.S. and Anders, E., Interstellar graphite in meteorites: growing complexity implied by its noble-gas components, Lunar Planet. Sci. XXI, 19-20, (1990).

Amari, S., Foote, J., Simon, C., Swan, P., Walker, R.M., Zinner, E. et al., SIMS chemical analysis of extented impacts on the leading and trailing edges of LDEF experiment AO187-2, *LDEF 69 Months in Space – 1st Post-Retrieval Symp.*, NASA CP-3194, 503-516, (1991).

Amari, S., Foote, J., Swan, P., Walker, R.M., Zinner, E. and Lange, G., SIMS chemical analysis of extented impacts on the leading and trailing edges of LDEF experiment AO187-2, *LDEF 69 Months in Space - 2nd Post-Retrieval Symp.*, NASA CP-3194, 513-528, (1993).

Arndt, P., Bohsung, J., Maetz, M. and Jessberger, E.K., The elemental abundances in interplanetary dust particles, *Meteoritics Planet. Sci.*, **31**, 817-833, (1996).

Astronomy Now, Deadly clouds, *Astronomy Now*, 49-51 (Dec 1996).

Barber, D.J., Matrix phyllosilicates and associated minerals in C2M carbonaceous chondrites, *Geochim. Cosmochim. Acta*, 45, 945-970, (1981).

Beckerling, W. and Bischoff, A., Occurrence and composition of relict minerals in micrometeorites from Greenland and Antarctica – implications for their origins, *Planet. Space Sci.*, **43**, 3, 4, 435-449, (1995).

Beech, M. and Brown, P., Impact probabilities on artificial satellites for the 1993 Perseid meteoroid stream, *Mon. Not. R. Astron. Soc.*, **262**, L35-L36, (1993).

Bernhard, R.P. and McKay, D.S., Micrometer-sized craters on the Solar Maximum satellite: the hazards of secondary ejecta, *Lunar Planet. Sci. XIX*, 65-66, (1988).

Bernhard, R.P., Durin, C. and Zolensky, M.E., Scanning electron microscope / energy dispersive X-ray analysis of impact residues in LDEF Tray clamps, *LDEF 69 Months in Space - 2nd Post-Retrieval Symp.*, 541-550, (1993a).

Bernhard, R.P., See, T.H. and Hörz, F., Projectile compositions and modal frequencies on the "Chemistry of micrometeorites" LDEF experiment, *LDEF 69 Months in Space - 2nd Post-Retrieval Symp.*, NASA CP-3194, 551-574, (1993b).

Berthoud, L., Micro-Impacts on HST Solar-Array-1 Surface, *Proc. Hubble Space Telescope Array Workshop*, ESA WPP-77, 477-492, (1995).

Berthoud, L. and Paul, K., Micro-Impacts on HST Solar-Array-1 Surfaces, *IKI Moscow Workshop on Space Debris*, (1995).

Bigg, E.K., Ono, A. and Thompson, W.J., Aerosols at altitudes between 20-37km. *Tellus XXII*, 550-563, (1970).

Bishop, A.N., Kearsley, A.T. and Patience, R.L., Analysis of sedimentary organic materials by scanning electron microscopy: the application of back-scattered electron imagery and light element X-ray microanalysis, *Org. Geochem.*, **18**, 4, 431-446, (1992).

Blanchard, M.B. and Davis, A.S., Analysis of ablation debris from natural and artificial iron meteorites, *J. Geophys. Res.*, **83**, B4 ,1793-1808, (1978).

Blanchard, M.B., Brownlee, D.E., Bunch, T.E., Hodge, P.W. and Kyte, F.T., Meteoroid ablation spheres from deep-sea sediments, *Earth Planet. Sci. Lett.*, **46**, 178-190, (1980).

Bland, P.A., Smith, T.B., Jull, A.J.T., Berry, F.J., Bevan, A.W.R., Couldt, S. and Pillinger, C.T., The flux of meteorites to the Earth over the past 50,000 years, *Mon. Not. R. Astron. Soc.*, **283**, 551-565, (1996).

Borg, J., Bibring, J-P., Langevin, Y., Salvetat, P.H. and Vassent, B., The COMET experiment, *Meteoritics*, **28**, 641-648, (1993).

Bradley, J.P. and Brownlee, D.E., *Lunar Planet. Sci. XIV*, 67-68, (1983).

Bradley, J.P. and Brownlee, D.E., Cometary particles: Thin sectioning and electron beam analysis, *Science*, **231**, 1542-1544, (1986).

Bradley, J.P., Carey, W., and Walker, R.M., Solar Max Impact Particles: Perturbation of Captured Material, *Lunar Planet. Sci.* XVII, 80-81, (1986).

Bradley, J.P., Analysis of chondritic interplanetary dust thin-sections, *Geochim.et Cosmochim.Acta.*, **52**, 889-900, (1988).

Bradley, J.P. and Brownlee, D.E., An interplanetary dust particle linked directly to type CM meteorites and an asteroidal origin, *Science*, **231**, 1542-1544, (1991).

Bradley, J.P., Mechanisms of grain formation, post-accretional alteration, and likely parent body environments of interplanetary dust particles (IDPs), In *Analysis of Interplanetary Dust Particles* (eds. M.E.Zolensky, T.L.Wilson, F.J.M.Rietmeijer and G.Flynn), AIP Conf. Proc. 310, AIP Press, Woodbury New York, 291-304, (1994).

Bradley, J.P., Keller, L.P., Brownlee, D.E. and Snow, T., The infrared space observatory resolution: Implications for the presolar origins for silicates in anhydrous interplanetary dust particles, *Meteoritics & Planet. Sci.*, **33**, 4, (abstract), A21-A22, (1998).

Bridges, J.C. and Grady, M.M., Evaporite mineral assemblages in Lafayette and the Nakhlites, *Meteoritics & Planet. Sci.*, **34**, 4, (abstract), A18, (1999).

Brownlee, D.E., Hodge, P.W. and Bucher, W., The physical nature of interplanetary dust as inferred by particles collected at 35km, In: Evolutionary and physical properties of meteoroids (Eds: C.L Hemenway, P.M. Millman and A.F. Cook), NASA SP-319, 291-295, (1973).

Brownlee, D.E., Hodge, P.W., Ablation debris and primary micrometeoroids in the stratosphere, *Space Res.*, **13**, 1139-1151, (1973).

Brownlee, D.E., Tomandl, D.A., Hodge, P.W. and Hörz, F., Elemental abundances in interplanetary dust, *Nature*, **252**, 667-669, (1974).

Brownlee, D.E., Ferry, G.V. and Tomandl, E.., Stratospheric alumininum oxide, *Science*, **191**, 1270-1271, (1976).

Brownlee, D.E., Tomandl, D.A. and Olszewski, E., Interplanetary dust: A new source of extraterrestrial material for laboratory studies, *Proc. 8th Lunar Planet. Sci. Conf.*, 149-160, (1977).

Brownlee, D.E., Bernhard, R.P. and Zolensky. M.E., Interplanetary dust: possible implication for comets and presolar interstellar grains, In: *Protostars and Planets: Studies of Star Formation and the Origin of the Solar System* (Eds. T.Gehrels and Matthew, M.S.), pp.134-150, Univ. Tucuson, Arizona, (1978).

Brownlee, D.E., Pilachowski, L.B. and Hodge, P.W., Meteorite mining on the ocean floor. *LPSC X*, 157-158, (1979).

Brownlee, D.E., Extraterrestrial components, In: The Sea (Ed: C.Emiliani), **7**, 733-762, (1981).

Brownlee, D.E., Bates, B.A. and Wheelock, M.M., Extraterrestrial platinum group nuggets in deep-sea sediments, *Nature*, **309**, 693-695, (1984)

Brownlee, D.E., Cosmic dust: Collection and research, *Ann. Rev. Earth Planet. Sci. Lett.*, **13**, 147-173, (1985).

Brownlee, D.E., Joswiak, D., Bradley, J.P. And Hörz, F., Interplanetary meteoroid debris in LDEF metal craters, *LDEF 69 Months in Space - 2nd Post-Retrieval Symp.*, NASA CP-3194, 577-584, (1993).

Brownlee, D.E., The origin and role of dust in the early solar system, In *Analysis of Interplanetary Dust Particles* (eds. M.E.Zolensky, T.L.Wilson, F.J.M.Rietmeijer and G.Flynn), AIP Conf. Proc. 310, AIP Press, Woodbury New York, 5-10, (1994).

Brownlee D.E. et al., The Stardust Mission: Returning comet samples to Earth, *Meteoritics & Planet. Sci.*, **32**, 4, (abstract), A22, (1997).

Brunn, A.F., Langer, E. and Pauly, H., Magnetic particles found by raking the sea floor, *Deep-Sea Res.*, **2**, 230, (1955).

Caistaing, R. and Fredriksson, K., Analyses of cosmic spherules with an X-ray microanalyser, *Geochim.et Cosmochim.Acta.*, **44**, 114-117, (1958).

Carr, R.H., Gibson, E.K., Rietmeijer, F.J.M., Grady, M.M., Wright, I.P. and Pillinger, C.T., Characterisation of carbonaceous materials in interplanetary dust particles, *Meteoritics*, **21**, 344-345, (abstract), (1986).

Carey, W.C., WP4: Analysis of impact residue studies, *Micrometeoroid & Debris Flux & Ejecta Models*. ESA Contract No. 1887/96/NL/JG, (1998).

Caswell, R.D., McBride, N. and Taylor, A., Olympus end of life anomaly – a Perseid meteoroid impact event?, *Int. J. Impact Engng.*, **17**, 149-150, (1995).

CDPET (Cosmic Dust Preliminary Examination Team), Cosmic Dust Catalog, JSC-27897, Houston Texas: NASA Johnson Space Center, **15**, (1991).

Christiansen, E., Bernhard, R. and Hartsough, N., Orbiter / Orbital Debris Impacts: STS-50 (6/92) through STS-86 (10/97), NASA JSC-28033, (1998).

Clemett, S.J., Chillier, X.D.F., Gillette, S., Zare, R.N., Maurette, M., Engrand, C. and Kurat, G., Search for polycyclic aromatic hydrocarbons in "gaint" carbonaceous Antarctic micrometeorites, *Orig. Life Evol. Biosphere*, In press, (1997).

Cour-Palais, B.G., The current micrometeoroid flux at the Moon for mases <10-7 g from the Apollo window and Surveyor 3 TV camera results, Proc. 5th Lunar Conf., *Geochim. Cosmochim. Acta*, **3**, 2451-2462, (1974).

Crutcher, E.R., Nishimura, L.S., Warner, K.J. and Wascher, W.W., Quantification of contaminants associated with LDEF, *LDEF 69 Months in Space – 1st Post-Retrieval Symp*, NASA CP-3134 (part1), 141-154, (1991).

Dohnanyi, J.S., Particle dynamics, In: *Cosmic Dust* (Ed: J.A.M. McDonnell), Wiley, 527-605, (1978).

Drolshagen, G., HST meteoroid and debris impact analysis: Overview, *Proc. Hubble Space Telescope Array Workshop*, ESA WPP-77, 295-300, (1995).

Drolshagen, G., *Personal Communication.*

Eaton, D., The Hubble Space Telescope first service mission, *ESA Bulletin*, **76**, 73-79, (1993).

Engrand, C. and Maurette, M., Antarctic micrometeorites: High carbon contents from C/O atomic ratios – the controversy, *Meteoritics & Planet. Sci.*, **31**, A39, (abstract), (1997).

Engrand, C. and Maurette, M., Carbonaceous micrometeorites from Antarctica, *Meteoritics & Planet. Sci.*, **33**, 565-580, (1998).

Everhart, T.E. and Thornley, R.F.M., *J. Sci. Instr.*, **37**, 246, (1960).

Farlow, N.H., Ferry, G.V. and Blanchard, M.B., Examination of surfaces exposed to a noctilucent cloud, August 1, 1968, *J. Geophys. Res.*, **75**, 6736-6750, (1970).

Finkelman, R.B., Magnetic particles extracted from manganese nodules: Suggested origin from stony and iron meteorites, *Science*, **167**, 982-984, (1970).

Finkelman, R.B., Relationship between manganese nodules and cosmic dust, *J. Mar.Tech. Soc.*, **6**, 34-39, (1972).

Fireman, E.L. and Kistner, G.A., The nature of dust collected at high altitudes, *Geochim. et. Cosmochim. Acta.*, **24**, 10-22, (1961).

Flam, F., Repairs rekindle 3-year-old dream, *Science*, **262**, 1810, (1993).

Flynn, G.J., Atmospheric entry heating of micrometeorites, *Proc. 19th Lunar Planet. Sci. Conf.*, 673-682, (1989a).

Flynn, G.J., Atmospheric entry heating: A criterion to distinguish between asteroidal and cometary sources of interplanetary dust, *Icarus*, **77**, 287-310, (1989b)

Flynn, G.J. and Sutton, S.R., Synchroton X-ray fluorescence analyses of stratospheric cosmic dust: New results for chondritic and low nickel particles, *Proc. 20th Lunar Planet. Sci. Conf.*, 335-342, (1990).

Fraundorf, P., Brownlee, D.E. and Walker, R.M., Laboratory studies of interplanetary dust, In: *Comets* (Ed. L.L. Wilkening), pp.383-409, Univ. Arizona Press, Tucuson, Arizona, (1982).

Genge, M.J., *Micrometeorite Catalogue*, The Natural History Museum, 1A, (1996).

Genge, M.J., Grady, M.M. and Hutchison, R., Evidence in a glassy cosmic spherule from Antarctica for grazing incidence encounters with Earth's atmosphere, *Meteoritics Planet Sci.*, 31, 627-632, (1996).

Genge, M.J., Grady, M.M. and Hutchison, R., The Textures and Compositions of Fine-Grained Micrometeorites: Implications for comparisons with meteorites, *Geochim. Cosmochim. Acta*, **61**, 23, 5149-5162, (1997).

Genge, M.J. and Grady, M.M., Melted Micrometeorites from Antarctic Ice with evidence for the separation of immiscible Fe-Ni-S liquids during entry heating, *Meteorit. Planet. Sci.*, **33**,425-434, (1998).

Gibson Jr., E.K., Zolensky, M.E., Lofgren, G.E., Lindstrom, D.J., Morris, R.V., Schmidt, S.D. and Yang, S.V., Monahans (1998) H5 chondrite: An unusual meteorite fall with extraterrestrial halite and sylvite, *Meteoritics Planet Sci.*, **33**(4), A57-58, (abstract), (1998).

Goldstein, J.I., Newbury, D.E., Echlin, P., Joy, D.C., Fiori, C. and Lifshin, E., Scanning electron microscopy and X-ray microanalysis, Plenum Press, New York and London, pp673, (1981).

Graham.G.A., Wright.I.P., Grady.M.M., Perreau.M., Maurette.M. & Pillinger.C.T., Carbon stable isotope analyses of Antarctic micrometeorites, *Lunar Planet. Sci. XXVII*, 441 - 442, (1996a).

Graham.G.A., Wright.I.P., Grady.M.M., Perreau.M., Maurette.M. & Pillinger.C.T., The carbon stable isotopic composition of Antarctic micrometeorites. *Meteoritics & Planet. Sci.*,**31**, 4, (abstract), A53-54, (1996b).

Graham, G.A., Sexton, A., Grady, M.M. And Wright, I.P., Further attempts to constrain the nature of the impact residues in the HST solar array panels, *Adv. Space Res.*, **20,** 8, 1461-1465, (1997a).

Graham, G.A., Kearsley, A.T., Grady, M.M. and Wright, I.P., The rapid identification of impact residues in solar array panels of the HST by digitised back-scattered electron and X-ray elemental imaging, *Proc. 2nd European Conf. On Space Debris*, ESA SP-393, 183-189, (1997b).

Graham, G.A., Kearsley, A.T., Grady, M.M. and Wright, I.P., Further impact residue chemistry analysis, *Executive Summary report*, ESA Contract No. 11887/96/NL/JG, (1998).

Graham, G.A., Kearsley, A.T., Grady, M.M., Wright, I.P., Griffiths, A.D. and McDonnell, J.A.M., Hypervelocity impacts in Low Earth Orbit: Cosmic Dust versus Space Debris, *adv. Space Res.*, **23**, 1, 95-100, (1999a).

Graham, G.A., Kearsley, A.T., Grady, M.M., Wright, I.P. Herbert, M.K. and McDonnell, J.A.M., Natural and simulated hypervelocity impacts into solar cells. *Int. J. Impact Eng.*, **23**, 319-330, (1999b).

Graham, G.A., Kearsley, A.T., Grady, M.M., Wright, I.P. and McDonnell, J.A.M., The collection of micrometeoroid remnants from Low Earth Orbit. *Adv. Space Res.*, **25**, 2, 303-307, (2000).

Grossman, L., Petrography and mineral chemistry of Ca-rich inclusions in the Allende meteorite,*Geochim. Cosmochim. Acta*, **39**, 433-454, (1975).

Gray, A.G., Source Book On Stainless Steels, American Soc. For Metals, 384-395, (1977).

Grün, E., Zook, H.A., Fechtig, H. and Gleen, R.H., Collisional balance of the meteoritic complex, *Icarus*, **62**, 244-272, (1985).

Grün, E., Zook, H.A., Baguhl, M., Balogh, A., Barne, S.J., Fechtig, H., Forsyth, R. et al., Discovery of Jovian dust streams and interstellar grains by Ulysses spacecraft, *Nature*, **362**, 428-430, (1993).

Heide, F. and Wlotzka, F., Meteorites – Messengers from space, *Springer-Verlag Berlin Heidleberg*, pp231, (1994).

Hiess, C. and Stadermann, F., Chemical analysis of hypervelocity impacts on solar cells from the Hubble Space Telescope, *Final Report*, ESA Contract No. WMA/94-335/GD/HST, (1995).

Hemenway, C.L. and Soberman, R.K., Studies of Micrometeorites obtained from recoverable sounding rockets, *Astron. J.*, **67**, 256-266, (1962).

Herbert, M.K. and McDonnell, J.A.M., Morphological classification on the EuReCa and Hubble Space Telescope solar arrays, *Proc. 2nd European Conf. On Space Debris*, ESA SP-393, 169-175, (1997).

Holtzclam, H.F.Jr., Robinson, W.R. and Odom, J.D., General Chemistry – 9th Edition, D.C. Heath & Company, pp1007, (1991).

Hughes, D.W., Meteors, In: *Cosmic Dust* (Ed: J. A. M. McDonnell), Wiley, 123-185, (1978).

Hörz, F., Brownlee, D.E., Fechtig, H., Hartung, J.B., Morrison, D.A., Neukum, G.A., Schneider, E. et al., Lunar microcraters: Implications for the micrometeoroid complex, Planet. Space Sci., **23**, 151-172, (1975).

Hörz, F., Fechtig, H. and Janicke, J., Mineralogy and chemistry of projectile residue in small experimental impact craters, Proc. 14th Lunar Planet. Sci. Conf., **88**, 1, B353-B363, (1983).

Hörz, F., Trajectory Determinations and Collections of Micrometeoroids on the Space Station, *LPI Tech Report 86-05*, Lunar and Planet. Inst., Houston Tex., pp102, (1986).

Hörz, F., Zolensky, M.E., Cress, G., Bernhard, R.P., See, T.H., et al., ODC: Aerogel particle capture during 18 months exposure on Mir, *Lunar Planet. Sci* XXIX, (CD-ROM abstr.), (1998).

Kearsley, A.T., Iron-rich ooids, their mineralogy and microfabric: clues to their origin and evolution, In: *Phanerozoic Ironstones* (Eds: T.P. Young and Taylor, W.E.G.), Geological Society, SP-**46**, 141-164, (1989).

Kearsley, A.T., *Personnel Communication.*

Kasten, F., Falling speeds of aerosol particles, *J. App. Met.*, **7**, 944, (1968).

Kessler, D.J., Reynolds, R.C. and Anz-Meador, P.D., Orbital debris environment for spacecraft designed to operate in low Earth orbit, NASA TM 100471, (1989).

Kessler, D.J., Reynolds, R.C. and Anz-Meador, P.D., Space station program natural environment definition for design, NASA SSP-30425, Rev. A., Houston Texas: NASA Johnson Space Center, (1991).

Kessler, D.J., Zhang, J., Matney, M.J., Eichler, P., Reynolds, R.C., Anz-Meador, P.D. and Stansbery, E.G., A computer based orbital debris environment model for spacecraft design and observation in low Earth orbit, NASA TM, (1996).

Klöck, W., Flynn, G.J., Sutton, S.R. and Nier, A.O., Mineralogy of IDPs with known 4He and trace element contents, *Meteoritics*, **27**, 243-244, (abstract), (1992).

Klöck, W. and Stadermann, F.J., Mineralogical and chemical relationships of interplanetary dust particles, micrometeorites and meteorites, In *Analysis of Interplanetary Dust Particles* (eds. M.E.Zolensky, T.L.Wilson, F.J.M.Rietmeijer and G.Flynn), AIP Conf. Proc. 310, AIP Press, Woodbury New York, 51-88, (1994).

Kurat, G., Brandstätter, F., Presper, T., Koeberl, C. and Maurette, M., Micrometeorites, *Russian Geology and Geophysics*, **34**, 12, 132-147, (1993).

Kurat, G., Koeberl, C., Brandstätter, F., Presper, T., Koeberl, C. and Maurette, M., Petrology and geochemistry of Antarctic micrometeorites, *Geochim. Cosmochim. Acta*, **58**, 3879-3904, (1994).

Laurance, M.R. and Brownlee, D.E., The flux of meteoroids and orbital space debris striking satellites in low Earth orbit, *Nature*, **323**, 136-138, (1986).

Levasseur-Regourd, A.C., Renard, J.B. and Dumont, R., The zodiacal cloud complex. In: *Origins and Evolution of Interplanetary Dust* (Eds: A.C. Levasseur-Regoud and H.Hasegawa), Kluwer Acad. Pub. Holland, 131-138, (1991).

Liou, J.C., Dermott, S.F., and Xu, Y.L., The contribution of cometary dust to the zodiacal cloud, *Planet. Space Sci.*, 43, 717-722, (1995).

Liou, J.C. and Zook, H.A., Comets as a source of low eccentricity and low inclination interplanetary dust particles, *Icarus*, 123, 491-502, (1996).

Liou, J.C., Zook, H.A. and Dermott, S.F., Kuiper belt dust grains as a source of interplanetary dust particles, *Icarus*, 124, 429-440, (1996).

Liou, J.C. and Zook, H.A., Evolution of interplanetary dust particles in mean motion resonances with planets, *Icarus*, 128, 354-367, (1997).

Love, S.G. and Brownlee, D.E., Heating and thermal transformation of micrometeoroids entering the Earth's atmosphere, *Icarus*, **89**, 26-43, (1991).

Love, S.G. and Brownlee, D.E., A direct measurement of the terrestrial mass accretion rate, *Science*, **265**, 550-553, (1993).

Mackay, N.S., Simulation of Earth's local particulate environment, *Unpublished PhD thesis*, University of Kent, (1994),

Mackinnon, I.D.R., McKay, D.S., Nace, G. and Isaacs, A.M., Classification of the Johnson Space Center Stratospheric Dust Collection, *Proc. 13th Lunar Planet. Sci. Conf., J. Geophys. Res.*, A413-421, (1982).

Mackinnon, I.D.R. and Mckay, D.S., Refinements and developments on the stratospheric dust database and the classification scheme, *Lunar Planet. Sci. XVII*, 510-511, (1986).

Martin, P.G., On the value of GEMS (glass embedded metal and sulfides), *Astrophys. J.*, **445**, L63-L66, (1995).

Mandeville, J-C., Profile and depth of microcraters formed in glass, *Earth and Planet Sci. Lett.*, **15**, 110-112, (1972).

Mandeville, J-C., Rival, M. and Durin, C., Small craters and X-ray analysis in HST solar cells: Preliminary results, *Hubble Space Telescope Solar Array Workshop: Results from Post-flight Investigations of the Returned HST Solar-Array*, ESA WPP-77, 513-525, (1995).

Maurette, M., Hammer, C., Brownlee, D.E., Reeh, N. and Thomsen, H.H., Placers of cosmic dust in the blue ice lakes of Greenland, *Science*, **233**, 869-872, (1986).

Maurette, M., Olinger, C., Christophe, M., Kurat, G., Pourchet, M., Brandstätter, F. and Buorot-Denise, M., A collection of diverse micrometeorites recovered from 100 tons of Antarctic blue ice, *Nature*, **351**, 44-47, (1991).

Maurette, M., Kurat, G., Perreau, M. and Engrand, C., Micro-analysis of Cap-Prudhomme Antarctic micrometeorites, *Microbeam Analysis*, **2**, 239-251, (1993)

Maurette, M., Immel, G., Hammer, C., Harvey, R., Kurat, G. and Taylor, S., Collection and curation of IDPs from the Greenland and Antarctic ice sheets, In: *Analysis of interplanetary dust particles* (eds. M.E. Zolensky, T.L. Wilson, F.J.M. Rietmeijer and G.J. Flynn), AIP Press, American Institute of Physics, Woodbury, New York, USA, 277-289, (1994).

McDonnell, J.A.M., Carey, W.C. and Dixon, D.G., Cosmic dust collection by capture cell technique on the space shuttle, *Nature*, 309, 237-240, (1984).

McDonnell, J.A.M., Extraterrestrial particulates: Their role in space science, *JBIS*, **41**, 387-392, (1988).

McDonnell, J.A.M., and the Canterbury LDEF MAP TEAM, Impact cratering from LDEF's 5.75 year exposure: decoding of the interplanetary and earth-orbital populations, *Proc. 22nd Lunar and Planet. Sci.*, 185-193, (1992).

McDonnell, J.A.M., Drolshagen, G., Gardner, D.J., Aceti, R. and Collier, I., EURECA's exposure in the near space environment. Hypervelocity impact cratering distributions at a time of space growth, *Adv. Space Res.*, **16**, 11, (11)73-(11)83, 1995.

McKeegan, K.D., Walker, R.M. and Zinner, E., Ion microprobe isotopic measurements of individual interplanetary dust particles, *Geochim. Cosmochim Acta*, 49, 1971-1987, (1985).

McKeegan, K.D., Hydrogen and magnesium isotopic abundances in aluminum-rich stratospheric dust particles, *Lunar Planet. Sci. XVII*, 539-540, (1986).

McKeegan, K.D., Oxygen isotopes in refractory stratospheric dust particles: Proof of extra-terrestrial origin, *Science*, **237**, 1468-1471, (1987).

McBride, N. and Taylor, E.A., The risk to satellite tethers from meteoroid and debris impacts, *Proc. 2nd European Conf. On Space Debris*, ESA SP-392, 643-647, (1996).

Melosh, H.J., *Impact cratering. A geologic process*, Oxford University Press, Oxford, (1996).

Messenger, S., Oxygen isotopic imaging of interplanetary dust particles, *Meteoritics & Planet. Sci.*, **33**, 4, A106-107, (1998)

Michel-Levy, M.C. and Bourot-Denise, M., Mineral compositions in Antarctic and Greenland micrometeorites, *Meteoritics*, **27**, 73-80, (1992).

Mosely, H.G.J., The high frequency spectra of the elements, *Philosophical Magazine*, **26**, 1024-1034, (1913).

Morrison, D.A. and Zinner, E., Distribution and flux of micrometeoroids, *Phil. Trans. R. Soc. London*, **A285**, 379-384, (1977).

Murray, S. and Renard, A.F., Measurement characters of volcanic ashes and cosmic dust and their origin in deep-sea sediment deposits, *Proc. Roy. Soc. Edinburgh*, **12**, 474-495, (1884).

Murray, S. and Renard, A.F., Report of the scientific results of the voyage of H.M.S. Challenger 3, *Neill and Co., Edinburgh*, (1891).

National Research Council, Orbital debris: A technical assessment, National Academy of Science, pp210, (1995).

New Scientist, Junk that goes bump, *New Scientist*, Reed Business Info. Ltd., 25-27, (11th May 1996).

Nier, A.O. and Schlutter, D.J., Helium and neon isotopes in stratospheric particles, *Metoritics*, **25**, 263-267, (1990).

Nier, A.O. and Schlutter, D.J., The thermal history of interplanetary dust particles collected in the Earth's stratosphere, *Meteoritics*, **28**, 675-681, (1993).

O'Neal, R.L and Lightner, E.B., Long Duration Exposure Facility – A general overview, *LDEF – 69 Months in Space Proc. Symp.*, NASA CP-3134, Part1, 3-48, (1991).

Opik, E.J., Interplanetary and terrestrial accretion of meteoritic matter, *Irish Astron. J.*, **4**, 84-135, (1956).

Olsson-Steel, D.I., The near Earth flux of microgram dust, In: *Dust in the universe* (Eds: M.E. Bailey and D.A. Williams), Cambridge University Press, 187-192, (1988)

Oxford Instruments Plc., The Oxford Guide to X-ray Microanalysis, Oxford Instruments Plc, Vol. 1 & 2 CD-Rom, (1997).

Parkin, D.W., Sullivan, R.A.L. and Andrews, J.N., Cosmic spherules as rounded bodies in space, *Nature*, **266**, 515-517, (1977).

Parkin, D.W., Sullivan, R.A.L. and Andrews, J.N., Further studies on cosmic spherules from deep-sea sediments, *Phil. Trans. R. Soc. Lond. A.*, **297**, 496-518, (1980).

Parkin, D.W., Sullivan, R.A.L. and Bull, R.K., Cosmic spherules and asteroidal collisions, *Geophys. J. R. astr. Soc.*, **75**, 473-491, (1983).

Reed, S.J.B., Electron microprobe microanalysis, In: *Microprobe Techniques in the Earth Sciences* (Eds: P.J. Potts, J.F.W. Bowles, S.J.B. Reed and M.R. Cave), Chapman and Hall, London, 49-89, (1995).

Reed, S.J.B., *Electron microprobe and scanning electron microscopy in geology*, Cambridge University Press, pp201, (1996).

Rietmeijer, F.J.M. and Mackinnon, I.D.R., Melting, ablation and vapor phase condensation during atmospheric passage of the Bjurböle meteorite, *J. Geophys Res*, 87, B, 597-604, (1984).

Rietmeijer, F.J.M., Silicone oil: A persistent contaminant in chemical and spectral microanalyses of interplanetary dust particles, *Lunar Planet. Sci. XVIII*, 836-837, (1987).

Rietmeijer, F.J.M. and Blandford, G.E., Capture of an olivine micrometeoroid by spacecraft in low Earth Orbit, *J. Geophys. Res.*, **93**, 11943-11948, (1988).

Rietmeijer, F.J.M., Interplanetary dust particles, In: *Planetary Materials* (Ed: J.J. Papike), Reviews in Mineralogy, Mineralogical Society of America, Washington D.C, 39, pp95, (1999).

Rival, M., Mandeville, J.C. and Durin, C., Impact phenomena on brittle materials: analysis of 1μm to 1mm impact features on solar arrays, *Adv. Space Res.*, (In press), (1997-1998).

Robin, E., Christophe, M., Bourot-Denise, M. and Jehanno, C., Crystalline micrometeorites from Greenland blue lakes: the chemical composition, mineralogy and possible origin, *Earth Planet. Sci. Lett.*, **97**, 162-176, (1990).

Russell, S., A carbon and nitrogen isotope study of chondritic diamond and silicon carbide, *Unpublished PhD thesis*, The Open University, (1993).

Sandford, S.A.. The collection and analysis of extraterrestrial particles, *Fundament. Cosmic. Phys.*, **12**, 1-73, (1987).

Sandford, S.A. and Bradley J.P., Interplanetary dust collected in the stratosphere: Observations of atmospheric heating and constraints on their interelationships and sources, *Icarus*, 82, 146-166, (1989).

Schramm, L.S., Barrett, R.A., Lieurance, M.L., McKay, D.S. and Wentworth, S.J., Particles associated with impact features in the main electronics box (MEB) thermal blanket from the Solar Max satellite, *Lunar Planet. Sci. XVII*, (1986).

Schramm, L.S., Brownlee, D.E. and Wheelock, M.M., Major element composition of stratospheric micrometeorites, *Meteoritics*, **24**, 99-112, (1989).

Scientific American, The future of space exploration, *Scientific American Inc.*, **10**, 1, 14-16, (1999).

Simon, C.G., Hunter, V.L., Griffis, D.P., Misra, V., Ricks, D.A., Wortman, J.J. and Brownlee, D.E., Elemental analysis of hypervelocity microparticle impact sites on interplanetary dust experiment sensor surfaces, *LDEF 69 Months in Space - 2nd Post-Retrieval Symp*, NASA CP-3194, 677-692, (1993).

Steele, I.M., Smith, J.V. and Brownlee, D.E., Minor-element signatures of relic olivine grains of deep-sea particles: Match with forsterites from C2 meteorites, *Nature*, **313**, 297-299, (1985).

Stadermann, F.J., Walker, R.M. and Zinner, E., Nanosims: The next generation ion probe for the microanalysis of extraterrestrial material, *Meteoritics & Planet. Sci.*, **34**, 4, A111-112, (abstract), 1999.

Stephan, T., Klöck, W., Jessberger, E.K., Rulle, H. and Zehnpfening, J., Multielement analysis of interplanetary dust particles using TOF-SIMS, *LPSC XXIV*, 1349-1350, (1993).

Stephan, T., Jessberger, E. and Bischoff, A., Hubble Space Telescope solar array microparticulate impact analysis. Final Report, ESA Contract No. WMA/94-335/GD/HST, (1995).

Sutton, S.R., Chemical composition of primitive solar system particles, In: *Analysis of interplanetary dust particles* (eds. M.E. Zolensky, T.L. Wilson, F.J.M. Rietmeijer and G.J. Flynn), AIP Press, American Institute of Physics, Woodbury, New York, USA, 145-158, (1994).

Taylor, A.D., Baggaley, W.J and Steel, D.I., Discovery of interstellar dust entering the Earth's atmosphere, *Nature*, 380, 323-325, (1996).

Taylor, E.A., Experimental and computational study of hypervelocity impact on brittle materials and composites, *Unpublished PhD thesis*, University of Kent, (1997).

Taylor, S., Lever, J. and Harvey, R.P., A new source of micrometeorites: The south pole water well, *Lunar Planet. Sci. XXVII*, 1319-1320, (1996).

Teetsov, A. and Bradley, J.P., Micromanipulation of extraterrestrial particles, *Lunar Planet. Sci.* XVII, 883-884, (Abstract.), (1986).

Thomas, K.L., Blandford, G.E., Keller, L.P., Klöck, W. and McKay, D.S., Carbon abundance and silicate mineralogy of anhydrous interplanetary dust particles, *Geochim. Cosmochim Acta*, **57**, 1551-1566, (1993).

Unispace Kent, Meteoroid & Debris Flux and Ejecta Models, *Final Report*, ESA Contract No. 1887/96/NL/JG, CD-ROM, (1998).

Walker, R.M., Isotopic constraints on interstellar material in chondritic IDPs, In: *Analysis of interplanetary dust particles* (eds. M.E. Zolensky, T.L. Wilson, F.J.M. Rietmeijer and G.J. Flynn), AIP Press, American Institute of Physics, Woodbury, New York, USA, 203-210, (1994).

Wallenwein, R., Blank, H., Jessberger, E.K. and Traxel, K., Photon microprobe analysis of interplanetary dust particles, *Anal. Chim. Acta*, **195**, 317-322, (1987).

Warren, J.L., Zook, H.A., Allton, J.H, Clanton, U.S., Dardano, C.B., Holder, J.A., et al., The detection and observation of meteoroid and space debris impact features on the solar max satellite, *Proc. 19th Lunar and Planet. Sci. Conf.*, 641-657, (1989).

Warren, J.L. and Zolensky, M.E., Collection and curation of interplanetary dust particles recovered from the stratosphere by NASA, In: *Analysis of interplanetary dust particles* (eds. M.E. Zolensky, T.L. Wilson, F.J.M. Rietmeijer and G.J. Flynn), AIP Press, American Institute of Physics, Woodbury, New York, USA, 245-254, (1994).

Wenthworth, S.J. and Gooding, J.L., Chloride and sulfate minerals in the Nakhla meteorite, *Lunar Planet. Sci. IXX*, 1261-1262, (1988)

Williams, C.T. and Spratt, J., Electron microprobe techniques in mineral analysis, *J. Russell Soc.*, **6**, 1, 5-12, (1995).

Whipple, F.L., The theory of micro-meteorites. Part I: In an isothermal atmosphere, *Proc. Nat. Acad. Sci.*, **36**, 12, 687-695, (1950).

Whipple, F.L., The theory of micro-meteorites. Part II: In hydrothermal atmosphere, *Proc. Nat. Acad. Sci.*, **37**, 1, 19-31, (1951).

Wright, I.P., Carr, R.H. and Pillinger, C.T., Carbon stable isotope analysis of individual deep-sea spherules, *Meteoritics*, **23**, 339-349, (1988).

Wright, I.P., Sexton, A. and Grady, M.M., EURECA Multi-lyer insulation impact morphology and residue analysis, *Final Report*, ESA Contract No. RFQ/3-8001/94/NL/JG, (1995a).

Wright, I.P., Sexton, A. and Grady, M.M., Impacts into HST solar array panels: Optical characterisation of impact damage and chemical analysis of residues, *Final Report*, ESA Contract No. WMA/94-335/GD/HST, (1995b).

Wright, I.P., Yates, P.., Hutchison, R. and Pillinger, C.T., The conent and stable isotopic composition of carbon in individual micrometeorites from Greenland and Antarctica, *Meteoritics & Planet. Sci.*, **32**, 79-89, (1997).

Yano, H., Identification of solid microparticles in ice cores and surface snow from Asuka station – comparative studies with NASA cosmic dust catalogue and microparticles retrieved at Mizuho station and Advance Camp, Antarctica, *Unpublished Baccalaureate Degree thesis*, (1991).

Yano, H., Comparative studies of chemical components of impact residues on LDEF, stratospheric particles and ice core particles, *Annal. Geophys.*, **11**, C481, (1993).

Yano, H., Fitzgerald, H.J. and Tanner, W.G., Chemical analysis of natural particulate impact residues on the long duration exposure facility, *Planet. Space. Res.*, **9**, 793-802, (1994).

Yates, P.D., The content and stable isotopic composition of carbon in spherical micrometeorites, *Unpublished Ph.D thesis*, The Open University, (1992).

Zarnecki, J.C., Giotto dust impact detection system: Instrument and In-flight performance, *JBIS*, **41**, 9, 403-410, (1988).

Zinner, E., Tang, M. and Anders, E., Interstellar SiC in the Murchison and Murray meteorites: isotopic compositions of Ne, Xe, Si, C and N., *Geochim. Cosmochim. Acta*, **53**, 3273-3290, (1989).

Zinner, E., Wopenka B., Amari, S. and Anders, E., Interstellar graphite and other carbonaceous grains from the Murchison meteorite: structure, composition and isotopes of C, N and Ne, *Lunar Planet. Sci. XXI*, 1379-1380, (1990)

Zolensky, M.E. and Mackinnon I.D.R., The abundance and origin of aluminium-rich particulates in the stratosphere, *EOS Trans. AGU*, **65**, 837, (1984).

Zolensky, M.E., Refractory interplanetary dust particles, *Science*, 237, 1466-1468, (1987)

Zolensky, M.E., Mckay, D.S. and Kaczor, L.A., A tenfold increase in the abundance of large solid particles in the stratosphere, as measured over the period 1976-1984, *J. Geophys. Res.*, **94**, D1, 1047-1056, (1989).

Zolensky, M.E., Zook, H.A., Hörz, F., Atkinson, D.R., Coombs, C.R., Watts, A.J et al., Interim Report Of Meteoroid and Debris Special Investigation Group, ***LDEF 69 Months in*** *Space - 2nd Post-Retrieval Symp*, NASA CP-3194, 277-302, (1993).

Zolensky, M.E., Hörz, F., See, T.H., Bernhard, R.P., Dardano, C., Barrett, R.A., Mackay, K., et al., Meteoroid Investigations Using The Long Duration Exposure Facility, In *Analysis Of Interplanetary Dust Particles* (eds M.E. Zolensky, T.L. Wilson, F.J.M. Rietmeijer and G.Flynn), AIP Conf. Proc. 310, AIP Press, Woodbury New York, 291-304, (1994).

Zolensky, M.E., *personnel communication.*

Zworykin, V.K., Hillier, J. and Snyder, R.L., *ASTM Bulletin 117*, 15, (1942).